

APPENDIX A

EXPERIMENT FACILITY DESCRIPTIONS



## ABSTRACT

This appendix provides summary descriptions of the capabilities and specifications of many of the experiment test facilities used for safety research. In general, each description provides the purpose of the facility, lists the issues it can address, reviews design specifications and range of operating parameters, and summarizes the scaling method(s) and considerations. References are cited which provide fuller detail about each facility.



## TABLE OF CONTENTS

<u>Section</u>	<u>Page</u>
LIST OF FIGURES .....	A-vii
LIST OF TABLES .....	A-x
A.1 SEMISCALE .....	A-1
A.2 LOSS OF FLUID TEST .....	A-15
A.3 LOOP BLOWDOWN INVESTIGATION FACILITY .....	A-27
A.4 PRIMARKREISLAUFE .....	A-35
A.5 CYLINDRICAL CORE TEST FACILITY .....	A-41
A.6 SLAB CORE TEST FACILITY .....	A-47
A.7 FULL LENGTH EMERGENCY COOLING HEAT TRANSFER .....	A-53
A.8 FLECHT-SEASET .....	A-63
A.9 TWO-LOOP TEST APPARATUS FACILITY .....	A-79
A.10 ROSA-III FACILITY .....	A-93
A.11 ROSA-IV LARGE-SCALE TEST FACILITY .....	A-99
A.12 MULTI-LOOP INTEGRAL SYSTEM TEST FACILITY .....	A-117
A.13 UNIVERSITY OF MARYLAND AT COLLEGE PARK 2x4 LOOP .....	A-125
A.14 SRI-2 INTEGRAL TEST FACILITY .....	A-133
A.15 THERMAL-HYDRAULIC TEST FACILITY .....	A-139
A.16 BOILING WATER REACTOR FULL INTEGRAL SIMULATION TEST FACILITY .....	A-147
A.17 UPPER PLENUM TEST FACILITY .....	A-155
A.18 CREARE ECC/CORE STEAM FLOW EXPERIMENTS .....	A-161
A.19 BATTELLE COLUMBUS LABORATORY ECC/CORE STEAM FLOW EXPERIMENTS .....	A-179

TABLE OF CONTENTS (Continued)

<u>Section</u>	<u>Page</u>
A.20 POWER BURST FACILITY .....	A-189
A.21 NRU FACILITIES .....	A-197
A.22 TWO-PHASE FLOW LOOP .....	A-201
A.23 30° STEAM SECTOR TEST FACILITY .....	A-203
A.24 ONCE-THROUGH INTEGRAL SYSTEM .....	A-211
A.25 MARVIKEN .....	A-221

## LIST OF FIGURES

<u>Figure</u>		<u>Page</u>
A.1-1	Semiscale Mod-1 .....	A-5
A.1-2	Semiscale Mod-3 .....	A-6
A.1-3	Semiscale Mod-2A .....	A-7
A.1-4	Semiscale Mod-2B .....	A-8
A.1-5	Semiscale Mod-2C .....	A-9
A.1-6	Semiscale Mod-2C core heater rod thermocouple and gamma densitometer locations .....	A-10
A.2-1	Cutaway view of the LOFT integral test facility.....	A-19
A.2-2	LOFT core configuration and typical instrumentation.....	A-20
A.2-3	The LOFT primary coolant system.....	A-21
A.2-4	LOFT ECCS equipment arrangement.....	A-22
A.2-5	LOFT reactor vessel and typical instrumentation.....	A-23
A.3-1	LOBI test facility.....	A-32
A.4-1	Primärkreisläufe (PKL) test facility .....	A-37
A.4-2	Pressure vessel internals of the Primärkreisläufe (PKL) test facility .....	A-38
A.4-3	Cross section of the PKL pressure vessel showing core arrangement of electrically heated core rod simulators ....	A-39
A.5-1	Cylindrical core test facility (CCTF) .....	A-43
A.5-2	Schematic diagram of cylindrical core test facility .....	A-44
A.5-3	Cylindrical core test facility core 1 pressure vessel .....	A-45
A.5-4	Cross section of the CCTF pressure vessel through core and primary loop nozzles .....	A-46
A.6-1	Slab core test facility (SCTF) .....	A-48
A.6-2	Arrangement of heater rod bundles in the slab core test facility (SCTF) pressure vessel .....	A-49
A.6-3	Horizontal cross section of the SCTF pressure vessel .....	A-50
A.6-4	Arrangement of the slab core test facility .....	A-51
A.7-1	FLECHT 7x7 test section simulating a PWR assembly power distribution .....	A-58
A.7-2	FLECHT 10x10 test section simulating a PWR assembly power distribution .....	A-58
A.7-3	FLECHT test facility .....	A-59
A.7-4	Group I flow blockage plate .....	A-60
A.7-5	Group II flow blockage plate .....	A-60
A.7-6	Various blockage configurations in Group II test series ...	A-61
A.7-7	FLECHT low-flooding-rate test configuration .....	A-62
A.8-1	Flow diagram for the SEASET forced reflood configuration ..	A-72
A.8-2	Flow diagram for the gravity reflood configuration .....	A-73
A.8-3	FLECHT-SEASET 161-rod unblocked bundle cross section .....	A-74
A.8-4	Flow diagram for the 21-rod blocked bundle configuration ..	A-75
A.8-5	21-rod blocked bundle cross section .....	A-76

LIST OF FIGURES (Continued)

<u>Figure</u>		<u>Page</u>
A.8-6	Flow diagram for the 163-rod blocked bundle configuration..	A-77
A.8-7	Blockage sleeve distribution, blockage island locations and bulge orientations for the 163-rod blocked bundle tests .....	A-78
A.9-1	Two-loop test apparatus configuration 5A (TLTA 5A) with emergency core cooling systems .....	A-84
A.9-2	TLTA simulation of BWR regions and flow paths .....	A-85
A.9-3	Comparison of jet pump size and elevation between TLTA and BWR .....	A-86
A.9-4	Flow paths at inlet region of a BWR fuel bundle and the TLTA simulation .....	A-87
A.9-5	Steam separator liquid reservoir which was removed for TLTA 5A .....	A-88
A.10-1	Schematic diagram of the ROSA-III facility .....	A-96
A.10-2	Diagram showing coolant flow in the ROSA-III vessel .....	A-97
A.11-1	Overall view of the ROSA-IV large scale test facility .....	A-104
A.11-2	Flow diagram of ROSA-IV (LSTF) .....	A-105
A.11-3	ROSA-IV large scale test facility pressure vessel .....	A-106
A.11-4	Cross section and heater rod arrangement of the ROSA-IV large scale test facility (LSTF) .....	A-107
A.11-5	Comparison of LSTF and PWR pressure vessel dimensions .....	A-108
A.11-6	Coolant flow path in pressure vessel .....	A-109
A.11-7	Fuel bundle power output distribution in core .....	A-109
A.11-8	Primary loop dimensions (plan view) for LSTF .....	A-110
A.11-9	Steam generator of LSTF .....	A-111
A.12-1	MIST reactor coolant system arrangement .....	A-121
A.12-2	MIST and prototype reactor vessels .....	A-122
A.12-3	MIST upper and lower downcomers .....	A-123
A.12-4	MIST RVVV circuit .....	A-124
A.13-1	Arrangement of the UMCP 2x4 loop reactor coolant system....	A-128
A.13-2	Principal features of the UMCP reactor vessel and downcomer .....	A-129
A.13-3	UMCP vent valve design .....	A-130
A.13-4	Spacing of tubes in the UMCP steam generator .....	A-131
A.14-1	Arrangement of the SRI-2 reactor coolant system .....	A-135
A.14-2	SRI-2 reactor vessel details .....	A-136
A.15-1	Diagram of the THTF .....	A-142
A.15-2	Schematic of THTF loop .....	A-143
A.15-3	Bundle and rod cross sections .....	A-144
A.15-4	Spacer grid and thermocouple locations within the THTF bundle .....	A-145
A.16-1	Schematic of the BWR FIST facility .....	A-150

## LIST OF FIGURES (Continued)

<u>Figure</u>	<u>Page</u>
A.16-2 FIST bundle inlet region and lower tie plate/electrode ...	A-151
A.16-3 FIST bundle outlet region and upper tie plate/electrode ..	A-152
A.16-4 FIST axial power profile .....	A-153
A.16-5 FIST local power profile .....	A-154
A.17-1 Top view of the upper plenum test facility (UPTF) .....	A-157
A.17-2 Upper plenum test facility pressure vessel and internals..	A-158
A.17-3 Flow diagram for the upper plenum test facility .....	A-159
A.18-1 1/30-scale CREARE transparent facility .....	A-166
A.18-2 Schematic of vessel geometry used for 1/30-scale countercurrent flow tests .....	A-167
A.18-3 Flow schematic for CREARE 1/15-scale high-pressure cylindrical vessel and facility .....	A-168
A.18-4 Cutaway view of CREARE 1/15-scale high-pressure cylindrical vessel .....	A-169
A.18-5 Six geometrical configurations of gap size, vessel length, and plenum depth possible with CREARE 1/15-scale vessel ..	A-170
A.18-6 Fluid flow paths in 1/15-scale CREARE planar facility ....	A-171
A.18-7 Schematic cross section of CREARE planar test apparatus ..	A-172
A.18-8 Hot and cold leg arrangement in downcomer of 1/15-scale apparatus .....	A-173
A.18-9 Drawing of CREARE 1/5-scale vessel .....	A-174
A.18-10 Drawing of 1/5-scale facility for flashing experiments ...	A-175
A.19-1 Drawing of BCL 1/15-scale transparent vessel model .....	A-182
A.19-2 Schematic of BCL transparent vessel facility .....	A-183
A.19-3 Schematic of BCL 1/15-scale 60 psi vessel model .....	A-184
A.19-4 Schematic of flow configuration for BCL 1/15-scale model..	A-185
A.19-5 Comparison of cold leg arrangements in the BCL 1/15-scale model vessels .....	A-186
A.19-6 Drawing showing as-built dimensions of the BCL 2/15-scale hot-wall vessel .....	A-187
A.20-1 PBF LOCA program target cladding temperature histories ...	A-193
A.20-2 PBF LOCA fuel train orientation .....	A-194
A.20-3 PBF LOCA test system .....	A-195
A.22-1 Diagram of two-phase flow loop .....	A-202
A.23-1 30° steam sector test facility (SSTF) .....	A-208
A.23-2 30° steam sector test section .....	A-209
A.24-1 Once-through integral system (OTIS) test facility .....	A-217
A.24-2 Comparison of full-size 205-FA plant OTSG to 19-tube OTSG of OTIS .....	A-218
A.24-3 OTIS general arrangement .....	A-219
A.24-4 Leak flow control orifice assembly .....	A-219
A.25-1 Marviken facility, showing flow paths during a flow test..	A-224

## LIST OF TABLES

<u>Table</u>	<u>Page</u>
A.1-1 Semiscale design specifications .....	A-11
A.1-2 Comparison of Semiscale modifications .....	A-13
A.2-1 PWR typicality requirements for the LOFT model design .....	A-24
A.2-2 LOFT - commercial PWR comparisons .....	A-25
A.3-1 LOBI large-break tests .....	A-33
A.3-2 LOBI small-break AI-tests preliminary .....	A-33
A.3-3 LOBI special transient experiment program .....	A-34
A.4-1 Summary of major features of PKL .....	A-36
A.5-1 Summary of major features of the CCTF .....	A-42
A.6-1 Summary of major features of the SCTF .....	A-52
A.7-1 FLECHT low flooding cosine test -- nominal initial conditions .....	A-56
A.7-2 FLECHT low flooding cosine test -- range of test conditions .....	A-56
A.7-3 FLECHT low flooding skewed test -- nominal initial conditions .....	A-57
A.7-4 FLECHT low flooding skewed test -- range of test conditions .....	A-57
A.8-1 Range of test conditions for the 161-rod unblocked bundle tests in FLECHT-SEASET .....	A-68
A.8-2 Blockage configurations tested in the 21-rod blocked bundle FLECHT-SEASET tests .....	A-69
A.8-3 Initial conditions and the ranges of test conditions for the 21-rod blocked bundle tests .....	A-70
A.8-4 Initial conditions and the ranges of test conditions for the 163 rod blocked bundle tests .....	A-71
A.9-1 TLTA test configurations .....	A-89
A.9-2 Flow areas and correlations for TLTA large-break tests .....	A-91
A.9-3 Relative volume distributions in TLTA .....	A-92
A.10-1 Scaling comparisons of ROSA-III and a BWR-6 .....	A-95
A.11-1 Major design characteristics of LSTF and PWR .....	A-112
A.11-2 Primary characteristics of pressure vessel and core .....	A-113
A.11-3 Major design characteristics of LSTF steam generators .....	A-114
A.11-4 Break locations in LSTF (ROSA-IV) .....	A-115
A.11-5 Break orifice sizes .....	A-116
A.11-6 ECCS injection locations .....	A-116
A.12-1 Significant events following a small-break LOCA test in MIST .....	A-120

LIST OF TABLES (Continued)

<u>Table</u>		<u>Page</u>
A.14-1	Scaling criteria for SRI-2 .....	A-137
A.15-1	THTF operating parameters .....	A-141
A.17-1	Summary of major features of UPTF .....	A-156
A.18-1	Parametric comparison of CREARE scale model experiments with typical PWR conditions .....	A-176
A.18-2	Combinations of parameters tested in the CREARE planar facility .....	A-177
A.20-1	Experimental envelope for operation of the PBF .....	A-196
A.21-1	Characteristics of the NRU reactor .....	A-198
A.21-2	Test conditions for the NRU LOCA simulation program .....	A-199
A.25-1	Summary of the Marviken CFT program test objectives .....	A-225



## APPENDIX A

### EXPERIMENT FACILITIES

#### A.1 SEMISCALE

The Semiscale facility, located at the Idaho National Engineering Laboratory, has been an important part of the NRC light water reactor safety program for more than a decade. Isothermal blowdown and refill tests were performed in the Semiscale facility prior to the ECCS hearing in 1973 and the results of these experiments were one of the major reasons for questioning ECCS effectiveness. However, for this report, only those experiments performed in the Semiscale facility after the ECCS hearings are described.

The Semiscale Mod-1 facility became operational in September 1974 and was scaled to the LOFT facility. Originally intended to study large-break loss-of-coolant accidents, subsequent facility modifications have provided data for LOCAs over a broad spectrum of sizes with additional experiments conducted to investigate reflood heat transfer, steam generator tube rupture, station blackout events, natural circulation, secondary induced transients, and power loss transients and has been operated to examine proposed recovery procedures for various transients.

The Semiscale Mod's simulated most of the large PWR counterpart's components such as pumps, loops, steam generators and vessel. The vessel included a non-nuclear electrically heated core which expedited experimental turnaround. The various Mod's of Semiscale were all high temperature, high pressure light water facilities with an initial thermal-hydraulic condition similar to the PWR counterpart (pressure, hot leg subcooling, core differential temperature).

There have been four major modifications to the original MOD1 facility. These will be discussed in the following sections along with the general area of investigation. Table A.1-1 summarizes the specifications for each of the modifications. Major differences between the Mod's are summarized in Table A.1-2. Also included in Table A.1-2 is the purpose of the facility which relates the Mod to the water reactor safety issue.

#### Semiscale Mod-1

The Mod-1, 1-1/2 loop facility (Ref. A.1-1) (so termed because it contains one active loop and one passive loop) was designed as a small-scale counterpart facility to LOFT. It was operated from September 1974 to September 1977. The Mod-1 facility is shown schematically in Figure A.1-1. The following experiment series were performed to address the indicated issues:

<u>Experiment Series</u>	<u>Type of Experiment</u>
S-01	Isothermal large break blowdown
S-02	Large break blowdown
S-03	Reflood heat transfer
S-29	Large break blowdown--reflood
S-04	Large break LOCA--ECC baseline
S-05	Large break LOCA--Alternative ECC
S-06	Large break LOCA--LOFT counterpart
S-28	Large break LOCA with steam generator tube rupture

### Semiscale Mod-3

The Semiscale Mod-3 facility (Ref. A.1-2) shown in Figure A.1-2 included several significant changes from the Mod-1 system. It was operated from June 1978 to October 1979. The changes included a new pressure vessel with an external down-comer, a new 25-rod bundle (3.7 m long), and active components in the broken loop. The Mod-3 system was based on a 4-loop PWR of Westinghouse design. The system changed from one active loop (intact loop) used for Mod-1 to a true two loop system by inclusion of a new full length active steam generator and a new high specific speed active pump in the broken loop. The facility was designed as a blowdown-refill-reflood facility to examine large break phenomena. The Mod-3 facility had no external heat loss makeup system and used augmented core power for some of the experiments to makeup for the large heat losses from the atypically large surface area. The inclusion of a vessel upper head with simulated guide tube and simulated support columns allowed simulation of small break LOCA experiments with upper head injection. The experiment series and issues addressed were:

<u>Experiment Series</u>	<u>Type of Experiment</u>
S-07	Large-break and small break LOCA Mod-3 baseline
S-UHD	Large-break LOCA with upper head injection
S-SB	2-1/2% small-break LOCAs
S-Tr	Station blackout transients

### Semiscale Mod-2A

The Mod-2A system (Ref. A.1-3) is shown in Figure A.1-3. The major changes to Mod-3 included a new Type II steam generator in the intact loop and a new pressure vessel with honeycomb insulators. External heaters were also added to loop piping to reduce heat losses. The experiments conducted from December 1980 to October 1982 were:

<u>Experiment Series</u>	<u>Type of Experiment</u>
S-UT	Small-break LOCA with UHI
S-NC	Natural circulation tests
S-IB	Intermediate-break LOCA
S-SR	Primary feed and bleed during natural circulation
S-SF	Secondary feed and steam line breaks

## Semiscale Mod-2B

The Mod-2B system (Ref. A.1-4) includes a new pressurizer, a new intact loop pump and pump suction piping, an upper head vent, a hot water makeup system, a modified steam generator relief valve, and crossover piping to connect both intact and broken loop steam generators. The heat loss makeup technique changed from band heaters to heater tape with a fairly uniform coverage of the tape (this was not possible with the band heaters). The upper head to upper plenum flow path was changed by plugging instrument holes and drain holes that had been used on the support column during Mod-2A testing. The bypass line between the vessel upper-head to downcomer inlet annulus used fixed orifices to set a desired bypass flow. The Mod-2B system is shown in Figure A.1-4. The experiment series listed below were conducted from November 1982 until May 1984.

<u>Experiment Series</u>	<u>Type of Experiment</u>
S-PL	Offsite power loss transients
S-SG	Steam generator tube rupture test
S-PBO	Primary system boiloff tests

## Semiscale Mod-2C

The major change in the facility for Mod-2C (Ref. A.1-5) was the new Type III broken loop steam generator, which was better scaled on the secondary side and includes an external downcomer and additional instrumentation appropriate for secondary steam and feed line breaks. Using an external downcomer allows better measurement of steam generator secondary hydraulic conditions during transients. The system was volume scaled to the PWR counterpart with a scaling factor of 1:1705. The Mod-2C system is shown in Figure A.1-5. This system was used to perform the following test series, then was shut down in early 1986.

<u>Experiment Series</u>	<u>Type of Experiment</u>
S-FS	Secondary feedline and steam line breaks
S-LH	Small-break LOCAs to investigate core bypass effects on core level depression.
S-NH	Small-break LOCAs with no high pressure coolant injection.

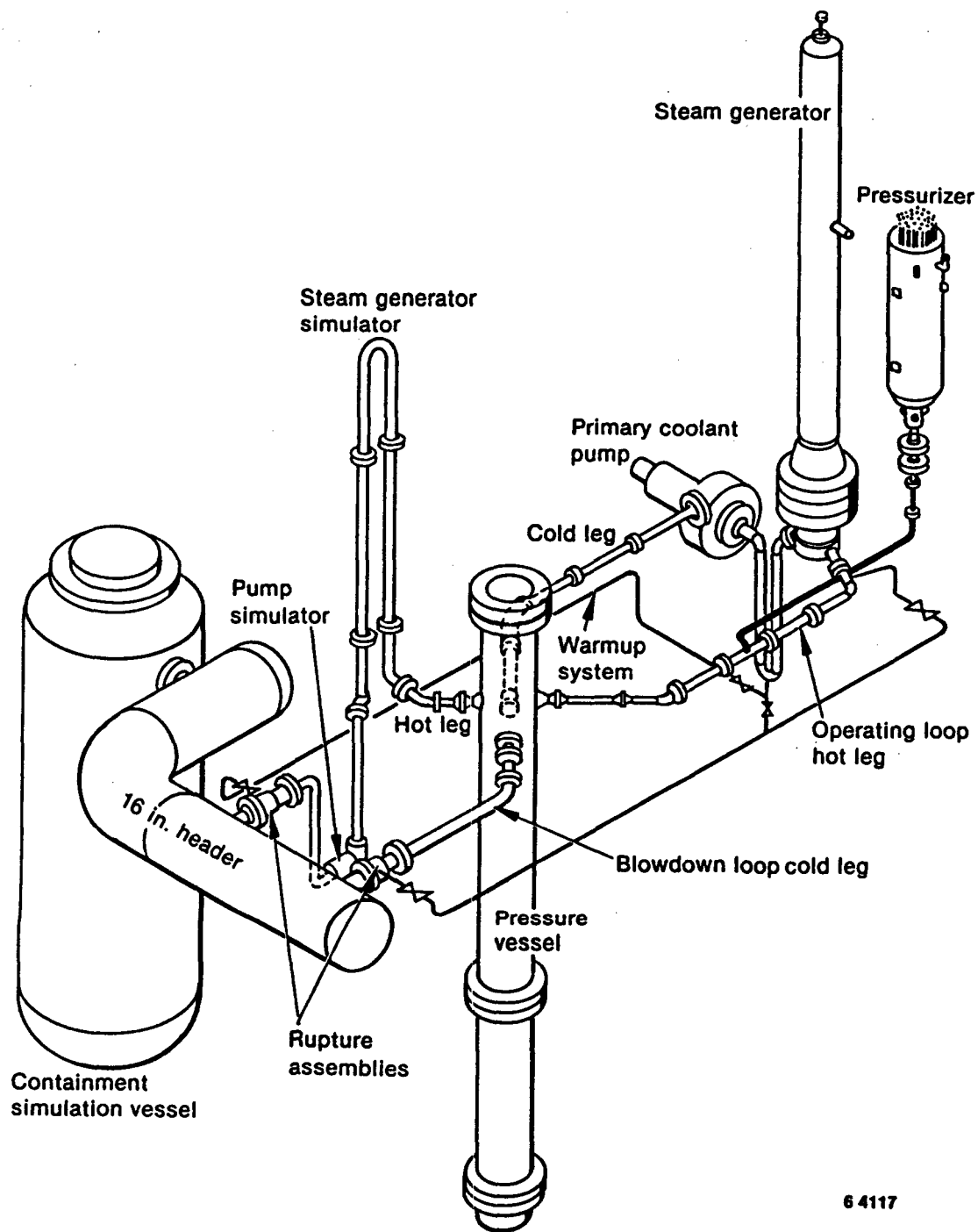
## Semiscale Measurement Techniques

As these various Mods evolved, there was a steady improvement in measurement techniques. Specifically, the early Mods used drag disks/screens to measure break flow; whereas the newer Mods used condensing systems and catch tanks. Improvements have been made in control and measurement of high pressure injection fluid into the system. As the Mods became more sophisticated, scaled relief valves were added to the steam generator secondaries also with condensing systems and catch tanks. The basic instrumentation in Semiscale is common to all the Mods including pressure cells, differential pressure cells to determine liquid level, loop and steam generator fluid and metal thermocouples, core heater rod cladding thermocouples, and gamma-ray and x-ray densitometers, turbine meters and drag disks to measure flow (at least single-phase initial conditions).

One of the most important features of the Semiscale Mods was the inclusion of extensive in-core measurements. The Mod 3, Mod-2A, Mod-2B and Mod-2C facilities all utilized a full height electrically heated core (3.66 m heated length) and a vessel with an external downcomer. This allowed using core gamma densitometers to measure the axial channel void fraction at various positions. Figure A.3.6 shows the cross section of the Mod 2C core with core rod heater temperatures measurement locations and gamma densitometer locations which help to track the mass distribution in the core.

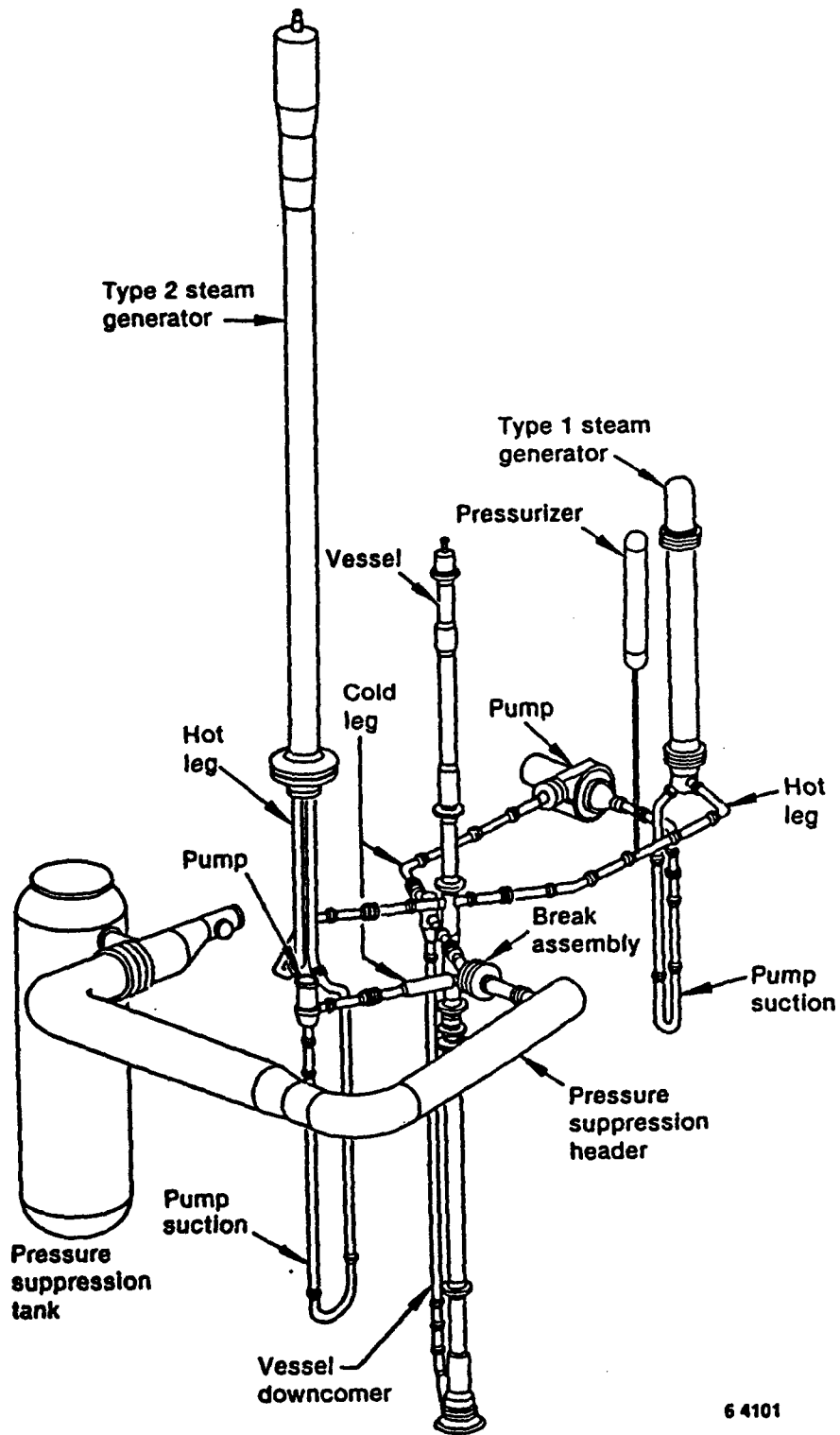
#### REFERENCES

- A.1-1 L. J. Ball et al., "Semiscale Program Description," EG&G Idaho, Inc., TREE-NUREG-1210, May 1978.
- A.1-2 M. L. Patton, Jr., "Semiscale Mod-3 System Description," NUREG/CR-0239, TREE-NUREG-1212, July 1978.
- A.1-3 System Design Description for the Mod-2A Semiscale System, Addendum I, "Mod-2A Phase I Addendum to Mod-3A System Description," EG&G Idaho, Inc., December 1980.
- A.1-4 L. J. Martinez, "Research Design Document for Semiscale Steam Generator Tube Rupture Experiment Series," EG&G Idaho, Inc. November 1982.
- A.1-5 T. J. Boucher and J. R. Wolf, "Experiment Operating Specification for Semiscale Mod-2C Feedwater and Steam Line Break Experiment Series," EGG-SEMI-6625, May 1965.



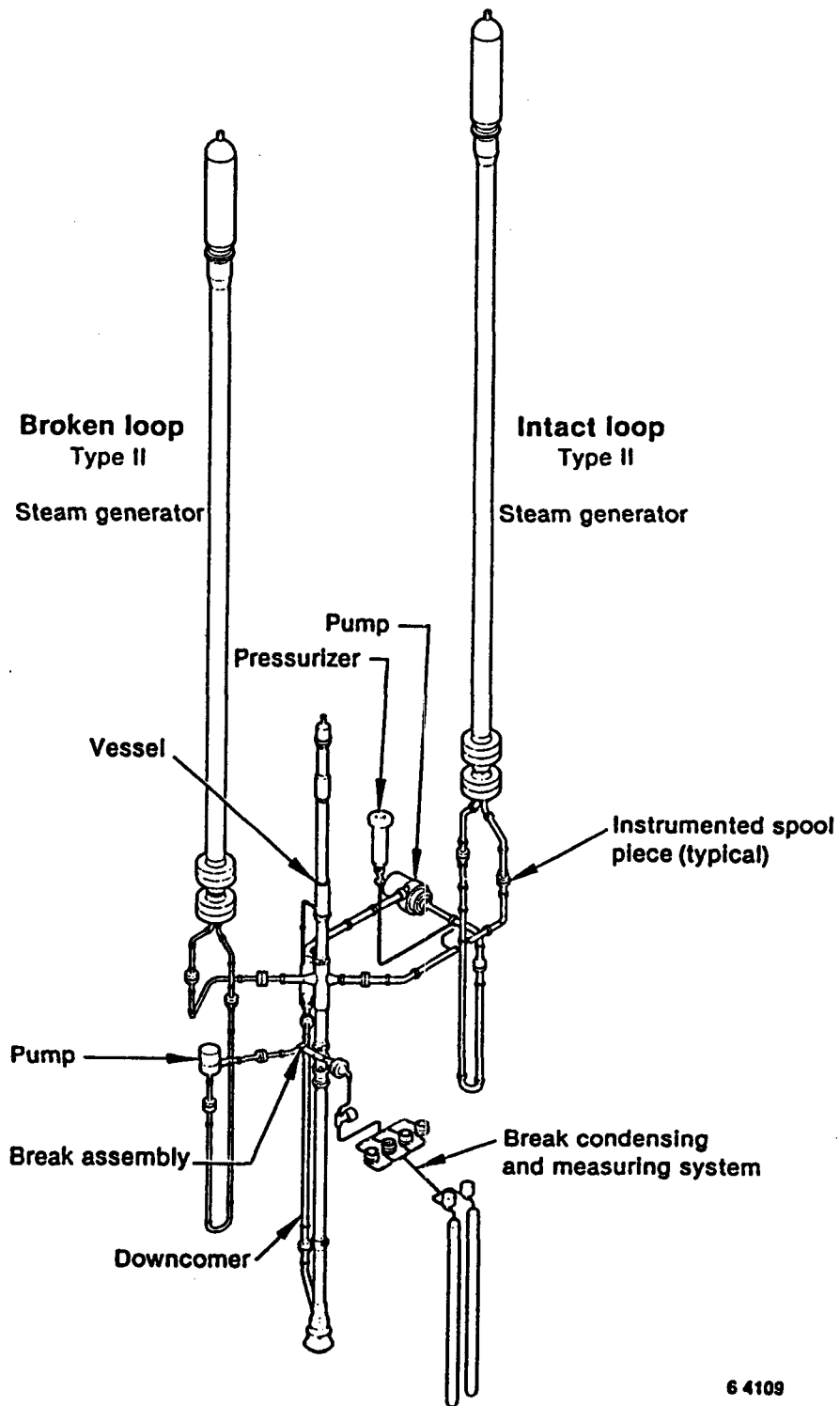
6 4117

Figure A.1-1 Semiscale Mod-1



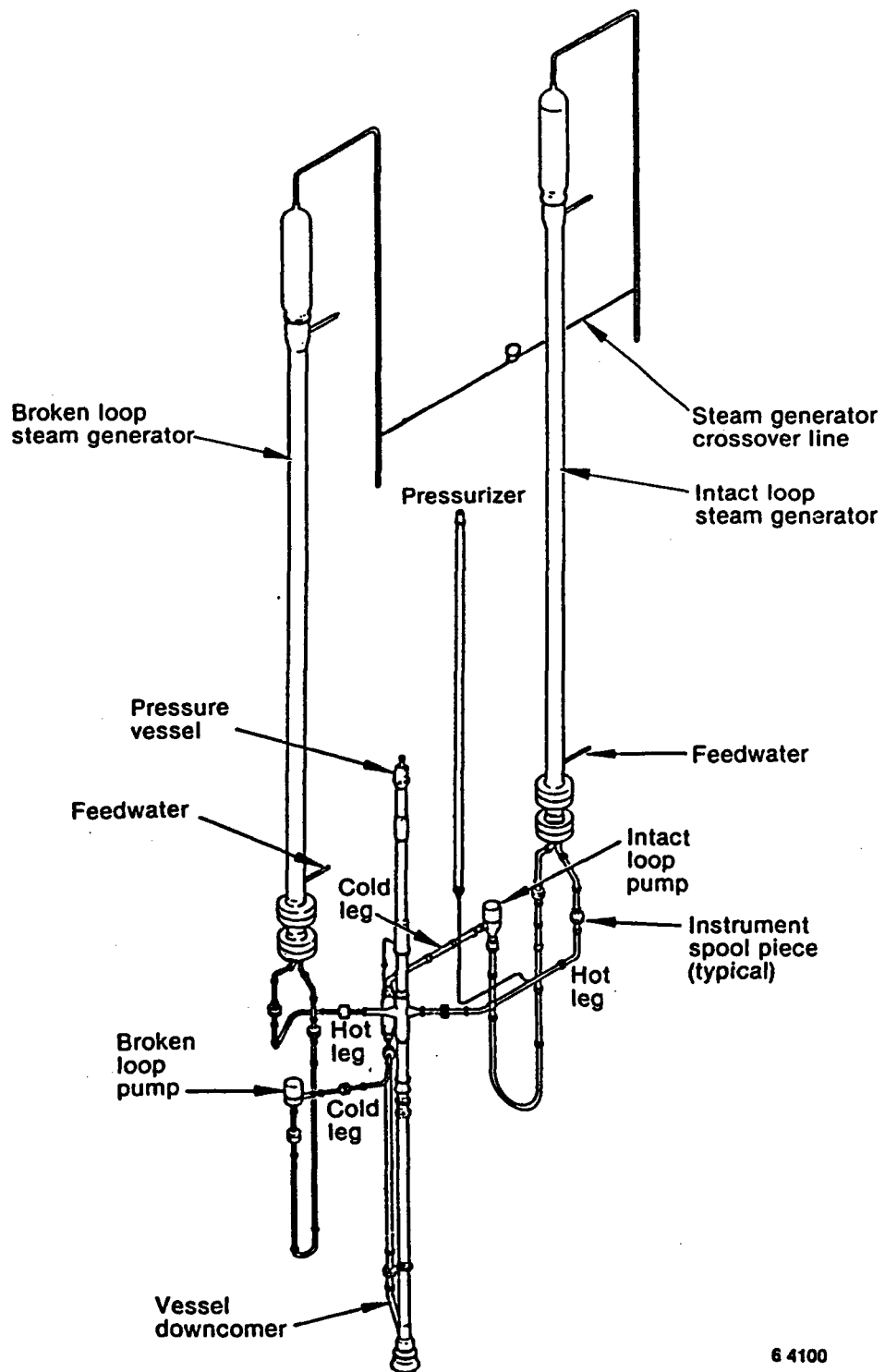
6 4101

Figure A.1-2 Semiscale Mod-3



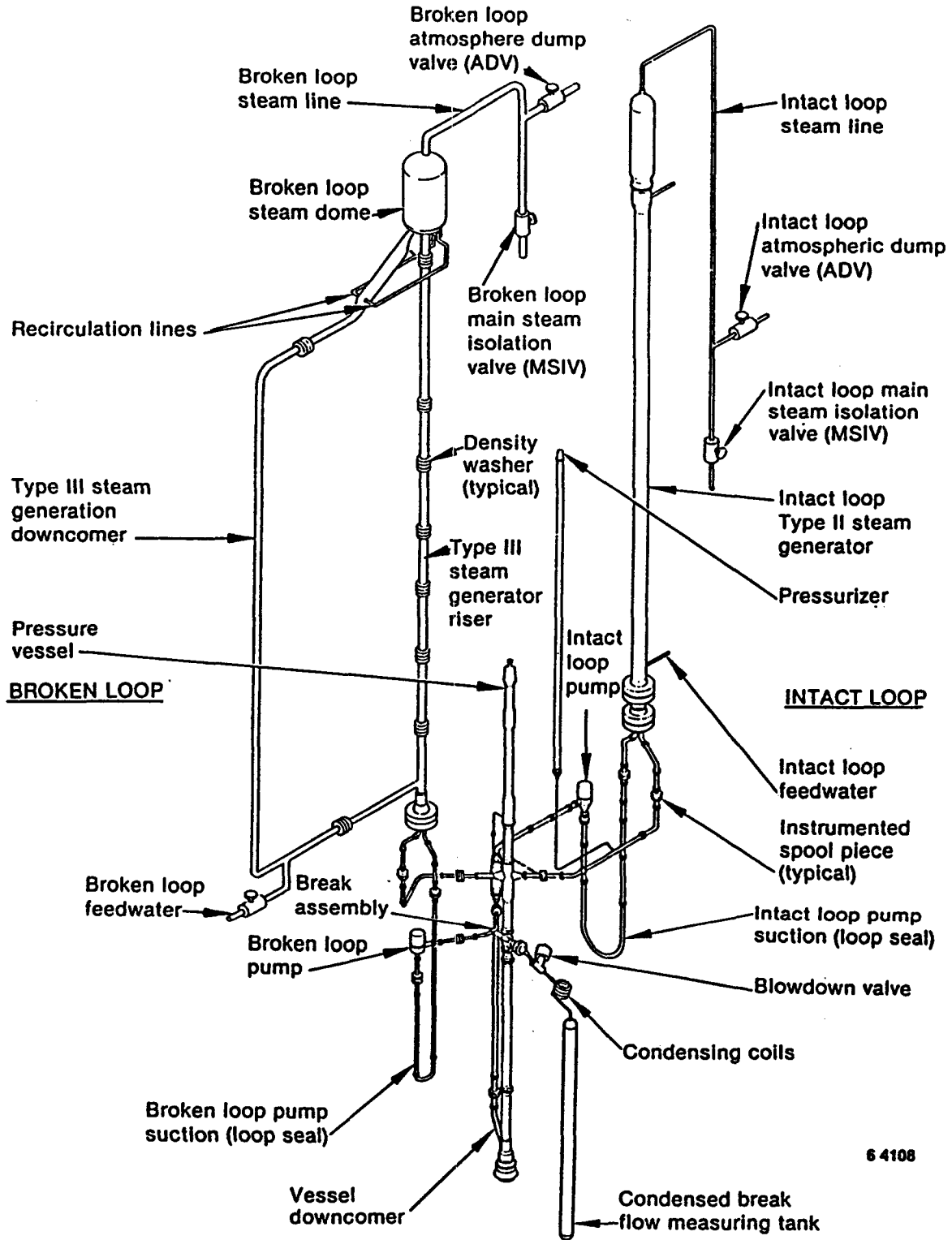
6 4109

Figure A.1-3 Semiscale Mod-2A



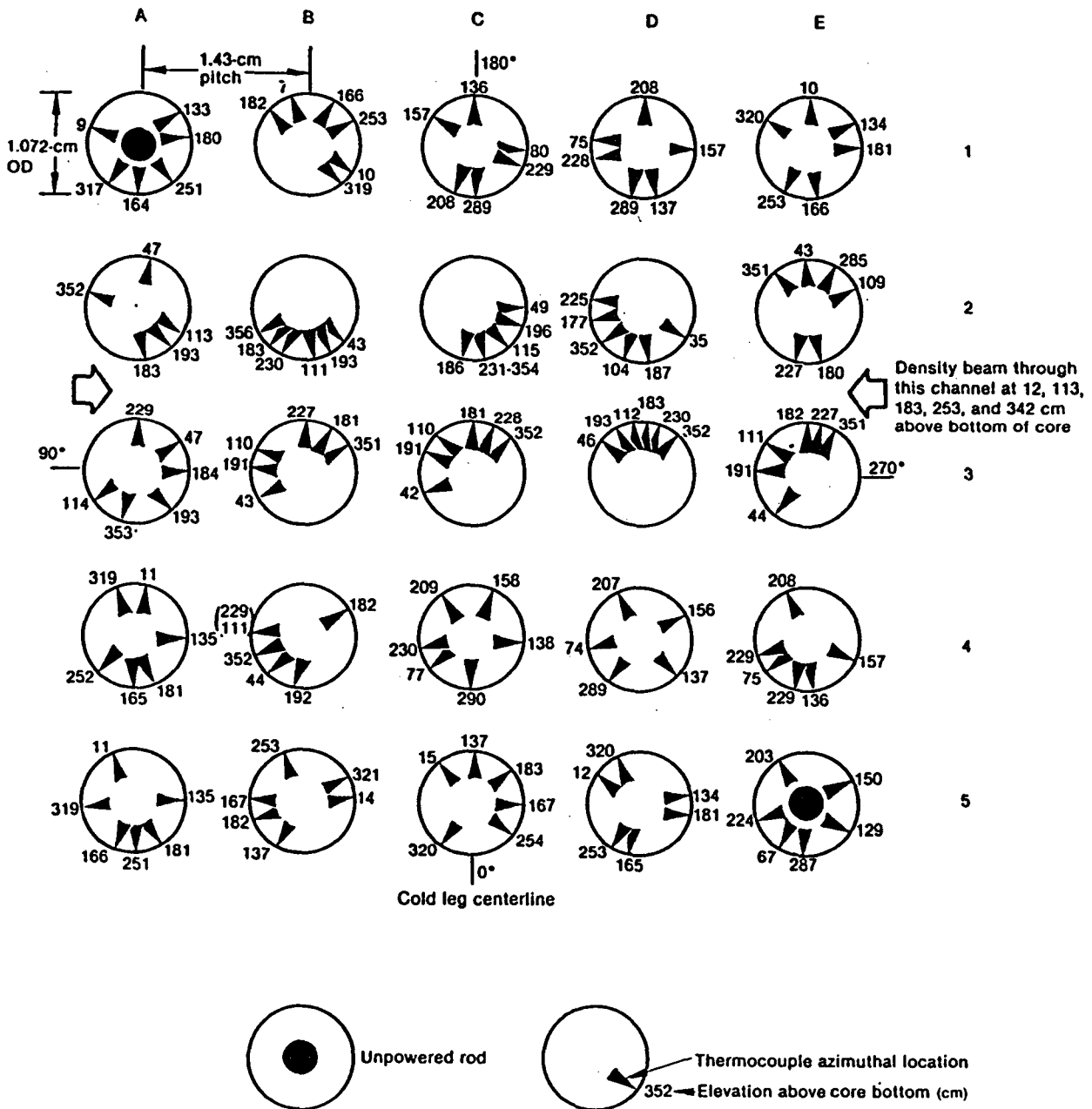
6 4100

Figure A.1-4 Semiscale Mod-2B



6 4108

Figure A.1-5 Semiscale Mod-2C



4 0403

Figure A.1-6 Semiscale Mod-2C core heater rod thermocouple and gamma densitometer locations

Table A.1-1 Semiscale design specifications

Item	Mod-1	Mod-3	Mod-2A	Mod-2B	Mod-2C
Reference plant	LOFT	W 4-loop PWR 3411 MW	W 4-loop PWR 3411 MW	W 4-loop 3411 MW	W 4-loop 3411 MW
Scaling	Full height volume scaled	Full height volume scaled 1/1705.5	Full height volume scaled 1/1705.5	Full height volume scaled 1/1705.5	Full height volume scaled 1/1705.5
Intact loop/broken loop flow	3/1	3/1	3/1	3/1	3/1
Maximum design pressure	17.2 MPa	17.2 MPa	17.2 MPa	17.2 MPa	17.2 MPa
Design temperature	616 K	616 K	616 K	616 K	616 K
Pressure vessel					
Downcomer	Internal	External	External	External	External
Core heated length	1.68 m	3.66 m	3.66 m	3.66 m	3.66 m
Number rods	40	25/23 heated	25/23 heated	25/23 heated	25/23 heated
Axial peaking factor	1.58	1.55	1.55	1.55	1.55
Total core power	1.6 MW	2.0 MW	2.0 MW	2.0 MW	2.0 MW
Intact loop					
Primary coolant pump	Horizontal centrifugal- volute	Horizontal centrifugal- volute	Horizontal centrifugal- volute	High speed centrifugal	High speed centrifugal

A-11

Table A.1-1 (Continued)

Item	Mod-1	Mod-3	Mod-2A	Mod-2B	Mod-2C
Steam generator	Type I U-tube	Type I U-tube	Type II U-tube	Type II U-tube	Type II U-tube
Number of tubes	54	54	6	6	6
Average tube length	5.14 m	5.14 m	19.29 m	19.29 m	19.29 m
Broken Loop					
Primary coolant pump	Hydraulic resistance simulator	Horizontal centrifugal volute	Horizontal centrifugal volute	Horizontal centrifugal volute	High speed centrifugal
Steam generator	Hydraulic resistance simulator	Type II U-tube	Type II U-tube	Type II U-tube	Type III U-tube
Number tubes		2	2	2	2
Average tube length		19.20 m	19.29 m	19.29 m	19.29 m
ECC systems	HPI, LPI, ACC	HPI, LPI, ACC	HPI, LPI, ACC, UHI	HPI, LPI, ACC, UHI	HPI, LPI, ACC, UHI

TABLE A.1-2 COMPARISON OF SEMISCALE SYSTEMS

Facility Mod	Intact Loop Steam Generator	Broken Loop Steam Generator	Intact Loop Pump	Broken Loop Pump	Electrically Heated Core
Bettis Flask (1965-1968) 500 Series 600 Series 700 Series	None	None	None	None	None
Single Loop- (1969-1971) 800 Series	3 ft; 43 tube once through	None	Canned rotor bottom vertical inlet	None	9 in.; 120 rods 1.2 MW
Single Loop- (1971) 900 Series	Same as 800 series	None	Same as 800 series	None	52 in.; 33-46 rods 1.6-1.8 MW
1-1 1/2 Loop (1973) Isothermal	Same as 800 series	None; simulated hydraulic resistance	Lawrence pump	None; orifice simulator	9 rods; 5.5 ft rods; used to heat system only
Mod 1 (1974-1977)	Type I; 54 tubes (5.13 m) (models LOFT facility)	None; resistance simulator	Lawrence pump	Orifice; locked rotor resistance only simulated	1.67 m (5.5 ft) active length core; rods extended out top of vessel; maximum power 1.6 MW; 40 rods with PWR pitch and size
Mod 3 (1981-1982)	Type I	Type II; 2 tubes 1:1 elevation scaling	Lawrence pump	High-speed vertical; bottom suction, side discharge; locked rotor resistance nozzle at discharge	3.66m (12 ft) length core; rods extended out top of vessel; maximum power 2.0 MW; 25 rods with PWR pitch and size
Mod 2A (1981-1982)	Type II; 6 tubes 1:1 elevation scaling	Type II; 2 tubes 1:1 elevation scaling	Lawrence pump (removed for natural circulation tests)	High-speed vertical; bottom suction side discharge; locked rotor resistance nozzle at discharge	3.66m (12 ft) length core; rods extended out top of vessel; maximum power 2.0 MW; 25 rods with PWR pitch and size
Mod 2B (1983-1984)	Type II; 6 tubes 1:1 elevation scaling; scaled relief valves on secondaries	Type II; 2 tubes 1:1 elevation scaling scaled relief valves on secondary	High-speed vertical; bottom suction; side discharge; locked rotor resistance nozzle at discharge	Same as Mod-2A	Same as Mod-2A
Mod 2C (1985-1986)	Type II; 6 tubes; 1:1 elevation scaling	Type III; 2 tubes; external downcomer; elaborate separator; 1:1 scaling; extensive instrumentation; improved secondary volume scaling	Same as Mod-2B	Same as Mod-2B	Same as Mod-2B

TABLE A.1-2 (CONT.)

Facility Mod	Piping	Heat Loss Makeup	Downcomer	Vessel Upper Head	Original Purpose of Facility
Bettis Flask (1965-1968) 500 Series 600 Series 700 Series	None	None	None	None	Subcooled Blowdown
Single Loop- (1969-1971) 800 Series	5 in. double extra strong	None	External piping	None	Large break LOCA; ECC bypass
Single Loop- (1971) 900 Series	Same as 800 series	None	Same as 800 series	None	Large break LOCA; core thermal response
1-1 1/2 Loop (1973) Isothermal	Intact loop: 3 in. sch 160; Broken Loop 2 in. sch 160	None	Internal annulus	None	Large break LOCA; ECC bypass
Mod 1 (1974-1977)	Intact loop 3 in. sch 160; broken loop 1-1/2 in. sch 160; carbon steel	None	Internal annulus in vessel; no incore densitometers	None	Large break LOCA
Mod 3 (1981-1982)	Intact loop 3 in. sch 160; broken loop 1-1/2 in. sch 160; carbon steel	Augmented core power	External pipe with core/ downcomer densitometers	Contains ECC injection port; simulated guide tube; two simulated support columns; support plate separates upper head from upper plenum	Large break LOCA
Mod 2A (1981-1982)	Intact loop 3 in. sch 160; broken loop 1-1/2 in. sch 160; carbon steel	Augmented core power and external band heaters on loop piping only (last natural circulation test used vessel heaters also)	External pipe with core/ downcomer densitometers	Same as Mod-3; however variation in bypass line resistance using valve	SBLOCA; natural circulation
Mod 2B (1983-1984)	Intact loop has a 2-1/2 in. sch 160 suction; mostly 3 in. sch 160 pipes; broken loop still has a 1-1/2 in. sch 160 piping. Most piping is stainless steel	Heater tape over both piping and vessel; no band heaters on suction	Same as Mod-2A	Basically same as Mod-3 bypass line used orifice; upper plenum/upper head resistance changed by plugging support columns	SBLOCA; power loss; anticipated transients without scram; steam generator tube rupture.
Mod 2C (1985-1986)	Most of intact loop all 2-1/2 in. sch 160 broken loop 1-1/2 in. sch 160 all stainless steel	Same as Mod-2B	Same as Mod-2B	Same as Mod-2B; bypass Line can be varied by chang- ing orifice	Steam and feed line break and further SBLOCA analysis

A-14

## A.2 LOSS OF FLUID TEST

The Loss-of-Fluid Test (LOFT) facility is located at the Idaho National Engineering Laboratory, Test Area North. This facility includes a 50-MW(t), volumetrically scaled, pressurized water reactor (PWR) system. With recognition of the differences in commercial PWR designs and inherent distortions in reduced scale systems, the design objective for the LOFT facility was to produce the significant thermal-hydraulic phenomena that would occur in commercial PWR systems in the same sequence and with approximately the same time frames and magnitudes. Experiments conducted in the LOFT facility provide "integral" system data for assessment of analytical licensing techniques and for identification of unexpected thresholds or events that may occur during a transient. The term integral implies that the entire system is modeled and the entire transient sequence is carried out as opposed to separate-effects tests in which specific phenomena, components or single systems are studied during a particular phase of a transient. A view of the facility is shown in Figure A.2.1.

A detailed description of the LOFT facility and instrumentation is provided in Reference A.2-1. The LOFT system and the scaling basis for the facility are described in Reference A.2-2. LOFT consists of five major systems:

1. Reactor system,
2. Primary coolant system,
3. Blowdown suppression system,
4. Emergency core cooling system,
5. Secondary coolant system.

### Reactor System

The reactor system consists of the reactor vessel and head, core support barrel, upper and lower core support structures, flow skirt, reactor vessel fillers, and a 1.68-m nuclear core.

The reactor core contains the nuclear fuel and provides a primary boundary to fission products, transfers the heat of fission to the primary coolant, contains a neutron source for initial criticality, and supports various experiment instrumentation.

The 1.68-m-long LOFT reactor core is about one-half the length of typical reactor cores (3.7 m long) in commercial plants. However, this is the only compromise made in the nuclear fuel for the LOFT core. PWR fuel rod assemblies are used in the geometry shown in Figure A.2.2. The triangular corner assemblies are partial square assemblies for simulation of a more circular core. The outer four square fuel assemblies have reactor control rods in the guide tubes. The center fuel assembly has instruments placed in the vacant guide tubes as well as on the fuel rods. The LOFT fuel assemblies are complete with upper and lower end boxes and fuel rod spacer grids at five elevations. More specific detail of the LOFT core design is contained in Reference A.2.2.

## Primary Coolant System

The primary coolant system, shown in Figure A.2-3, consists of two coolant loops connected to the reactor system. The loops are designated the intact loop and the broken loop. The primary system removes heat from the reactor system during normal, upset, emergency, and faulted conditions; provides and maintains a primary coolant and fission product envelope; provides the capability for producing a coolant environment and time behavior during an experiment that will be similar to that found during an accident in a commercial PWR; provides the capability for removing residual heat from the reactor system during normal, upset, emergency, and faulted conditions; and simulates the three unbroken loops (intact loop) and one broken loop of a four-loop PWR during transients. Some of these functions are performed by the reactor system and the emergency core cooling system (ECCS) in combination with the primary system.

The intact loop simulates the three unbroken loops in a four-loop PWR during a LOCA. The principal (active) components contained in the intact loop are the steam generator, primary coolant pumps, pressurizer, primary coolant venturi (flow measuring device), and intact loop piping.

The broken loop simulates the broken loop of a four-loop PWR during a LOCA. The loop is not closed in the LOFT system; its hot and cold legs end in quick-opening blowdown valves (QOBVs) that discharge to the blowdown suppression system. To maintain the dead-ended legs of the loop at specified hot and cold leg temperatures, two 25.4-mm (1 in.) warmup lines are provided. The principal components of the broken loop are the QOBVs and upstream isolation valves, reflood assist bypass system, break simulating orifices, and a passive simulator that represents the flow resistances of the steam generator and primary coolant pump.

## Blowdown Suppression System

The purpose of the blowdown suppression system is to simulate the containment back pressure response of commercial PWRs during LOCAs and to contain the blowdown effluent. This system also prevents containment contamination during a LOCA experiment.

The major components of the blowdown suppression system are the blowdown suppression header and downcomers, blowdown suppression tank, and blowdown suppression tank spray system.

## Emergency Core Cooling System

The basic functions of the ECCS are to protect the LOFT plant and to simulate the ECCSs of commercial PWRs. The plant protection functions are to provide required core cooling over the full range of break sizes and locations and the capability for long-term core cooling in conjunction with the purification system.

LOFT ECCSs simulate the ECCS response of various commercial PWRs during a LOCA, investigate the margin available in engineered safety features of commercial PWRs, and provide flexibility for investigations beyond the capability of commercial PWRs. The LOFT ECCS has the capability of injecting ECC to any of

several locations including the intact loop hot or cold legs, and the reactor vessel downcomer, lower plenum, or upper plenum. An identical backup ECCS is also available which functions separately from the ECCS used in an experiment.

The LOFT ECCS is arranged in two separate groups of equipment (Groups A and B in Figure A.2-4). Each group contains three subsystems: the high-pressure injection systems, accumulator, and low-pressure injection system. The groups can act singly or simultaneously. In general, the groups use separate piping, but it is possible to valve them into the same piping. Only one group is normally used, however (in one experiment, both were used with one injecting into the upper plenum and the other into the intact loop cold leg); the other group is maintained in the standby mode and is under the control of the plant protection system or the control room.

### Secondary Coolant System

The secondary coolant system removes (to the environment) the heat transferred to the secondary system in the steam generator, controls reactor power during power operation and influences the primary coolant and reactor systems in a manner similar to the secondary coolant system of a commercial PWR, and removes decay heat under normal conditions.

The main loop of the secondary system consists of the shell side of the steam generator, an air-cooled condenser, a condensate receiver, condensate subcooler, main feedwater pump, and the main steam control and feedwater flow regulating valves.

### Scaling

The LOFT facility was scaled to generic PWRs by maintaining the system and component coolant-volume-to-total-power ratio whenever possible (Ref. A.2.1). Inherent in scaling are some compromises of geometric similarity. Scaling compromises must be such as to not adversely affect the requirements for typicality, as defined in Table A.2.1, that must exist between the LOFT model and the generic PWR. The LOFT scale model of the generic 4-loop PWR that resulted is summarized in Table A.2.2 which contains comparisons of geometric and physical parameters between LOFT and commercial PWRs. The physical parameters listed are for nominal operating conditions in the Westinghouse 4-loop ZION PWR and in the LOFT PWR prior to the experiment designated L2-3. The values listed in Table A.2.2 indicate that the coolant volume-to-total core power ratio is not exactly the same between LOFT and ZION. The differences are due to design compromises that were made.

### Instrumentation

The LOFT facility is augmented with an extensive "experimental" measurements system in addition to the normal PWR instrument systems for reactor operation and control. State measurements of the coolant in the primary system provide the capability of following the redistribution of mass and energy in the primary coolant system following the initiation of a transient. Extensive thermal measurements in the nuclear core provide detailed information on the thermal response of the fuel cladding. Nuclear measurements in the core assist in

determining the initial or steady-state energy distribution. The philosophy followed on measurement locations in the nuclear core, as shown in Figure A.2.2, was to instrument one-half of the core on a circular symmetry basis with emphasis on the center fuel assembly. The intent is to permit determination of the thermal and mechanical effects of instrumentation on the fuel rods during post-irradiation analysis. Utilizing circular symmetry simplified the core structure by permitting identical fuel assemblies to be used in core locations 2, 4, 6, in locations 1 and 3, and in locations 7 and 9. Experimental measurements are also placed at other locations within the reactor vessel. The reactor vessel and a typical set of instruments for transient are shown in Figure A.2.5. Experimental measurements are also located on the ECC systems, the secondary coolant system, the pressure suppression system, and on components such as pumps, valves, and control rod drive mechanisms for mechanical operation measurements during a transient. Details of these instrument systems are contained in Reference A.2.2.

#### REFERENCES

- A.2-1 D. L. Reeder, "LOFT System and Test Description (5.5 ft Nuclear Core 1 LOCE's)," NUREG/CR-0247, TREE-1208, July 1978.
- A.2-2 L. J. Ybarrondo et al., "Examination of LOFT Scaling: 74-WA/HT-53," Proceedings of the 95th Winter Annual Meeting of the ASME, New York, New York, August 1974.

## LOFT INTEGRAL TEST FACILITY

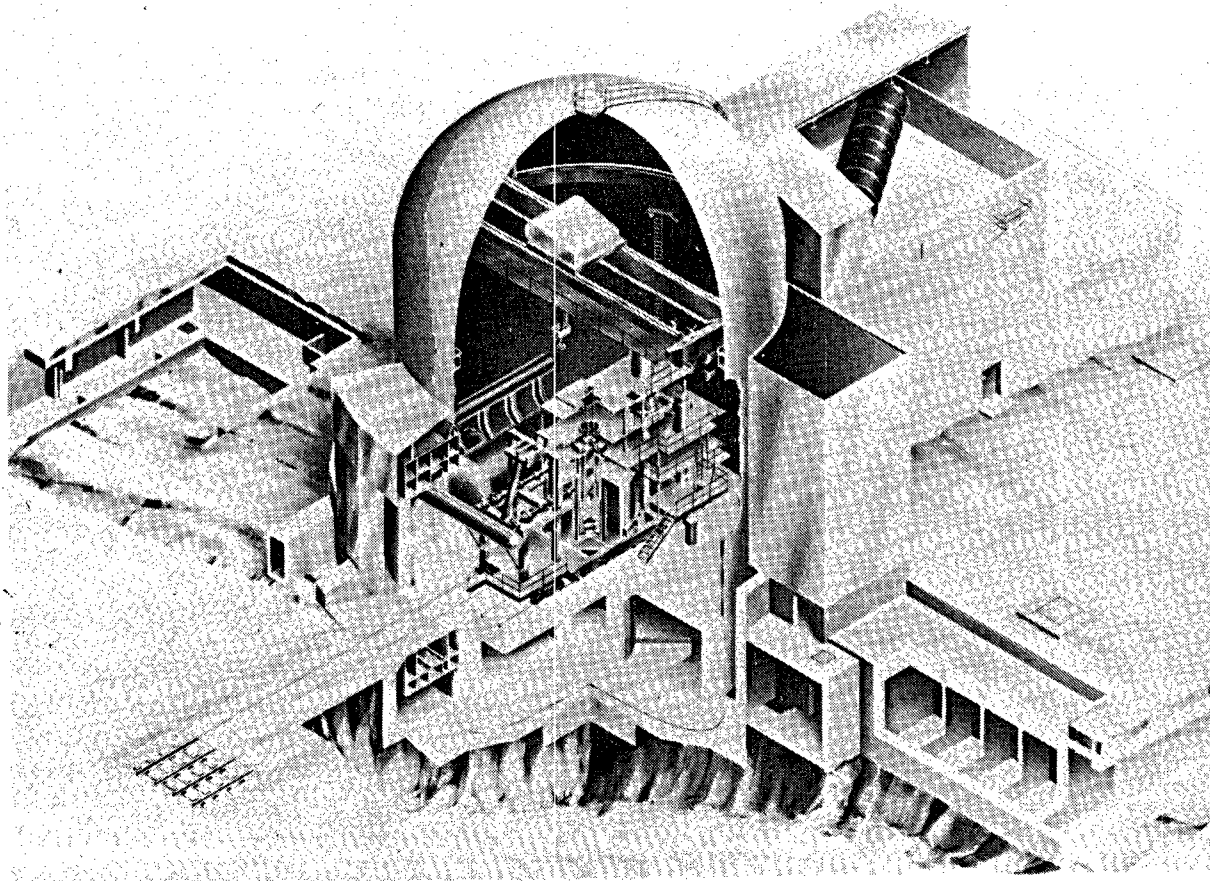


Figure A.2-1 Cutaway view of the LOFT Integral Test Facility

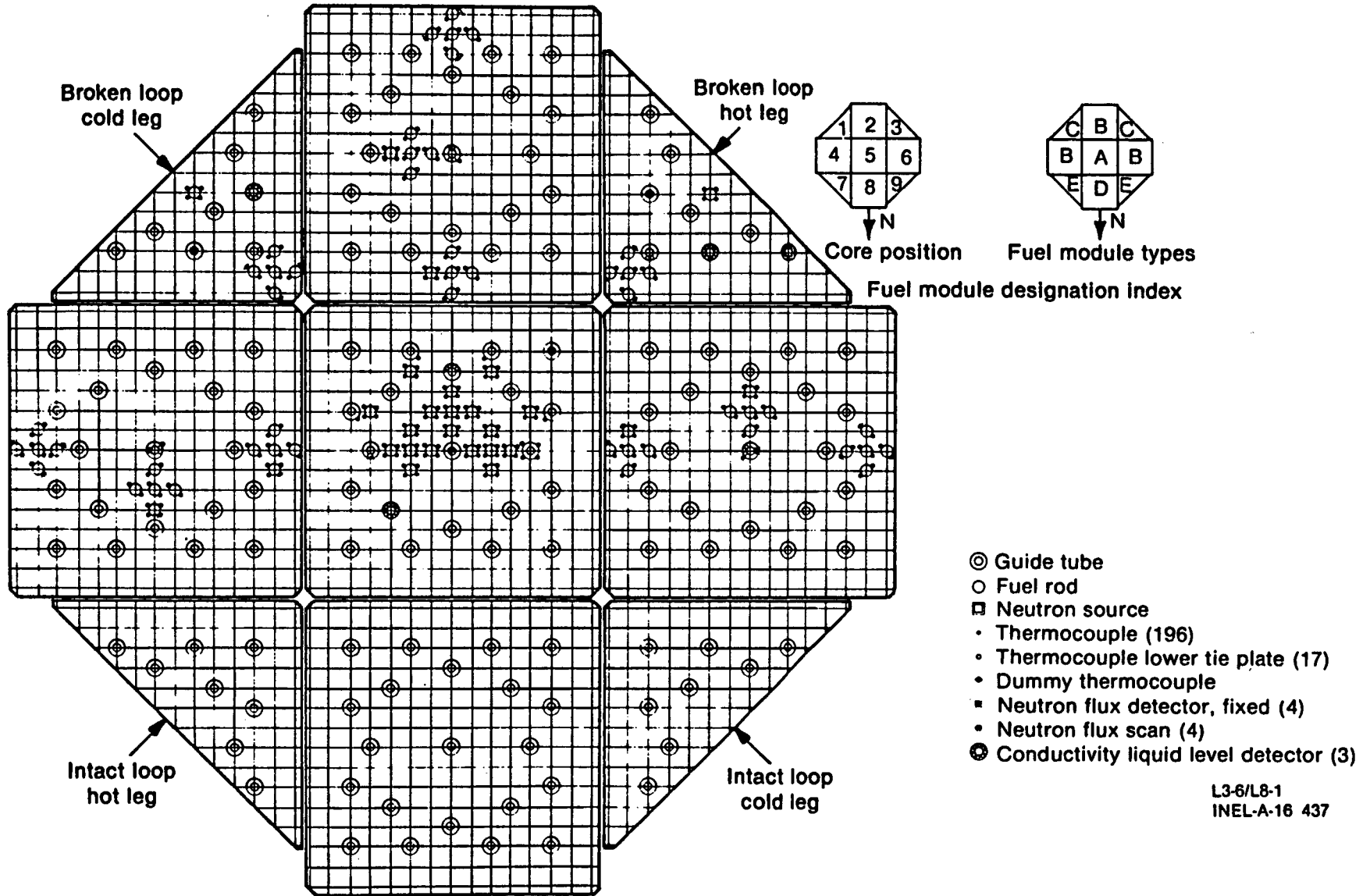


Figure A.2-2 LOFT core configuration and typical instrumentation

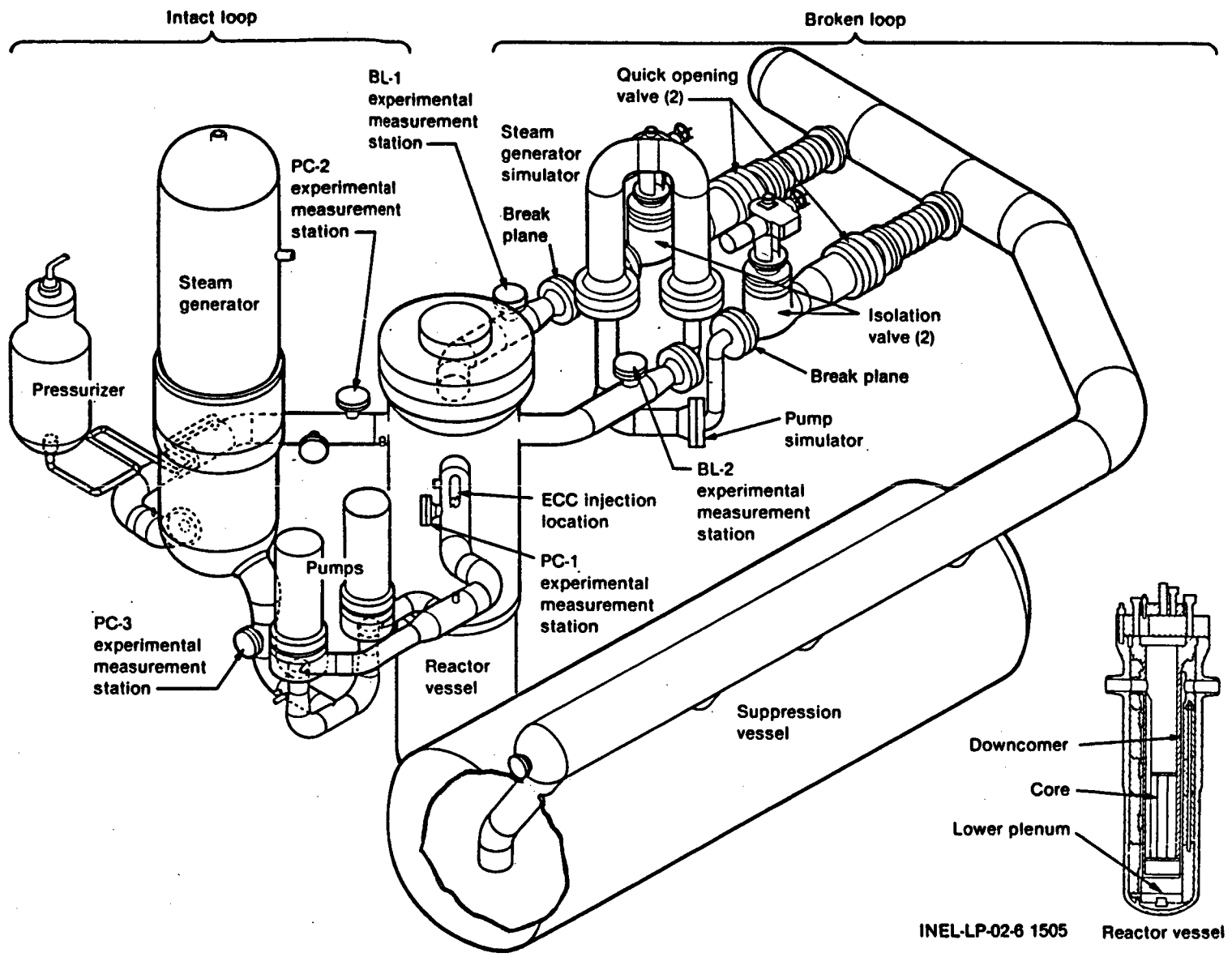


Figure A.2-3 The LOFT primary coolant system

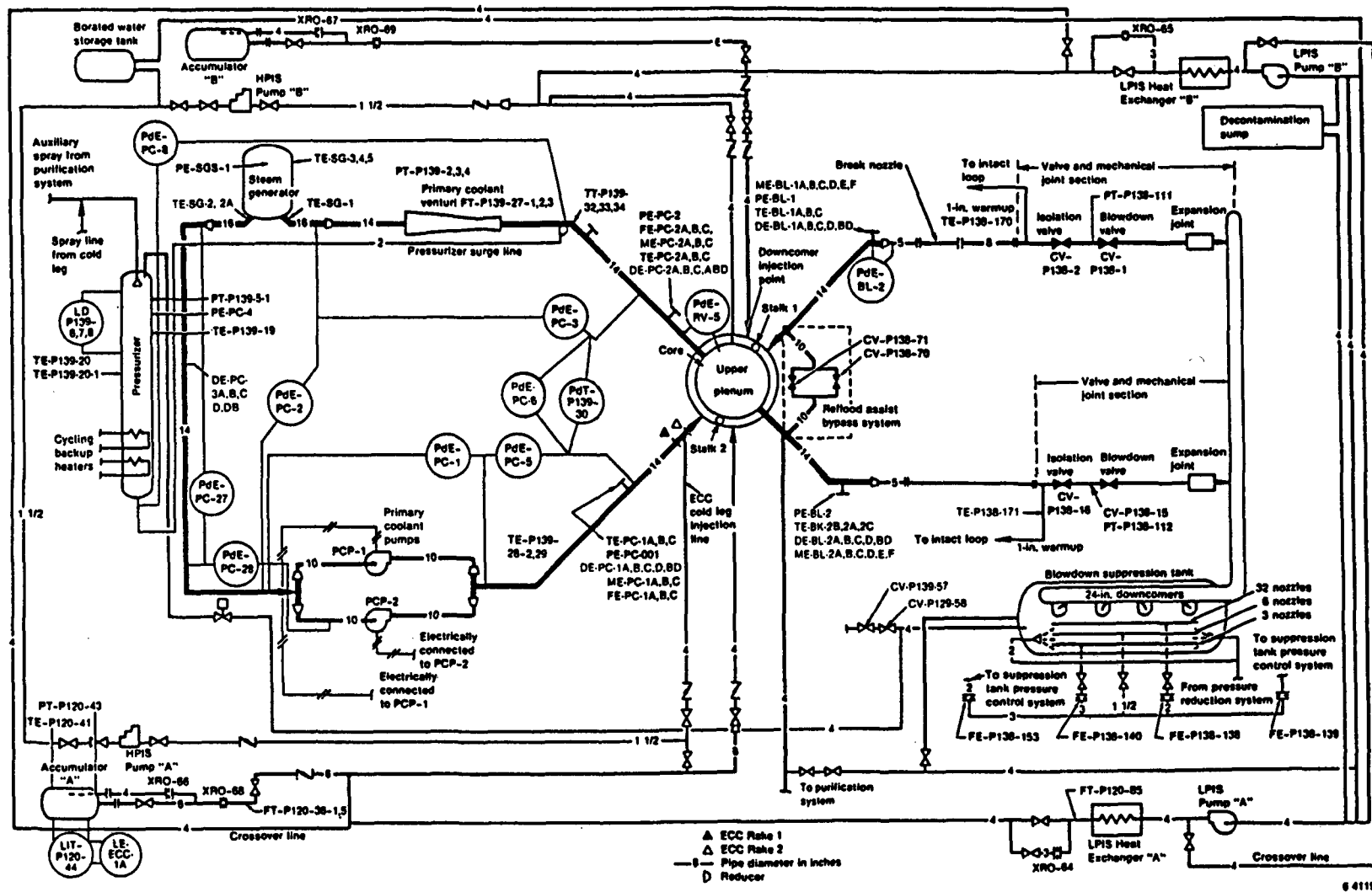


Figure A.2-4. LOFT ECCS Equipment Arrangement

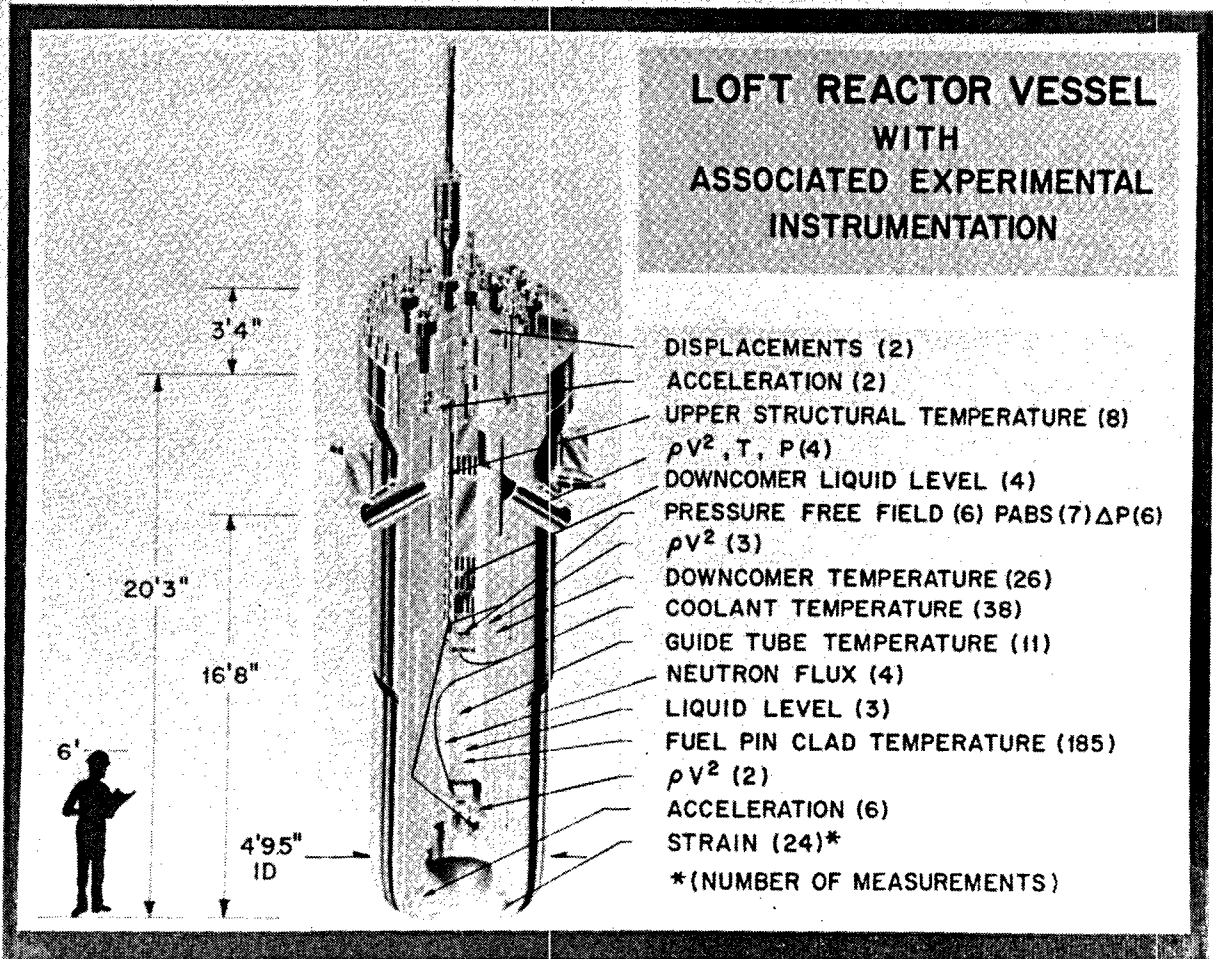


Figure A.2-5 LOFT Reactor Vessel and Typical Instrumentation

Table A.2-1 PWR Typicality Requirements for the LOFT Model Design

Item	Reason
System volume to core power ratio	Distribution of energy
Break area to system volume ratio	Depressurization and event time similarities
Length-to-diameter ratios (system resistance)	Pressure drop balance
Elevations	Pressure distribution (reflood)
Surface area to volume ratios	Heat transfer distribution
Core power distribution	Thermal response

Table A.2-2 LOFT - Commercial PWR Comparisons

Item	LOFT		TROJAN	
	Volume (m <sup>3</sup> )	% Total	% Total	Volume (m <sup>3</sup> )
Reactor Vessel				
Outlet Plenum	0.95	12.51	15.95	55.47
Core and Bypass	0.31	4.12	7.50	26.05
Lower Plenum	0.71	9.32	8.58	29.73
Downcomer and Inlet Annulus	0.69	<u>9.00</u>	<u>5.89</u>	20.42
Subtotal		34.95	37.92	
Intact Loop <sup>a</sup>				
Hot Leg Pipe	0.35	4.60	1.94	6.71
Cold Leg Pipe	0.37	4.85	2.08	7.22
Pump suction Pipe	0.33	4.38	3.09	10.70
Steam generator	1.45	18.97	26.40	94.49
Pump	0.20	<u>2.60</u>	<u>1.96</u>	6.80
Subtotal		35.40	35.47	
Broken Loop				
Cold Leg to Break <sup>b</sup> Vessel to Steam Generator	0.16	2.16	1.72	5.97
Steam Generator	0.15	1.98	0.65	2.24
Pump	0.52	6.88	8.80	30.50
Additional Volume Part of Outlet Plenum	0.05	0.72	0.65	2.27
Additional Volume Part of Inlet Plenum	0.19	2.46	N/A	N/A
Subtotal	0.22	<u>2.83</u>	<u>N/A</u>	N/A
Pressurizer	0.96	12.62	14.79	50.97
Total	7.63	100.00	100.00	349.54

Table A.2-2 (Continued)

Item	LOFT	ZION
Fuel rod number	1300	39372
Length (m)	1.68	3.68
Inlet flow area (m <sup>2</sup> )	0.16	4.96
Coolant volume (m <sup>3</sup> )	0.295	20.227
Maximum linear heat generation rate	39.4	39.4
Coolant temperature rise (K)	32.2	32.2
Power (MW)	36.7	3540.5
Peaking factor	2.34	1.60
Power/coolant volume (MW/m <sup>3</sup> )	124.4	175.0
Core volume/system volume	0.038	0.057
Mass flux (kg/s-m <sup>2</sup> )	1248.8	3707.3
Core mass flow/system volume (kg/s-m <sup>3</sup> )	25.6	51.7

<sup>a</sup>TROJAN values are for three loops combined.

<sup>b</sup>Includes pump suction piping.

### A.3 LOOP BLOWDOWN INVESTIGATION FACILITY

The Loop Blowdown Investigation (LOBI) facility is a high-pressure integral system test facility. LOBI research is conducted under a research and development contract between the Bundesminister für Forschung and Technologie, Bonn, and the Commission of European Communities. The facility is located at the Euratom Joint Research Center in Ispra, Italy.

The purpose of the original LOBI facility was to investigate the transient thermal-hydraulic behavior of a simulated primary cooling system during LOCAs covering the blowdown and the initial part of the refill phase and to simulate LOCAs caused by a pipe rupture within the primary cooling system. The results are also used to check and improve blowdown computer codes and associated analytical models used for the safety analysis of LWRs.

#### Facility Design and Operating Parameters

The facility simulates the primary and secondary system of a four-loop 1300-MW(e) PWR, primarily of German design (Ref. A.3-1). Pipe ruptures of various sizes ranging from double-ended large breaks to single-ended small leaks, may be simulated at three different locations within the broken loop (hot leg, cold leg, and pump suction); capability is also provided for simulating other rupture locations in the lower plenum of the reactor pressure vessel and in the steam generator U-tubes.

The facility was designed for a primary system pressure of 160 bars (2300 psi) and a temperature of 325°C (615°F). The system consists of two primary cooling loops connected to a reactor vessel (Fig. A.3-1). Both loops are fully active, each containing a radial circulation pump and a steam generator. One loop (an intact loop) has three times the capacity (of water volume and mass flow) of the other loop (single or broken). The reactor core is simulated by a bundle of 64 heater rods (hollow tubes) in an 8 by 8 array, which are uniformly heated over the bundle cross section.

Heat is removed from the steam generators by an active secondary cooling circuit containing two condensers and a cooler (simulating the heat sink provided by the turbines and condensers in the real plant) and a feedwater circulation pump. The nominal operating conditions of the secondary circuit are 54 bars (780 psi) and 270°C (520°F); this may be extended to about 80 bars (1160 psi) and the corresponding saturation temperature of 295°C (565°F).

Only the intermediate-pressure (up to 60 bars or 880 psi) accumulator portion of an ECCS was included in the original LOBI facility. This system provides ECCS water for both cold leg and combined cold and hot leg injection into both test loops.

The process control system allows the simulation of both the reactor pump behavior, by controlling the speeds of the PCS pumps, and the fuel decay heat and stored heat, by controlling the power input to the heater rod bundle during the transient.

### Facility Scaling Criteria

A scaling factor of 712 has been applied to the thermal power, coolant mass flow, and coolant volume of the primary coolant system of the reference plant. The values for the LOBI facility are then:

1. A heating power of 5.3 MW supplied to the 64 heater rod bundle of 1:1 PWR size,
2. A coolant mass flow of up to 21 kg/s for the intact loop and 7 kg/s for the broken loop, resulting in 28 kg/s core mass flow, and
3. A coolant volume of 0.82 m<sup>3</sup> within the primary loop system (pressurizer included) with a 50-mm downcomer gap width; a configuration with a 12-mm gap is also used. (Correct volumetric scaling would indicate a 7-mm gap, but this was not done to avoid CCFL and other problems resulting from LOBI's small size.)

Design of the experimental primary loops and the individual components was such that the following are as close as possible to the corresponding value in the reference plant:

1. Ratio of power to volume,
2. Ratio of the volume of various components and pipework sections to each other,
3. Ratio of rupture size to PCS volume, and
4. Single-phase pressure drop and temperature distribution along the flow paths.

For the pipework within each loop, these criteria led to a reduced length and a relatively too large diameter. As a consequence, the single-phase steady-state coolant velocity and mass flux are reduced by about a factor of 2 with respect to the reference plant.

The height above floor level and the height (elevation) relative to other components are scaled 1:1 relative to the reference plant, thus preserving gravitational pressures. The heat transfer surfaces (rod bundle and steam generators) are full length.

### LOBI-MOD2 Modifications

A thorough review of the small-break experiment program performed in the second half of 1979 after the Three Mile Island accident revealed the need for several modifications of the test facility so it could handle special requirements of small-break experiments. As a result of this review, the LOBI facility was modified to accommodate several new design features (Ref. A.1-2).

A new reactor pressure vessel model contains additional differential pressure measurements. From these, the following may be obtained: the individual collapsed levels, the overall collapsed level, the void fraction distribution, and possibly the bubble rise velocity within the bundle region.

New steam generators with the following characteristics were installed:

1. A much more detailed and accurate (to within 6%) volume scaling within the various regions of both the primary and secondary sides,
2. A 1:1 scaling of various volume ratios within and between both primary and secondary sides, and
3. A 1:1 scaling of all heights between the centerline of the main coolant piping and the lowest U-tube bend.

Preservation of the height above the highest U-tube bend and the height within the steam dome was not considered necessary because gravitational pressure heads are not present within this region. A throttling device installed in the downcomer allows the adjustment of the internal recirculation ratio.

Extensive instrumentation includes thermocouples on the inside and outside of the U-tubes and differential pressure measurements on the primary and secondary side. These measurements allow a local determination of the fluid flow and heat transfer conditions.

A high-pressure injection system (HPIS) was added to the primary cooling system as part of the ECCS. It consists of a positive displacement pump with a special speed control device for pressure and flow rate variation and a flooding tank and injection lines connected to the already existing ones for the accumulators. Throttling devices have been installed in the injection lines to provide a 1:3 subdivision of the injection rate between the broken and intact loops.

The secondary cooling circuit was modified by installing shutoff valves in the steam lines and feedwater lines to allow isolation of the steam generator secondary side and pressure relief valves in the steam lines to allow blowdown of the steam generator secondary side. An auxiliary feedwater system was added to the secondary cooling circuit. It consists of a storage tank and two positive displacement pumps (one for each steam generator) with special speed control devices and corresponding injection lines.

### Test Program

The LOBI test program (Ref. A.3-1) included 28 tests, 25 of which are summarized in Table A.3-1, and 3 of which were small-break scoping tests. Fourteen tests were performed with a 50-mm downcomer gap width and 14 with a 12-mm gap width.

The first six tests were 2 x 100% cold leg breaks performed with the 50-mm gap width. These tests were aimed at establishing the final nominal heating power time function and investigating the effect of different ECCS injection modes.

The next three tests were scoping tests (SD or "shakedown" tests) to establish facility specification criteria for modifications to be made for small break testing. These tests were 10, 1, and 0.4% single-ended cold leg breaks.

Five additional tests were performed before installation of the 12-mm gap width. These interim tests investigated the effects of break geometry, break size, and reproducibility for 1 x 25%, 1 x 50%, 2 x 50%, and 1 x 100% cold leg breaks.

Fourteen large- and medium-break tests were performed with the 12-mm gap width for investigating the effects of pump operation, ECCS injection mode and rate, break geometry and size, downcomer gap width, and heating power input. Breaks varied from 1 x 25% to 2 x 100% in the cold leg, hot leg, and pump suction.

### LOBI-MOD2 Test Program

The LOBI-MOD2 plan includes additional loss-of-coolant experiments and special transient experiments (Ref. A.3-2, -3).

The LOCA experiments will be subdivided into two phases. The first phase will continue with 16 small- and intermediate-break tests. These tests cover a break size spectrum ranging from 0.4% to 10% and include two quasi-steady-state natural circulation tests. Priority has been assigned to 8 of the 12 tests (Table A.3-2).

The objectives of these 16 tests are:

1. To investigate the natural circulation characteristics of the primary coolant system, particularly with respect to heat transport performances between reactor and steam generators, under single- and two-phase flow conditions,
2. To establish mixture levels due to phase separation and study their behavior as a function of break location and size and of pump operation mode, and
3. To determine the heat removal characteristics of both the steam generator secondary side and the secondary loop system, which may be operated in different modes according to reactor plant type and the safety and emergency system operation mode applied by the utility.

The LOBI-MOD2 facility commissioning program includes pressure drop and environmental heat loss measurement tests and a large-break "link test." One of the early LOBI-MOD2 tests will be a 1% cold leg break test, which has been designated for OECD-CSNI International Standard Problem (ISP) No. 18.

The tests to be performed during the second phase have not been finally defined. Although the break size to be simulated with these tests will again cover the whole range of interest, emphasis will be placed on small- and intermediate-size breaks.

The special transient experiments program proposed for LOBI-MOD2 is aimed at the investigation of whole plant behavior resulting from the class of intact circuit faults referred to as special transients. The recent modifications and the overall scaling concept make LOBI-MOD2 well suited for a variety of special transients. In the experiment program, emphasis will be placed on the simulation of key phenomena governing the course of the transient. The preliminary

test matrix consists of 11 tests, 6 short-term (e.g., station blackout ATWS) and 5 long-term (e.g., loss-of-feedwater) transients. For each transient, key phenomena have been identified (Table A.3-3). Three scoping test have been selected to provide initial experiment results, which, together with results of survey calculations, will form the basis for establishing the final test matrix.

#### REFERENCES

- A.3-1 W. L. Riebold and H. Staedtke, "LOBI-Influence of PWR Primary Loops on Blowdown: First Results," NUREG/CP-0024, Proceedings of the 9th Water Reactor Safety Research Information Meeting at Gaithersburg, Md., October 26-30, 1981.
- A.3-2 W. L. Riebold, L. Piplies, and H. Staedtke, "LOBI Experimental Programme Results and Plants: Status Sept. 1982," NUREG/CP-0041, Proceedings of the 10th Water Reactor Safety Research Information Meeting at Gaithersburg, Md., October 12-15, 1982.
- A.3-3 W. L. Riebold, C. Adabbo, L. Piplies, and J. Sanders, "Some Salient Results of LOBI Tests, and Programme Plans for LOBI-MOD2 Facility," NUREG/CP-0048, Proceedings of the 11th Water Reactor Safety Research Information Meeting at Gaithersburg, Md., October 24-28, 1983.

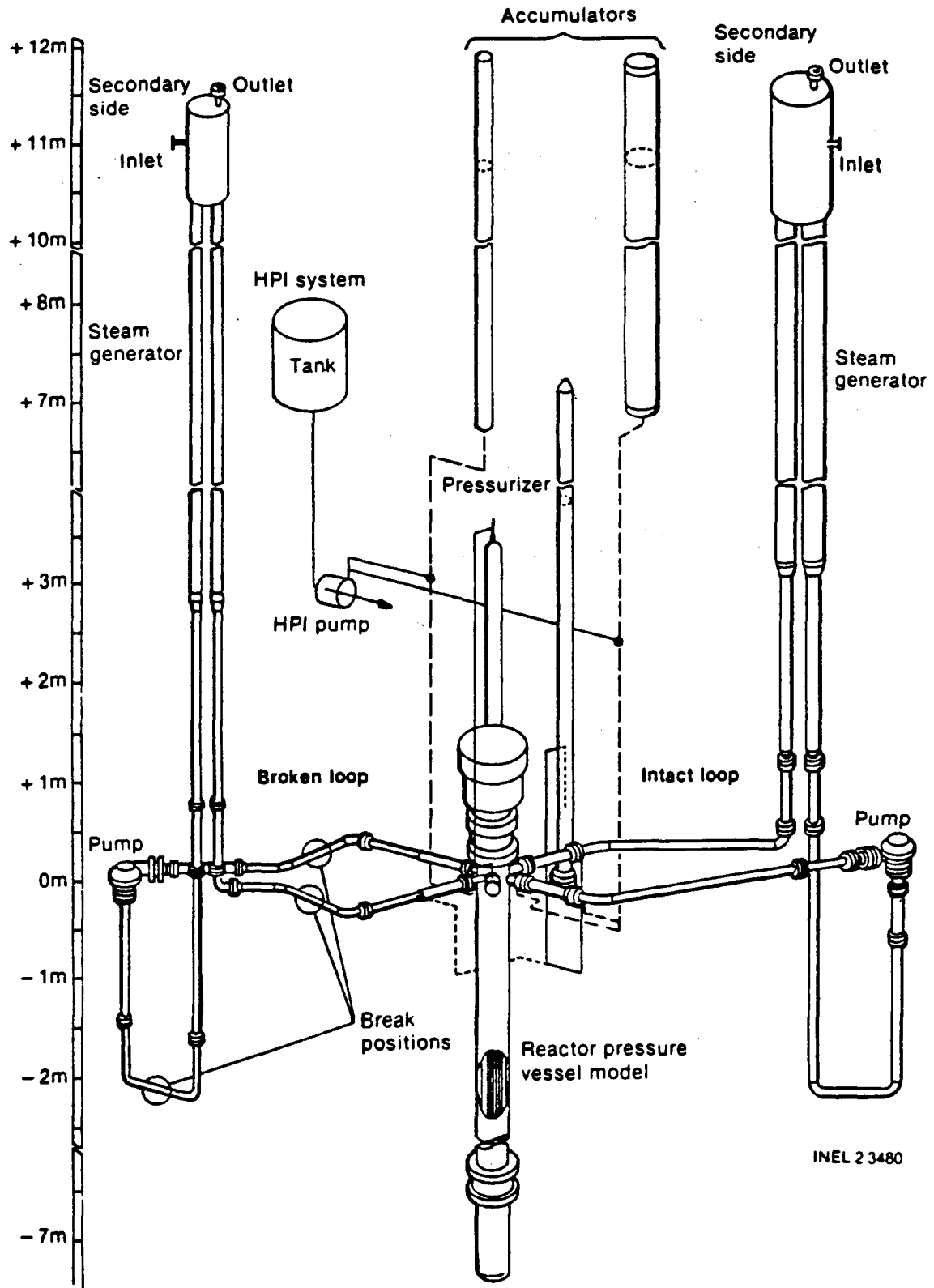


Figure A.3-1 LOBI test facility

Table A.3-1 LOBI large-break tests (1980-1982)

BREAK LOCATION		BREAK SIZE										ECC INJECTION MODE
		2 x 1A		2 x 0.5A		1 x 1A		1 x 0.5A		1 x 0.25A		
		A1-04 A1-04R	A1-66	B-101	B-222	A2-58 A2-59R		A2-55		B-RIM		
COLD												COLD LEG INJ.
LEG	A1-01 A1-02 A1-03 A1-05	A1-72 A1-74				A1-69		A1-68		A1-67		COMBINED INJECT.
		A1-07										NO INJECT.
PUMP SUCTION												COLD LEG INJ.
LEG		A1-70										COMBINED INJECT.
HOT				B-302								COLD LEG INJ.
LEG		A1-10A A1-10B								A1-73		COMBINED INJECT.
		50	12	50	12	50	12	50	12	50	12	
DOWNCOMER GAP WIDTH (MM)												

Table A.3-2 LOBI small-break A1-tests preliminary (1983-198 )

BREAK LOCATION		BREAK SIZE										ACCUMULATION INJECTION MODE
		1 x 0.1A		1 x 0.02A		1 x 0.01A		1 x 0.004A				
			BL-04			A1-82	A2-81 BL-06 BL-08	A1-80 A1-88		BL-10		
Cold												Off
Leg	A1-83			A1-78 A1-79 A1-89					BL-16			Combined Inject.
Pressurizer								A1-85				Off
Relief Valve											BL-18	Cold Leg
Hot									BL-07		BL-26	Cold Leg
Leg	A1-84			A1-86 BL-09								Combined Inject.
		H.L.	C.L.	H.L.	C.L.	H.L.	C.L.	H.L.	C.L.	H.L.	C.L.	
HPIS INJECTION LOCATION												

Table A.3-3 LOBI special transient experiment program

Preliminary list; Transients tests and key phenomena ( ● = phenomenon expected).

Phenomena	Short-Term Transients						Long-Term Transients				
	1	2	3	4	5	6	7	8	9	10	11
	LOFW/ATWS	Station Blackout ATWS	Loss of Heatsink ATWS & non ATWS	One loop steam line isolation, valve fails in closed position	Steam line break PTS	100% Steam line break	LOFW	LOFW, Natural Circulation	Cool down with isolated SG with and without pumps	LOFW + LOAF + Open PORV, with Safety Injection	U-Tube Rupture
Surge Line Thermohydraulics	●	●	●	●	●	●	●	●		●	
Pressurizer fluid and Thermohydraulics	●	●	●	●	●	●	●	●	●	●	●
Steam Generators	Primary TH	●	●	●	●	●	●	●	●	●	●
	Secondary TH	●	●	●	●	●	●	●	●	●	●
Pump Behavior	●	●	●				●	●		●	●
Natural Circul. (inc. Interruption)	Single Phase		●				●	●	●	●	●
	Two Phase		●				●	●	●	●	●
Non-condensable Gases		●					●	●		●	●
Spatial Flow and Temperature Dist.					●	●			●	●	
Core TH (inc. uncover)	●	●	●	●	●	●	●	●	●	●	●
Scoping Test Proposals	●						●		●		
Test Date	Oct 1987	Mar 1985			Jan 1986	June 1987	Nov 1985		1988	May 1987	Jan 1987

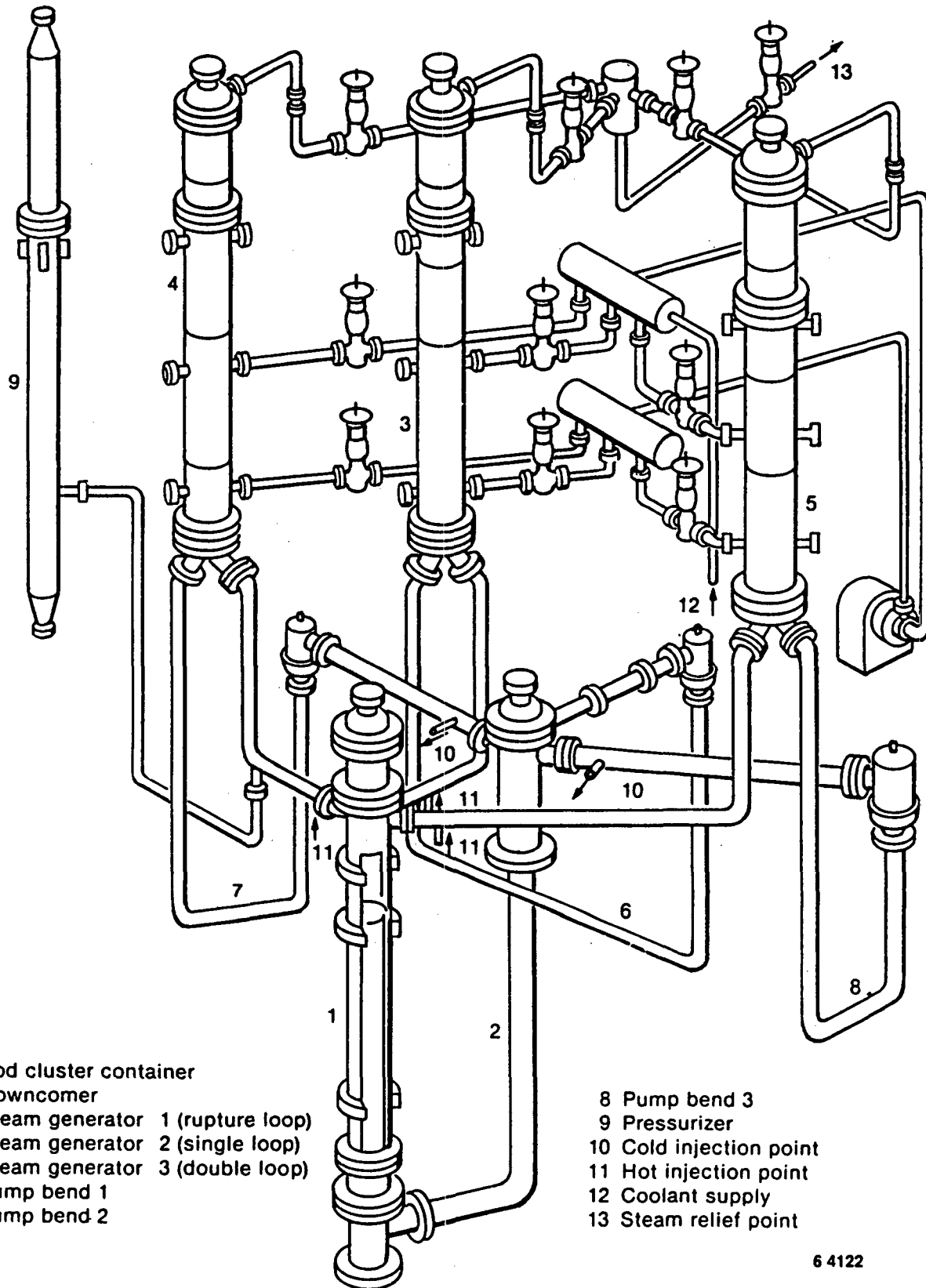
#### A.4 PRIMÄRKREISLÄUFE

The Primärkreisläufe (PKL) test facility, operational since 1977, is located in Erlangen, West Germany, and supported by the German Ministry for Research and Technology. The overall arrangement of the PKL is shown in Figure A.4-1. The design of this facility is similar to the design of the reactor core and primary loops of a typical 1300 MWe German PWR and simulates the essential components of the primary system with respect to their thermal-hydraulic effect.

The facility models a four-loop PWR on a 1:134 scale with three loops: a double intact loop, a single intact loop, and a single loop equipped to model a large break. Each loop contains a pump resistance simulator and a steam generator simulator. The primary pressure vessel houses a lower plenum, core, and upper plenum (Figure A.4-2). Several cores have been used over the life of the facility. The first core, which is typical, has a fuel rod simulation bundle consisting of 340 rods, 337 of which are electrically heated (Figure A.4-3). The vessel includes an internal downcomer, but it was sealed off from the core and lower plenum and connected to the upper plenum by a pressure equalization line. The testing utilized an external downcomer scaled to simulate PWR flow characteristics more accurately (see Figure A.4-1). The cross sections and lengths of the primary loop piping have been designed so that pressure losses are approximately equal to those arising in corresponding lines in the reactor facility. All elevations were designed to correspond to actual reactor dimensions. Table A.4-1 summarizes major features of the PKL.

Originally PKL was designed to examine the refill and reflood phases of large-break LOCAs but it was modified in 1980 to model small-break experiments by adding a heated pressurizer on the hot leg of the single intact loop and by refining the steam generator secondary sides. The small-break experiments focus on the role of steam generators as heat sinks because small breaks require the removal of most of the core decay heat while secondary cooling is maintained. The most recent modification of PKL has allowed testing of the end-of-blowdown phase of a postulated large-break LOCA.



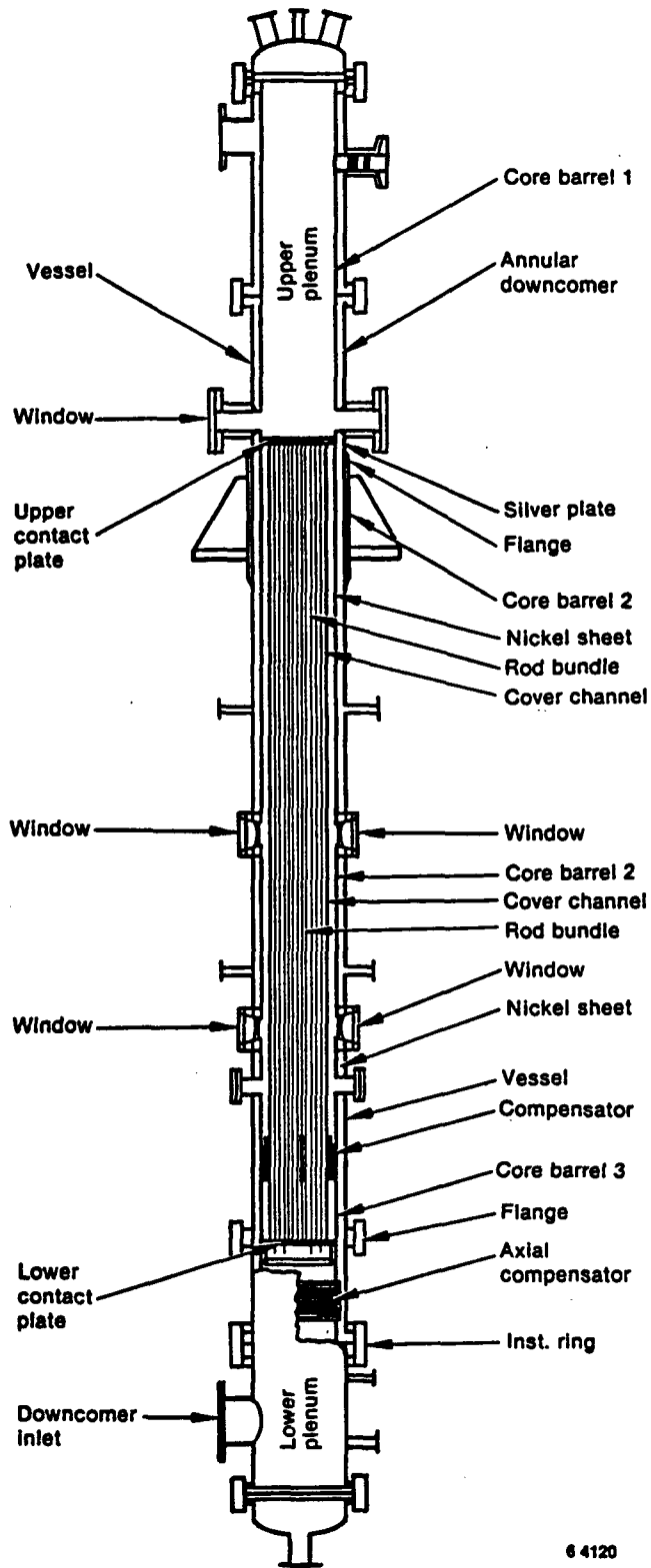


- 1 Rod cluster container
- 2 Downcomer
- 3 Steam generator 1 (rupture loop)
- 4 Steam generator 2 (single loop)
- 5 Steam generator 3 (double loop)
- 6 Pump bend 1
- 7 Pump bend 2

- 8 Pump bend 3
- 9 Pressurizer
- 10 Cold injection point
- 11 Hot injection point
- 12 Coolant supply
- 13 Steam relief point

6 4122

Figure A.4-1 Primärkreisläufe (PKL) test facility



6 4120

Figure A.4-2 Pressure vessel internals of the Primärkreisläufe (PKL) test facility

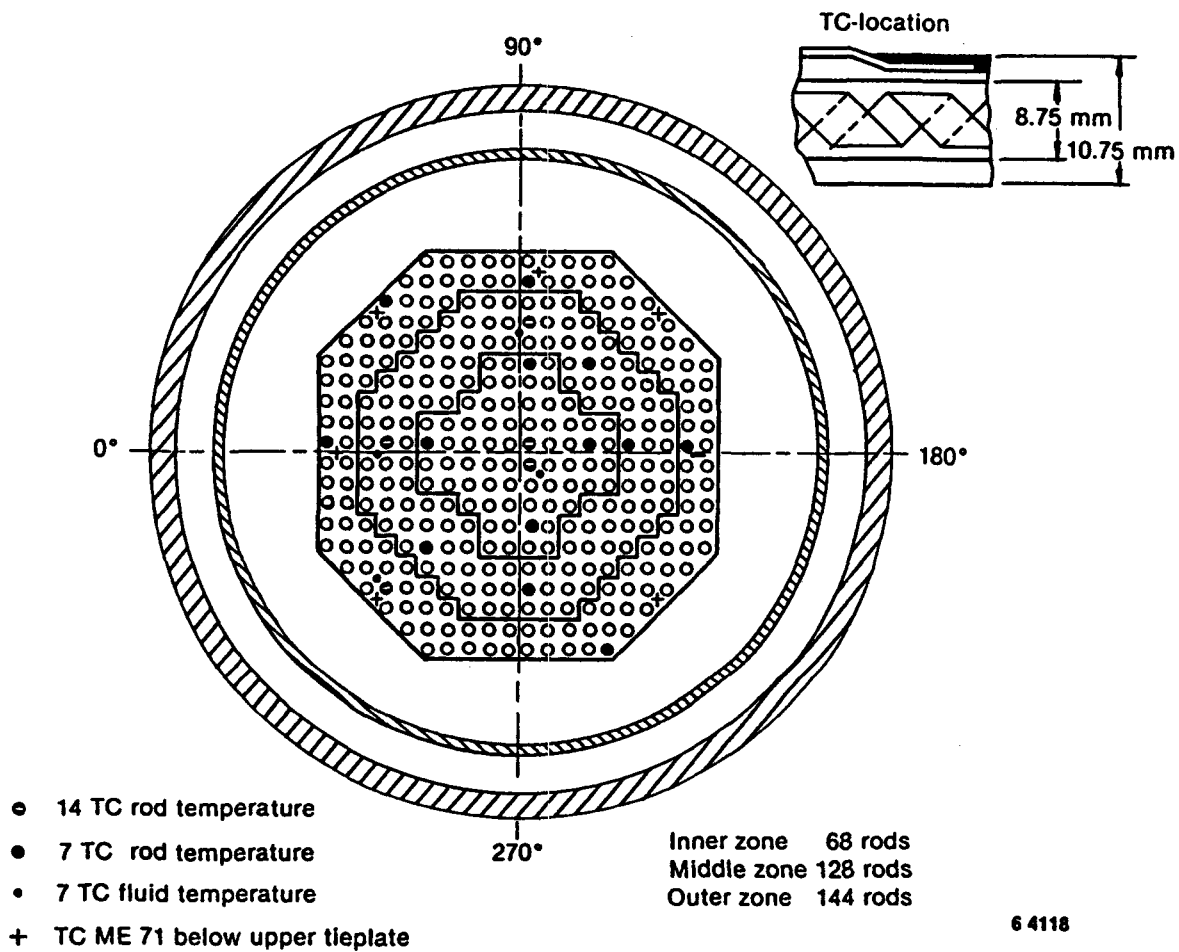


Figure A.4-3 Cross section of the PKL pressure vessel showing arrangement of electrically heated core rod simulators



## A.5 CYLINDRICAL CORE TEST FACILITY

The Cylindrical Core Test Facility (CCTF), operational since 1979, is located in Tokai, Japan, and is supported by the Japan Atomic Energy Research Institute (JAERI). The overall arrangement of the CCTF is shown in Figure A.5-1. The NRC provided advanced instrumentation for installation in the facility and computer code analysis support of the testing. CCTF is one of three test facilities included in the trilateral 2D/3D Program. (The other test facilities are the Slab Core Test Facility in Japan and the Upper Plenum Test Facility in Germany.) The CCTF is a full-height, scaled-cross-section model of an 1100 MWe PWR with four primary loops. The principal reference PWR is the Trojan Nuclear Generating Station, although certain aspects of the Ohi reactor in Japan are also incorporated. A schematic flow diagram for CCTF is shown in Figure A.5-2.

At the center of the CCTF facility is a full-height pressure vessel that houses a heated core and includes a downcomer as well as upper and lower plena (Figure A.5-3). The core contains 2048 rods, 1824 of which are electrically heated. The core is composed of 32 8 x 8 assemblies, arranged to obtain a roughly cylindrical array (Figure A.5-4). The pressure vessel and attached piping flow areas are based on the core area scaling ratio of 1/21.4 as compared to an 1100 MWe PWR. The pressure vessel downcomer annulus is 61.5 mm (2.42 inches) wide. This is larger than the width that results from an exact 1/21.4 scaling because the scaled core bypass area is included as part of the downcomer area. The annulus was further widened to offset the hot-wall effect. The upper plenum internals model those used in the reference plant but are reduced in size by the ratio of 8/15. This approach of using a larger number of internal structures that are smaller in size was chosen because the use of larger structures resulted in only a few structures in the upper plenum and hence in the possibility of strong asymmetries and unrealistic flow distributions. The smaller structures give a much more uniform and realistic flow distribution.

The four full-length primary loops include passive pump simulators and active steam generators, although the steam generator tubes are 25% shorter than those in a commercial reactor. Three of the loops are intact while the fourth loop is designed to allow for simulation of a full-size double-ended offset cold leg break about 2 meters from the vessel wall. Table A.5-1 summarizes major features of CCTF.

The CCTF was designed to simulate the thermal-hydraulic behavior of a commercial 1100 MWe PWR during the refill and reflood phases of a large-break LOCA with the break in the cold leg. The first series of experiments (Core I) was designed to investigate system thermal-hydraulics and core response during the reflood phase. The Core II testing included additional reflood tests as well as refill and performance evaluation test of alternative ECC systems. A second core was used because of the limited life cycle of the electric heater rods.

Table A.5-1 Summary of major features of CCTF

PRIMARY VESSEL

General

Height: 9.44 m  
 Inside Diameter: 1084mm  
 Downcomer Gap: 61.5 mm  
 Design Pressure: 6 bar  
 Design Temperature: 300°C

Downcomer

Area: 0.198 m<sup>2</sup>  
 Height (Bottom of LP  
 to Cold Leg Nozzle: 4849 mm

Lower Plenum

Volume: 1.38 m<sup>3</sup>  
 Structures: Extension of  
 Heater Rods

Core

No. heated/unheated  
 rods: 1824/224  
 Rod O.D.: 10.7 mm  
 Rod Pitch: 14.3 mm  
 Heated Length: 3660 mm  
 Axial Peaking Factor: 1.49

Upper Plenum

Volume: 2.04 m<sup>3</sup>  
 Structures: 8/15 Scale Simu-  
 lated Structures

PRIMARY LOOPS

Piping

No. Loops: 4  
 Hot Leg Flow Area: 0.019 m<sup>2</sup>  
 Cold Leg Flow Area: 0.019 m<sup>2</sup>

Pumps

No.: 4  
 Type: Resistance Simulator

Steam Generator

Number: 4  
 Type: U-Tube and Shell  
 No. Tubes: 158  
 Tube O.D./I.D.: 25.4/19.6 mm  
 Tube Length: 15.2 m  
 Secondary Pressure: 52 bar

Break

Location: Cold Leg, 2 m from Vessel  
 Type: 100% Offset

Pressurizer

No.: None  
 Location:

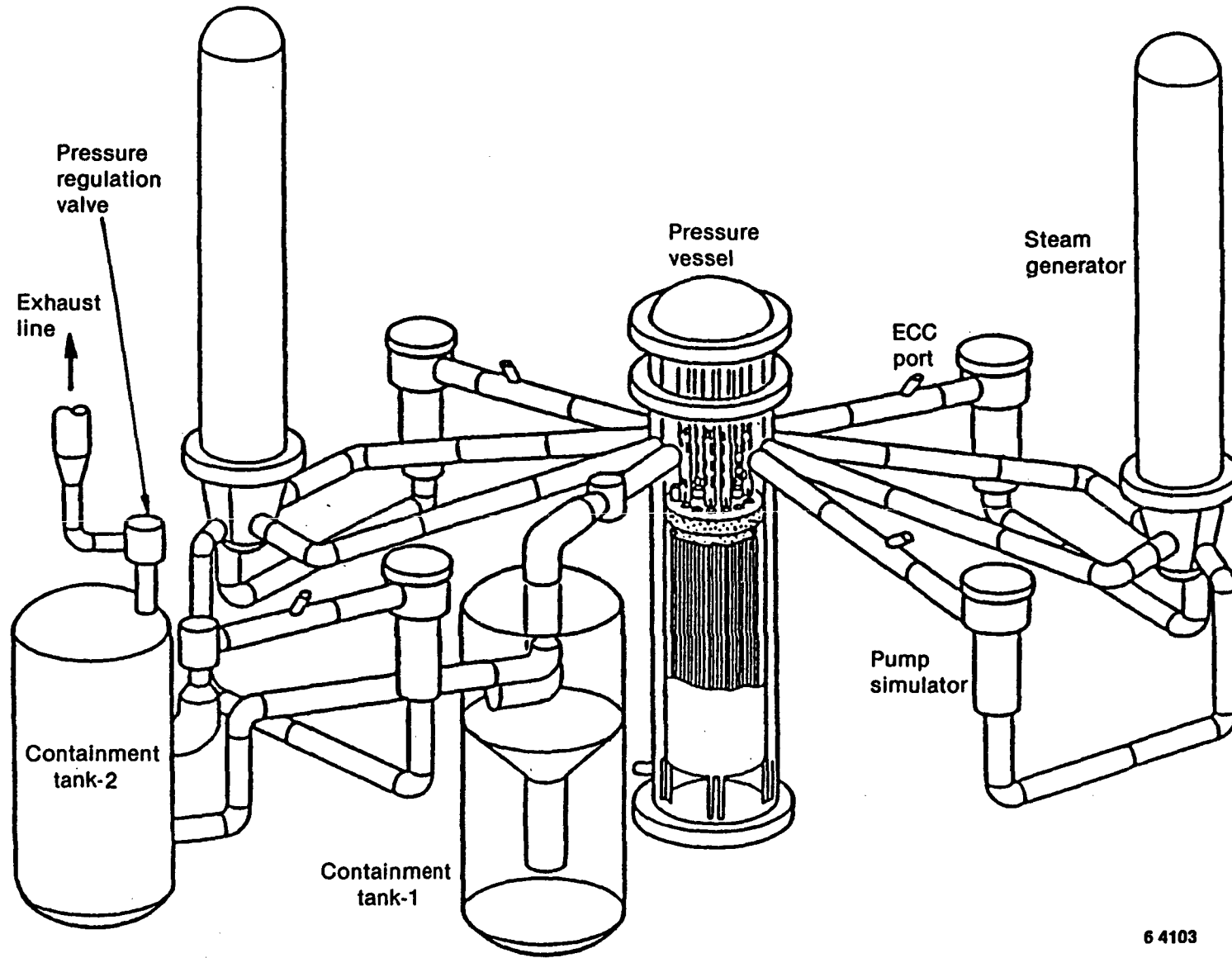
ECC SYSTEMS

Injection Locations

Cold Leg  
 Lower Plenum  
 Upper Plenum  
 Hot Leg  
 Downcomer

Injection Sources

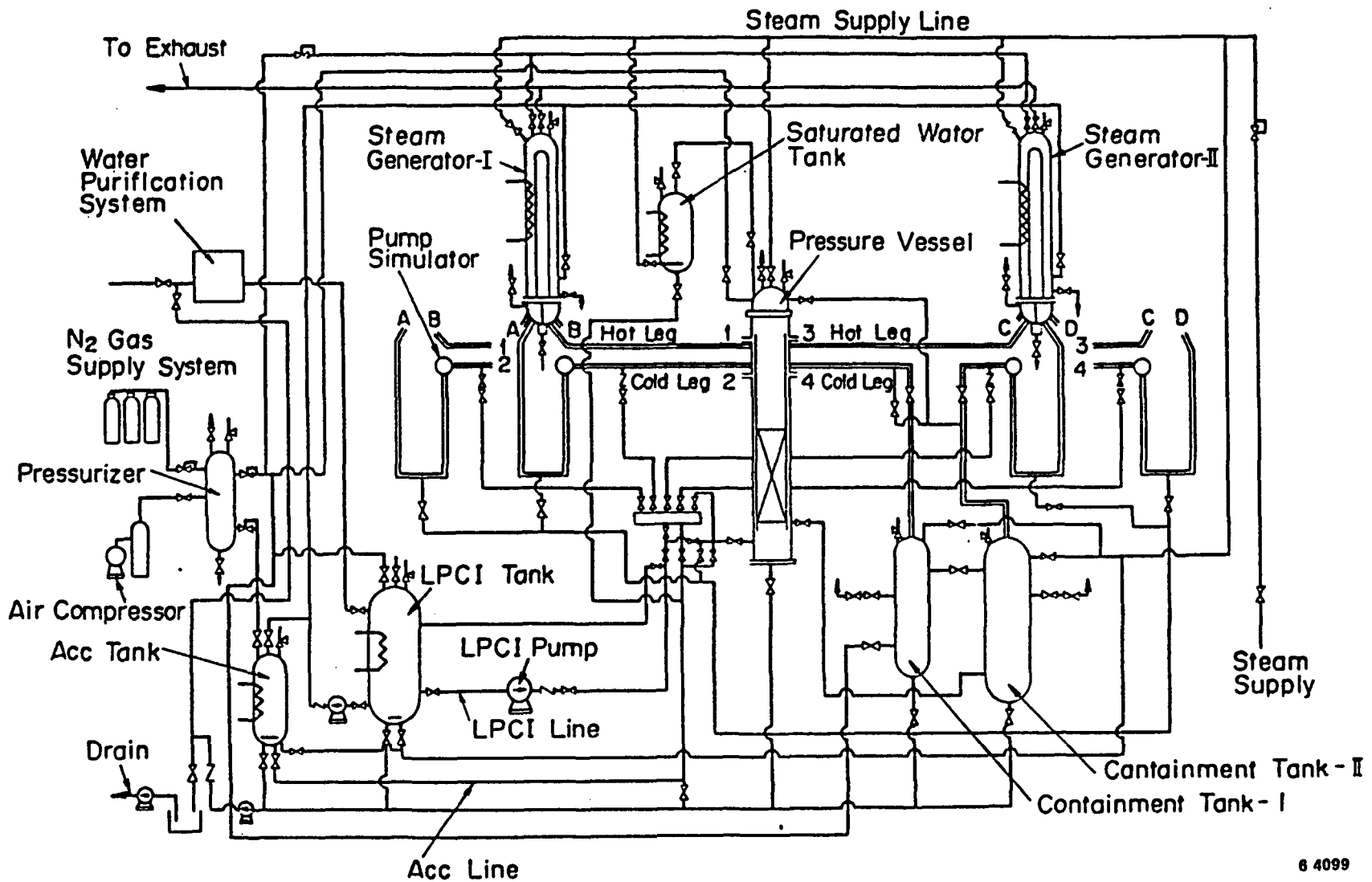
Accumulator  
 LPCI



6 4103

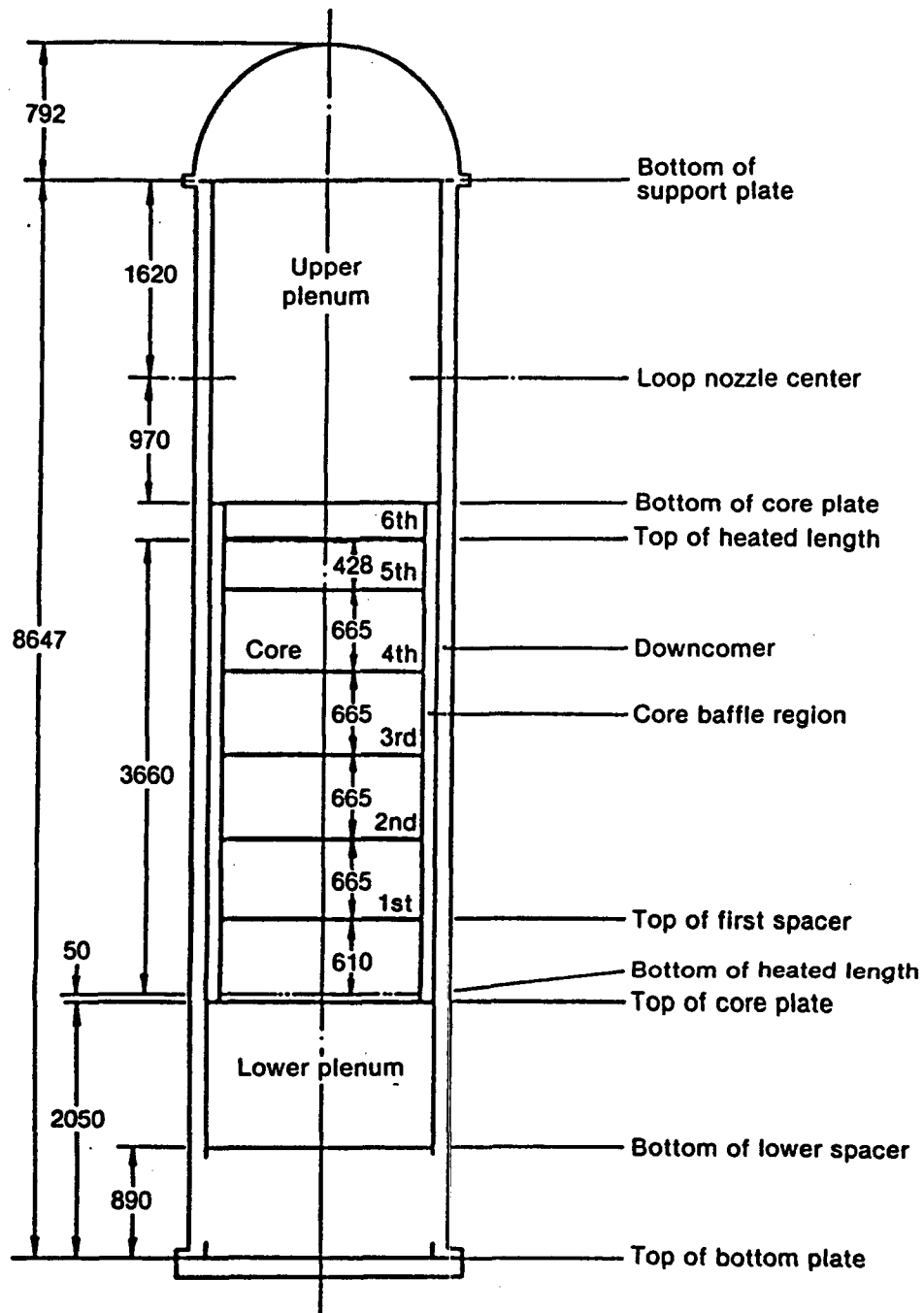
Figure A.5-1 Cylindrical Core Test Facility (CCTF)

A-44



6 4099

Figure A.5-2 Schematic diagram of Cylindrical Core Test Facility (CCTF)



6 4104

Figure A.5-3 Cylindrical Core Test Facility Core 1 pressure vessel

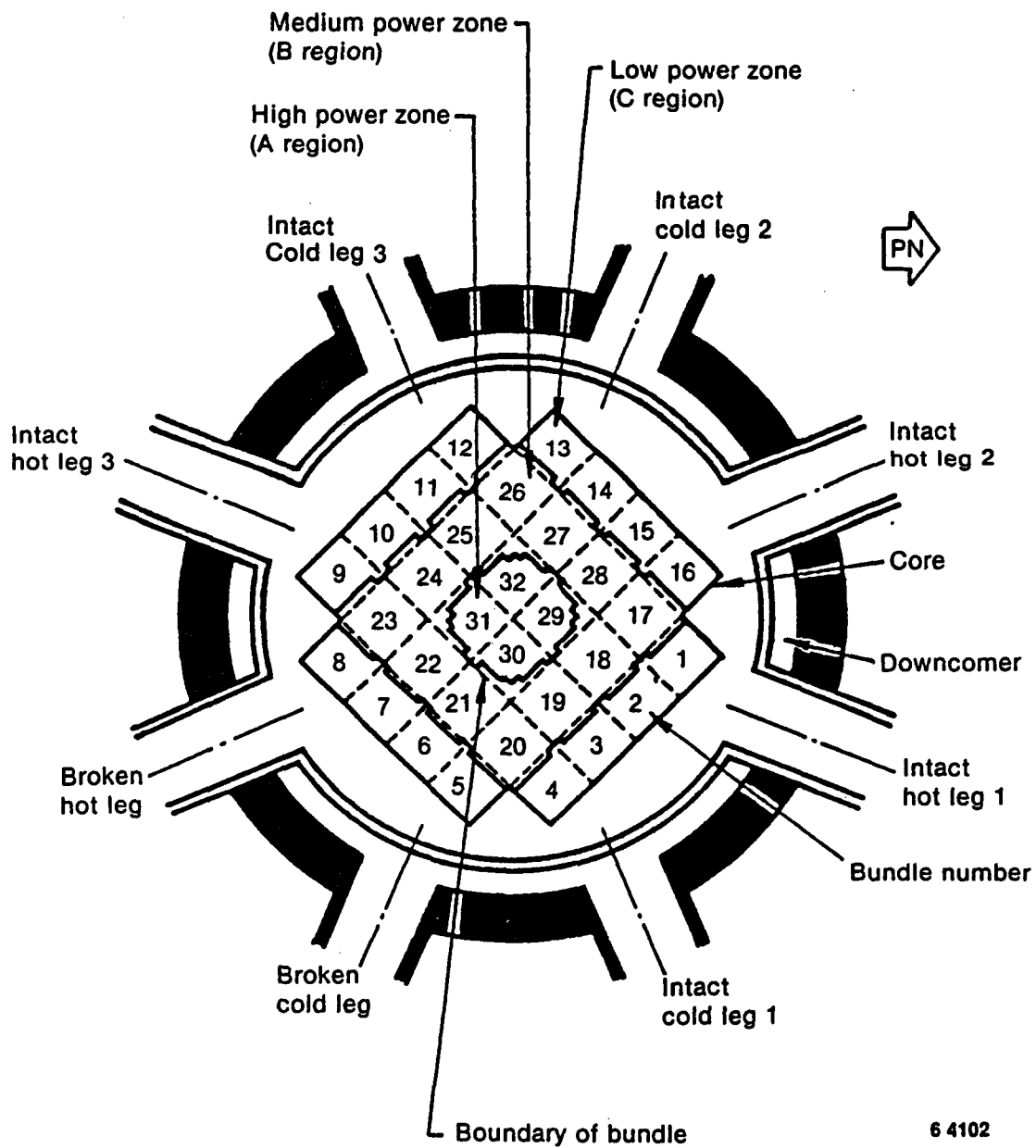


Figure A.5-4 Cross section of the CCTF pressure vessel through Core 1 core and primary loop nozzles

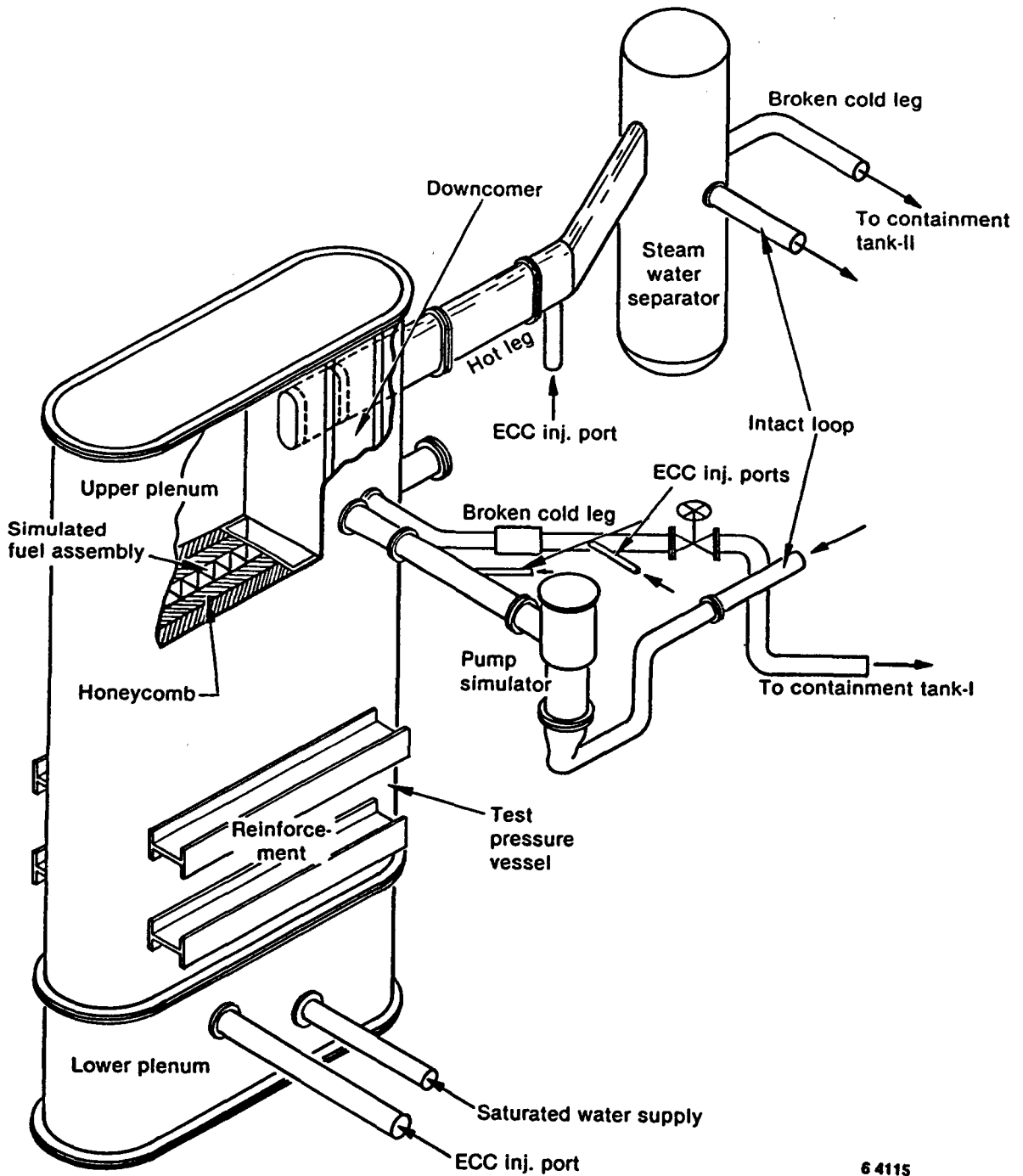
## A.6 SLAB CORE TEST FACILITY

The Slab Core Test Facility (SCTF), operational since 1981, is located in Tokai, Japan, and is supported by the Japan Atomic Energy Research Institute (JAERI). The arrangement of the SCTF is shown in Figure A.6-1. The NRC provided advanced two-phase flow instruments for installation in the facility and computer code analysis support of the testing. SCTF is one of three test facilities included in the trilateral 2D/3D Program. The reference PWR is the 4-loop 3300 Mwt Trojan reactor in the U.S.

The SCTF is provided with a full-height, full-radius, one-bundle-width, electrically heated core. The core consists of eight 16 x 16 fuel bundles arranged in a row to produce a slab core configuration, each bundle containing both heated and unheated rods (Figure A.6-2). There are a total of 1872 heated rods and 176 unheated rods. The downcomer is located at one end of the pressure vessel, which corresponds to the periphery of the actual reactor pressure vessel (Figure A.6-1). The upper plenum region contains 1/2-scale structures to simulate a PWR (Figure A.6-3). Half-scale structures were chosen to give a realistic flow path simulation in the upper plenum since it appeared that full-scale structures would result in nearly complete flow blockage at some points.

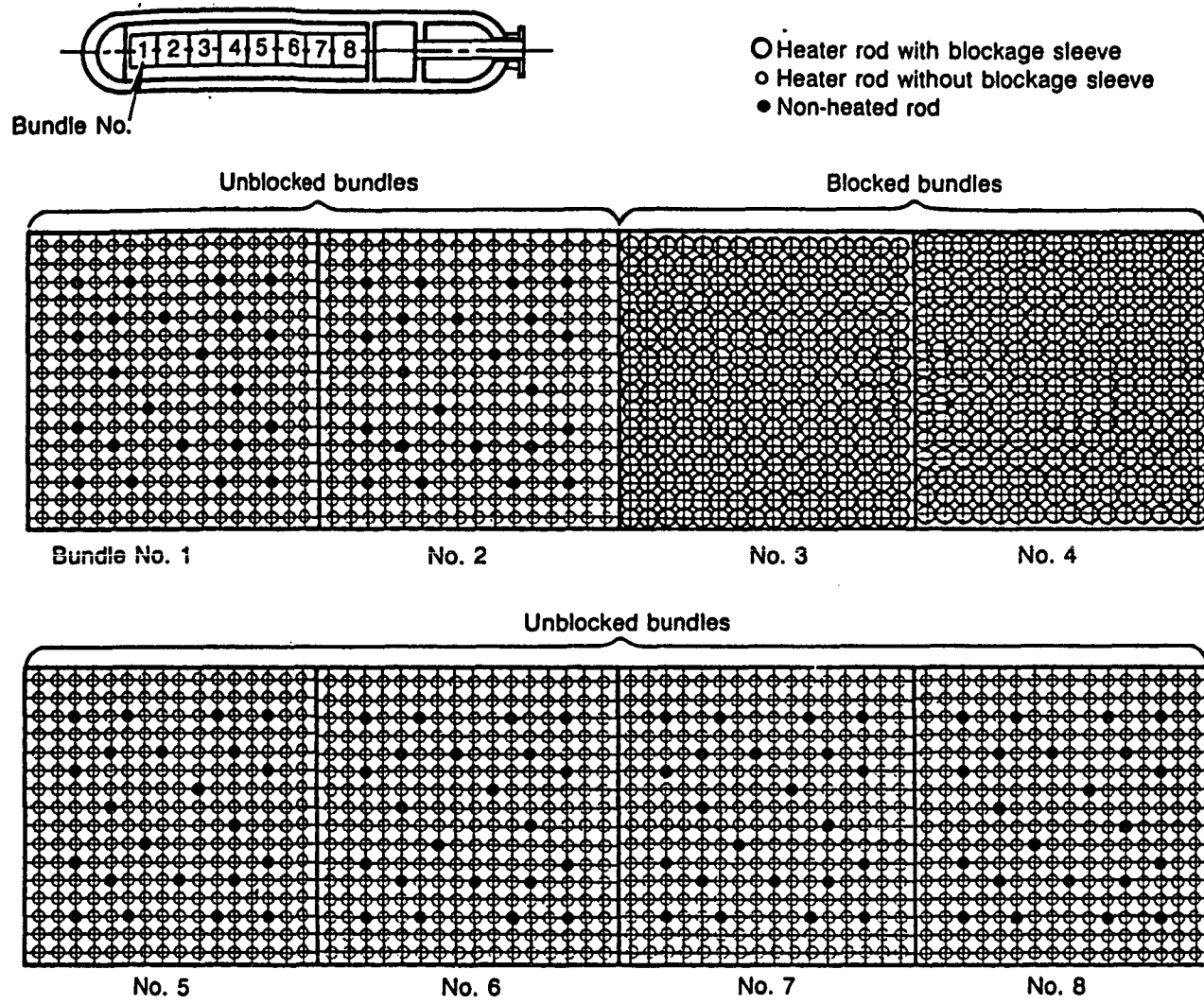
The flow area and fluid volume of components are scaled down based on the nominal core flow area scaling of 1/21. The primary loops consist of a hot leg equivalent to four hot legs in area, a steam/water separator for measuring the flow rate of carryover water, an intact cold leg equivalent to the cold legs of three intact loops, a broken cold leg on the pressure vessel side and a broken cold leg on the steam/water separator side (Figures A.6-1 and A.6-4). The intact cold leg has a pump simulator and a loop seal. The heights of the hot leg and cold legs are as close as possible to those of the reference PWR. Table A.6-1 summarizes major features of the SCTF.

The objectives of the SCTF testing are to study two-dimensional hydrodynamics and heat transfer in the core and the performance of the ECCS during the end of blowdown and during the refill and reflood phases of a LOCA in a PWR. The SCTF test program includes the testing of three simulated cores. Core I simulates a blocked core of a Westinghouse PWR in which all heater rods in two fuel bundles out of the eight have blockage sleeves simulating fuel rod ballooning. Core II simulates an unblocked core of a Westinghouse PWR. With the exception of the fuel rod blockages, Cores I and II are nearly identical. Multiple cores were used because of the limited lifetime of the heater rods. Core III simulates a KWU PWR of the Federal Republic of Germany. Modified upper core and upper plenum hardware is to be used in Core III, and use of the UCSP injection/extraction system is planned, to simulate the German combined injection system.



6 4115

Figure A.6-1 Slab Core Test Facility (SCTF)



6 4096

Figure A.6-2 Arrangement of heater rod bundles in the Slab Core Test Facility (SCTF) pressure vessel

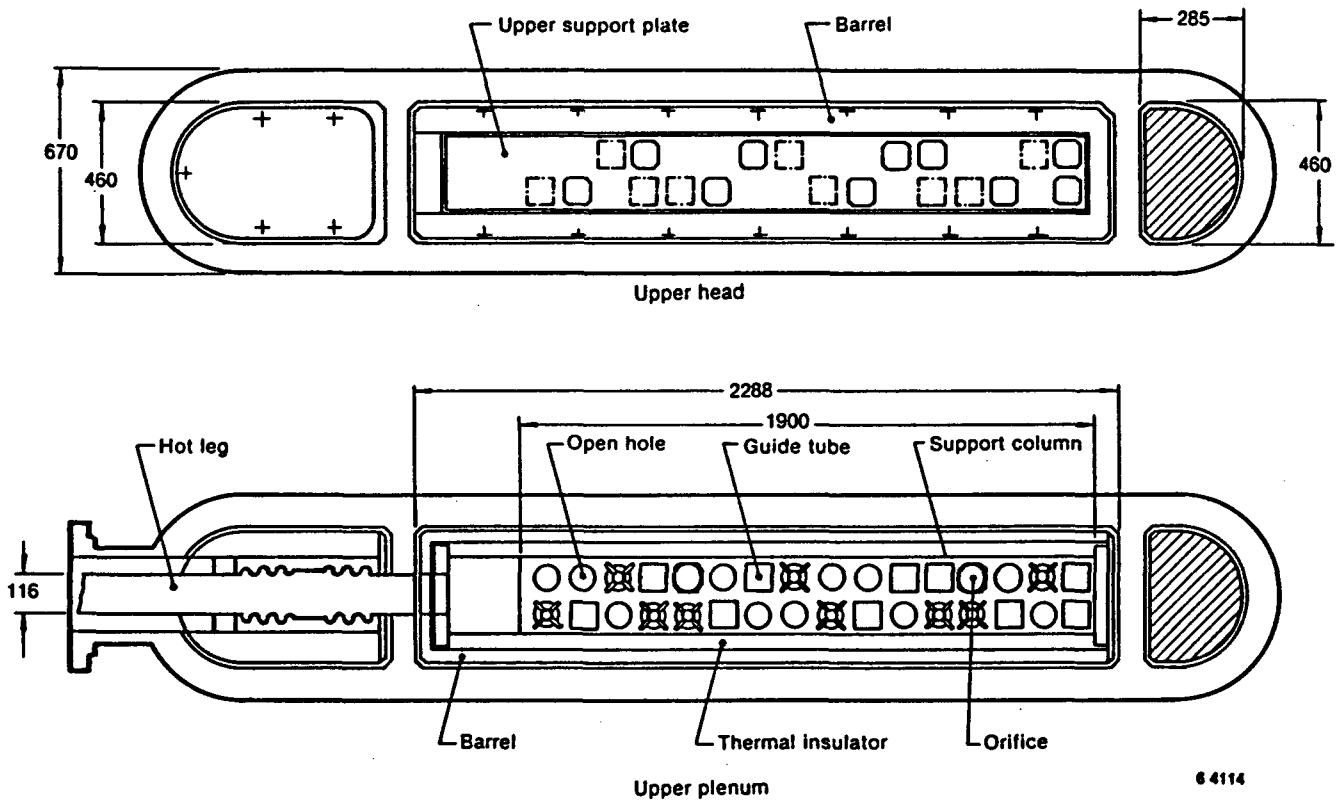
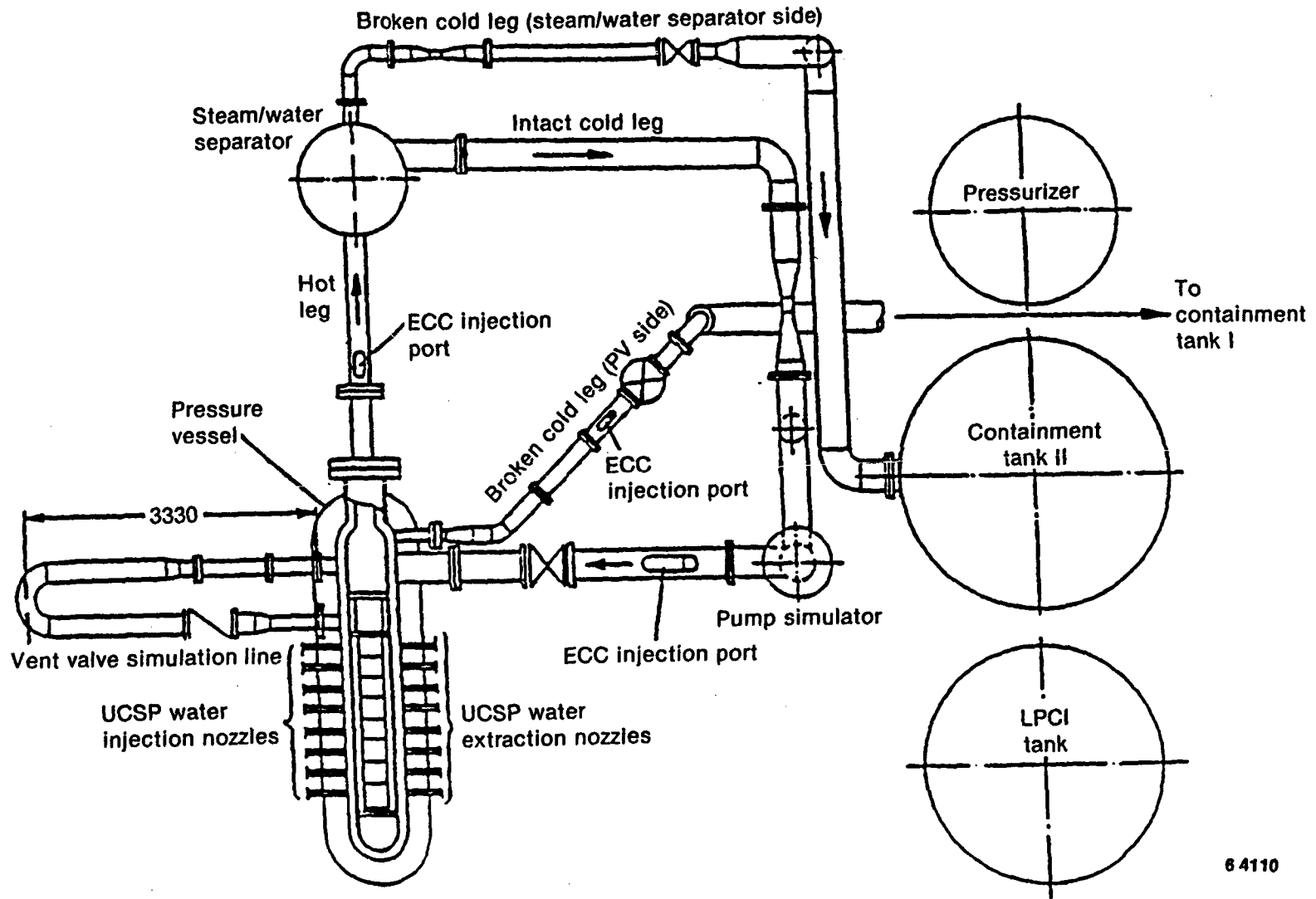


Figure A.6-3 Horizontal cross section of the SCTF pressure vessel

A-51



64110

Figure A.6-4 Arrangement of the Slab Core Test Facility

Table A.6-1 Summary of major features of the SCTF

---

PRIMARY VESSEL

---

General

Height: 8957 mm  
 Inside Diameter: N/A  
 Downcomer Gap: 250 mm  
 Design Pressure: 7 bar  
 Design Temperature: 350°C

Core

No. heated/unheated rods: 1872/176  
 Rod O.D.: 10.7 mm  
 Rod Pitch: 14.3 mm  
 Heated Length: 3660 mm  
 Axial Peaking Factor: 1.4

Downcomer

Area: 0.121 m<sup>2</sup>  
 Height (Bottom of LP to Cold Leg Nozzle): 8004 mm

Lower Plenum

Volume: 1.38 m<sup>3</sup>  
 Structures: Heater Rod Extension

Upper Plenum

Volume: 1.16 m<sup>3</sup>  
 Structures: 1/2 Scale, Simulation

---

PRIMARY LOOPS

---

Piping

No. Loops: 1  
 Hot Leg Flow Area: 0.0826 m<sup>2</sup>  
 Cold Leg Flow Area: 0.0696 m<sup>2</sup>

Steam Generator

Number: 1  
 Type: Steam/Water Separator  
 No. Tubes: ---  
 Tube O.D./I.D.: ---  
 Tube Length: ---  
 Secondary Pressure: ---

Pumps

No.: 1  
 Type: Resistance Simulator

Break

Location: Cold Leg  
 Type: 100% Offset

Pressurizer

No.: None  
 Location:

---

ECC SYSTEMS

---

Injection Locations

Lower Plenum  
 Cold Leg  
 Downcomer  
 Hot Leg  
 UCSP

Injection Sources

Accumulator  
 LPCI  
 UCSP Injection Tanks I and II

---

## A.7 FULL LENGTH EMERGENCY COOLING HEAT TRANSFER

The objective of the PWR Full Length Emergency Cooling Heat Transfer (FLECHT) test program was to obtain test data on reflooding heat transfer under simulated loss-of-coolant accident conditions for use in evaluating the heat transfer capabilities of PWR emergency core cooling systems (Ref. A.7-1). To achieve this objective, the test program was planned to investigate the effects of such parameters as initial clad temperature, flooding rate, power, inlet subcooling, and system pressure on transient heat transfer coefficient.

### Test Bundle

The FLECHT tests were conducted with 7 x 7 and 10 x 10 heater rod bundles having the following principal dimensions, which are typical of commercial PWR fuel assemblies:

Heated length:	12 feet
Heater pitch:	0.5563 inch, square pitch
Heater diameter:	0.422 inch
Control rod thimble diameter:	0.545 inch
Instrumentation tube diameter:	0.463 inch

Figure A.7-1 shows the location of the non-power-producing elements (control rod guide thimbles and instrumentation tube) and the radial power profile for the heater rods (1.1, 1.0, and 0.95 radial peak to average) in the 7 x 7 assembly. The non-power-producing elements and a radial power profile for the 10 x 10 bundle are shown in Figure A.7-2. The axial and radial power distributions employed are typical of those found in actual PWR fuel assemblies.

Chromel-Alumel thermocouples located on the inside surface of the heater rod cladding were distributed radially and axially throughout the bundle. In each test bundle, five of the instrumented heater rods contained five thermocouples. These five thermocouples were placed at positions 2, 4, 6, 8, and 10 feet above the bottom of the heated rods. The remaining heater rods contained three thermocouples at the 4-, 6-, and 10-foot positions. Figure A.7-2 shows the instrumentation layout for the 10 x 10 test bundle. One of the three thermocouple rods provided a check on the test bundle symmetry.

Pressure transducers were utilized to obtain axial and radial pressure measurements. Five pressure taps were located along the flow housing wall at locations 0, 2, 4, 6, and 8 feet from the bottom of the active heater length. Radial pressure measurements at the bottom of the heated length were obtained by means of pressure taps in two of the control rod thimbles.

### Test Facility

The FLECHT facility, shown schematically in Figure A.7-3, was operated as a once-through system. It consisted of a flow housing for the test bundle, a coolant accumulator, a coolant catch vessel, a steam boiler for back-pressure regulation, a gas supply system for coolant injection, and the required piping and valves.

The flow housing was fabricated from 0.7-inch-thick carbon steel and was designed for operation at up to 100 psig and 800°F. Separate square housings having internal dimensions of 4.2 and 5.9 inches, were used for testing 7 x 7 and 10 x 10 assemblies, respectively. The plenum chambers were flanged and could be used with either flow housing.

The 10 x 10 flow housing was equipped with three rectangular quartz glass ports for viewing and photographic study. The upper plenum had one circular quartz glass port. Power was supplied by a 1500-kVA transformer to three silicon-controlled rectifier power control units. To simulate the decay heat generated by a shut-down reactor, the three power control units were biased automatically through a curve-follower programmer. The programmer consisted of an instrument with a pen following the decay heat curve drawn on electrostatic paper. The pen of the programmer mechanically drove three potentiometers to bias each power control unit. The potentiometers were offset to obtain the required radial power profile.

The test program was divided into three groups according to the type of heater rods employed:

- Group I - Stainless steel cladding, low-peak-temperature tests
- Group II - Stainless steel cladding, high-peak-temperature tests
- Group III - Zircaloy 4 cladding, high-peak-temperature tests

Flow blockage tests were performed in the Group I and Group II test series. The objective of these tests was to simulate subchannel blockage that may be caused by clad swelling and axial rod distortion during a loss-of-coolant accident and to determine its effect on heat transfer.

The blockage was effected by a 3/8-inch-thick flat plate approximately an inch below the bundle midplane. In the Group I tests, the plate blocked from 50 to 75% of the flow area of sixteen central flow channels of a 49-rod bundle, allowing bypass flow around the plate in the outer channels. A sketch of the plate is shown in Figure A.7-4. Flooding rates for these tests were 6, 4, and 2 ins. The Group II blockage plate initially blocked 75% of the total flow area in the 10 x 10 bundle with no bypass. The blockage of 16 central flow channels could be increased up to 100 percent with the rest of the bundle blocked 75 to 90 percent. This was the most severe blockage configuration investigated. The Group II blockage plate is shown in Figure A.7-5.

Figure A.7-6 is a schematic of the various blockages used in the Group II tests. Note that the severity of blockage was increased in going from Blockage Geometry 1 to Blockage Geometry 4. For this series, flooding rates were 4, 1, and 0.6 in./s. In addition, a test was performed using variable flooding rates. Special thermocouples were installed at 6 ft 4 in. and 6 ft 8 in. for the Group II flow blockage tests. In both plate designs, blockage was increased by means of special pins inserted into the plate.

#### FLECHT Low-Flow Test

This program was undertaken to expand to data base in the low-flow range, i.e., less than 1 in./s. Two test series were performed, one with the cosine power profile (Ref. A.7-2) and another with the skewed power profile (Ref. A.7-3).

The test facility was basically similar to that used for earlier FLECHT forced flooding tests. A number of refinements were made to improve the quality of data obtained from the testing. A schematic of the facility is shown in Figure A.7-7. The principal components of the facility include:

1. A pressurized temperature-controlled water supply to provide forced flooding of the test bundle.
2. A flow control valve and flow metering devices to set flooding rates from 0.5 to 12 in./s.
3. A close-couple carryover tank connected to the test section upper plenum with a minimum capacity of 145 lb.
4. A steam separator with a capacity of 2500 lb/hr and a liquid collection tank with a volume of 2.8 gal to collect liquid entrained in the exhaust steam.
5. Exhaust piping with a system pressure control valve and an orifice plate flow meter to measure steam flow rate.
6. A 10 x 10 test section consisting of a 12-ft-long instrumented rod bundle in a pressure housing for the cosine test series.
7. A new low-mass circular housing test section with 105 12-ft-long instrumented heater rods for the skewed test series.

The range of test conditions for the cosine and skewed test series are shown in Tables A.7-1 through -4. The effects of the following parameters were studied:

1. Constant flooding rate,
2. Pressure,
3. Inlet subcooling,
4. Initial clad temperature,
5. Peak power,
6. Radial power,
7. Hot/cold channel,
8. Gravity reflood,
9. Variable step flow.

#### REFERENCES

- A.7-1 F. F. Cadek, D. P. Dominicis, and R. H. Leyse, "PWR FLECHT, Final Report," WCAP-7665, April 1971.
- A.7-2 E. R. Rosal et al., "FLECHT Low Flooding Rate Cosine Test Series Data Report," WCAP-8651, December 1975.
- A.7-3 E. R. Rosal et al., "FLECHT Low Flooding Rate Skewed Test Series Data Report," WCAP-9108, May 1977.

Table A.7-1 FLECHT low flooding cosine test -- nominal initial conditions

Parameter	Initial Condition
Initial clad temperature	1600°F
Radial power distribution	1.1, 1.0, and 0.95 peak to average
Peak power	0.9 kW/ft
Coolant $\Delta T$ subcooling	140°F
Containment pressure	40 psia
Injection rate	0.8 in./s (~.56 lb/sec)
Upper plenum flow area	Lower plenum initially full
Axial power shape	Nominal
	Cosine

Table A.7-2 FLECHT low flooding cosine test -- range of test conditions

Parameter	Range
Pressure	19 - 62 psia
Initial clad temperature	300 - 1813°F
Rod peak power	.55 - 1.27 kW/ft
Flooding rates	
Constant	0.4 - 5.8 in./s
Variable in steps	12 $\rightarrow$ 0.4 in./s
Continuously variable (programmed)	12 $\rightarrow$ 0 in./s
Coolant $T_{subcooling}$	8 - 155°F
Housing temperature	FLECHT Criteria - $T_{sat}$

Table A.7-3 FLECHT low flooding skewed test -- nominal initial conditions

Parameter	Initial Condition
Initial clad temperature	1600°F
Radial power distribution	1.1, 1.0, and 0.95 peak to average
Peak power	0.7 kW/ft
Coolant $\Delta T$ subcooling	140°F
Containment pressure	40 psia
Injection rate	1.0 in./s (~0.7 lb/sec) Lower plenum initially full
Upper plenum flow area	Nominal
Axial power shape	Skewed to the top

Table A.7-4 FLECHT low flooding skewed test -- range of test conditions

Parameter	Range
Pressure	18 - 60 psia
Initial clad temperature	293 - 1630°F
Rod peak power	0.216 - 1.0 kW/ft
Flooding rates	
Constant	0.7 - 6.0 in./s
Variable in steps	6 → 0.5 in./s
Injection rates	
variable steps	12.6 → 1.4 lb/s
Coolant $T_{\text{subcooling}}$	2 - 143°F
Housing temperature	$T_{\text{sat}}$ - 800

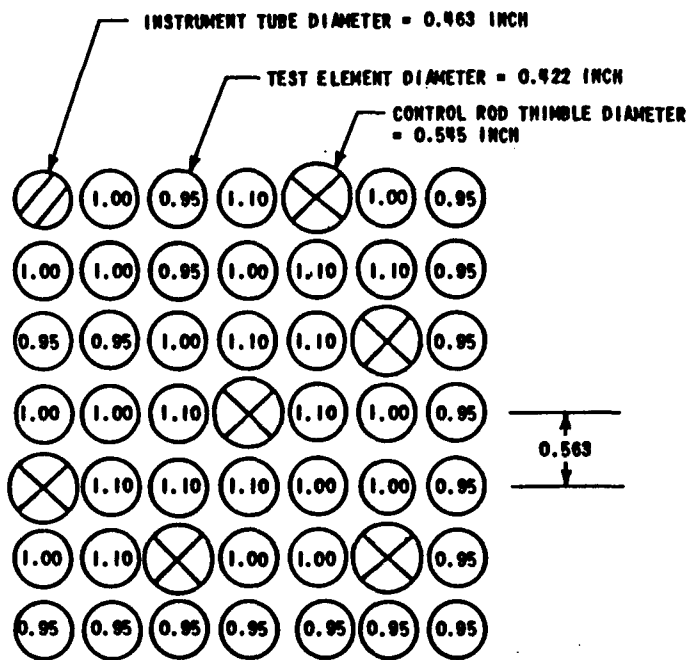


Figure A.7-1 7 x 7 test section simulating a PWR assembly power distribution

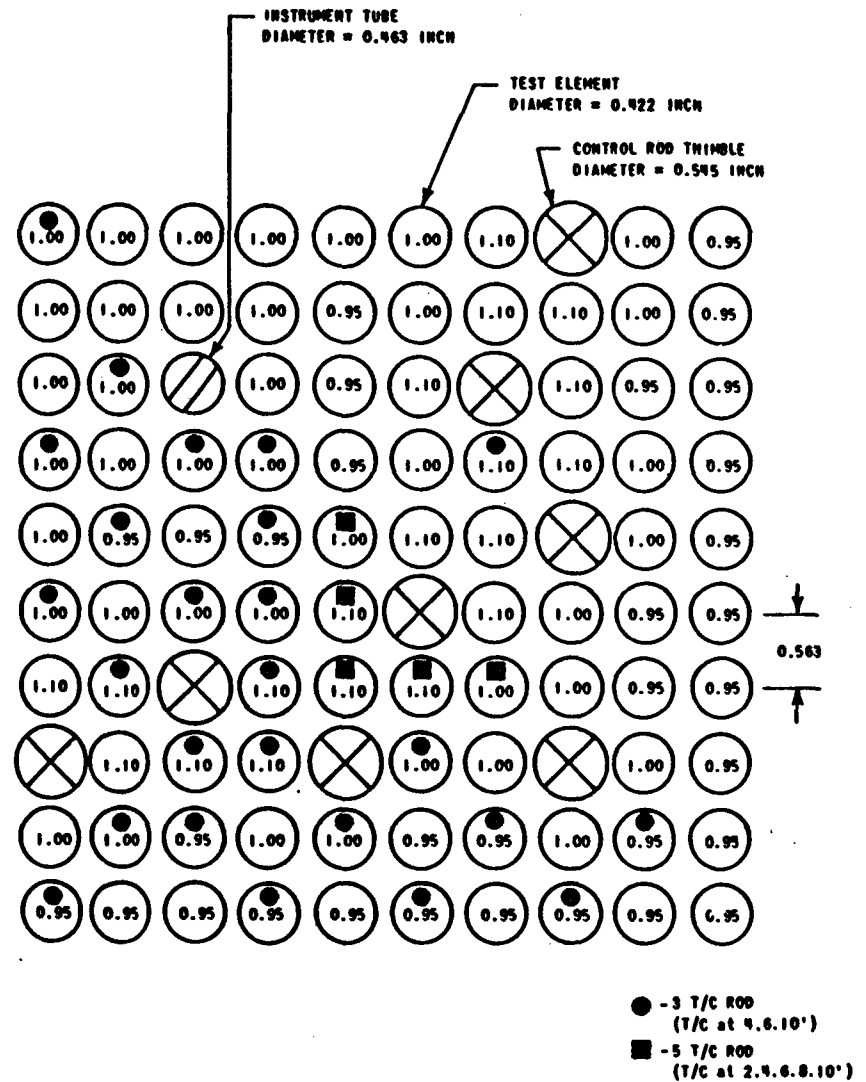


Figure A.7-2 10 x 10 test section simulating a PWR assembly power distribution

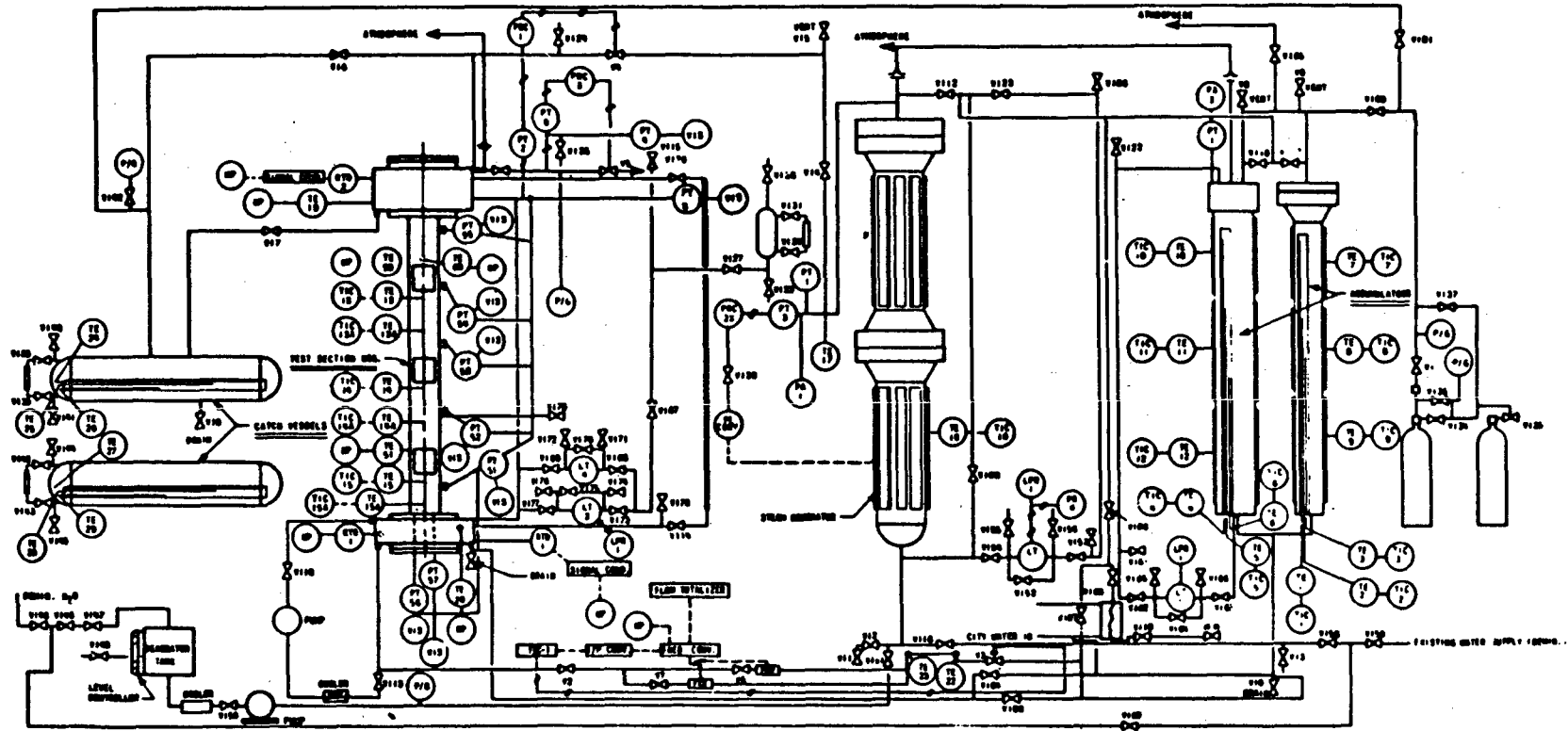


Figure A.7-3 FLECHT test facility

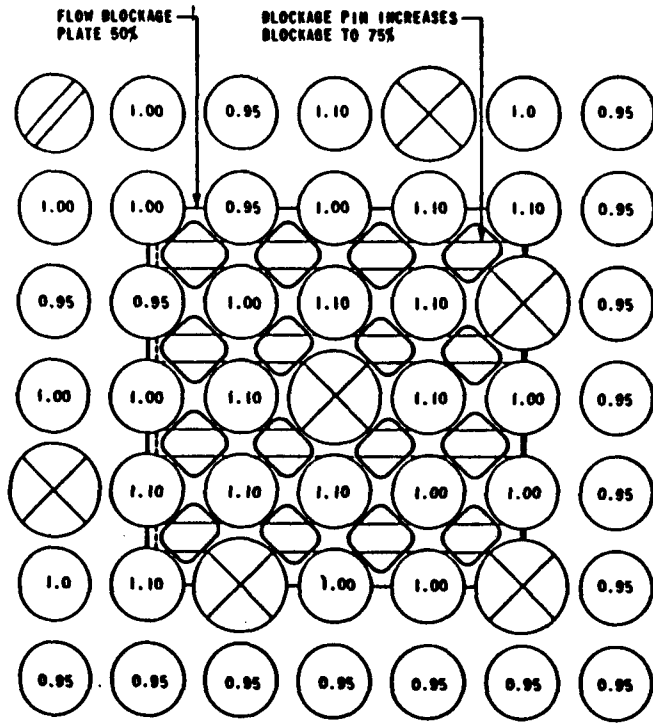


Figure A.7-4 Group I flow blockage plate

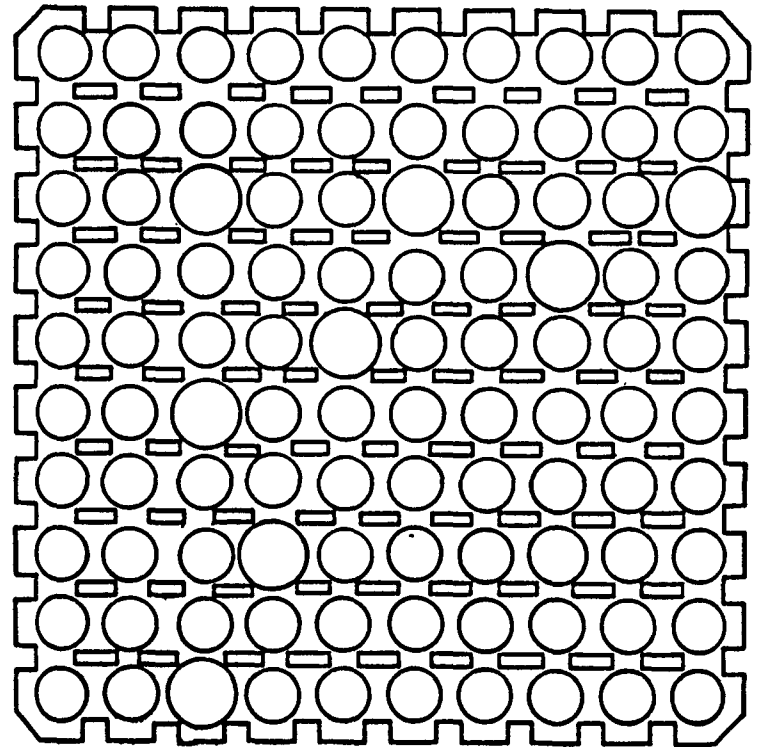
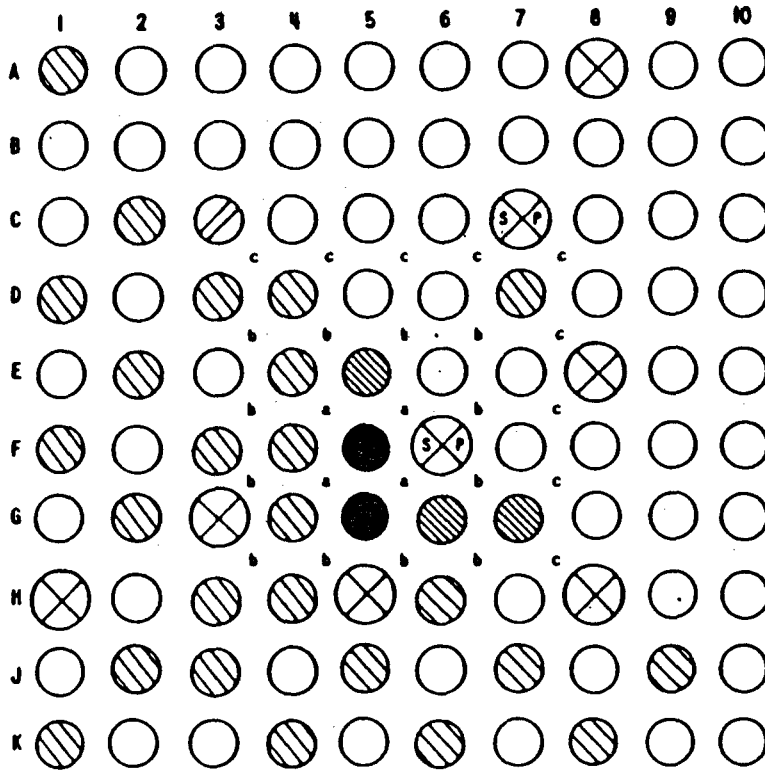


Figure A.7-5 Group II flow blockage plate



BLOCKAGE GEOMETRY	BLOCKAGE OF FLOW AREA IN CHANNELS DESIGNATED:			
	a	b	c	ALL OTHERS
1	75%	75%	75%	75%
2	90%	90%	90%	75%
3	100%	90%	90%	75%
4	100%	100%	90%	75%

Figure A.7-6 Various blockage configurations used in Group II test series



## A.8 FLECHT-SEASET\*

### 161-Rod Unblocked Bundle Facility

The FLECHT-SEASET facility used to conduct the unblocked bundle forced and gravity reflood experiments is a separate-effect test facility in which the bundle is isolated from the system and the thermal-hydraulic conditions are prescribed at the bundle entrance and exit (Ref. A.8-1). Within the bundle, the dimensions are full scale compared to a PWR except for the overall radial dimension. A low-mass housing used in the test was designed to minimize the wall effects so that the rods one row or more away from the housing in the bundle are representative of any region in a PWR core. To preserve proper thermal scaling of the facility with respect to a PWR, the power-to-flow-area ratio is nearly the same as that of a PWR fuel assembly. Thus the vapor superheat, entrainment, and fluid flow behavior should be similar to that expected in a PWR for the same boundary conditions. In addition to examining the effects of fuel assembly geometry on reflood heat transfer and carryout rate fraction behavior, the data resulting from these experiments could be utilized as a baseline in assessing the effects of flow blockage.

The FLECHT-SEASET facility (Fig. A.8-1) was a modification of the FLECHT facility described in the previous section. The following changes or additions were made:

1. A new low-mass housing test section and upper and lower plenum.
2. An upper plenum baffle to improve liquid carryover separation.
3. The 161-rod bundle and related instrumentation.
4. The pressurized water supply accumulator and injection line with three rotameters and a turbine meter to measure injection rates from 0.4 in./s in forced flooding tests to 14.3 lb/s in gravity reflood tests.
5. A closed-coupled carryover tank with a storage capacity of 145 lb connected to the upper plenum of the test section.
6. A steam separator with a capacity of 2500 lb/hr and a liquid collection tank to collect liquid entrained in the exhaust line. The steam separator had a storage capacity of approximately 425 lb.
7. Exhaust piping with a system pressure control valve and an orifice plate flowmeter to measure exhaust steam flow rate.
8. An electric steam boiler with a capacity of 125 lb/hr to established initial loop pressure and temperature.

---

\*Full Length Emergency Cooling Heat Transfer - Separate Effects and System Effects Test.

The facility was modified as shown in Figure A.8-2 to conduct gravity reflood tests. The modifications consisted of connecting the downcomer to the lower plenum, moving the injection line from the lower plenum to the bottom of the downcomer, installing a resistance orifice plate to simulate the hot leg resistances between the test section outlet pipe and the inlet flange of the entrainment separator, venting the top of the downcomer to the entrainment separator, and installing additional differential pressure cells. A cross section of the test bundle is shown in Figure A.8-3. The bundle is composed of 161 heater rods, 4 instrumented thimbles, 12 steam probes, 8 solid triangular fillers, and 8 grids. The fillers were welded to the grids to maintain the proper grid location. The fillers also reduced the amount of excess flow area.

The ranges of the test conditions are listed in Table A.8-1. Best-estimate conditions were included in the range of conditions and were reflected in the low-power, low-initial-temperature, and high-flooding-rate tests. The effects of the following parameters were studied:

1. Flooding rate,
2. Pressure,
3. Subcooling,
4. Initial cladding temperature,
5. Rod peak power,
6. Variable flooding rate,
7. Gravity.

#### 21-Rod Blocked Bundle Facility

The 21-rod blocked bundle task examined the reflooding phenomena in simple blockage configurations to obtain a fundamental understanding of the heat transfer change effected by blockage and to select a worst blockage shape in terms of heat transfer for use in the 163-rod blocked bundle test with ample bypass flow. The effects of blockage on heat transfer due to flow bypassing the blockage zone and local flow behavior in and downstream of the blockage. Bypass flow is expected to reduce heat transfer in the blocked region because of a reduction in fluid flow, but the blockage itself may increase heat transfer as a result of increased turbulence and droplet disintegration. These two heat transfer effects are counteracting. For a clear understanding, it was necessary to determine which effect would dominate under which thermal-hydraulic conditions. This test series, therefore, studied these effects to determine the relative importance of flow bypass and local blockage geometry on reflood heat transfer.

A new facility was designed and built for conducting the 21-rod blocked bundle tests as shown in Figure A.8-4. It was designed to be capable of performing forced flooding, steam cooling, and gravity reflood tests with a 21-rod bundle. The upper and lower plenums, carryover tank, and steam separator tanks have the same volume-to-flow-area ratio as the unblocked bundle facility. The downcomer and crossover pipe flow areas were scaled down from the unblocked bundle flow area to the 21-rod bundle flow area. The test section was designed to facilitate disassembling the bundle for changing blockage configurations.

Detailed analyses and discussions on choosing the blockage configurations are contained in Reference A.8-2. The six 21-rod bundle tests are described in

Table A.8-2, with an explanation of the different effects that were expected to be observed in the experiments. Three of the five blockage configurations utilized a noncoplanar blockage sleeve distribution because most of the out-of-pile data indicated that bursting occurs in a noncoplanar fashion. Coplanar blockage is defined as bursting that occurs at the same elevation. Noncoplanar blockage is defined as bursting that occurs at different elevations; however, the blockage strain may overlap from rod to rod. The sleeves for all the test series were smooth; no attempt was made to simulate the burst opening in the clad. Tests were conducted with no blockage in the same facility at the same thermal-hydraulic conditions to serve as a basis for evaluating the effect of the flow blockage on heat transfer. The bundle, which is composed of 21 instrumented heater rods and four solid triangular fillers, is shown in Figure A.8-5.

To help ascertain both the hydraulic and the heat transfer effects of the flow blockage configurations relative to the unblocked bundle, single-phase hydraulic tests, steam cooling, forced reflood, and gravity reflood scoping tests were performed on each of the six bundles, except that gravity reflood tests were not performed on the final configuration.

The initial conditions and the ranges of test conditions are listed in Table A.8-3. The effects of the following parameters were studied:

1. Flooding rate,
2. Pressure,
3. Subcooling,
4. Variable flooding rate,
5. Gravity reflood.

#### 163-Rod Blocked Bundle Facility

The tests performed in the 163-rod blocked bundle are classified as separate-effect tests. The primary objectives of the tests were to obtain, evaluate, and analyze thermal-hydraulic data using a 163-rod bundle to determine the effects of flow blockage and flow bypass on reflood heat transfer and to assess analytical or empirical methods for use in analyzing the blocked bundle heat transfer data. A new test facility was designed and built specifically for conducting flow blockage tests following the 21-rod blocked bundle test program. A schematic diagram of the facility is shown in Figure A.8-6.

The 163-rod blocked bundle test facility, like the 21-rod blocked and 161-rod unblocked bundle test facilities, contained the following major components.

1. A heater rod bundle.
2. A low-mass housing coupled directly to the upper and low plenums.
3. A coolant injection system and a steam heating system.
4. A phase separation and liquid collection system.
5. A downcomer and crossover leg.

The above components were thoroughly instrumented to measure flow blockage effects within the bundle and the boundary conditions at the bundle inlet and

outlet. The volumes of the upper and lower plenums, downcomer, crossover leg, and steam separator tanks were essentially the same as those in the 161-rod unblocked bundle facility. The carryover tank volume was increased to accommodate additional water. Both forced flooding and gravity reflood tests were performed in the 163-rod blocked bundle test facility (Ref. A.8-3).

The large 163-rod bundle was blocked to investigate the flow bypass effects on reflood heat transfer in the simulated fuel rod assembly. The blockage in the bundle was arranged so that fluid was not forced through the blocked zone. Several methods could be used to produce a sufficient bypass area in the bundle. However, the following limitations affect how the blockage should be arranged radially:

1. The 163-rod bundle has only one symmetry line because of thimble locations, as shown in Figure A.8-7.
2. The test should be linked to the 21-rod blocked bundle test to better utilize information.
3. Lateral symmetry in the blocked bundle for the bypass area and blockage zone is desirable in view of possible data scattering and computer time for flow calculations.
4. The blockage zone must be large enough to provide a detectable flow field distortion and a maximum flow depletion in the blocked zone.

The above considerations resulted in the choice of the blockage configuration with two 21-rod bundle islands as shown in Figure A.8-7. The rods in the island are blocked exactly as in the 21-rod bundle. This blockage configuration has a higher bypass area because of the smaller and isolated blockage zone.

Data from Westinghouse multirod burst tests (Ref. A.8-4) showed an effect of thimbles on the circumferential location of the burst. The burst locations were not random, and were usually directed away from thimbles. This indicated that the thimbles were good heat sinks, causing nonuniform circumferential temperature distributions on neighboring rods. It must be noted that a burst occurs at the hottest point of a rod; however, the major flow blockage due to the nonconcentric bulge is on the side opposite the burst.

Although observations from the Westinghouse tests indicate that bursts can occur toward either adjacent subchannels or rods, it was decided that simulated bursts would occur only toward adjacent subchannels for the following reasons:

1. Blockage tests were not intended to investigate detailed variations in a subchannel but to determine average subchannel behavior.
2. The additional parameter of burst orientation makes data analysis complicated without an apparent improvement of understanding.
3. There were physical limitations in installing the blockage sleeves on the rods.

The above decision provided the basis for selecting bulge directions of the nonconcentric sleeves in the 21-rod bundle. First it was necessary to find the hottest subchannel of the four subchannels surrounding each rod. The bulge then occurred on the side opposite the hottest point.

Since an effort had been made to relate the results from (Ref. A.8-4), the 21-rod bundle to those from the 163-rod bundle tests to maximize data utilization, it was necessary to consider the relative location of the 21-rod island in a fuel assembly in applying the method to the small bundle, as shown in Figure A.8-7. For this case, the determination of the hottest subchannel (or subchannels) associated with each rod was straightforward because of the unique distribution of the thimbles.

The above arguments were used to determine the possible bulge directions in the 21-rod bundle, as indicated by dots in island A of Figure A.8-7. The bulge directions of some rods were determined uniquely; others had several possible locations. Bulge directions of the rods with multiple choices could be chosen from the possible locations so that the four center subchannels had high blockages. The locations of the peripheral rods with multiple choices could be chosen arbitrarily from the possible locations. The resulting bulge directions are shown in island B of Figure A.8-7.

The initial conditions and the ranges of test conditions are listed in Table A.8-4. The effects of the following parameters were studied:

1. Flooding rate,
2. Pressure,
3. Peak power,
4. Subcooling,
5. Stepped flow,
6. Hot/cold channel,
7. Gravity reflood.

#### REFERENCES

- A.8-1 L. E. Hochreiter et al., "PWR FLECHT-SEASET Unblocked Bundle, Forced and Gravity Reflood Task: Task Plan Report," NRC/EPRI/W Report No. 3, March 1978.
- A.8-2 L. E. Hochreiter et al., "PWR FLECHT-SEASET 21 Rod Bundle Flow Blockage Test; Task Plan Report," WCAP-9658, March 1980.
- A.8-3 L. E. Hochreiter et al., "PWR FLECHT-SEASET 163-Rod Bundle Flow Blockage Task: Task Plan Report," WCAP-9692, July 1980.
- A.8-4 R. E. Schreiber et al., "Performance of Zircaloy-Clad Fuel Rods during a Simulated Loss-of-Coolant Accident: Multirod Burst Tests," WCAP-7795-L, April 1970.

Table A.8-1 Range of test conditions for the  
161-rod unblocked bundle tests

Parameter	Parameter Range
Initial clad temperature	149 - 871°C (330 - 1600°F)
Peak power	1.30 - 3.10 kW/m (0.4 - 0.95 kW/ft)
Upper plenum pressure	0.14 - 0.4 MPa (20 - 60 psia)
Flooding Rates:	
Constant	8 - 150 mm/s (0.3 - 6 in./s)
Variable in steps	150 to 15 mm/s (6.0 to 0.6 in./s)
Injection Rates (Gravity Reflood)	
Variable in steps	6.49 to 0.77 kg/s (14.3 to 1.7 lb/s)
Coolant subcooling ( $\Delta T$ )	3 - 78°C (5 - 140°F)

Table A.8-2 Blockage configurations tested in the 21-rod blocked bundle tests

Test Series	Configuration Description	Comments
A	No blockage on the rods	This configuration served as a reference.
B	Short concentric sleeve, coplanar blockage on center nine rods	This series provided for both blockage effects and some bypass effects.
C	Short concentric sleeve, coplanar blockage on all 21 rods	This series was easiest to analyze, since it provides no flow bypass effects with maximum flow blockage effect at one axial plane.
D	Short concentric sleeve, noncoplanar blockage on all 21 rods	This test series examined a noncoplanar blockage distribution and was comparable to Series C.
E	Long nonconcentric blockage sleeve, noncoplanar blockage on all 21 rods	This test series permitted a one-to-one comparison with Series D in which all rods were blocked. Comparison of Series D and E with unblocked data indicated the worst shape.
F	Test series E with increased blockage sleeve strain, noncoplanar blockage on all 21 rods	This test series increased the blockage effect relative to series E.

**Table A.8-3 Initial conditions and the ranges of test conditions  
for the 21-rod blocked bundle tests**

<b>Parameter</b>	<b>Initial Condition</b>	<b>Range of Conditions</b>
<b>Initial clad temperature</b>	871°C (1600°F)	260°C - 871°C (500°F - 1600°F)
<b>Peak power</b>	2.3 kW/m (0.7 kW/ft)	0.88 - 2.3 kW/m (0.27 - 0.7 kW/ft)
<b>Upper plenum pressure</b>	0.28 MPa (40 psia)	0.14 - 0.28 MPa (20 - 40 psia)
<b>Flooding rate:</b>		
Constant	25 mm/s (1 in./s)	10.2 - 152 mm/s (0.4 - 6 in./sec)
Variable in steps		152 to 20 mm/s (6.0 to 0.8 in./s)
<b>Injection rate (gravity reflood)     Variable in steps</b>		0.82 to 0.09 kg/s (1.8 to 0.2 lb/s)
<b>Coolant ΔT subcooling</b>	78°C (140°F)	3°C - 78°C (5°F - 140°F)

Table A.8-4 Initial conditions and the ranges of test conditions for the 163 rod blocked bundle tests

Parameter	Initial Condition	Range of Conditions
Initial clad temperature	871°C (1600°F)	260°C - 871°C (500°F - 1600°F)
Peak power	2.3 kW/m (0.7 kW/ft)	1.31 - 3.3 KW/m (0.4 - 1.0kW/ft)
Upper plenum pressure	0.28 Mpa (40 psia)	0.14 - 0.42 MPa (20 - 60 psia)
Flooding rate:		
Constant	25 mm/s (1 in./s)	15 - 152 mm/s (0.6 - 6 in./s)
Variable in steps	--	152 to 20 mm/s (6.0 to 0.8 in./s)
Continuously variable	--	36 - 17 mm/s (1.4 - 0.65 in./s)
Injection rate (gravity reflood)	--	5.80 to 0.785 kg/s (12.8 to 1.73 lb/s)
Coolant ΔT subcooling	78°C (140°F)	8°C - 78°C (15°F - 140°F)

A-72

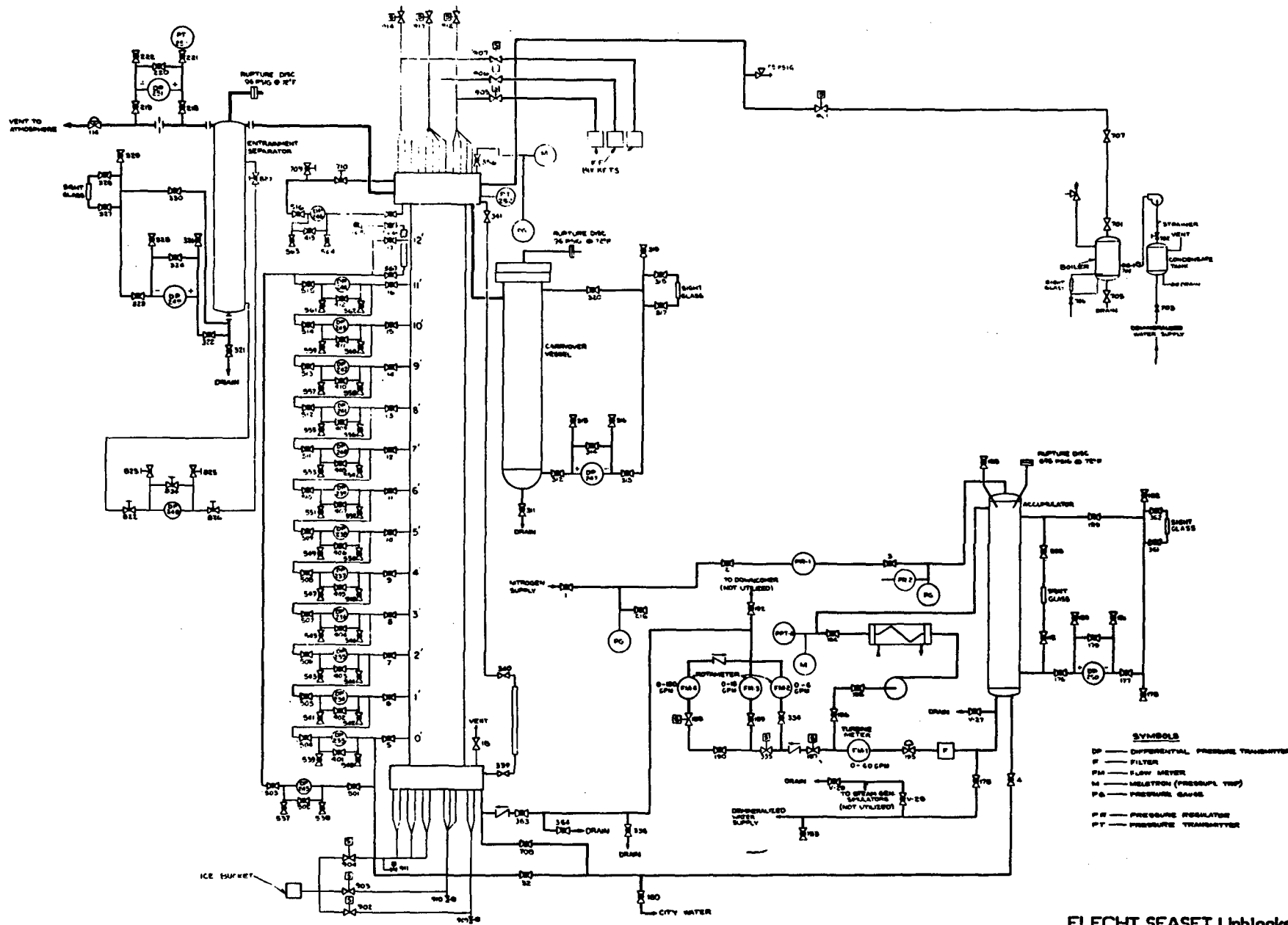


Figure A.8-1 Flow diagram for the forced reflow configuration

FLECHT SEASET Unblocked Bundle Flow Diagram, Forced Reflood Configuration

A-73

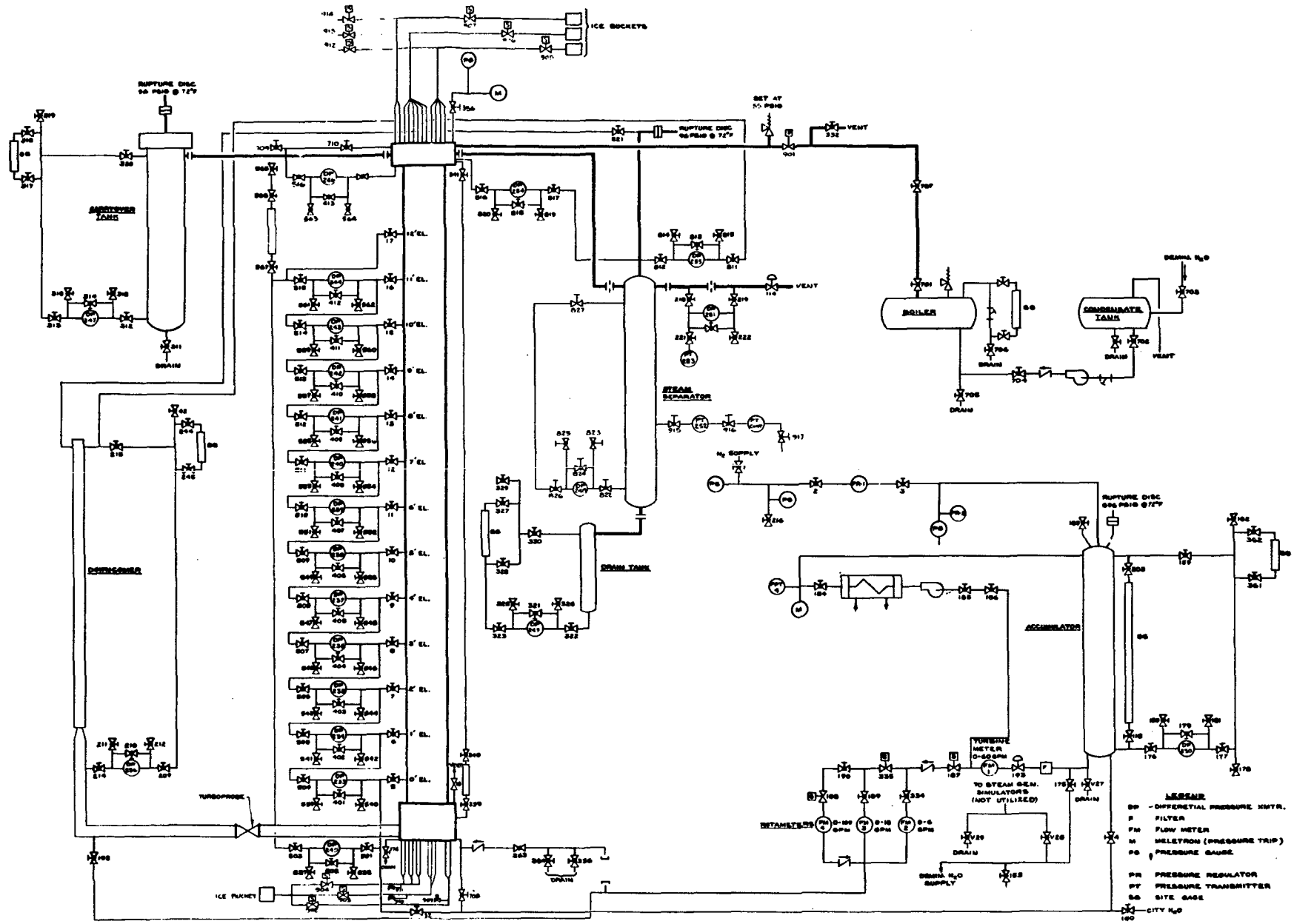


Figure A.8-2 Flow diagram for the gravity reflood configuration

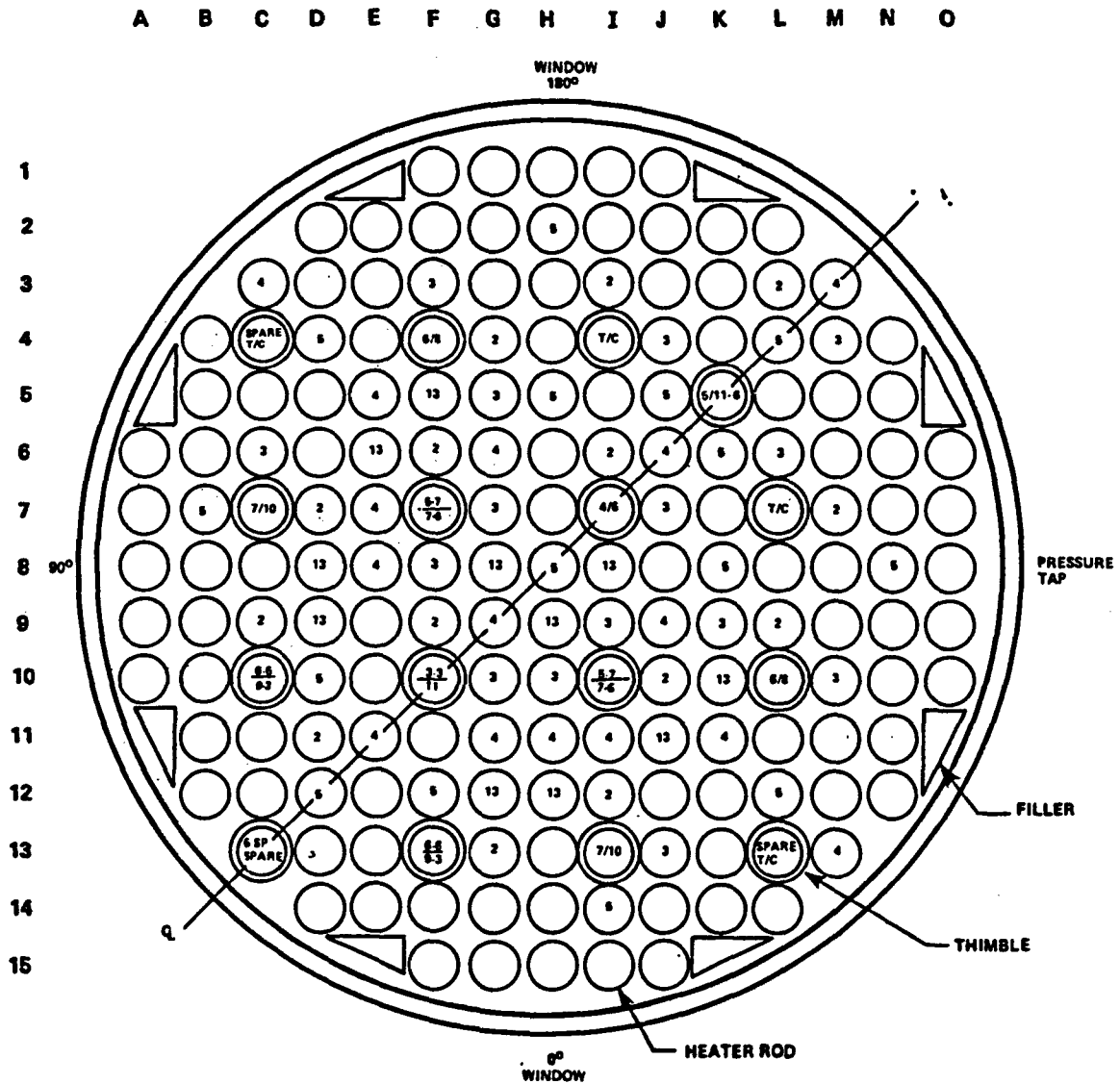


Figure A.8-3 161-rod unblocked bundle cross section

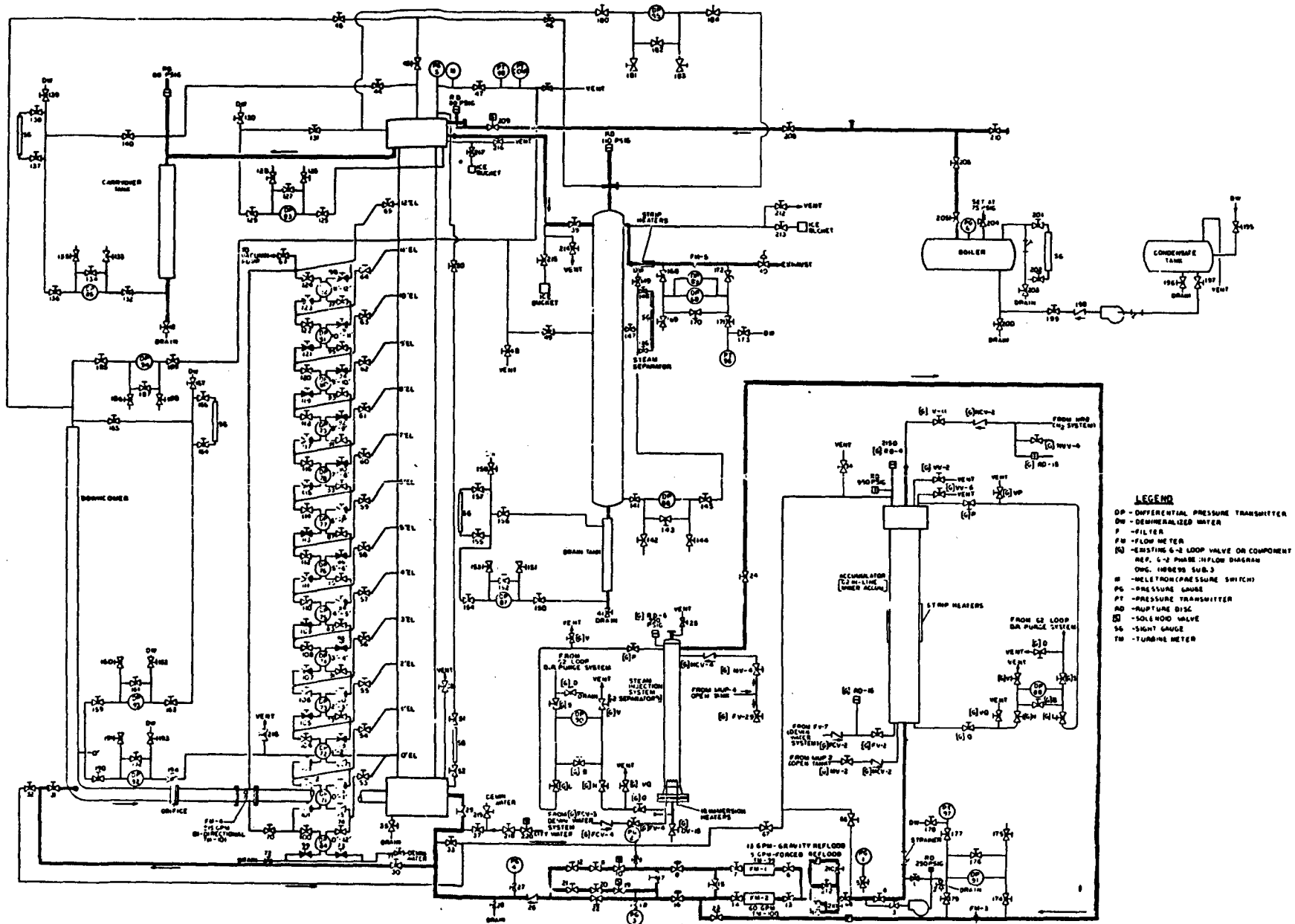


Figure A.8-4 Flow diagram for the 21-rod blocked bundle configuration

7.62 cm (3") OD X 6.82 cm (2.687") ID  
X 3.99 mm (0.157") WALL 304 SS

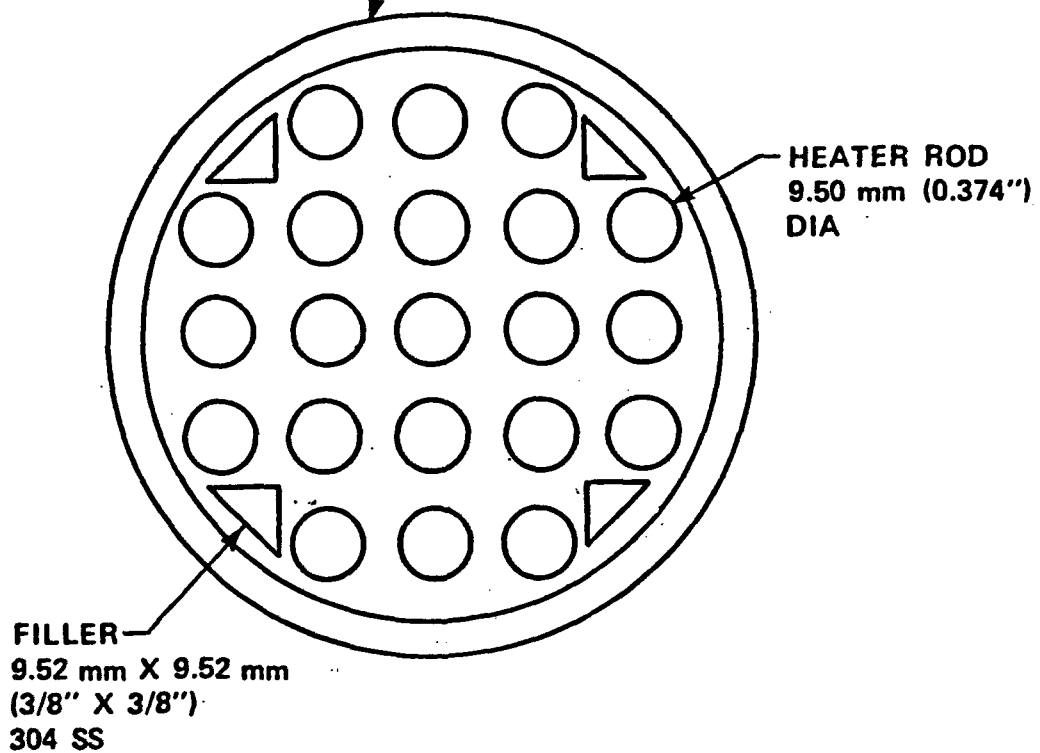


Figure A.8-5 21-rod blocked bundle cross section



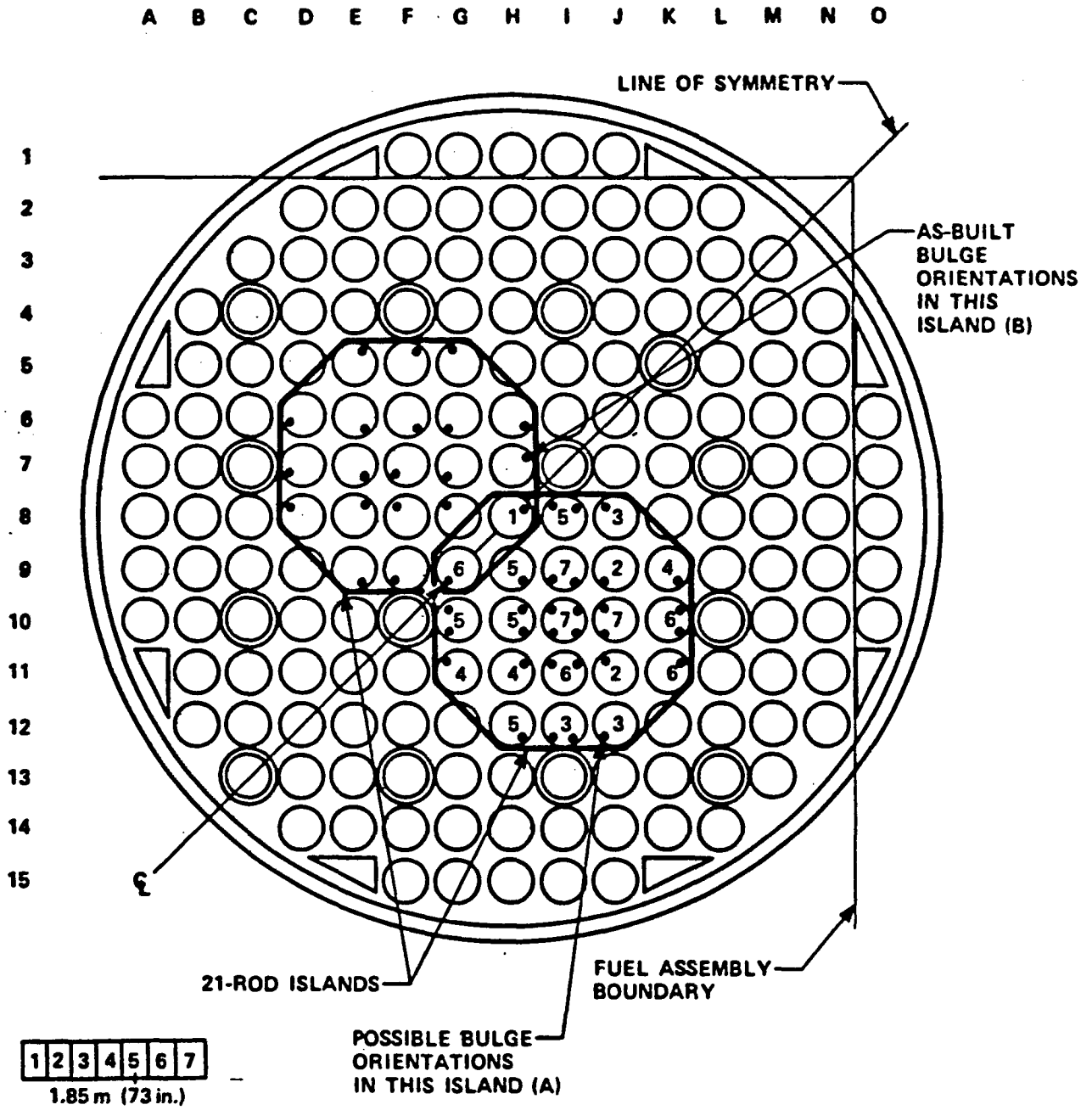


Figure A.8-7 Blockage sleeve distribution, blockage island locations and bulge orientations for the 163-rod blocked bundle tests

## A.9 TWO-LOOP TEST APPARATUS FACILITY

The BWR system simulator Two-Loop Test Apparatus (TLTA) was modified many times to reflect different plant configurations, different test objectives and in order to improve the simulation capability of the facility. These major configurations are summarized in Table A.9-1 and in Reference A.9-1. Configurations TLTA 1-TLTA 4 were used in the Blowdown Heat Transfer program to study the blowdown phase of the BWR LOCA and are described in Reference A.9-2. Reference A.9-3 describes the TLTA 5 configuration which included the addition of emergency core coolant injection and a capability to simulate the entire BWR LOCA. The facility was further improved to the TLTA 5A version described in Reference A.9-1. Small break LOCA configurations, TLTA 5B and TLTA 5C, are described in Reference A.9-4. This facility description primarily describes the TLTA 5 and TLTA 5A configurations, with reference to earlier configurations.

### General Description

Salient features of TLTA 5 and 5A included:

- a. integral system,
- b. full-size bundle,
- c. full power,
- d. typical BWR operating pressure and temperature, and
- e. emergency core cooling systems.

The full-size electrically heated bundle (which is capable of duplicating the power output of a BWR fuel bundle from full initial power to the decay heat power) is enclosed in a pressure vessel. Also contained inside the vessel are such BWR counterparts as guide tube, jet pumps, and steam separator, as shown in Figure A.9-1. Connected to the vessel outside are two recirculating loops, a feedwater system, and a steam line with pressure regulation capability.

The configurations of the TLTA simulate the reference BWR system in all the major regions. Figure A.9-2 depicts the TLTA representation of the BWR regions. These regions include the lower plenum, guide tube, core region (viz., the bundle and bypass region), upper plenum, steam separator, steam dome, annular downcomer, recirculation loops, and ECC injection systems. The regional fluid volumes and their relative distributions within the reference BWR system are simulated.

All significant internal flow paths between adjacent regions are preserved. These paths are identified in Figure A.9-2; the flow areas are given in Table A.9-2. Key elements along the flow paths are provided to ensure that the anticipated phenomenon is preserved. In an effort to preserve the counter-current flow limiting (CCFL) characteristics at the bundle inlet and exit, for instance, a typical side entry orifice and a simulated upper tie plate are used in TLTA. The leakage paths, as will be discussed later, were modified during the program to improve the simulation.

The external flow paths are also simulated to give close simulation to a BWR system. These include the steam line flow, recirculation flow, feedwater flow, break flow, and ECC flow. The steam line contains a pressure regulator which duplicates the function of a reactor pressure control system and the

main steam isolation valve. The intact loop recirculation pump has coastdown characteristics similar to the BWR counterpart. The broken loop recirculation lines are connected to the two blowdown lines. Flow limiters are installed in the blowdown lines to simulate and vary the break size. The ECC injection systems have flow characteristics similar to those of a BWR system. The feedwater system is not representative, however.

### Scaling Considerations and Compromises

The fundamental scaling consideration in TLTA is to achieve the real-time response objective. Both Configurations 5 and 5A of TLTA were scaled to a reference BWR/6 - 218 having 624 fuel bundles. Each bundle consists of 64 rods in an 8x8 array. The ratio of TLTA to BWR bundles is 1/624. This same ratio is the basis for scaling the regional volumes, masses, energies, and flow rates.

The TLTA was designed with the constraint of accommodating a full-size test bundle and to achieve the fundamental objective of real-time response. A number of compromises have been made in order to satisfy these scaling considerations and geometric limitations. The compromises on the regional volumes, as can be seen from Table A.9-3, are the larger steam space and the recirculation loops. The larger steam space was found (Ref. A.9-3) to have a negligible effect on the system response. The large recirculation loop volume can be expected to retard the system depressurization because the larger fluid mass will flash into vapor and interact with the rest of the system.

Additional compromises included flow area to fluid volume ratio and the boundary surface area to volume ratio, the flow area being larger in the downcomer region and the lower plenum. This larger flow area renders the fluid velocity slower. However, in both the BWR and TLTA the fluid velocities are typically very low. The higher surface to volume ratio can lead to higher heat addition from the vessel stored energy to the fluid.

In order to assure realistic recirculation flow coastdown performance for the early portion of the blowdown transient, the jet pumps were linearly scaled to height and diameter (Ref. A.9-3). The resultant TLTA jet pumps are much shorter than the BWR counterparts. However, the mass flux through these jet pumps was scaled to produce the typical mass flux as in the BWR. Other fluid regions in the TLTA, typically in the downcomer region, were correspondingly made shorter to produce a real-time response. The size of the TLTA jet pumps and vessel relative to the reference BWR can be seen in Figure A.9-3. The short jet pumps result in a lower hydrostatic head. This lower head can have a significant effect during the reflooding phase of the transient. The height of the jet pumps can affect the height to which the bundle region can be reflooded because the bundle is in a hydraulic path parallel with the jet pumps. The elevation distortion can also affect the level response even though the timings of the controlling events in the early transient are preserved in TLTA.

Finally, any radial or parallel channel effects which might exist in the multi-bundle BWR would be much less prominent in the single bundle TLTA. Effects such as core spray injection on CCFL breakdown and parallel channel hydraulics on bundle reflood are expected to be important after ECC injection. They are not well represented in TLTA.

## Test Apparatus Modifications

The TLTA has been modified to meet the primary objective of each test phase with the overall objective of maintaining a real-time, thermal-hydraulic system response. Each modification of TLTA is assigned a number to identify with that configuration. The evolution of the configurations is summarized in Table A.9-1.

The key features of TLTA 5 are the ECC injection systems and a simulated upper tie plate. The significant modifications made to TLTA to transform Configuration 5 to 5A were: improved leakage path simulations and improved bundle power supply controller. Other modifications include recirculation line isolation and removal of the separator liquid reservoir. These modifications are summarized below. A schematic of the TLTA Configuration 5A is shown in Figure A.9-1. During the course of TLTA 5A tests there were also other minor additions: improved break flow instrumentation and improved pressure control simulation. These are discussed later.

### Leakage Paths

The inlet region of a BWR fuel bundle and that of TLTA 5A are shown in Figure A.9-4. Various flow paths of a fuel bundle and the TLTA representations are shown.

Two core-bypass flow paths are included in TLTA 5A. One path allows a proportion of a bundle inlet flow that passes through the side entry orifice to be diverted to the bypass region. Another path permits fluid to flow from the lower plenum through the guide tube and into the bypass region. The orifices (Table A.9-2) in each path have been sized to give the correct flow rates under normal operating conditions.

### Recirculation Line Volume

The volume of the intact recirculation line was 2.79 ft<sup>3</sup> in TLTA 5. In comparison, the volumetrically scaled value is 0.48 ft<sup>3</sup>. The excessive volume of fluid flashes into steam and interacts with the pressure vessel as the blowdown transient progresses. The added steam generation tends to retard the system depressurizations.

In order to improve the simulation of the post lower plenum flashing response, two isolation valves were used in TLTA 5: one each in the suction and drive lines of the intact recirculation loop. These valves were closed after the recirculation pumps coasted down (at ~20 sec). This isolated the major portion of the excess volume, with the remaining volume of ~0.53 ft<sup>3</sup> being close to the desired scale volume.

The blowdown loop has only one valve that closes at the beginning of the transient. This valve does not isolate the mass in the loop but only stops the flow through the recirculating pump.

### Separator Liquid Reservoir

The separator liquid reservoir in TLTA 5 (Figure A.9-5) contained in ~0.52 ft<sup>3</sup> of saturated liquid which, upon flashing, could affect the system response.

It was initially installed to assure that the separator would perform the desired function. Subsequent testing after this reservoir was removed showed that the desired function could still be realized. It was removed in TLTA 5A to improve the blowdown response simulation.

### Measurement System

The basic philosophy of the measuring system is one of obtaining sufficient measurements in order to characterize the system response and perform a mass and energy balance throughout the system. The quantities measured in TLTA include: system pressure, nodal (controlled volume) differential pressure, flow differential pressure, fluid conductivity, fluid temperature, cladding temperature, vessel temperature, valve positions, pump speed, power supply, volume flow, and momentum flux.

The measurement system and its application have been described in detail in the facility description report (Ref. A.9-3). A summary is provided below.

### Measurement Objectives

The measurement system was developed in keeping with the following objectives:

- a. assure that the initial conditions specified for each test were established;
- b. measure the bundle temperature distribution and the power input;
- c. measure fluid conditions in various regions; and
- d. measure the global system pressure response and obtain sufficient data to perform, as practicable, mass and energy balance on the total system and key components, e.g., lower plenum.

### Instrumentation

The instruments used to collect various data in the tests include four pressure transducers, 70 differential pressure transducers, 30 loop thermocouples, 80 cladding thermocouples, 10 conductivity probes, and various other devices such as turbine meters, drag discs, potentiometer (valve position), tachometer, ampmeter, voltmeter, and wattmeter. The output signals from these measuring devices were recorded on a Hewlett-Packard data acquisition system and reduced for further processes on a Honeywell H-6070 system. The details of the function, installation, and application of these instruments are documented in Reference A.9-3. Reference A.9-1 provides detailed schematics of the instrumentation for the TLTA 5 and 5A configurations.

## REFERENCES

- A.9-1 L. S. Lee, et al., "BWR Large Break Simulation Tests - BWR Blowdown/Emergency Core cooling Program," NUREG/CR-2229, April 1982.
- A.9-2 W. S. Hwang and B. S. Schneidman, "BWR Blowdown/Emergency Core Cooling Program 64-Rod Bundle Blowdown Heat Transfer (8x8 BDHT) Final Report," GEAP-NUREG-23977, September 1978.
- A.9-3 W. J. Letzring, "BWR Blowdown/Emergency Core Cooling Program Preliminary Facility Description Report for the BD/ECC1A Test Phase," GEAP-23592, December 1977.
- A.9-4 W. S. Hwang, "BWR Small-Break Simulation Tests With and Without Degraded ECC Systems - BWR Blowdown/Emergency Core Cooling Program," NUREG/CR-2230, January 1982.

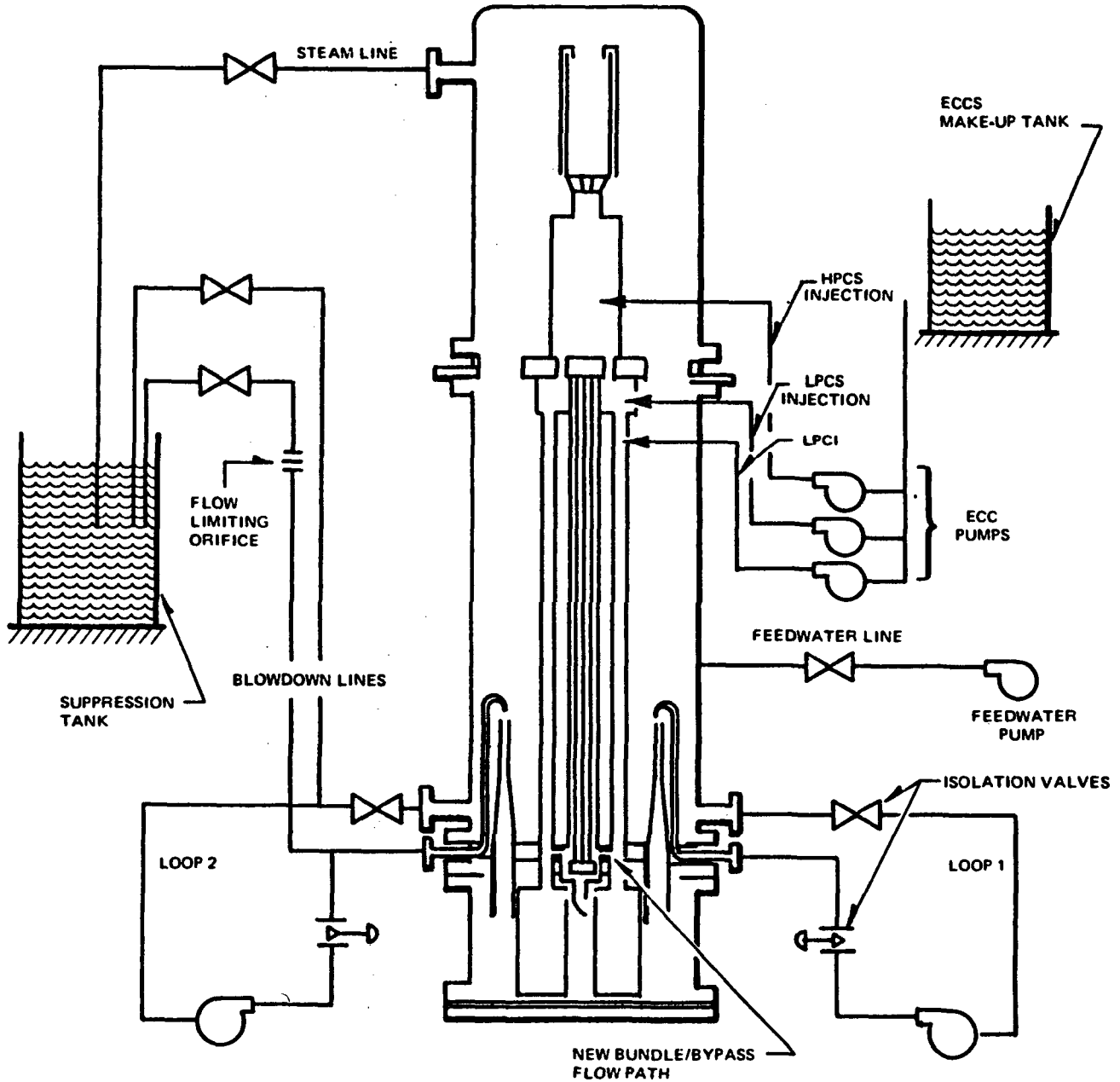


Figure A.9-1 Two-Loop Test Apparatus Configuration 5A (TLTA 5A) with Emergency Core Cooling Systems

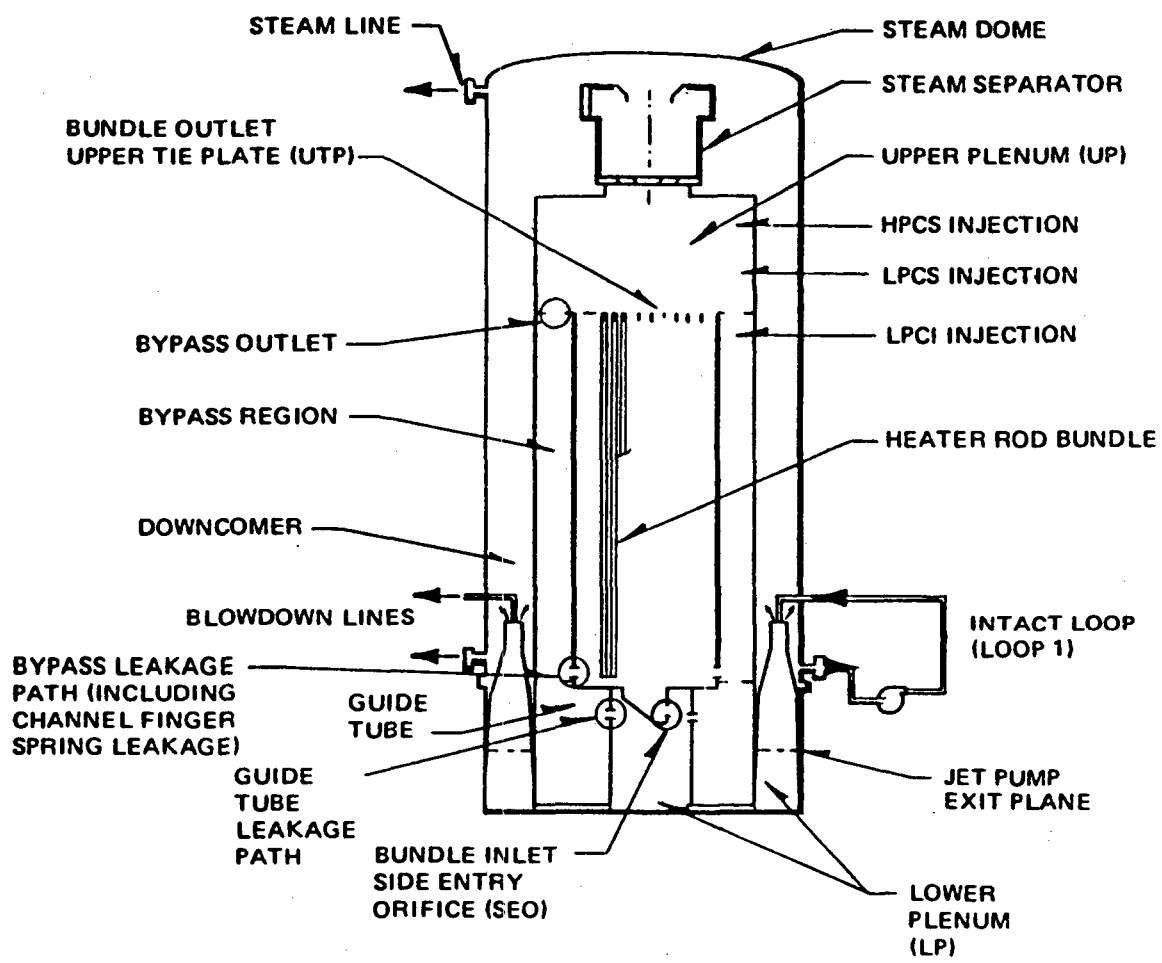


Figure A.9-2 TLTA simulation of BWR regions and flow paths

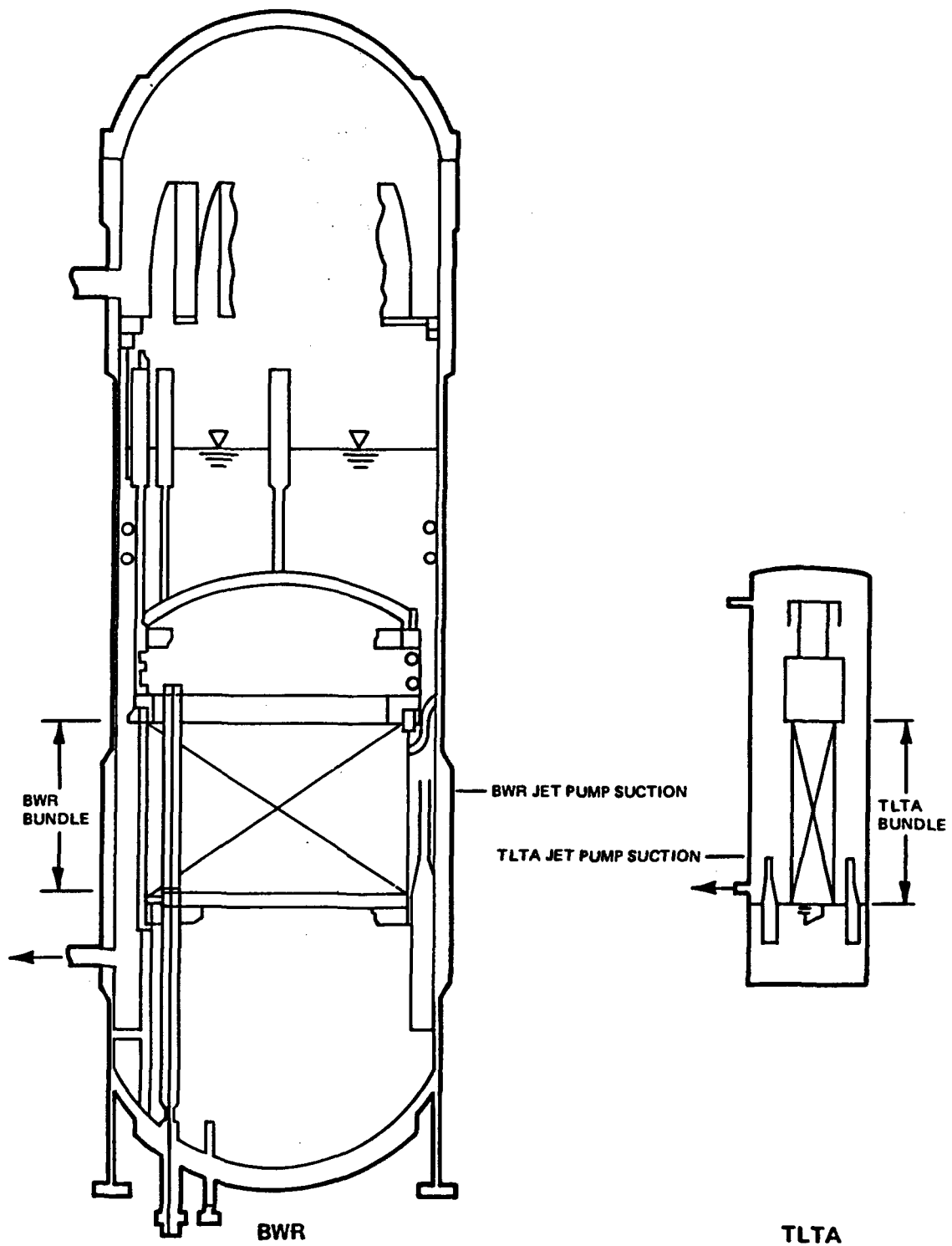


Figure A.9-3 Comparison of jet pump size and elevation between TLTA and BWR (height only to scale, width not to scale)

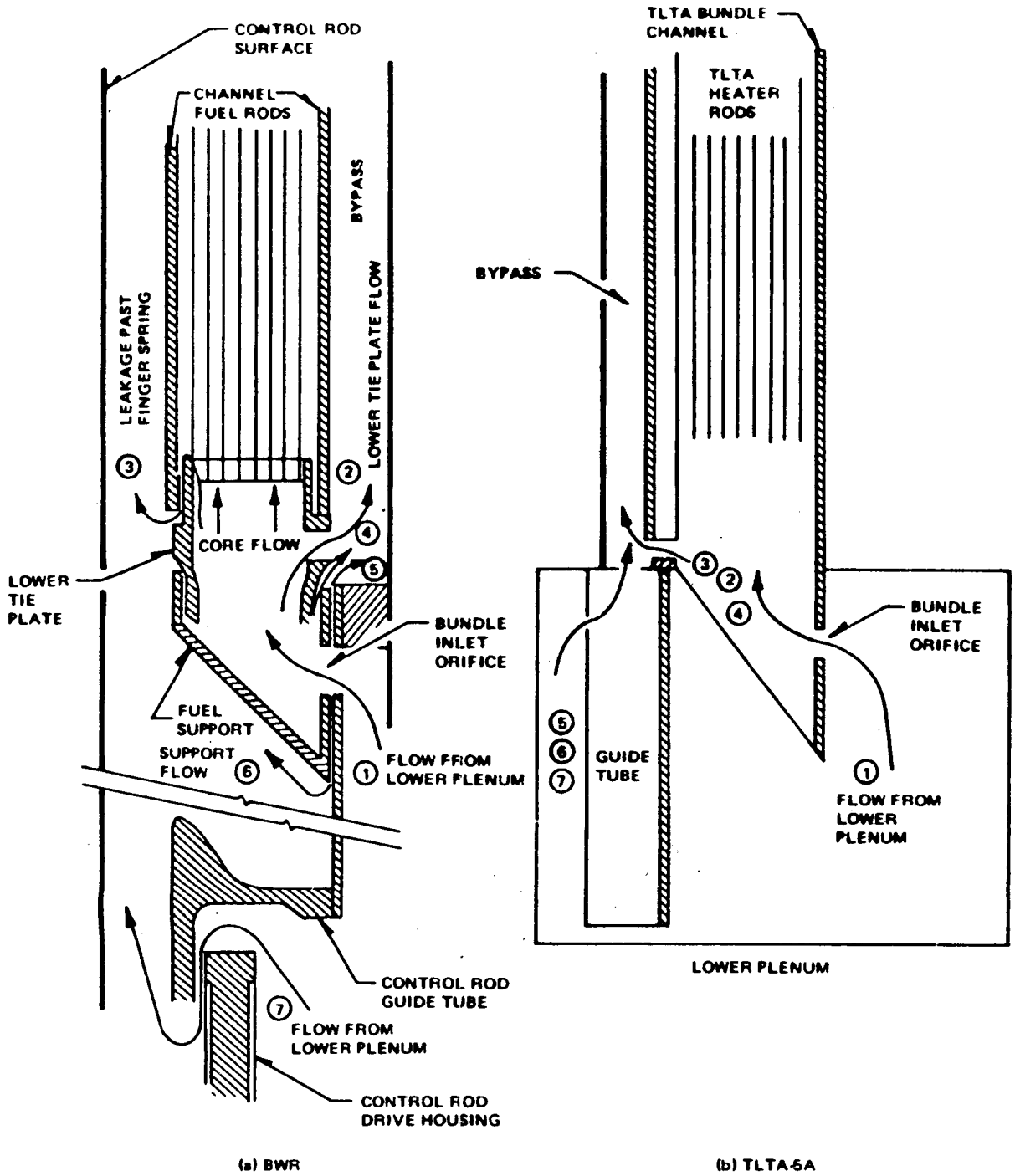


Figure A.9-4 Flow paths at inlet region of a BWR fuel bundle and the TLTA simulation

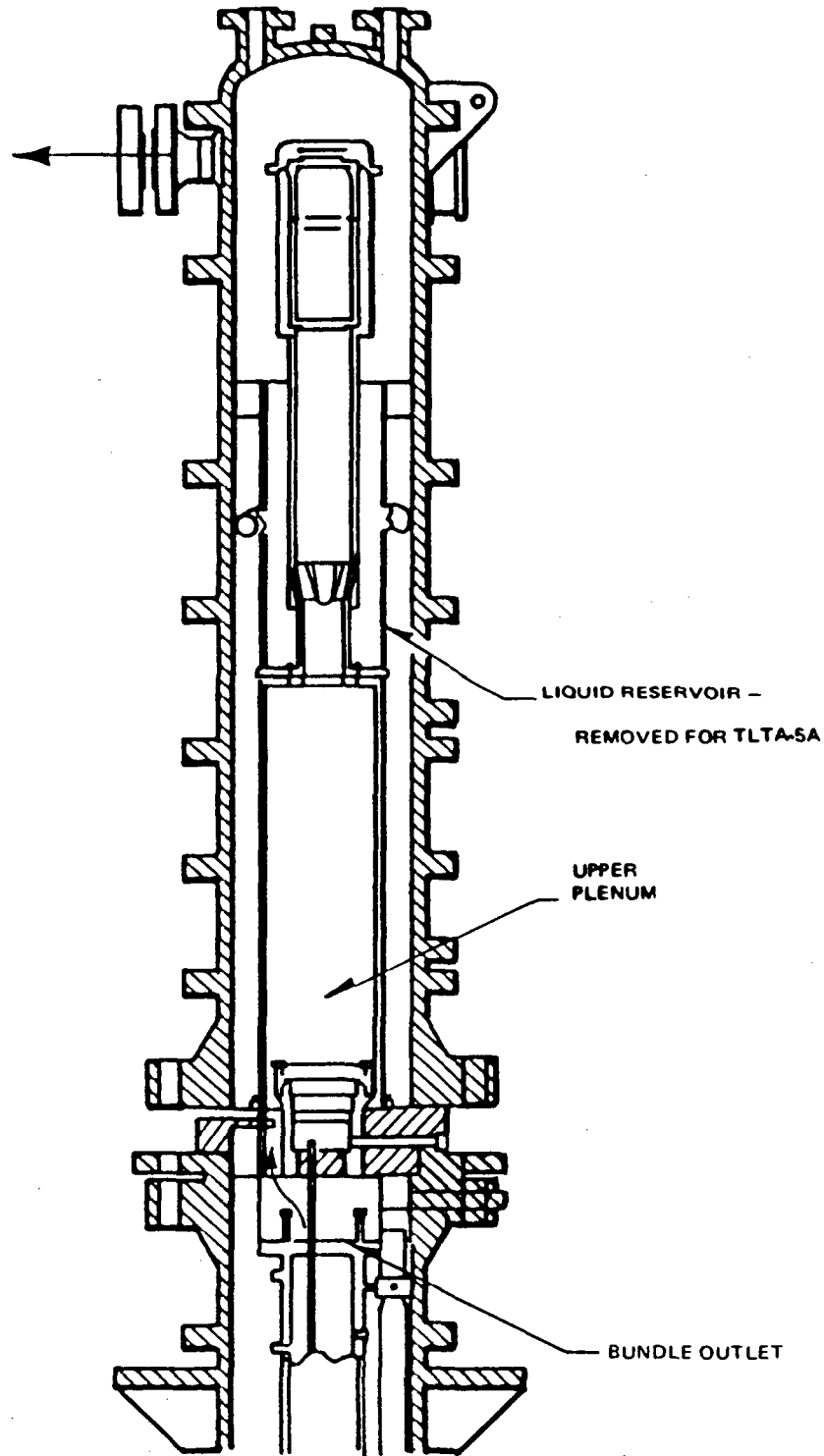


Figure A.9-5 Steam separator liquid reservoir which was removed for TLTA 5A

Table A.9-1 TLTA Test Configurations

TLTA Configuration Number	Scaling Basis	Design Considerations
1	BWR/4, 560 bundles, 7x7 BDHT base line	1. TLTA design used in the 7x7 BDHT program.
2	BWR/4, 560 bundles, 8x8 BDHT base line	1. Replace 7x7 bundles with 8x8 bundles in TLTA. 2. Modify bundle electrode plate and include new electrode connector design.
3	BWR/6, 624 bundles, 8x8 BDHT (same scaling basis as TLTA 1 for BWR/4)	1. Modify lower plenum volume to match BWR/6. 2. Adjust initial mixture level in annulus to match hydraulic timing of BWR/6. 3. Lower feedwater sparger to provide the proper amount of subcooled liquid in downcomer. 4. Steam line pressure control characteristics of BWR/6. 5. Initial power for 8x8 bundle in BWR/6. 6. Break geometry modified to provide scaled BWR/6 break flow for entire transient (including the subcooled discharge regime). 7. Scaled single side entry orifice for core inlet flow.
4	BWR/6, 624 bundles, 8x8 BDHT, base line design for BD/ECC	1. Modify flow geometry at core exit and at bypass exit to account for counter-current flow limiting (CCFL) phenomena along these flow paths.

Table A.9-1 (Continued)

TLTA Configuration Number	Scaling Basis	Design Considerations
4 (cont)		<ol style="list-style-type: none"> <li>2. Lower the jet pump suction inlet and extend the jet pump diffuser/tailpipe into the lower plenum to preserve the timing of the cost-down period and to achieve a more representative lower plenum geometry.</li> <li>3. Provide for more representative stored heat effects by adding insulation to lower plenum.</li> </ol>
5	BWR/6, 624 bundles, BD/ECC 1A, early ECC interaction scoping series	<ol style="list-style-type: none"> <li>1. Implemented ECCS injection systems.</li> </ol>
5A	BWR/6, 624 bundles, BD/ECC 1A, ECC interaction with improved simulation	<ol style="list-style-type: none"> <li>1. Add bundle to bypass leakage paths to improve simulation of the flow paths at the inlet region of a BWR/6.</li> <li>2. Include an isolation valve in both the suction and drive lines of the intact recirculation loop to improve simulation of post lower plenum flashing response.</li> <li>3. Remove the separator liquid reservoir to improve transient simulation.</li> <li>4. Improve power control by using a new controller for the bundle power supply.</li> </ol>

Table A.9-2 Flow areas and correlations for TLTA large-break tests

Flow location	Flow area	Correlation*
	(in <sup>2</sup> )	W(lbm/sec), ΔP(psi), ρ(lbm/ft <sup>3</sup> )
Bundle inlet orifice	4.638	$W = 2.48 [\Delta P \times \rho]^{1/2}$
Bypass leakage	0.2732	$W = 0.119 [\Delta P \times \rho]^{1/2}$ forward flow $W = 0.113 [\Delta P \times \rho]^{1/2}$ reverse flow
Guide tube leakage	0.0908	$W = 0.0379 [\Delta P \times \rho]^{1/2}$
Bypass outlet	0.160	
Bundle outlet (UTP)	11.3	
Bundle	15.15	
Bypass	15.83	
Steam line orifice	3.237	
Suction line break nozzle	0.4336	
Drive line break orifice	0.0804	
HPCS orifice	0.1307	$W = 0.0645 [\Delta P \times \rho]^{1/2}$
LPCS orifice	0.1706	$W = 0.069 [\Delta P \times \rho]^{1/2}$
LPCL orifice	0.1225	$W = 0.0515 [\Delta P \times \rho]^{1/2}$

\*Note: Determined for single-phase water calibration data.

Table A.9-3 Relative volume distributions

Region	Volumes (ft <sup>3</sup> ) "Ideal" TLTA <sup>a</sup>	TLTA 5 and 5A
Lower Plenum	2.97	3.09
Core	1.38	1.38
Upper Plenum	2.34	2.78
Separation Region	8.21	11.76
Downcomer	2.88	2.88
Recirculation Loop No. 2	0.48	2.09
Recirculation Loop No. 1	0.48	2.79 (0.53) <sup>b</sup>
Bypass	1.05	1.01
Steam Dome	5.09	5.29
Guide Tube Volume	2.03	1.90
<u>Fluid Volumes Governing</u> <u>Key Events Timing</u>		
Volume of saturated liquid in the separation region	3.26	3.26
Volume from jet pump support plate to jet pump throat	1.37	1.37
Volume of inventory in annulus	6.15	6.15
Volume of subcooled liquid in annulus	2.89	2.89

<sup>a</sup>Ideal TLTA Volumes = BWR/6 Volumes ÷ 624.

<sup>b</sup>TLTA 5A recirculation loop volume after isolation valves closed.

## A.10 ROSA-III FACILITY

The Rig of Safety Assessment (ROSA)-III program is conducted by the Japan Atomic Energy Research Institute (JAERI). It was begun in 1976 to study the thermal-hydraulic response of a BWR to postulated LOCA conditions. In addition, the program was intended to provide data for and perform assessments of thermal-hydraulic computer codes. The ROSA-III facility was completed in 1978 to provide a test bed for the program. The design objective of the facility was to produce the significant thermal-hydraulic phenomena that would occur in commercial BWRs in the same sequence and with approximately the same time frames and magnitudes, (Ref. A.10-1). Of particular interest to the prediction of LOCA response is the performance of the emergency core cooling systems (ECCS). The ROSA-III program was thus designed to provide data to evaluate the quantitative margins of safety inherent in the performance of the ECCS.

The ROSA-III facility is a volumetrically scaled (1/424) simulated BWR system with an electrically heated core. It was designed to simulate a LOCA in a standard BWR/6 plant of the General Electric Co. product line. Table A.10-1 lists important scaling comparisons between ROSA-III and a BWR/6 with a vessel inside diameter of 251 in. Figure A.10-1 is a schematic diagram of the facility, and Figure A.10-2 shows the steady-state coolant flow in the vessel and the ECCS flows during a LOCA. Both figures were taken from Reference A.10-2, which contains details of the design, operation, and instrumentation of the facility.

Two symmetrical recirculation loops are provided. Each loop contains two jet pumps that receive their drive flow from the same recirculation pump. The simulated broken loop is equipped with a sharp-edged orifice and a quick-opening blowdown valve. A typical BWR ECCS is simulated with high-pressure core spray (HPCS) and low-pressure core spray (LPCS) injected into the upper plenum. Low-pressure coolant injection (LPCI) is pumped through a circular sparger in the upper core bypass region. The automatic depressurization system (ADS) is simulated in one branch of the steam line. Also located in the steam line are a simulated main steam isolation valve (MSIV) and a safety relief valve (SRV).

Four half-length electrically heated bundles make up the ROSA-III core. This allows the simulation of multibundle behavior. Each bundle contains 62 heated rods and 2 water rods in an 8 x 8 array. One bundle represents a high-power bundle, and the others represent average-power bundles.

Several series of tests have been conducted in the ROSA-III facility. Natural circulation tests yielded the following results (Ref. A.10-3):

1. The ROSA-III test facility can simulate the ratio of the water level heights inside and outside the core shroud in a BWR system during natural circulation in the low-power or low-flow-rate region.
2. The decay heat can be removed by natural circulation if the downcomer liquid level is maintained above the jet pump suction line.

Steam line break tests have been conducted for a variety of break sizes. Results indicate a peak cladding temperature of 1008 K (Ref. A.10-3). Small-break tests (Ref. A.10-4) and large-break tests (Ref. A.10-5) have also been performed.

Results from the double-ended (large break LOCA) break test series and analysis indicate that (Ref. A.10-5):

1. The similarity between the ROSA-III test and a BWR LOCA has been confirmed through the comparison of calculated results for the ROSA-III and a BWR system.
2. The measured peak cladding temperature was well below the present safety criterion of 1473 K, even with the single failure assumption in ECCS.

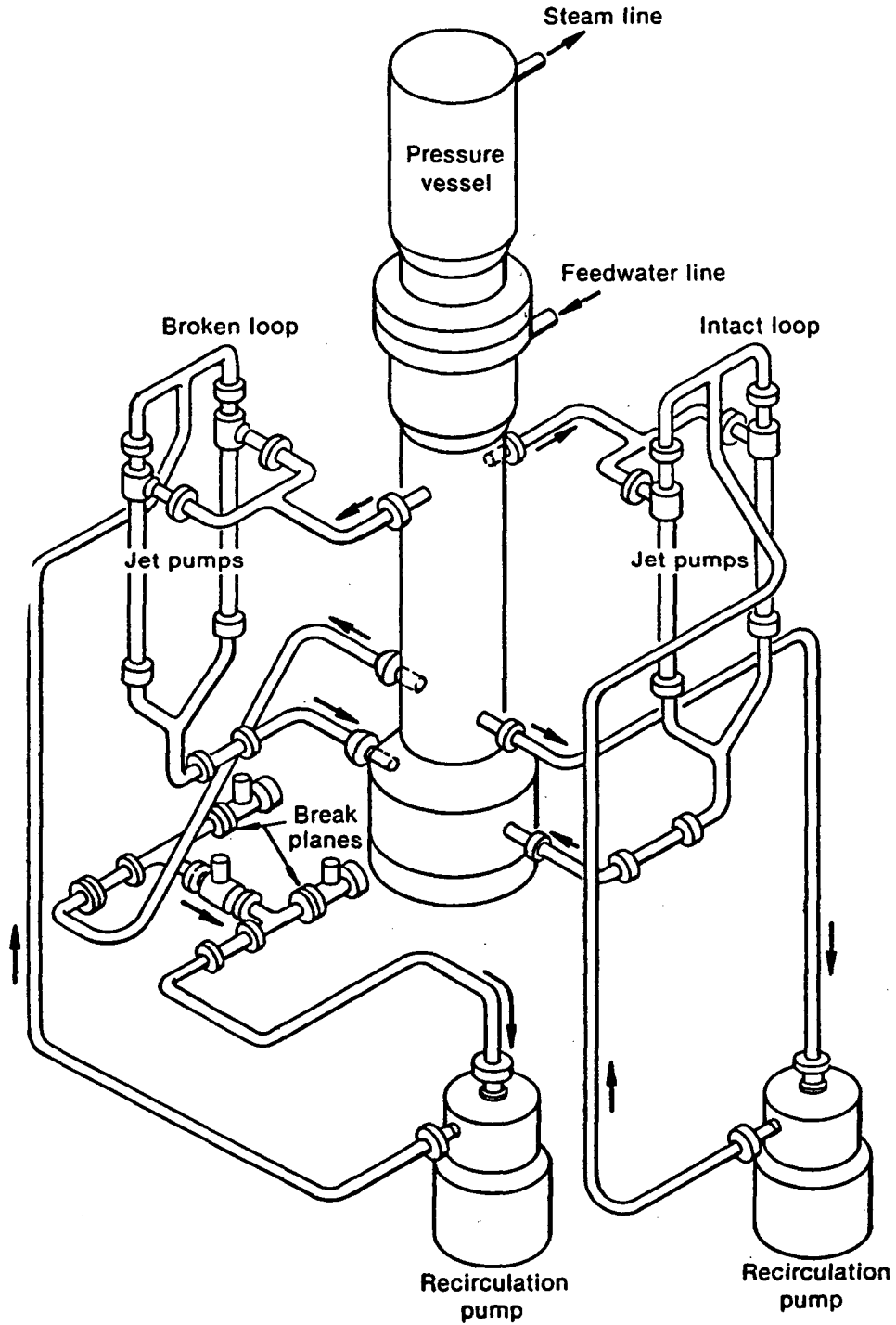
It is anticipated that, as further test data are analyzed and released by JAERI, the impact of ROSA-III on nuclear safety issues will be realized.

#### REFERENCES

- A.10-1 K. Tasaka and M. Shiba, "ROSA-III Program at JAERI for BWR LOCA/ECCS Integral Tests," ANS Conference on Thermal Reactor Safety, Knoxville, Tennessee, April 6-10, 1980.
- A.10-2 Yoshinari Anoda et al., "ROSA-III System Description for Fuel Assembly No. 4," JAERI-M 9363, February 1981.
- A.10-3 K. Tasaka et al., "Steam Line Break, Jet Pump Drive Line Break and Natural Circulation Tests in ROSA-III Program for BWR LOCA/ECCS Integral Tests," Eleventh Water Reactor Safety Research Information Meeting, Gaithersburg, Maryland, October 24-28, 1983.
- A.10-4 Yoshinari Anoda et al., "Experiment Data of ROSA-III Integral Test Run 912 (5% Split Break Test Without HPCS Actuation)," JAERI-M 82-010, 1982.
- A.10-5 K. Tasaka et al., "ROSA-III Double-Ended Break Test Series for a Loss-of-Coolant Accident in a Boiling Water Reactor," Nuclear Technology, 68, January 1985.

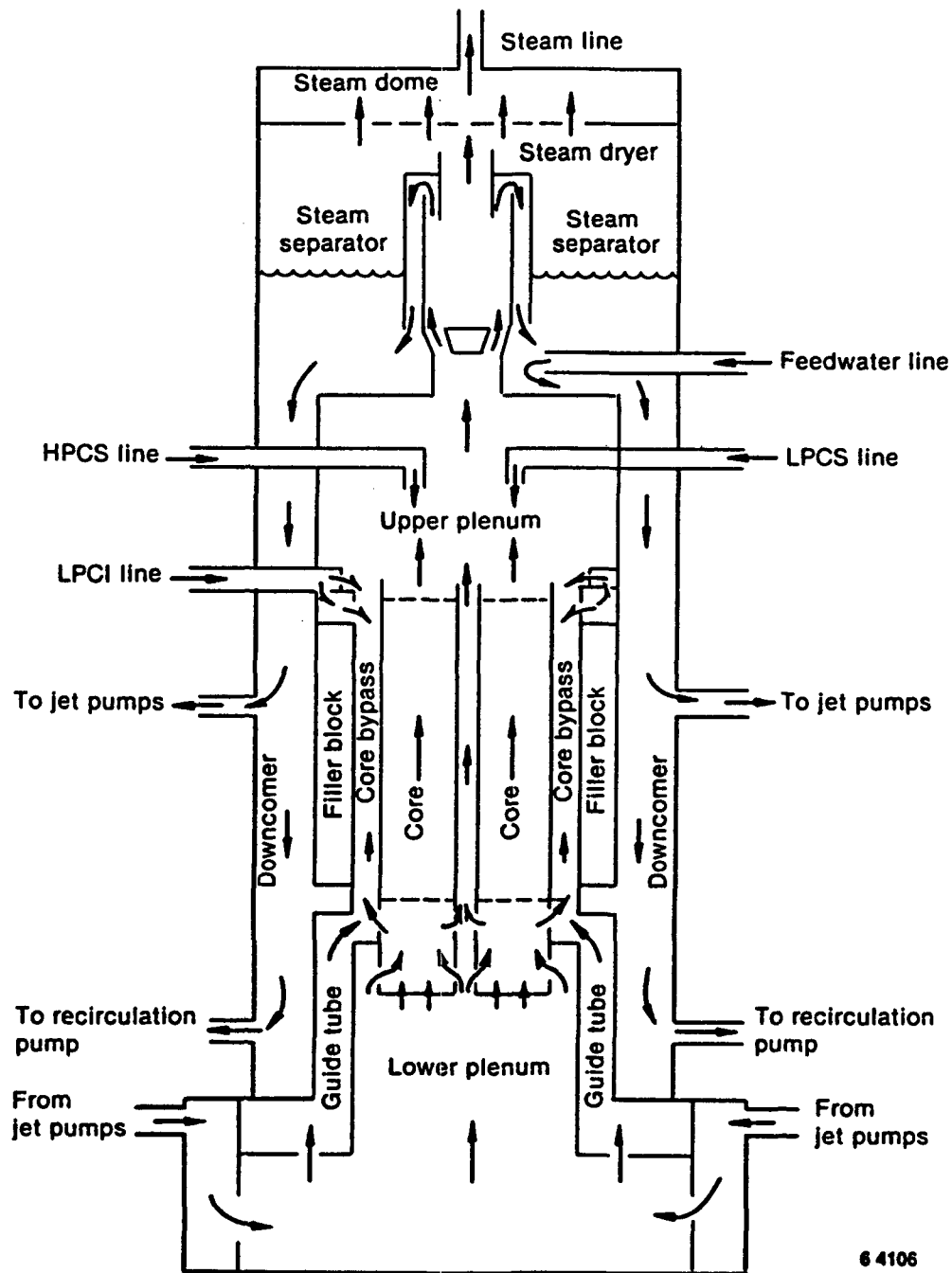
TABLE A.10-1 Scaling comparisons of ROSA-III and a BWR-6

	<u>BWR-6</u>	<u>ROSA-III</u>	<u>BWR-6/ROSA-III</u>
Number of recirculation loops	2	2	1
Number of jet pumps	24	4	6
Number of separators	251	1	251
Number of fuel assemblies	848	4	212
Active fuel length (m)	3.76	1.88	2
Total volume (m <sup>3</sup> )	621	1.42	437
Power (MW)	3800	4.40	864
Pressure (MPa)	7.23	7.23	1
Core flow (kg/s)	1.54 x 10 <sup>4</sup>	36.4	424
Recirculation flow (l/s)	2970	7.01	424
Feedwater flow (kg/s)	2060	4.86	424
Feedwater temperature (K)	489	489	1



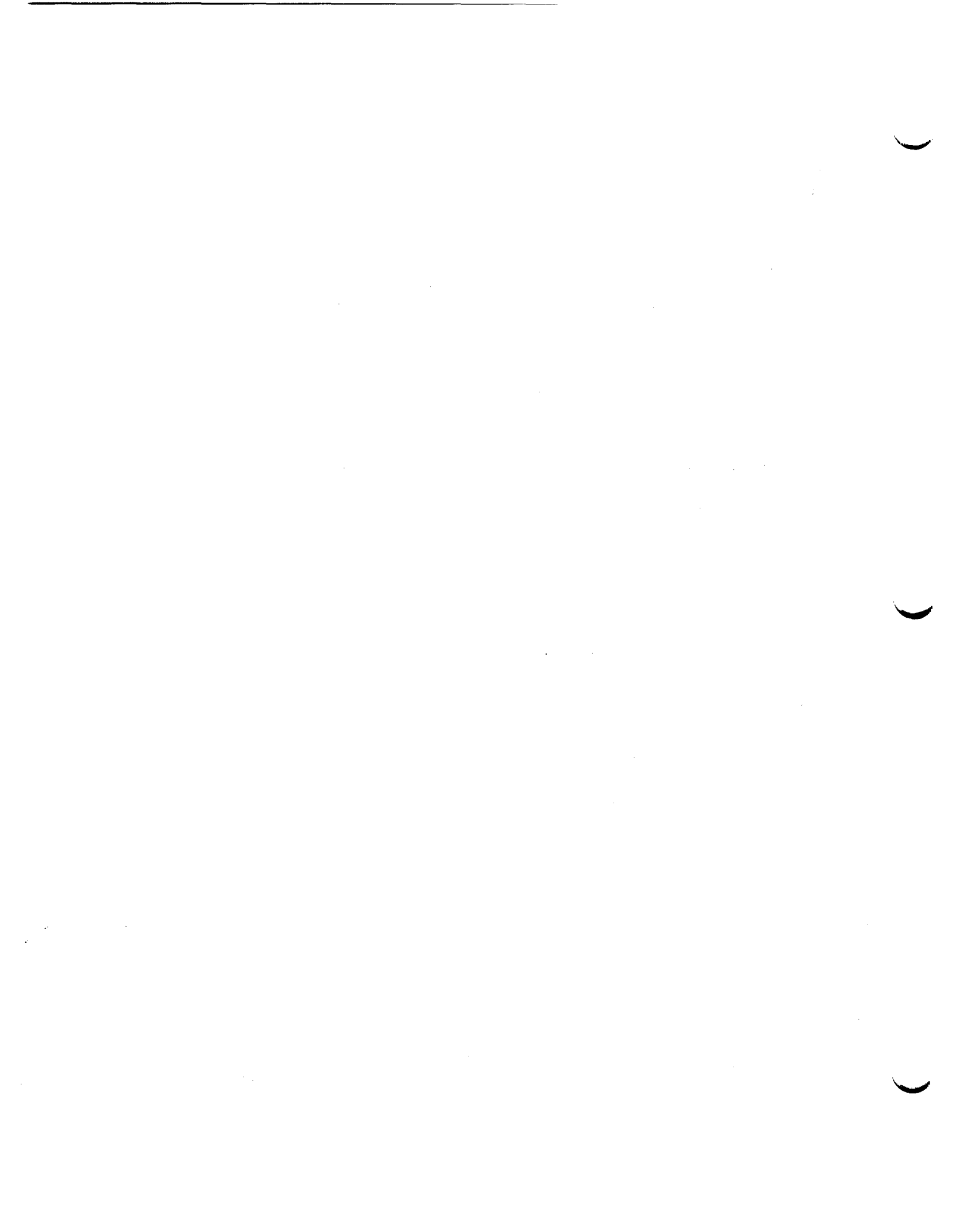
6 4105

Figure A.10-1 Schematic diagram of the ROSA-III facility



6 4106

Figure A.10-2 Diagram showing coolant flow in the ROSA-III vessel



## A.11 ROSA-IV LARGE-SCALE TEST FACILITY

The Rig of Safety Assessment No. 4 (ROSA-IV) Program (Ref. A.11-1) was instituted in 1980 by the Japan Atomic Energy Research Institute (JAERI). One of the major tasks of the ROSA-IV Program is that of conducting large-scale integral simulation of a typical 3423 Mwt, 4-loop Westinghouse (W) PWR using the ROSA-IV Large-Scale Test Facility (LSTF). An artist's overall view of the ROSA-IV LSTF is shown in Figure A.11-1. The flow diagram of ROSA-IV is shown in Figure A.11-2. The NRC joined the ROSA-IV Program in early 1984 and is providing advanced two-phase instruments, computer codes, and analysis assistance in support of the LSTF testing.

### Objectives

The purpose of the tests underway and planned at LSTF is to provide large-scale test data on the transient performance of PWRs under small-break LOCA and transient conditions and on the effectiveness of emergency safeguards systems and procedures under such conditions. The tests will also provide experimental data on two-phase flow in PWRs. Specifically, LSTF is being used to:

1. Study the effectiveness of the ECCS under small-break LOCA and plant transient conditions. Both standard and potential alternative ECCSs will be evaluated.
2. Study the effectiveness of secondary-side cooling via the steam generators under small-break LOCA and plant transient conditions.
3. Examine the nature of forced and natural circulation cooling in PWRs in various flow regimes and cooling modes and in transition from one flow regime or mode of cooling to another.
4. Examine the effect of break size and location on system behavior.
5. Study the effects of incondensable gases on system behavior during a small-break LOCA or plant transient.
6. Investigate alternative design systems and procedures that are being considered to improve system performance during small-break LOCA or plant transient.
7. Provide test data for developing or assessing the small-break LOCA analytical models.

### Safety Issues To Be Addressed

Since the ROSA-IV LSTF is a very large scale integral test facility, data obtained from the tests cannot only expand the existing data base, but also address the scaling issues for these tests. The tests identified below are underway or planned.

Small-Break LOCA Tests. These tests are direct, continuous simulations of PWR small-break LOCAs from the time of break to completion of plant recovery. Parameters to be investigated are:

1. Break area,
2. Break location,
3. Break orientation,
4. Break size,
5. ECCS capacity.

Operational Transient Tests. These tests are direct, continuous simulations of PWR operational transients from the scram to the completion of plant recovery. Transients to be investigated are:

1. Reactor undercooling transients resulting from loss of feedwater, loss of load, or loss of residual heat removal (RHR) system.
2. Reactor overcooling transients resulting from sudden increase in the feedwater flow or a main steam line or feedwater line rupture.
3. Loss of electric power transients resulting from loss of offsite power or loss of total AC power (station blackout) will be simulated.

TMI Simulation Tests. These tests are simulations of TMI-type accidents in Westinghouse PWRs.

Advanced Tests. These tests are simulations of the performance of alternative ECCS designs, alternative plant recovery procedures, or both during a small-break LOCA or a transient.

Core Cooling Tests (Separate-Effects Tests). These tests are experiments on the overall system behavior of a PWR under specific, predetermined thermal-hydraulic conditions. Series of steady-state or relatively slow transient tests are planned. These tests will supplement separate-effects tests at the TPTF (Ref. A.11-2), and will provide data for developing and assessing the best-estimate codes. Tests to be performed include:

1. Forced (pumped) circulation core cooling tests with circulation flow rate, reactor coolant inventory, and core power level as parameters.
2. Natural circulation core cooling tests with reactor coolant inventory, secondary coolant inventory, core power level, and amount of noncondensables, etc., as parameters.
3. Once-through mode core cooling tests with once-through core flow due to break flow or due to feed and bleed through the pressurizer PORVs and without forced or natural circulation.

#### Design Specification and Scaling Method

The LSTF is an experiment facility designed as a full-height model of the primary system of the reference PWR. The four primary loops of the reference PWR are represented by two equal-volume loops. The overall facility scaling factor is 1/48. Table A.11-1 shows the major design characteristics of the ROSA-IV LSTF and reference PWR plant. The overall scaling factor used for designing LSTF is described below.

1. Elevations are preserved; i.e., there is one to one correspondence with the reference PWR (Fig. A.11-3). Because the LSTF hot and cold leg inner diameters (IDs) are smaller than those of the reference PWR, only the top of the primary hot and cold legs (IDs) were set equal to those of the reference PWR. The primary characteristics of the pressure vessel and core are summarized in Table A.11-2.
2. Volumes are scaled by the facility scaling factor, 1/48.
3. Flow areas are scaled by 1/48 in the pressure vessel and by 1/24 in the steam generators (see Table A.11-2). However, the hot and cold legs were scaled to conserve the ratio of the length to the square root of pipe diameter, i.e.,  $L/\sqrt{D}$ , for the reference PWR. Such an approach was taken to better simulate the flow regime transitions in the primary loops.
4. Core power is scaled by 1/48 at core powers equal to or less than 14% of the scaled reference PWR rated power. The LSTF rated and steady-state power is 10 Mwt, i.e., 14% of the rated reference PWR core power scaled by 1/48.
5. Fuel assembly dimensions, i.e., fuel rod diameter, pitch and length, guide thimble diameter pitch and length, and ratio of number of fuel rods to number of guide thimbles, are designed to be the same as those of a 17x17 fuel assembly of the reference PWR to preserve the heat transfer characteristics of the core. The total number of rods was scaled by 1/48 and is 1064 for heated and 104 for unheated rods (Fig. A.11-4).
6. Design pressures are roughly the same as those in the reference PWR.
7. Fluid flow differential pressures ( $\Delta P$ s) are designed to be equal to those in the reference PWR for scaled flow rates.
8. Flow capacities are scaled by the overall scaling factor where practical.

#### Description of Primary and Secondary Coolant Systems and Other Systems

Primary Coolant System. The primary system consists of the pressure vessel, primary loop piping, including steam generator U tubes, primary coolant pumps, and a pressurizer. Figure A.11-5 compares LSTF and PWR pressure vessel dimensions. The coolant flow paths inside the vessel under normal and accident or transient conditions are shown in Figure A.11-6. The core contains 16 square 7x7 and 8 semi-crescent electrically heated rod assemblies. These assemblies are divided into three groups to simulate heat generation in the reference PWR core, as shown in Figure A.11-7. The bundle peaking factor can be changed according to test needs. The rod axial power profile is chopped cosine in shape with a peaking factor of 1.495.

The LSTF primary coolant loop consists of two identical loops, each representing two loops of the reference four-loop PWR. Figure A.11-8 shows the primary loop dimensions in plan view. There are only two different pipe sizes used in the whole loop. Pipes with 207 mm ID and 295 mm OD are used for hot and cold legs, while pipes with 168.2 mm ID and 240.2 mm OD are used for the cross-over legs.

The primary coolant pumps used in the loops are canned centrifugal pumps. The pump capacity is approximately 20% of the scaled capacity at 1/24. The pump speed can be adjusted to simulate the transient flow characteristics of the reference PWR primary coolant pump.

The pressurizer is scaled to have 1/48 of the volume and the same height-to-diameter ratio as the pressurizer of the reference PWR. It consists of a cylindrical vessel 4.19 m high. It has immersion-type electrical heaters. Normally the pressurizer is connected through the surge line to the hot leg, but provisions have been made to allow connection to the upper head of the vessel. The purpose is to test the effectiveness of system pressure control for this alternative method. Any incondensable gas or vapor accumulating in the vessel upper head can be vented through this line. The power-operated relief valve and safety valve are also designed to simulate those in the reference PWR.

Secondary Coolant System. The secondary system consists of the steam generators, main and auxiliary feedwater pumps, and the steam condensing system, which simulates the turbine generator and condensing system of the reference PWR.

Figure A.11-9 shows the steam generators used in LSTF, and Table A.11-3 presents the primary design characteristics in comparison with the reference PWR. The LSTF steam generator has a scaled height of 1/1. The downcomer is simulated by four pipes located outside the steam generator vessel to give satisfactory simulation of the downcomer volume and width.

The main feedwater pump is a canned centrifugal pump. Its characteristics can be simulated by the pump and the control valves. The auxiliary feedwater pump is a plunger-type pump. It can simulate the flow characteristics of the reference PWR pumps. The steam condensation system is the so-called jet condenser, which is composed of a spray and cooling unit.

Other Systems. The blowdown system consists of a break unit, blowdown piping, and a break flow storage tank. Nineteen break locations are provided in LSTF as summarized in Table A.11-4. LOCA induced by the malfunctions of the pressurizer relief or safety valve can be simulated by opening the valve without using the break unit. The break orifice sizes are summarized in Table A.11-5.

The emergency core cooling systems consist of a high-pressure injection system (HPIS), a low-pressure injection system (LPIS), an accumulator (ACC) injection system, and a residual heat removal (RHR) system. The injection locations are summarized in Table A.11-6. The injection locations are selected in accordance with test conditions.

The control system has a process control unit and operation and monitoring sections. The process control unit includes the feedback control system, the sequence control system, and the arithmetic computing unit. By using this system, most reference PWR control systems can be simulated.

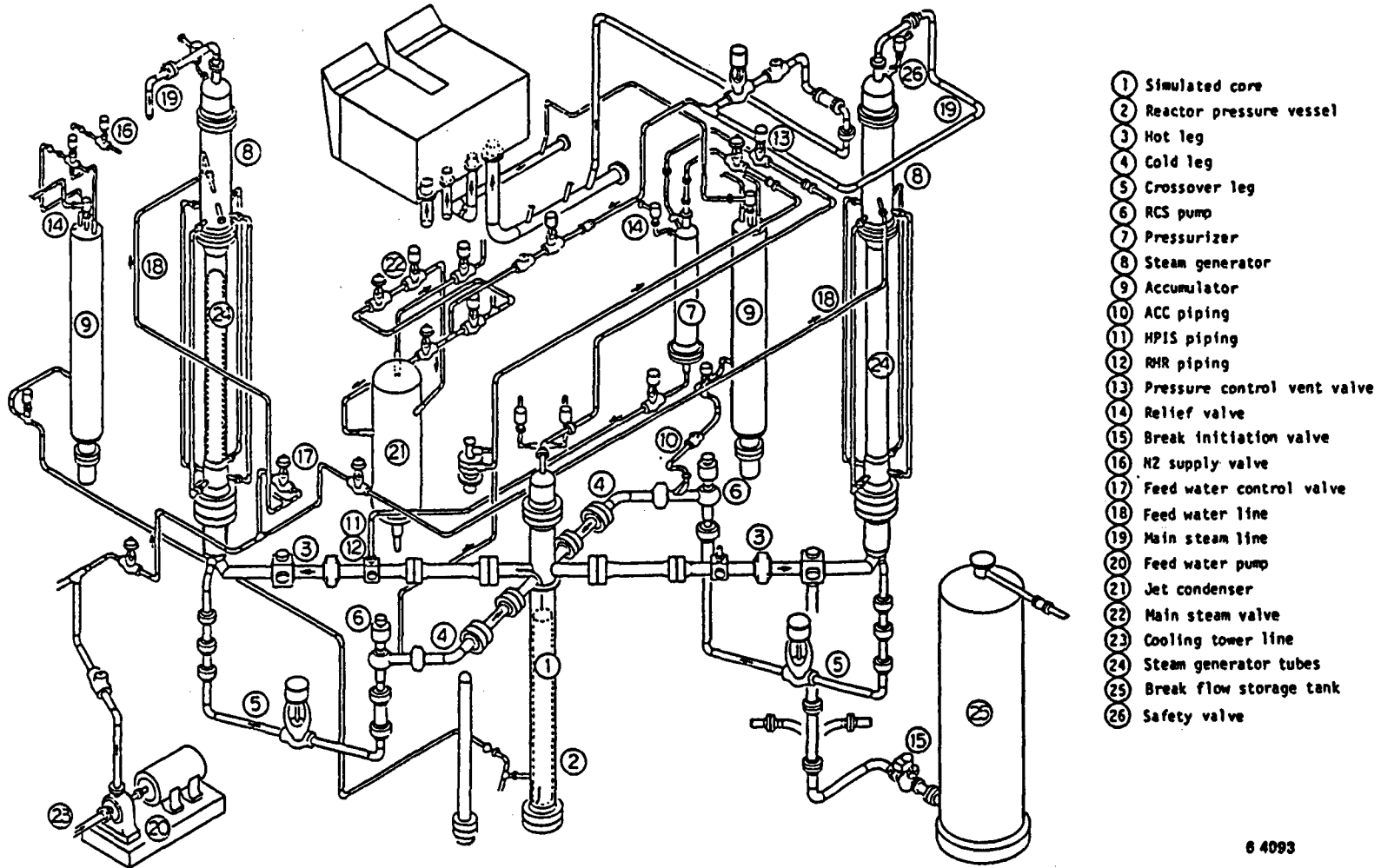
### Summary

The LSTF is the integral test facility for PWR small break LOCAs and operational transients. The facility is well designed to preserve the thermal-hydraulic

phenomena in a PWR and well instrumented to measure the thermal-hydraulic response during the accidents and transients.

#### REFERENCES

- A.11-1 The ROSA-IV group, "ROSA-IV Large Scale Test Facility (LSTF) System Description," Japan Atomic Energy Research Institute, JAERI-M 84-237, 1985.
- A.11-2 H. Nakamura et al., "System Description for ROSA-IV Two-Phase Test Facility (TPTF)," Japan Atomic Energy Research Institute, JAERI-M 83-042, 1983.



- ① Simulated core
- ② Reactor pressure vessel
- ③ Hot leg
- ④ Cold leg
- ⑤ Crossover leg
- ⑥ RCS pump
- ⑦ Pressurizer
- ⑧ Steam generator
- ⑨ Accumulator
- ⑩ ACC piping
- ⑪ HPIS piping
- ⑫ RHR piping
- ⑬ Pressure control vent valve
- ⑭ Relief valve
- ⑮ Break initiation valve
- ⑯ N2 supply valve
- ⑰ Feed water control valve
- ⑱ Feed water line
- ⑲ Main steam line
- ⑳ Feed water pump
- ㉑ Jet condenser
- ㉒ Main steam valve
- ㉓ Cooling tower line
- ㉔ Steam generator tubes
- ㉕ Break flow storage tank
- ㉖ Safety valve

6 4093

Figure A.11-1 Overall view of the ROSA-IV Large Scale Test Facility



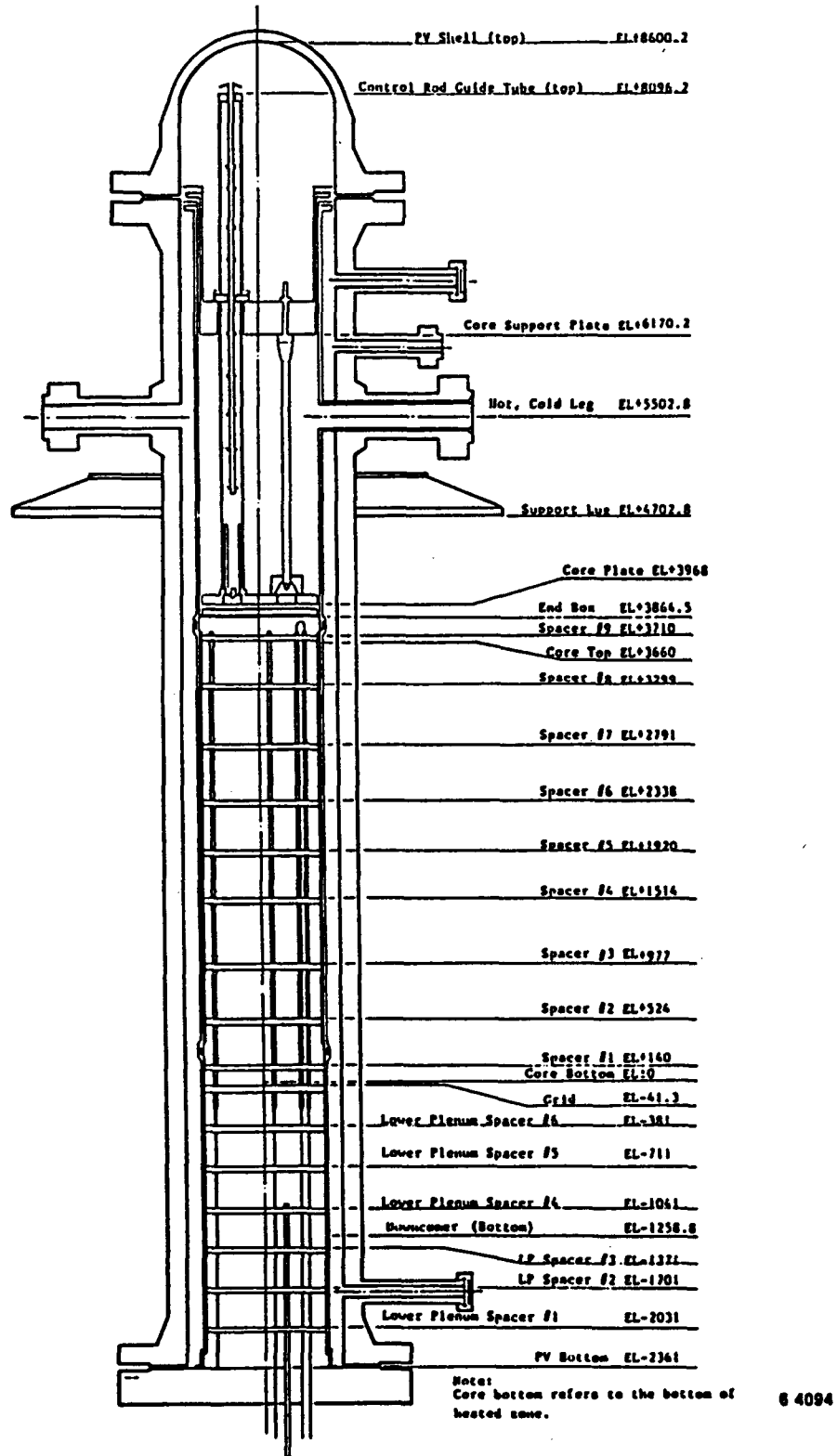
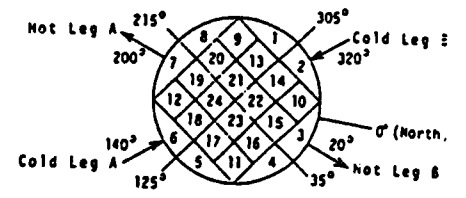
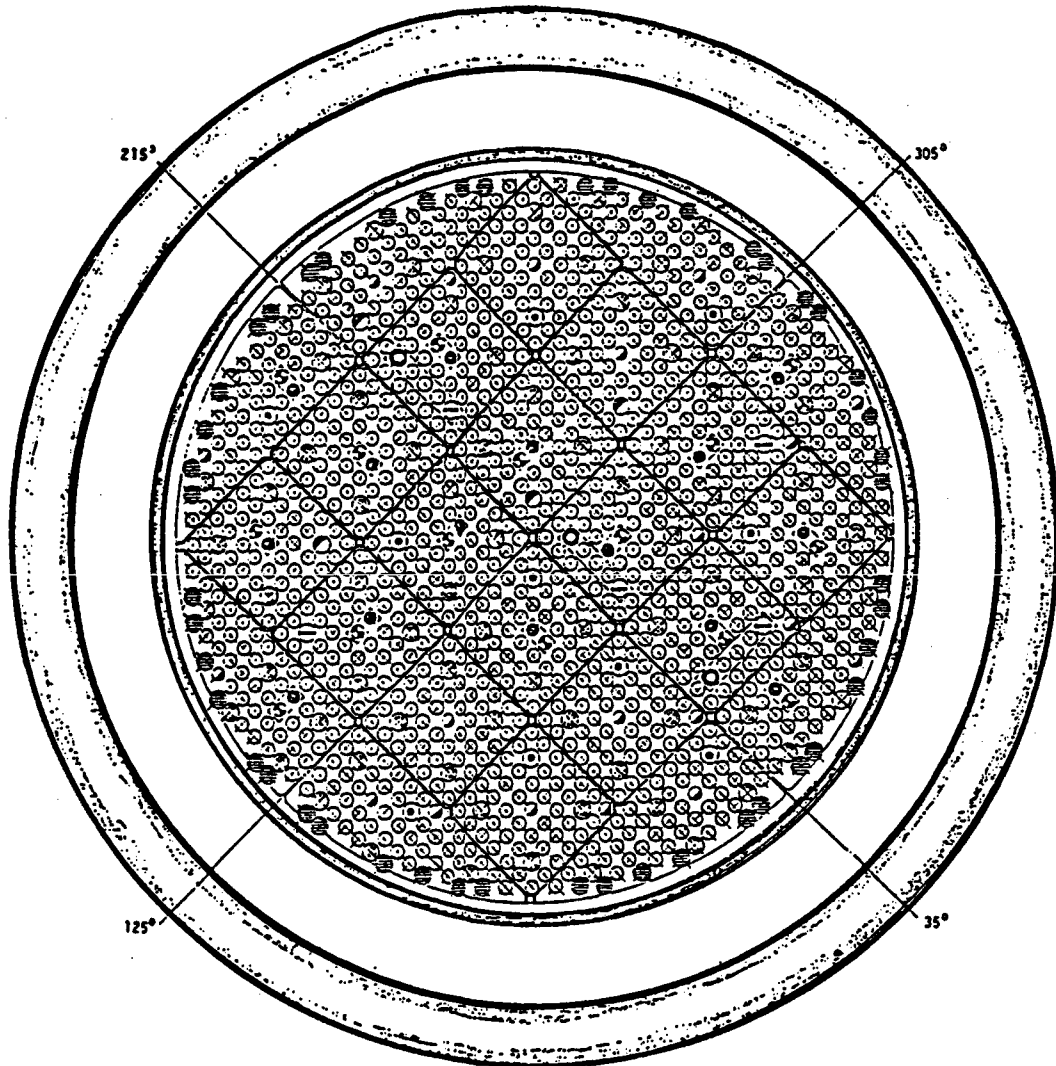


Figure A.11-3 ROSA-IV Large Scale Test Facility pressure vessel

A-107



- Heater Rods
- Non Instrumented
  - } with Cladding Temp. TCs
  - ⊙ } with Cladding Temp. TCs
- Non-Heating, Instrumented Rods
- with Conduction Probes
  - ⊙ with Fluid Temp. TCs
  - ⊙ with Fluid Temp. TCs
  - ⊙ with Rod Surface Temp. TCs
- ⊙ Tie Rod
- ⊙ Dummy Rod

6 4095

Figure A.11-4 Cross section and heater rod arrangement of the ROSA-IV Large Scale Test Facility

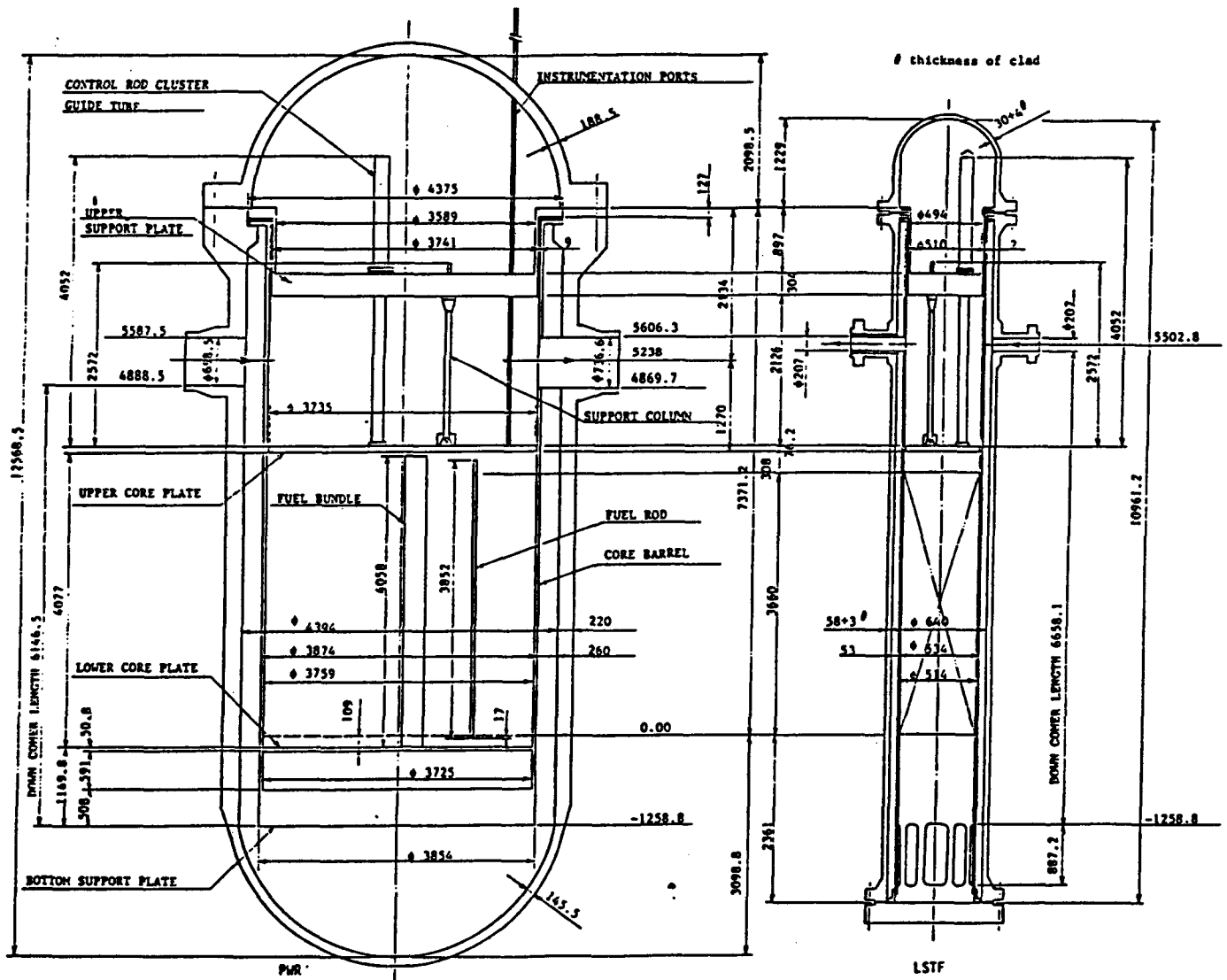
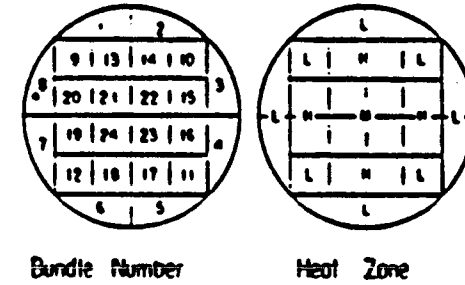
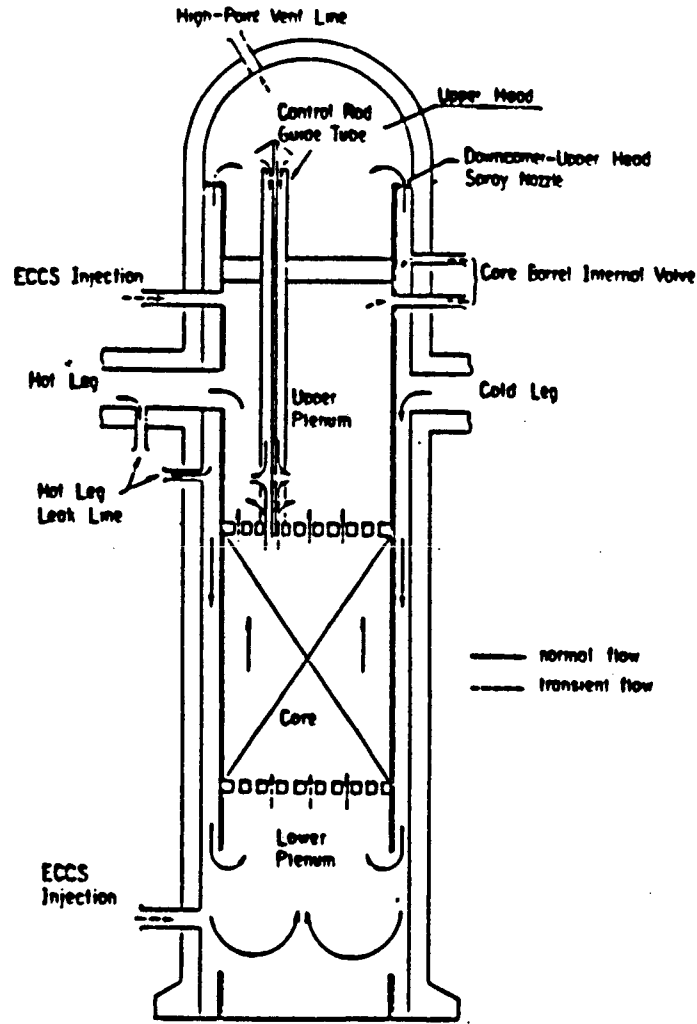


Figure A.11-5 Comparison of LSTF and PWR pressure vessel dimensions



Heat Zone	Peaking Factor		
	Case 1	Case 2	Case 3
L	1.00	0.71	0.66
M	1.00	1.0	1.00
H	1.00	1.44	1.51

Figure A.11-6 Coolant flow path in pressure vessel

Figure A.11-7 Fuel bundle power output distribution in core

A-110

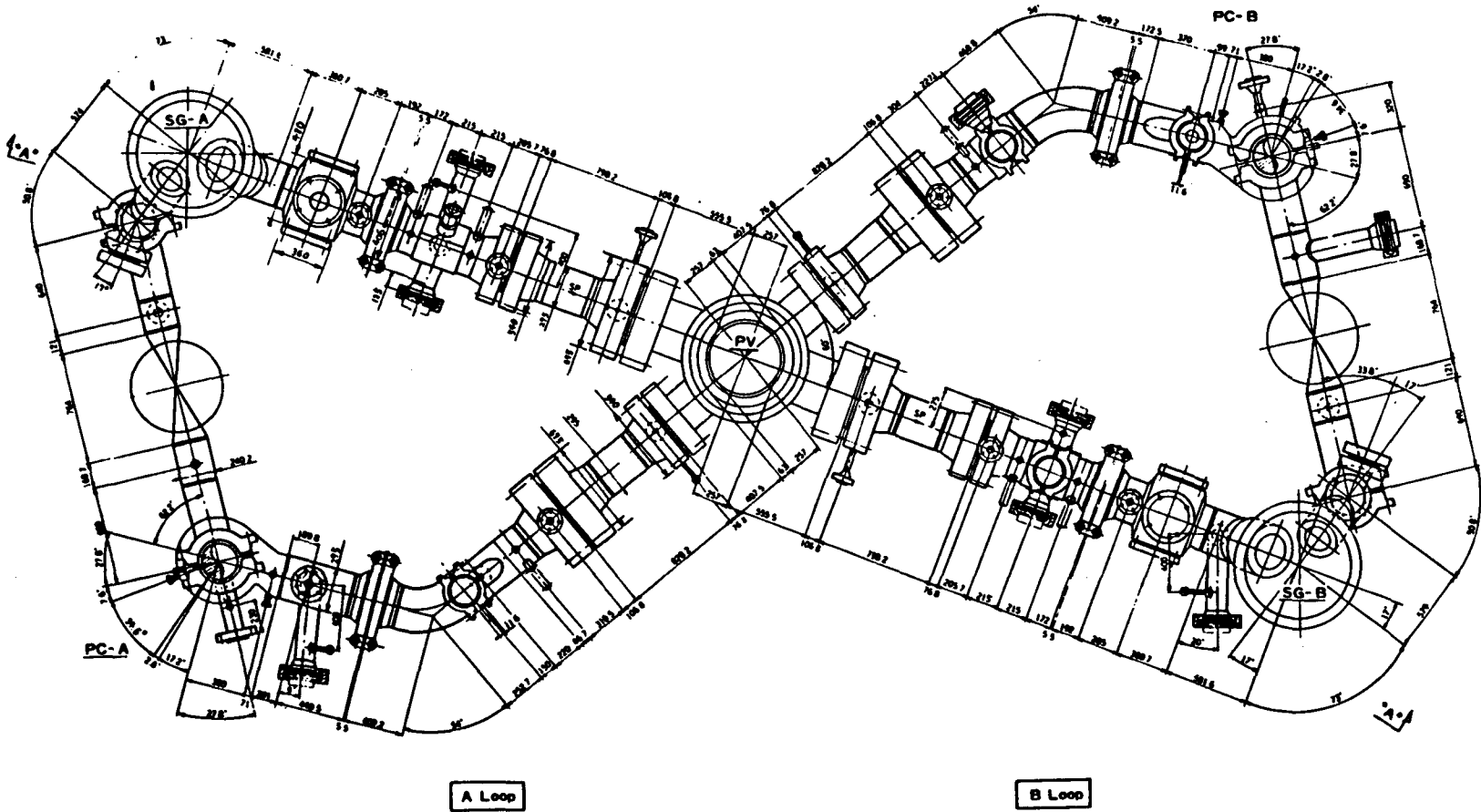


Figure A.11-8 Primary loop dimensions (plan view)

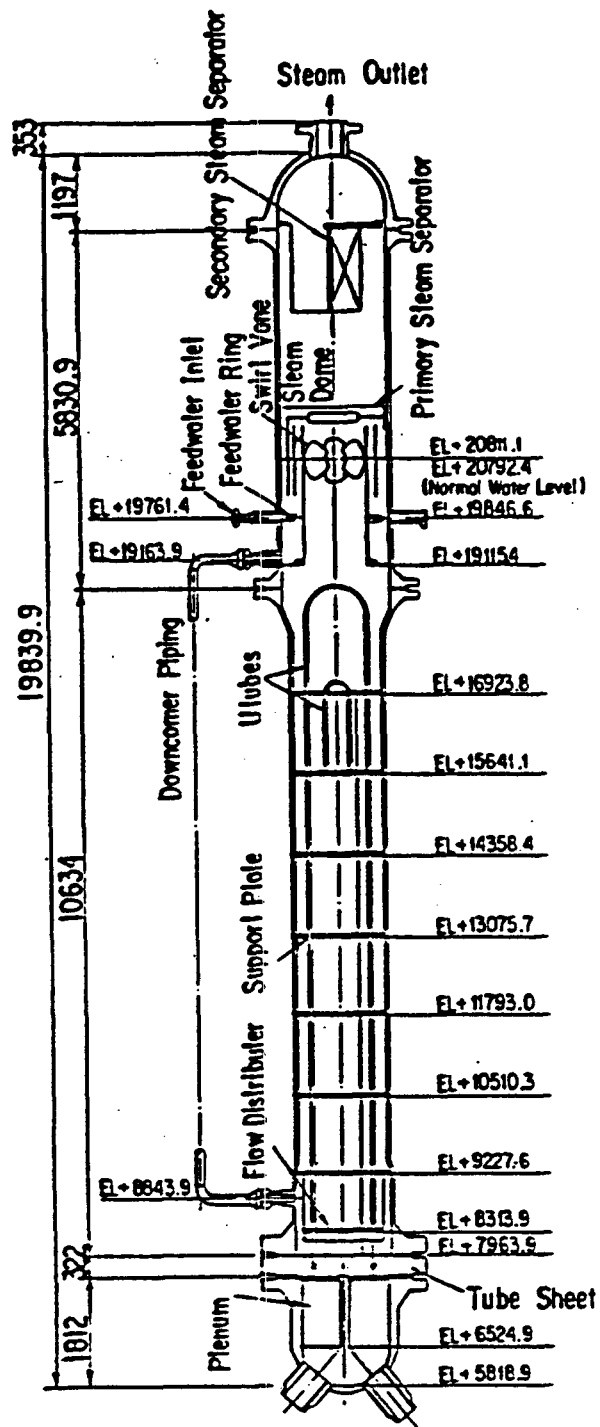


Figure A.11-9 Steam generator of LSTF

Table A.11-1 Major design characteristics of LSTF and PWR

Parameter	LSTF	PWR	PWR/LSTF
Pressure (MPa)	16	16	1
Temperature (K)	598	598	1
No. of fuel pins	1064	50952	48
Core height (m)	3.66	3.66	1
Fluid volume, V (m <sup>3</sup> )	7.23	347	48
Core power, P (MW)	10	3423(t)	342
P/V (MW/m <sup>3</sup> )	1.4	9.9	7.1
Core inlet flow (ton/s)	0.0488	16.7	342
Downcomer gap (m)	0.053	0.260	4.91
Hot leg, D (m)	0.207	0.737	3.56
L (m)	3.69	6.99	1.89
$L/\sqrt{D}$ (m <sup>1/2</sup> )	8.15	8.15	1.0
$\frac{\pi}{4}D^2L$ (m <sup>3</sup> )	0.124	2.98	24.0
No. of loops	2	4	2
No. of tubes in steam generator	141	3382	24
Length of steam generator tube (average) (m)	20.2	20.2	1.0

Table A.11-2 Primary characteristics of pressure vessel and core

Item	LSTF	PWR	LSTF/PWR
<b>Pressure Vessel</b>			
Total volume (m <sup>3</sup> )	2.6748	131.7	1/49
Core volume (m <sup>3</sup> )	0.4078	17.5	1/43
Core flow area (at spacer) (m <sup>2</sup> )	0.06774	3.70	1/55
Core flow area (m <sup>2</sup> )	0.1134	4.75	1/42
Downcomer flow area (m <sup>2</sup> ) (incl. Bypass)	0.09774	5.23	1/54
Downcomer gap width (m)	0.053	0.26	1/5
Spray nozzle flow area (mm <sup>2</sup> )	72.63	3552	1/49
Normal core flow rate (m <sup>3</sup> /s)	0.0651	22.30	1/343
Leakage bet. D.C. and upper head		0.5% of Core Flow	
Number of rod bundles	24	193	
Bundle size	7 x 7 (square) 48 rods (semi-crescent)	17 x 17	
Total number of rods	1,168	55,777	1/48
Heater rods	1,064	50,952	1/48
Non-heating rods	104	4,825	1/46
Rod diameter (mm)			
Heater rod	9.5	9.5	1/1
Non-heating rods	12.24	12.24	1/1
Rod pitch (mm)	12.6	12.6	1/1
Effective heated length (m)	3.66	3.66	1/1
Output power (Mwt)	10.0	3,423	1/342
Peaking factor	1.495	1.495	1/1
Cladding thickness (mm)	1.0	0.57	1.8/1
Number of spacers in core	9	9	1/1
Core barrel inner diameter (mm)	514	3759	1/7.3

Table A.11-3 Major design characteristics of steam generators

Item	LSTF	PWR	LSTF/PWR
Number of steam generators	2	4	1/2
Number of U-tubes*	141	3382	1/24
Feedwater flow rate* (kg/s)	2.76	469	1/170
Steam flow rate* (kg/s)	2.76	468	1/170
Pressure in SG steam dome (MPa)	7.34	6.13	1.2/1
Temperature difference between SG inlet and outlet (K)	35.7	35.7	1/1
Inner diameter of U-tube (mm)	19.6	19.6	1.1
Outer diameter of U-tube (mm)	25.4	22.23	1.14/1
Pitch of U-tubes (mm)	32.5	32.5	1/1
Inner height of SG vessel (m)	19.84	19.97	1/1.0
Height of U-tube (max.) (m)	10.62	10.62	1/1.0
Height of U-tube (min.) (m)	9.16	9.16	1/1.0
Height of downcomer (m)	14.10	14.10	1/1.0
Total secondary coolant volume (m <sup>3</sup> )	7.480	163.1	1/22
Boiler section flow area (m <sup>2</sup> )	0.229	5.10	1/22
Lower downcomer flow area (m <sup>2</sup> )	0.0296	0.663	1/22

\* : per steam generator

Table A.11-4 Break locations

Number	Location
1	Hot Leg B Bottom
2	Hot Leg B Middle
3	Hot Leg B Top
4	Cold Leg B Bottom
5	Cold Leg B Middle
6	Cold Leg B Top
7	Hot Leg A
8	Cold Leg A
9	Crossover Leg B Bottom
10	Crossover Leg B near SG
11	Hot Leg B near SG
12	PV Lower Plenum
13	PV Upper Head
14	Pressurizer Top
15	SG B Secondary FW Line
16	SG A Secondary FW Line
17	SG Tube Rupture
18	SG B Main Steam Line
19	SG A Main Steam Line

Table A.11-5 Break orifice sizes

Scaled Size %	Diameter mm
0.1	3.2
2.5	16.0
5	22.5
7.5	27.6
10	31.9

Table A.11-6 ECCS injection locations

Injection location	Charging system	HPIS	ACC	Hot ACC	LPIS (RHR)
Hot leg A	√	√	√	√	√
Cold leg A	√	√	√	√	√
Crossover Leg A	√	√			
Hot leg B	√	√		√	√
Cold leg B	√	√	√	√	√
Crossover leg B	√	√			
Pressure vessel lower plenum	√	√	√	√	√
Pressure vessel upper plenum	√	√		√	√

## A.12 MULTI-LOOP INTEGRAL SYSTEM TEST FACILITY

The Multi-Loop Integral System Test (MIST) facility is an integral testing facility sponsored by the Nuclear Regulatory Commission, the Babcock and Wilcox Company, the Babcock and Wilcox Owners Group, and the Electric Power Research Institute. The facility is a scaled 2x4 loop model of the lowered-loop B&W reactor system. The purpose of the facility is to generate integral system data on specific issues and phenomena following a small-break LOCA to verify analytical models used in computer codes for assessing thermal-hydraulic safety.

### Facility Description

The MIST facility is an integral 2x4 test loop that consists of a reactor vessel, downcomer, four reactor vessel vent valves (RVVV), two hot legs, two 19-tube once-through steam generators (OTSG), four cold legs, and four reactor coolant pumps. Figure A.12-1 illustrates the overall arrangement of the MIST reactor coolant system and identifies the diameters and schedules of the pipe sections and components. The reactor coolant system is approximately 75 feet tall and 11 feet across (including the pressurizer). As indicated on Figure A.12-1, the downcomer is outside the reactor vessel and is centrally located in the MIST configuration. The four cold legs (two from each loop) enter the downcomer around its circumference at 90° spacings. The four reactor coolant pumps are located at the highest elevation of each cold leg. The two 91-tube OTSGs are full-length subsections of their plant counterparts and are located to preserve similarity in flow path and length for each loop. The two hot leg takeoffs from the reactor vessel are spaced and angled to maintain equal flow lengths. The horizontal length of the hot leg takeoffs has been minimized to preserve flow typicality. The pipe length from the reactor vessel nozzle to the hot leg U-bend is approximately 45 feet. A pipe section is included between the hot leg U-bend and the upper tubesheet of each OTSG to simulate the elevation and volume occupied by the upper primary plenum of the prototype steam generator. Details of each loop component are included in Reference A.12-1.

The core simulator consists of 45 electrically heated filament-type heater rods. Each heater rod is geometrically similar to a B&W PWR fuel rod and is designed to simulate the fuel rod surface heat flux during small-break LOCA transients. Each of them is capable of operating at 70 kW, which corresponds to a 100% scaled power simulation. However for the MIST program, each of them operates over a range of 0 to 7 kW corresponding to 0 to 10% of scaled power.

The upper plenum and top plenum are designed to afford prototypical phase separation upstream of the RVVVs and top plenum. Volume to power scaling sets the elevations of the plenum cover plate at 8.2 feet above the end of the heated length of the core and the top of the reactor vessel at 4.1 feet above the plenum cover plate. Figure A.12-2 compares reactor vessel elevations in the model with those in the plant.

The MIST downcomer consists of two separate regions as shown in Figure A.12-3, an upper downcomer and a lower downcomer. The upper downcomer provides an annular mixing chamber for the loop, high-pressure injection, low-pressure injection, and RVVVs. This annular region is believed to allow loop-to-loop coupling for asymmetric loop behavior and provides limited geometric similarity

to prototypical downcomer regions. The lower downcomer consists of a single pipe, power to volume scaled, that maintains the current liquid level and volume in the downcomer and core region.

The MIST RVV arrangement simulates the eight prototype vent valves with four valves as illustrated in Figure A.12-4. A differential pressure measurement between the reactor vessel (at the RVV elevation) and the upper downcomer quadrant corresponding to each MIST vent valve line is used to control the condition (open or closed) of each valve. In addition, each valve can be operated in automatic or manual mode. In the automatic mode, the valves open and close at a preset differential pressure. The differential pressure set-points for each valve is continuously adjustable over the calibrated range of the differential pressure (1/8 to 1/4 psi) transmitter used.

Each of the two MIST steam generators contains nineteen full-length plant-typical tubes. Each models an OTSG of the B&W (177 fuel assembly) lowered-loop plant. The power scaling of the model is set by the ratio of the number of steam generator tubes in the plant to that in the model,  $15520/19 = 817$ . Auxiliary feedwater injections are available at both high and low elevations in MIST.

The MIST pressurizer provides a scaled power of 2 kW. The bottom of the pressurizer is connected to the one of hot legs by the pressurizer surge line. The pressurizer vessel and the surge line have a guard heater to minimize heat loss.

The MIST facility reactor coolant system contains four reactor coolant pumps, one in each of the four cold legs. Each coolant pump has scaled head-flow characteristics so that pump on-off operation (running, locked rotor, pump bumps) during a small-break LOCA can be simulated.

The secondary loop in the MIST facility is limited to providing the steam generators with a secondary-side inventory and those fluid boundary conditions that affect a small-break LOCA. This includes steam generator secondary-side level control, auxiliary feedwater, and controlled cooldown (at 50-100°F/hr).

### Scaling

The 25 events shown in Table A.12-1 were identified as being of importance to small-break LOCA transients (Ref. A.12-2). The four scaling criteria used in the design of MIST were elevation, two-phase behavior, volume, and irrecoverable pressure losses.

Elevation is considered the most significant model characteristic for the preservation of small-break LOCA events. It is crucial to nine of the 25 events in Table A.12-1, particularly in decoupling of primary-to-secondary heat transfer and events involving fluid buoyancy forces. System two-phase behavior encompasses the hot leg U-bend voiding and phase separation, hot leg (horizontal and vertical) flow regimes and lower region (reactor vessel upper head, downcomer, and cold leg discharge piping) voiding and condensation. This was identified to be significant in more than two-thirds of the small-break LOCAs considered. System volume scaling governs fluid transport time as well as the rate of change of fluid energy content. The ideal model system scales volume as power and retains volume-versus-elevation proportions. Coupled with power-scaled boundary flowrates, the ideal system loses inventory and level and

changes fluid properties in entirely prototypical fashion. In order to avoid whole-pipe slugging behavior, the hot and cold leg diameters were oversized compared to ideal volume scaling. As a result, the hot and cold leg volumes are three to four times larger than would result from ideal volume scaling. The other major primary loop component volumes are sized according to ideal volume scaling. The ideal model preserves plant irrecoverable pressure drops (fluid momentum losses) at power-scaled flowrates. Furthermore, the ideal model preserves component as well as system losses, and the loss fractions due to form (shock) and to friction. When other scaling considerations were accommodated, irrecoverable pressure losses were adjusted to plant-typical values in various components of the system.

MIST atypicalities are summarized below; detailed discussions are given in Reference A.12-1.

1. Hot leg separation
2. Excess steam generator metal mass
3. AFW multidimensionality
4. Downcomer flow & density field, tangential resistance
5. RVVV simulation
6. Excess piping metal mass
7. No low pressure injection
8. Limitation of secondary side depressurization
9. Stratified single-phase flow in hot leg
10. RCP two-phase characteristic

#### Testing Capability

The MIST facility is currently scheduled to conduct 41 tests to obtain the integral system data identified below.

1. RVVV, guard heater, and steam generator effects
2. Break configuration and ECCS effects
3. Feed and bleed
4. Steam generator tube rupture
5. Effects of incondensables and vents
6. Effects of pump operation

#### REFERENCES

- A.12-1 "Multi-Loop Integral System Test (MIST) Facility Specification," NRC-04-83-168, Babcock & Wilcox, Lynchburg, Virginia.
- A.12-2 "Test Advisory Group: Final Report, Integral Systems Testing Program for B&W Designed NSS Systems," BAW-1787, Babcock & Wilcox, Lynchburg, Virginia, June 1983.

Table A.12-1 Significant events following a small-break LOCA

---

Initiation

1. Leak flow
2. Pressurizer draining
3. Primary depressurization
4. Power and flow transient; reactor and reactor coolant pump trips, transfer of steam generator feed
5. Single-phase natural circulation

Intermittent Spillover Circulation

6. Hot leg U-bend saturation and voiding
7. Reactor vessel upper head voiding
8. Reactor vessel vent valve actuation
9. Decoupling of steam generator, steam generator depressurization
10. Primary repressurization
11. Leak-HPI (high pressure injection) cooling
12. Feed and bleed (primary) cooling
13. Downcomer and cold leg voiding and condensation
14. Asymmetric conditions among cold legs

Boiler Condenser Mode

15. Steam generator condensation of primary steam
16. Primary depressurization to CFT/LPI pressures
17. Steam generator repressurization

Primary Refill

18. Compression of primary steam
19. Venting of primary fluid
20. Subcooling of primary components
21. Spillover circulation (hot leg U-bend refilled)
22. "Pump bump"

Cooldown

23. Controlled steam generator depressurization and primary cooldown
  24. Reinitiation of natural circulation
  25. Cooling of idled loop
-

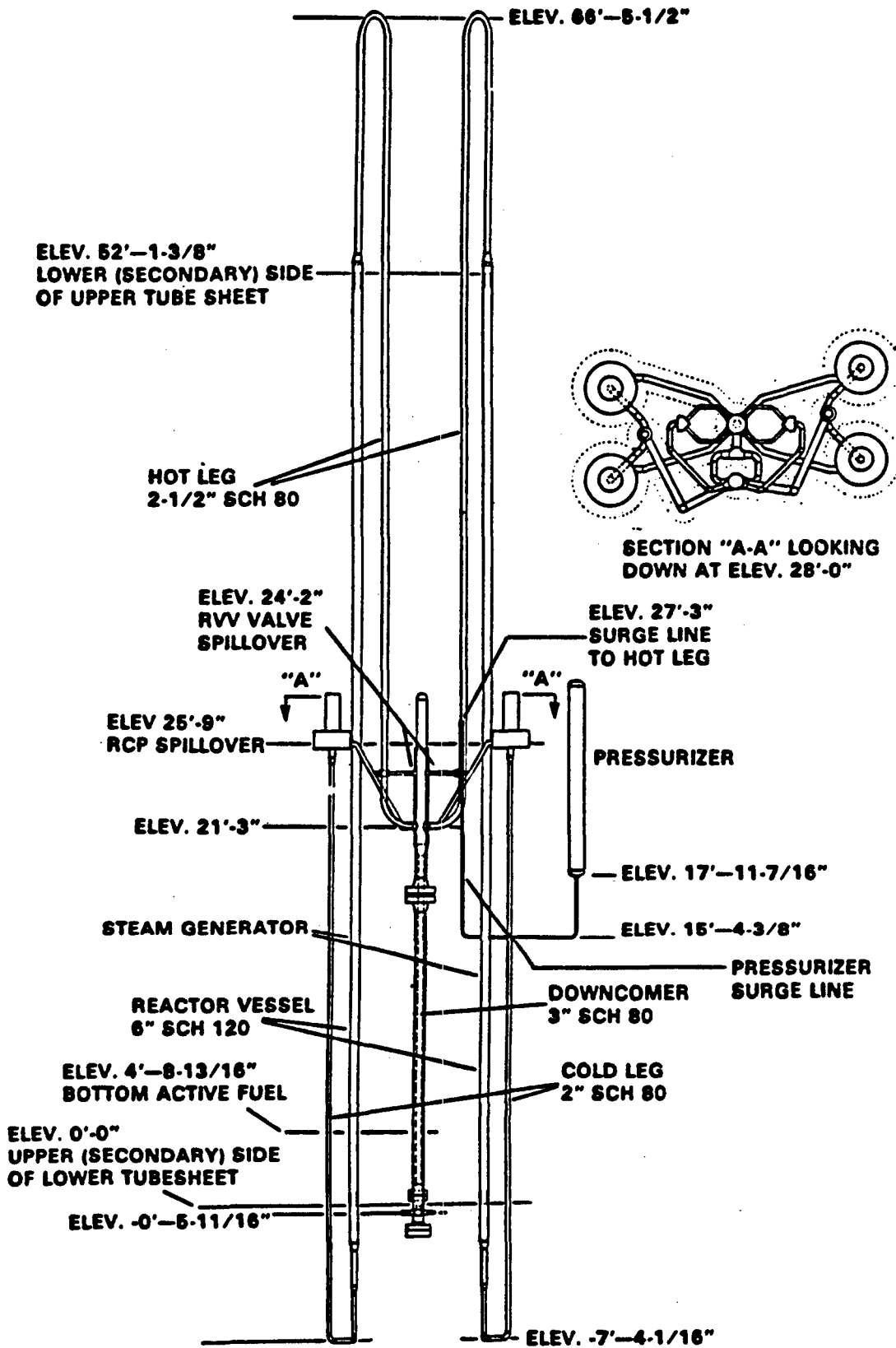
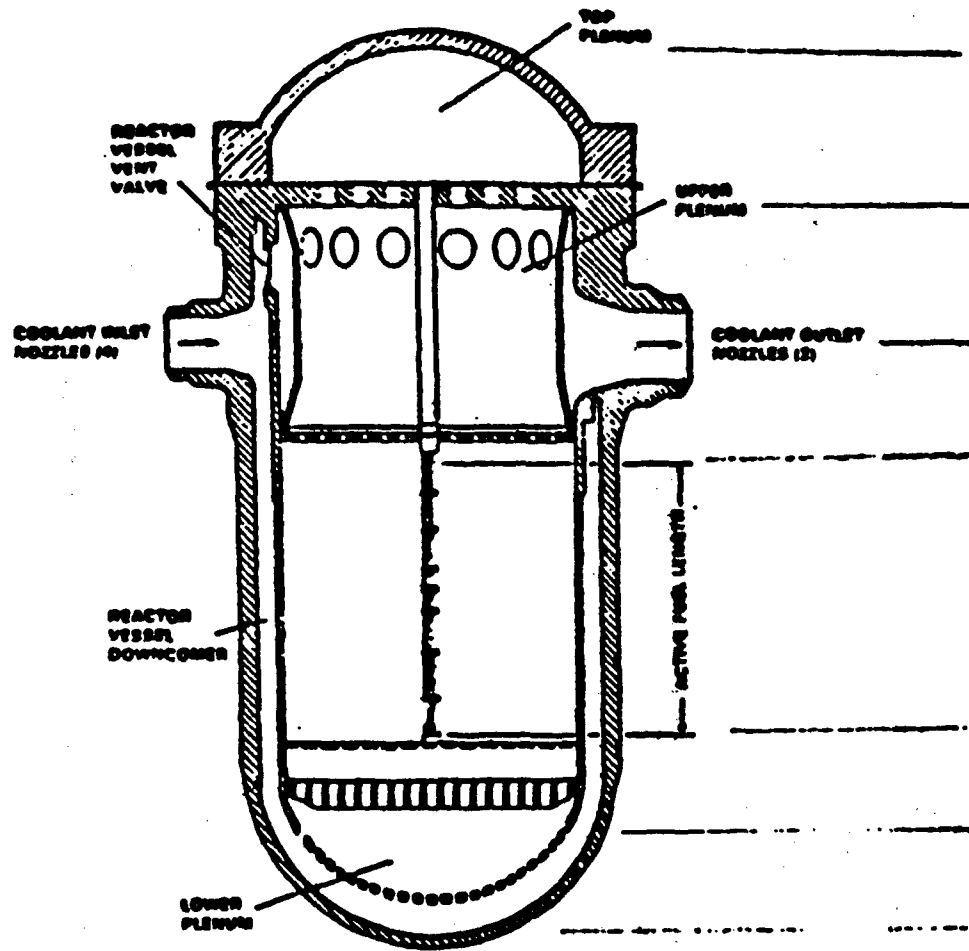
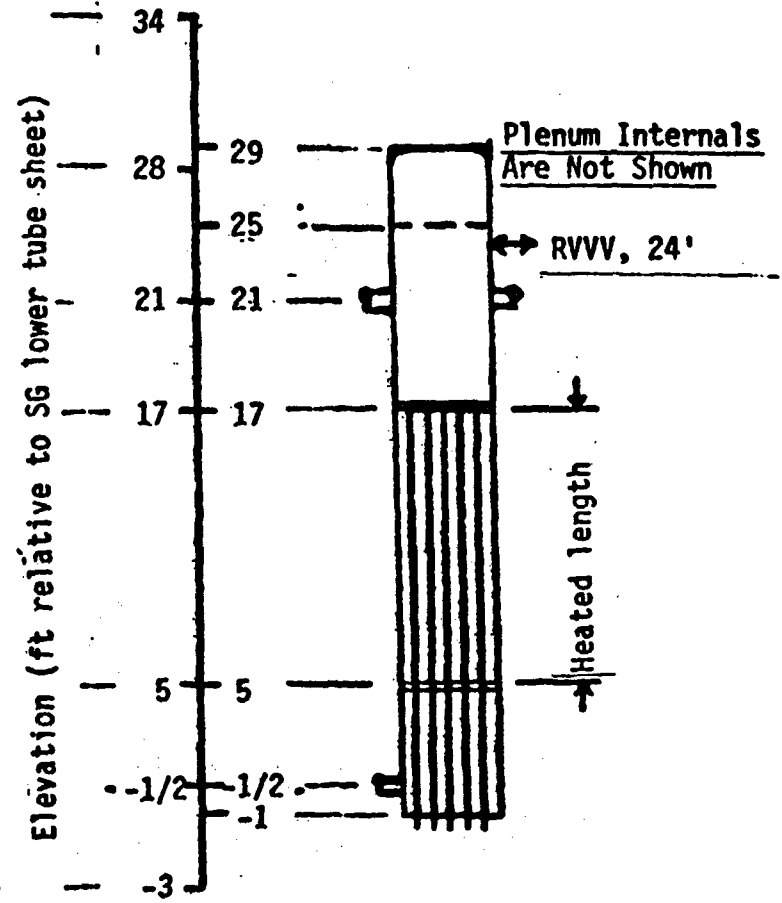


Figure A.12-1 MIST reactor coolant system arrangement

A-122



**REACTOR VESSEL FOR A 177 FUEL ASSEMBLY PLANT**



**MIST RV CONCEPT**

Figure A.12-2 MIST and prototype reactor vessels

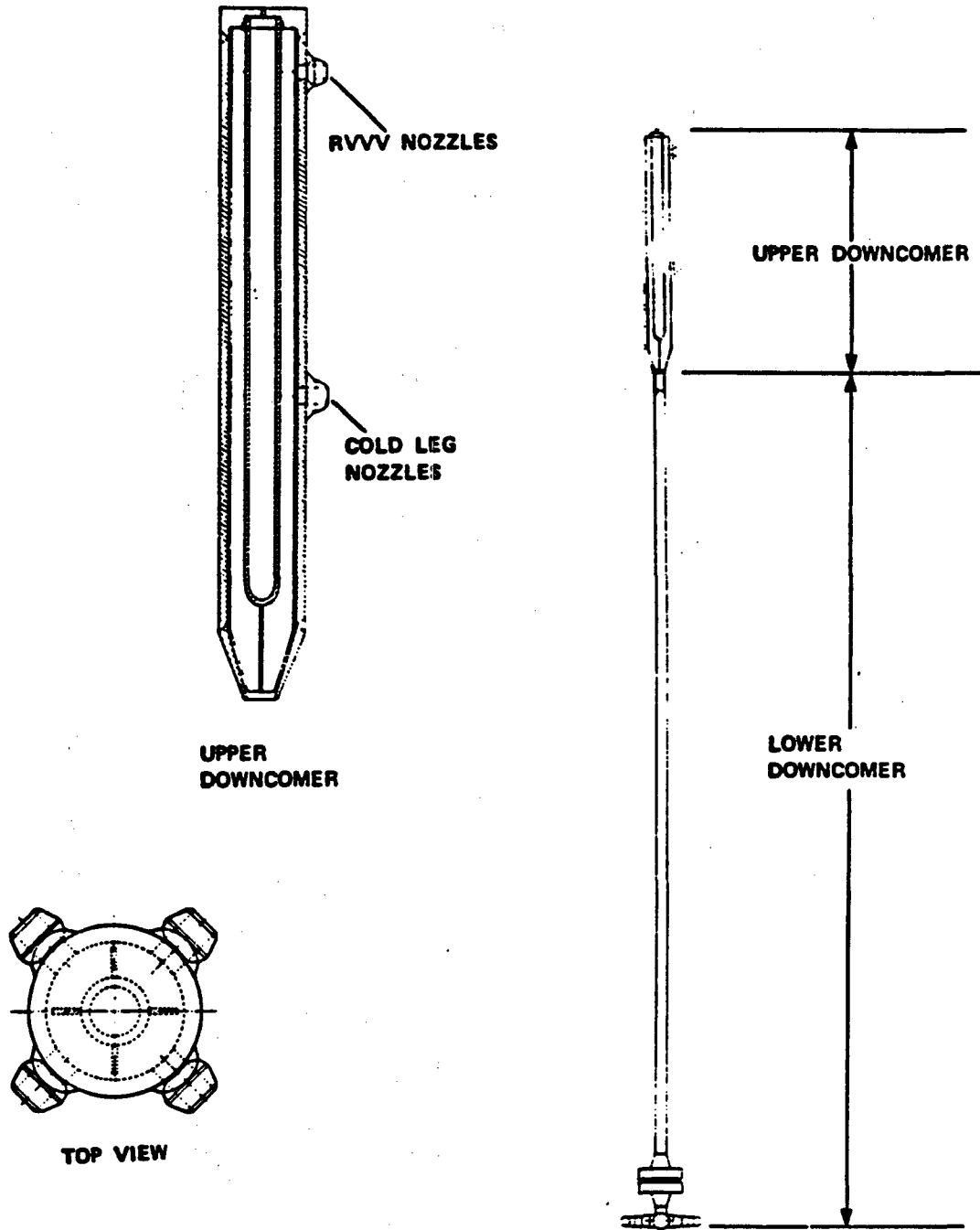


Figure A.12-3 MIST upper and lower downcomers

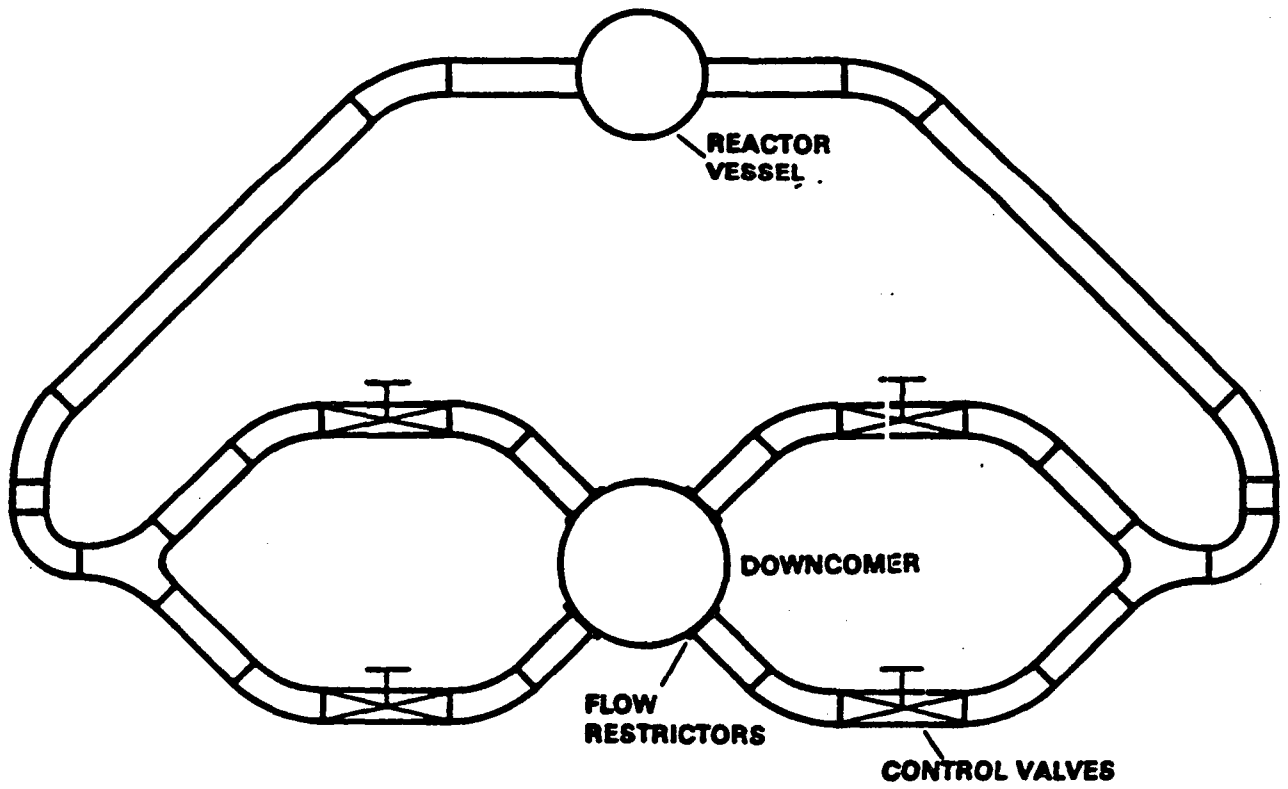


Figure A.12-4 MIST RVV circuit

### A.13 UNIVERSITY OF MARYLAND AT COLLEGE PARK 2x4 LOOP

The University of Maryland at College Park (UMCP) 2x4 loop is an integral facility sponsored by the Nuclear Regulatory Commission. The facility is a scaled 2x4 loop model of the lowered-loop B&W reactor system. The purpose of the facility is to generate integral system data on phenomena related to small-break LOCAs to verify analytical models used in computer codes for assessing thermal hydraulic safety.

#### Facility Description

The UMCP 2x4 loop is a scaled integral experimental facility constructed entirely of stainless steel and operates at a maximum pressure of 300 psi. It is volume-scaled by a ratio of 1/500. Its short height is proportionally compensated in its cross-sectional area. The loop consists of a reactor vessel with core barrel and annular downcomer, two hot legs, four cold legs, two once-through steam generators, and a pressurizer (Figure A.13-1). The principal features of the reactor vessel and core barrel are shown in Figure A.13-2. The vessel is 20 inches in diameter and 50.25 inches in height. The downcomer gap is 1.25 inches. The core barrel can be skirted to decrease the downcomer size; an increase in size would require replacement of the core barrel. The vessel has 19 top head penetrations for the heater rods and for instrumentation and four view ports that allow visual observation of the reactor vessel vent valves (RVVV).

The core barrel has eight reactor vessel vent valves. Penetrations through the vessel allow selected valves to be held fully closed or at any open position by externally controlled set screws. The valves open on differential pressure; the onset of opening and the dynamic characteristics of the valve action can be altered by using machined weights on the flapper. The vent valve design is shown in Figure A.13-3.

Heat is added to the loop by 16 heater rods 1 inch in diameter and 49 inches in total length. Fifteen of the 16 heaters are used during operation leaving one heater as a spare. Only the bottom 24 inches of the heater rods are heated. The total maximum heater input is approximately 200 kW.

The hot legs are made of 3.5 inch ID Schedule 40 Type 304 stainless steel piping and 300 lb weld neck flanges as shown in Figure A.13-1. Three view ports are included in each hot leg: one in the horizontal section near the reactor vessel, one in the vertical section, and one in the candy cane. The view ports are designed to minimize any dead water region or flow disturbance. High-point vents have been installed in each of the hot leg U-bends. They could be used to fill the loop or for certain experiments in which high-point venting or spraying is desired. The loop also contains safety valves at the top of the pressurizer and the reactor vessel.

The cold legs are made of 3.0 inch ID Schedule 40 Type 304 stainless steel piping and 300 lb stainless steel weld neck flanges. The cold legs have provisions for HPI injection and spray lines and for connection to a water treatment system.

The K-factor (the flow losses due to pipe friction and entrance losses) of the model loop can be changed (increased) by inserting screens and orifice plates at various locations within the loop. For this reason, a small recess has been machined into every flanged connection within the loop.

Each steam generator contains 28 12.8-ft-long stainless steel tubes with a 1.18 inch ID and a 1.25 inch OD. The tube sheet pattern is shown in Figure A.13-4. The outer shell is 12 inch Schedule 20 stainless steel pipe with a 12.75 inch OD and a 12.25 inch ID. A middle tube sheet divides the secondary side into two equal half sections. This feature was included in the design of the steam generator to provide more flexibility in the positioning of the thermal center. The top and bottom sections may be connected together allowing inlet main feedwater to exit the top section or controlled separately using water, air, or steam as a secondary fluid. There are four nozzles near the top of the shell side for the auxiliary feedwater spray.

The pressurizer is made of 12 inch Schedule 20 stainless steel pipe and is 52 inches in length. It is connected to the hot leg by a 3/4 inch stainless steel pipe. A plant-typical loop seal is included in the surge line. Two electric heaters (2.5 kW each) are inserted near the bottom of the pressurizer. Penetrations at the top of the pressurizer are for the spray, instrumentation, and pressure relief valve. The spray line is connected to the nearest cold leg.

The secondary system is a closed loop that pumps water from the cooling tower, through the steam generators, and back to the tower. System pressure is approximately 45 psi and can be increased to approximately 150 psi by replacing the pump. As already discussed, the secondary of each steam generator is split into two equal halves. Depending on the configuration, the secondary system pumps water into one or two inlets on each steam generator.

### Scaling

The overall scaling logic for both single-phase and two-phase flow begins with consideration of the fundamental laws of conservation of mass, energy, and momentum. For single-phase steady-state natural circulation, these equations relate the balance of buoyancy forces due to density differences to flow losses in the loop due to friction and form losses. For one-phase non-steady-state natural circulation, the analysis concluded that for a maximum power output of the model of 200 kW and a model loop pressure of 300 psi will permit simulation of the natural circulation in the prototype starting within 2 seconds after prototype shutdown from full power, assuming the prototype pressure drops rapidly to 600 psi, or a simulation starting at 4 seconds after shutdown, assuming the prototype pressure remains at the operating pressure level. For two-phase flow, using the conservation equations, the usual set of nondimensional parameters (Froude number, subcooling number, etc.) are developed. Using these parameters, values for each are calculated and compared to those of the prototype. The comparison shows that most model values compare well (factor of 1 to 2) to the prototype. This indicates that, during a transient, the flow regime for the crucial components (hot leg, downcomer, etc.) should be preserved. For two-phase flow, the additional scaling logic is to require the void fractions to be the same in the prototype and the model. The relative vapor content within the loop is determined by (1) the vaporization due to depressurization, (2) the

vaporization and consequent energy loss due to inventory loss, (3) the vaporization due to the decay heat input, and (4) the condensation of steam during HPI actuation. Therefore, the pressure history as characterized by the sequence of a particular transient is simulated. Detailed description of the single- and two-phase scaling is presented in Reference A.13-1.

### Testing Capabilities

The UMCP 2x4 loop is currently scheduled to conduct tests to obtain integral system data identified below.

1. Interruption of natural circulation - hot leg phase separation
2. Establishment of boiler-condenser mode - auxiliary feedwater effects
3. Reestablishment of natural circulation - downcomer flow and density fields, RVVV simulation
4. Long-term cooling - downcomer flow and density fields, RVVV
5. Interloop interaction - effect of steam generator, RVVV, etc.
6. Combined primary and secondary side blowdown - auxiliary feedwater multidimensionality

### REFERENCE

- A.13-1 "Coordination of Support Projects for the B&W Integral System Test Program," edited by J. Sursock and M. W. Young, NUREG-1163, March 1987.

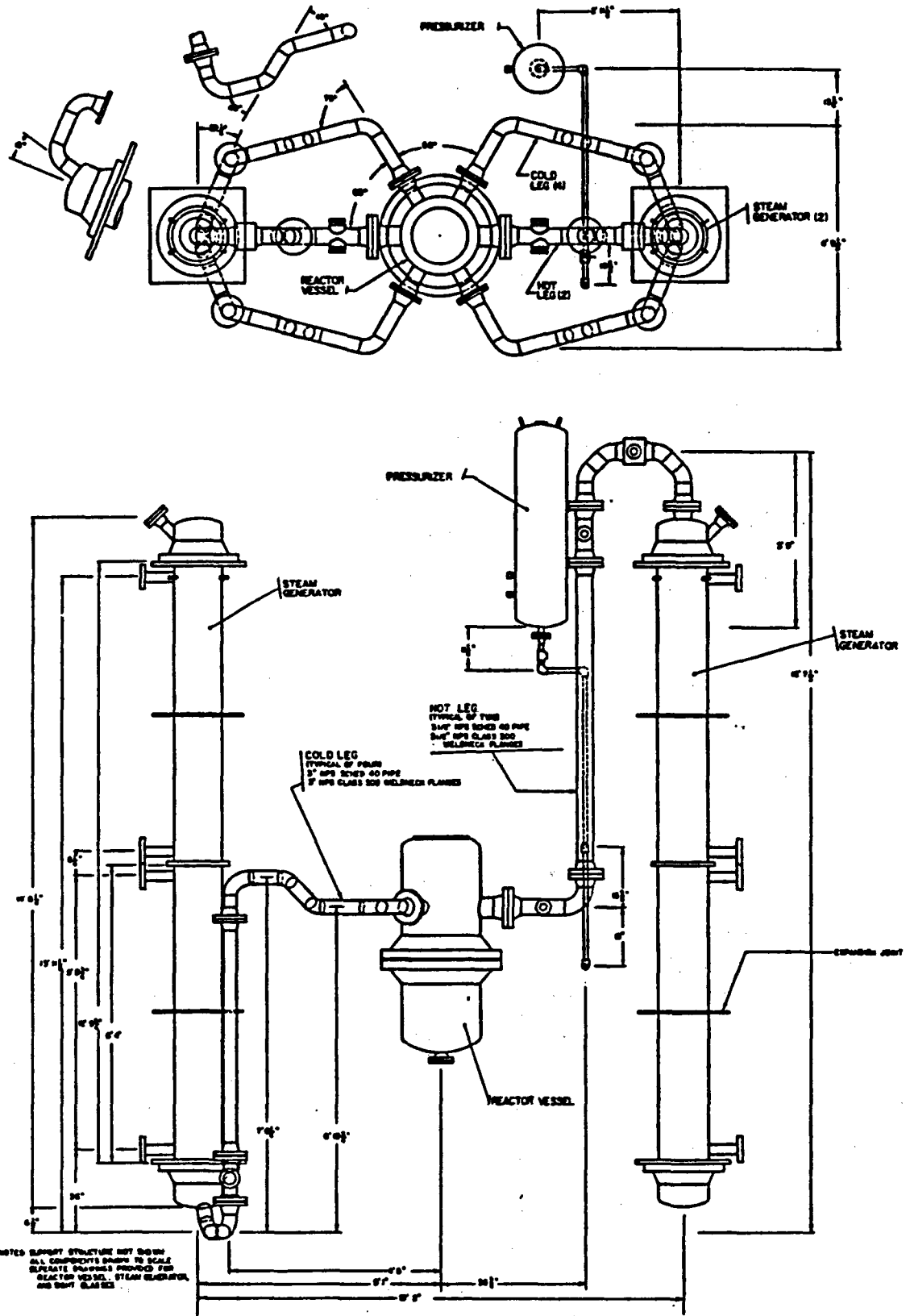


Figure A.13-1 Arrangement of the UMCP 2x4 loop reactor coolant system

A-129

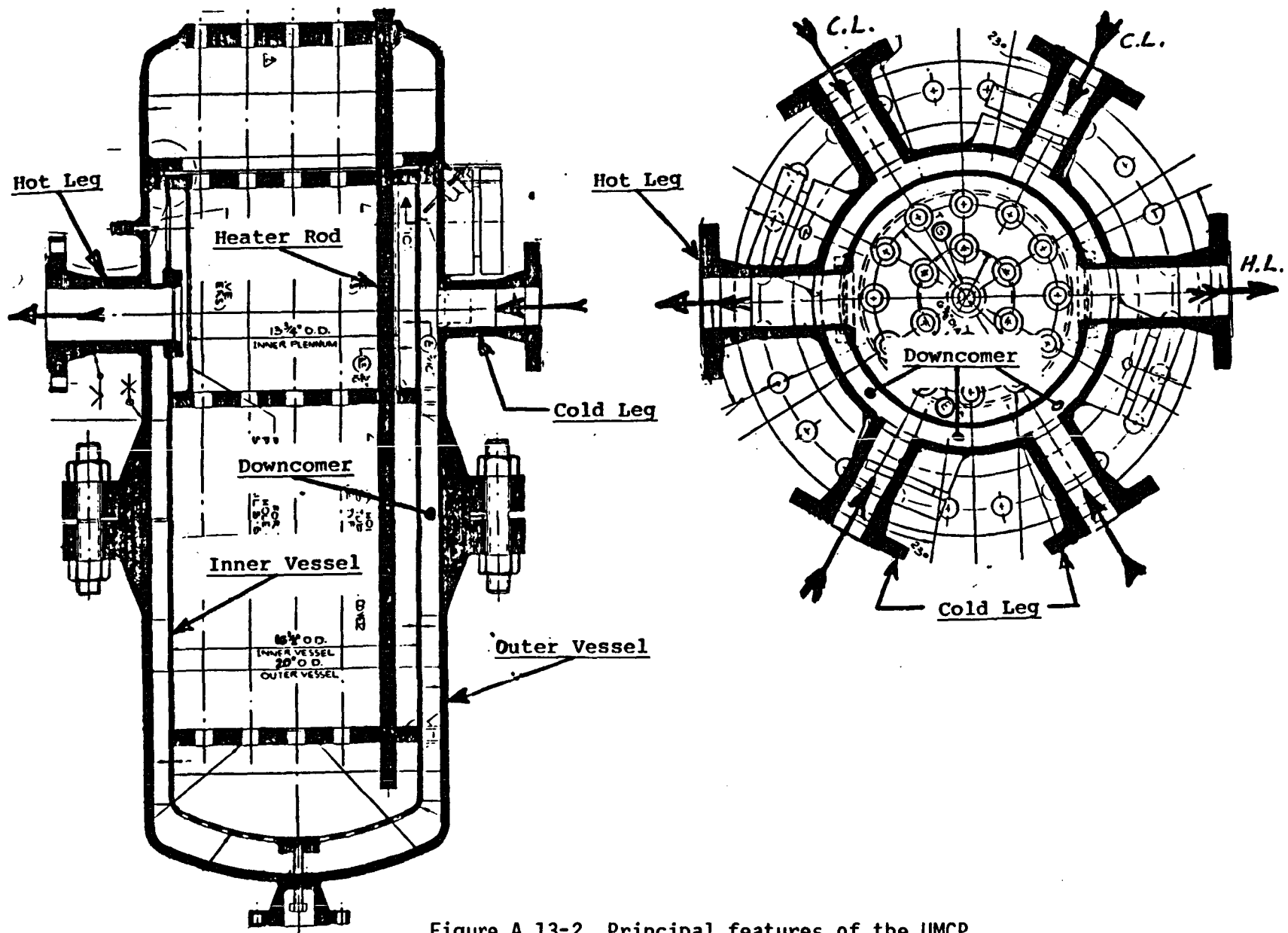
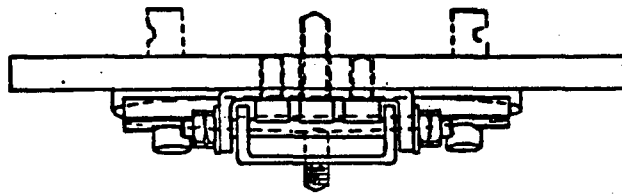


Figure A.13-2 Principal features of the UMCP reactor vessel and downcomer



TOP VIEW

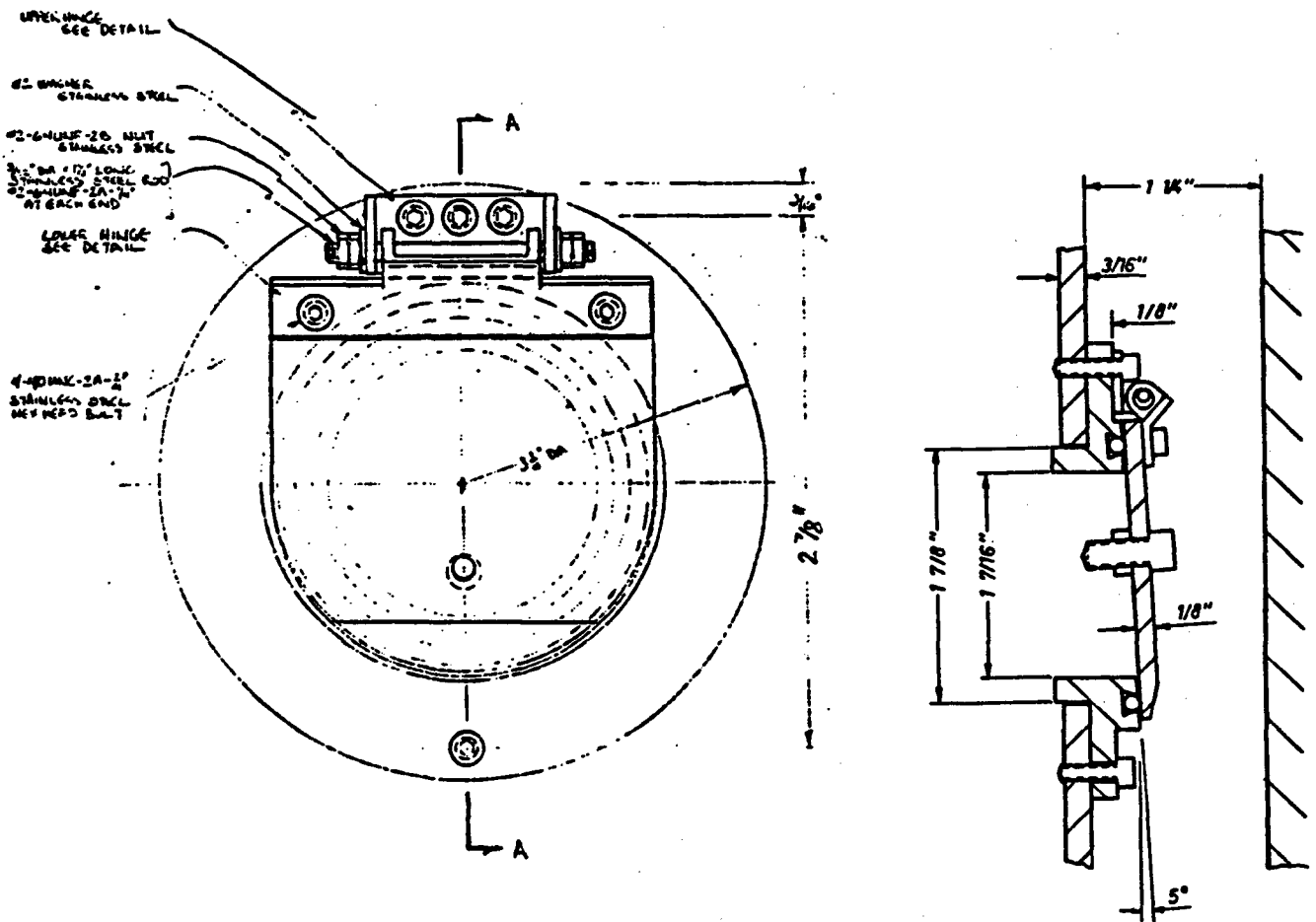


Figure A.13-3 UMCP vent valve design





## A.14 SRI-2 INTEGRAL TEST FACILITY

The SRI-2 facility at Stanford Research Institute is an integral test facility sponsored by the Electric Power Research Institute. It is a scaled 2x4 test facility modeled after TMI-2. The major objective of the facility is to obtain experiment data for the qualification and assessment of safety analysis codes and models used for simulating B&W plants.

### Facility Description

The facility is a 2x4 integral test facility modeled after TMI-2. All vertical dimensions are 1/4 of the prototypical heights. All flow are as in the primary loop except that in the core are 1/324 of the prototypical areas. Horizontal segments of the pipes are not scaled. Overall views of the facility and the reactor vessel are shown in Figures A.14-1 and A.14-2. The nominal operating pressure is 0.7 MPa (100 psia).

The reactor vessel is a circular cylinder 2.58 m (102 in.) high and 25 cm (10 in.) in diameter. It has an internal downcomer with four vent valves. Similar to the prototypical valves, the hinges for the valves are placed on the inside of the downcomer rather than the outside. Such an arrangement allows the valve to open under 1/4 psia pressure difference without having to design a valve of excessive weight. Each of the four valves simulates the vent valve in the prototype. Its opening area is therefore twice that of the scaled area of a prototypical valve.

The core is simulated by 18-element rod electric heaters which provide a total of 88 kW. The heater control allows continuous variation of the core power below its maximum output.

The vessel is equipped with a high point vent which also serves as an injection port for incondensable gas. The hot legs are made of 2 in. Schedule 40 stainless steel pipe. The nominal pair of the hot legs have a radius of curvature at the U-bend of  $R=4D$ , which is slightly larger than the prototypical radius of curvature. An alternate pair of hot legs having an  $R/D$  of 11.5 could be installed to study the effect of U-bend radius phase separation. Cold legs are made of Schedule 40 steel pipe with a 1.5 inch ID. A centrifugal pump with a vertical axis will be installed in each of the four legs. The loop seal around the pump is properly configured.

The pressurizer will be equipped with a 3-kW electric heater and a relief valve at its top. The loop seal between the hot leg and the pressurizer is scaled correctly for elevation. The fluid-to-metal mass ratio is also preserved.

Two counterflow exchangers were modified to serve as once-through steam generators. Each steam generator has 48 tubes. The tube dimensions are prototypical, i.e., 0.625-inch OD with a 0.034-inch wall. The main feedwater, the downcomer, and the annular flow path for the steam are modeled. The steam outlet is located near the top tube sheet. Opposite the steam line is the auxiliary feed nozzle, which is designed to spray on three tubes to simulate the effect of partial wetting. The fluid-to-metal mass ratio is simulated. The hydraulic resistance of the tube section is about 1/3 that of the prototype.

Auxiliary systems include (1) a high-pressure injection system, (2) a break flow measurement system, (3) a tertiary cooling system for the secondary steam, (4) a proportional control system for the auxiliary feedwater, and (5) a pressurizer heater control system.

### Scaling

The design of the facility is based on the scaling rationale presented by Ishii (Ref. A.14-1). The scaling approach was modified to account for the nonprototypical pressure (i.e., 0.7 MPa instead of 10 MPa). The scaling laws for both single-phase and two-phase flow are summarized in Table A.14-1. Table A.14-1 shows that, for a particular quantity such as the core power density, its functional dependence on the length scale is the same for single-phase and two-phase flow. However, the numerical multipliers are different. This difference is the result of nonprototypical fluid properties. With due consideration to the two-phase flow limitation, a component height ratio of 1/4 and an area ratio of 1/324 were chosen. The core heater is sized to give a maximum of 5% scaled decay power under single-phase conditions. This turned out to be 88 kW. Because of the difference in scaling, this power represents 17% scaled decay power under two-phase conditions. A detailed discussion on scaling is presented in Reference A.14-2.

### Testing Capabilities

The SRI-2 is expected to conduct tests to provide information related to the following areas:

1. Interruption and reestablishment of natural circulation - hot leg U-bend separation, hot leg flow regime, RVV simulation
2. Interloop interaction and oscillations - effect of heat losses, downcomer configuration/resistance, scaling rationales
3. Feed and bleed
4. Small-break loss-of-coolant accidents

### REFERENCES

- A.14-1 M. Ishii and I. Kataoka, "Similarity Analysis and Scaling Criteria for LWR's under Single-Phase and Two-Phase Natural Circulation," NUREG/CR-3267, 1983.
- A.14-2 "Coordination of Support Projects for the B&W Integral System Test Program," edited by J. Sursock and M. W. Young, NUREG-1163, March 1987.

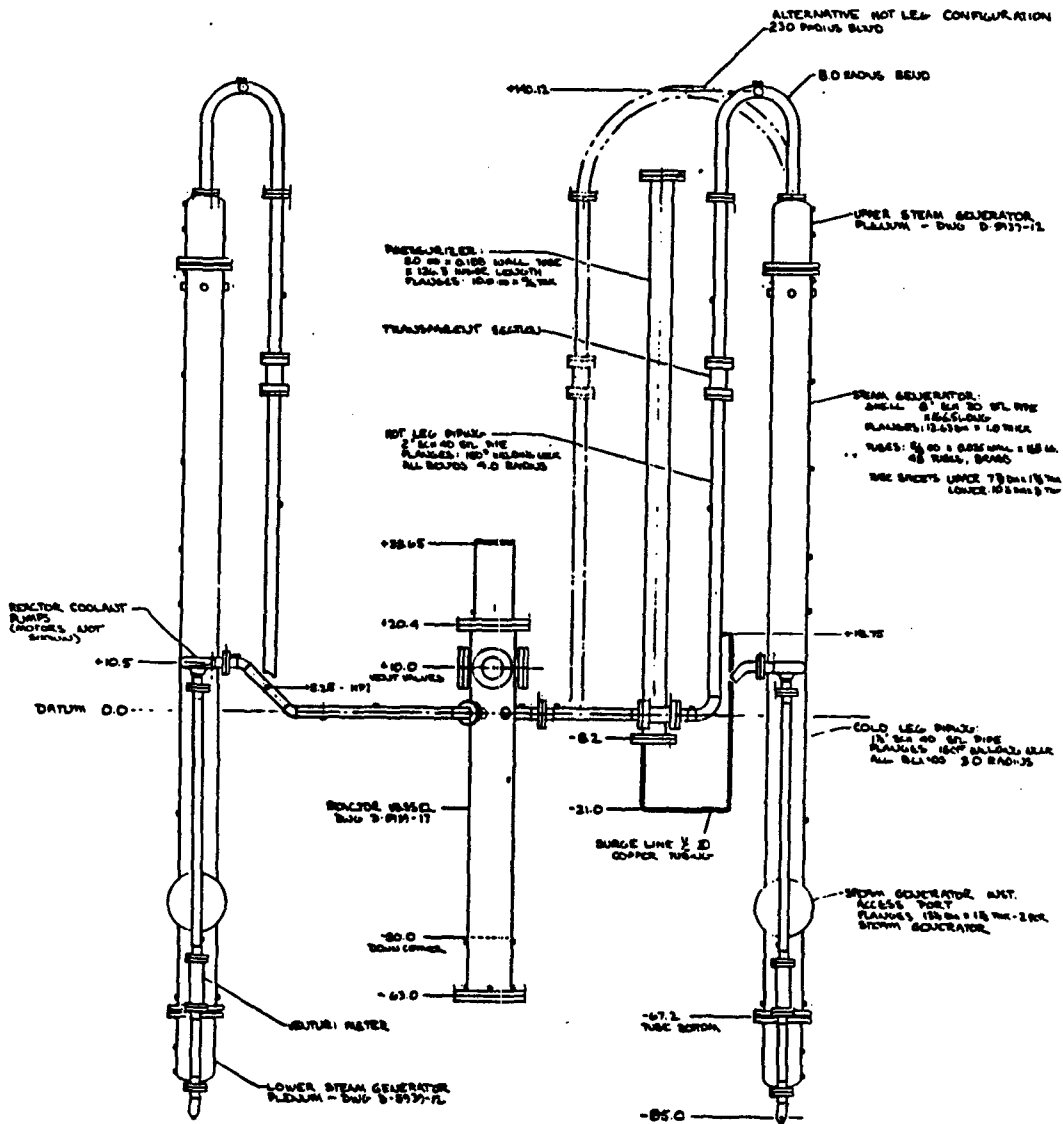
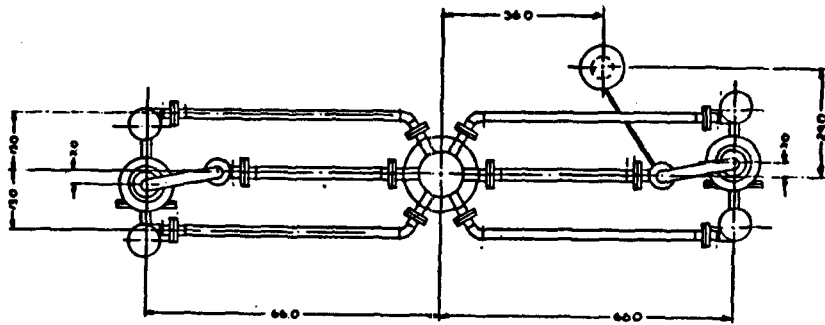


Figure A.14-1 Arrangement of the SRI-2 reactor coolant system



Table A.14-1 Scaling criteria for SRI-2

	Single-Phase	Two-Phase
Component height	$(L_i/L_o)_R = 1$	$(L_i/L_o)_R = 1$
Flow area	$(A_i/A_o)_R = 1$	$(A_i/A_o)_R = 1$
Flow resistance	$(f \frac{L}{d} + K)_R = 1$	$(f \frac{L}{D} + K)_R = 1$
Pipe wall	$(a_{si}/a_i)_R = 1$	$(a_{si}/a_i) = 1$
Core power	$(q''')_R = 0.42 L_{OR}^{-1/2}$	$(q''')_R = 0.12 L_{OR}^{-1/2}$
Velocity	$U_R = 0.56 L_{OR}^{1/2}$	$U_R = 0.96 L_{OR}^{1/2}$
Time	$t_R = 1.8 L_{OR}^{1/2}$	$t_R = 1.04 L_{OR}^{1/2}$

NOTE: Subscript R refers to ratio of model to prototype.

The numerical coefficients result from the fact that SRI-2 does not operate at prototypical pressure.



## A.15 THERMAL-HYDRAULIC TEST FACILITY

The Thermal-Hydraulic Test Facility (THTF) is a nonnuclear high-pressure water loop designed explicitly to gather accurate transient heat transfer data within a rod bundle geometry. It consists of an array of 64 electrically heated fuel rod simulators, a primary loop to provide desired fluid conditions to the test section, and a high-speed data acquisition system. A detailed description of the THTF is given in Reference A.15-1; maximum system operating parameters are listed in Table A.15-1.

### Loop Design

The THTF, shown in Figure A.15-1, is operated with fluid flowing upward through the vertical test section. Several spool pieces for measuring fluid conditions are located in the primary flow loop near the test section to provide accurate determination of fluid velocity, temperature, and pressure at both the entrance and the exit of the 64-rod bundle. Each spool piece contains a drag disk, a turbine meter, a gamma attenuation densitometer, and rapid-response temperature and pressure measurement devices. Four separate spool pieces in the test section inlet line and three in the outlet line allow redundant measurements on both sides of the test section, providing a check on individual instrument responses. A schematic of the system is shown in Figure A.15-2. System pressure is maintained using a pressurizer located between the test section exit and pump inlet (the exact location may vary from test to test). Forty-five kW of independent heat input to the pressurizer maintains system pressure.

The primary pump provides flow to the test section through a 4-inch inlet line. Flow control valves (FCV-18 and HCV-2 in Figure A.15-2) are used to trim the flow to desired values by bypassing a portion of the flow around the test section.

The test section itself was originally designed with an internal downcomer between the 1-inch barrel and the bundle shroud (Figure A.15-3). An external downcomer was added later with means for completely isolating and bypassing either internal or external downcomers. Using the facility with the internal downcomer activated simulates downcomer behavior in an actual reactor core by providing both fluid and thermal interaction between the core and downcomer fluid. The external downcomer is used when accurate measurement of bundle inlet fluid conditions are desired. A 4-inch test section exit line routes the fluid through three Graham Heliflow heat exchangers that are used to establish the desired bundle thermal conditions. They may also be used as condensers if steady-state operation of the loop under two-phase conditions is desired. Transient behavior is controlled by selecting appropriate orifices at the break location and by controlling bundle power and primary pump flow during the transient. During transient tests, the two-phase mixture leaving the test section enters a large pressure suppression tank. Steam is condensed within the tank using a subcooled water spray provided by a separate pump and heat exchanger.

### Bundle

The bundle contains 64 12-ft long rods, 60 of which are resistance heated using DC electric power. Each rod is capable of providing 125 kW of power. Four unheated rods are positioned at locations corresponding to control rod locations within an actual 17 x 17 nuclear fuel assembly. Both axial and radial power pro

files within the bundle are flat. A cross section of the THTF bundle is presented in Figure A.15-3.

Figure A.15-4 shows the location of thermocouples and spacer grids within the bundle. Rod temperature measurements are made at 25 axial locations within the heated length of the bundle; spacer grids are located at 0.61-m intervals along the test section.

Individual rods (see Figure A.15-3 for the cross section) consist of a stainless steel outer sheath with an Inconel heating element centered by boron nitride filler material. The rods are manufactured using boron nitride preforms which ensure the accurate placement of both the heating element and rod sheath thermocouples. Once in place, the preforms are compressed and powdered both by packing longitudinally and swaging the outer sheath. This process ensures direct contact between the sheath thermocouples and the sheath itself. Boron nitride was chosen because of its thermal similarity to stainless steel, as well as its electrical insulating capability. Each rod contains a maximum of twelve sheath thermocouples and four centerline thermocouples.

In order to measure local steam temperatures, the bundle contains fluid thermocouples, some protruding from the unheated instrument rods and some located within subchannels at the end of the heated length of the bundle. Differential pressure taps used to determine void fraction and bundle pressure drop are located at various axial positions within the bundle.

#### Data Acquisition System

The data acquisition system consists of a Digital Equipment Corporation (DEC) PDP-11/34 minicomputer and various peripheral devices and interfaces. The minicomputer employs DEC's real-time multitasking executive software, RSX-11M, while all application software is written in FORTRAN.

Multiple cartridge disks are used as storage for the operating system, application programs, instrumentation data base, plots, and short data scans. Magnetic tape units are used to record and process data acquired from the loop instrumentation during loop calibration, checkout, and test operations. Because the units are industry compatible, the magnetic tapes are also used to interchange data and software programs with other computers. The high-speed analog input system consists of two data acquisition subsystems. The first subsystem acquires data from the 256 loop instruments, and the second acquires data from up to 1024 bundle and loop thermocouples. The analog input system collects data at a maximum of 20,000 samples per second. Typically, this corresponds to an individual channel frequency response of 10-20 Hz. The present software package allows the first subsystem to sample each of the 256 loop instruments five times more frequently than the second subsystem samples each of the 1024 bundle thermocouples; this allows every loop instrument to be sampled 100 times per second and bundle and loop thermocouples to be sampled 20 times per second. A custom computer interface for the analog input subsystems provides equally spaced data values at the full sampling rate while allowing hardware limit checking to be carried out concurrently on all thermocouples.

#### REFERENCE

- A.15-1 D. K. Felde et al., "Facility Description, THTF MOD 3 ORNL PWR BDHT Separate-Effects Program," ORNL/TM-7842, Oak Ridge National Laboratory, September 1982.

Table A.15-1 THF operating parameters

---

Maximum loop conditions	17.2 MPa/616 K
Heat removal capacity	7.5 MW
Maximum rod bundle power	7.5 MW
Pump design flow/head	700 gpm/590 m
Data acquisition scan rate	20,000 channels per second
Maximum rod temperature	1088 K
Rod length	3.66 m

---

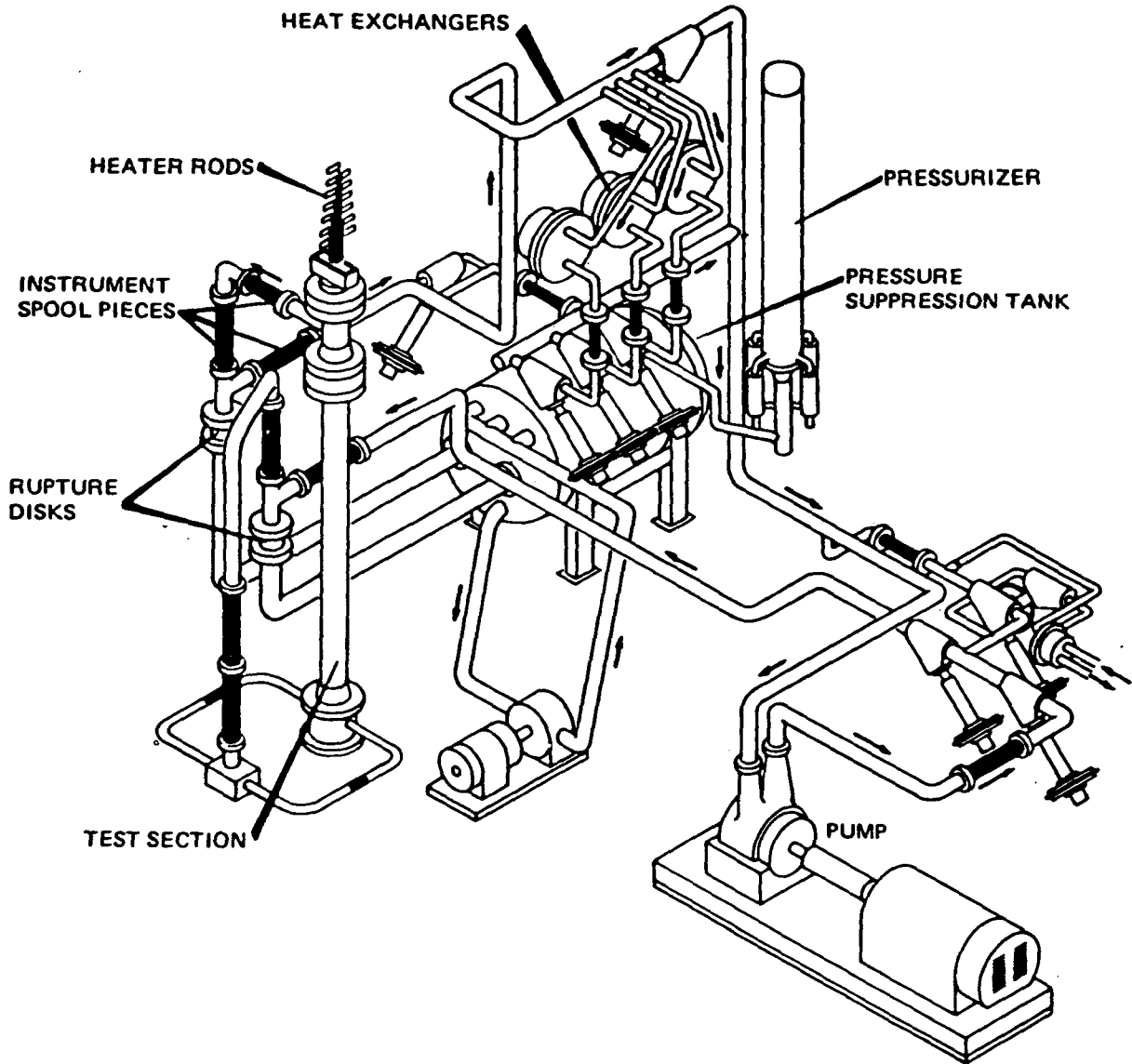


Figure A.15-1 Diagram of THTF

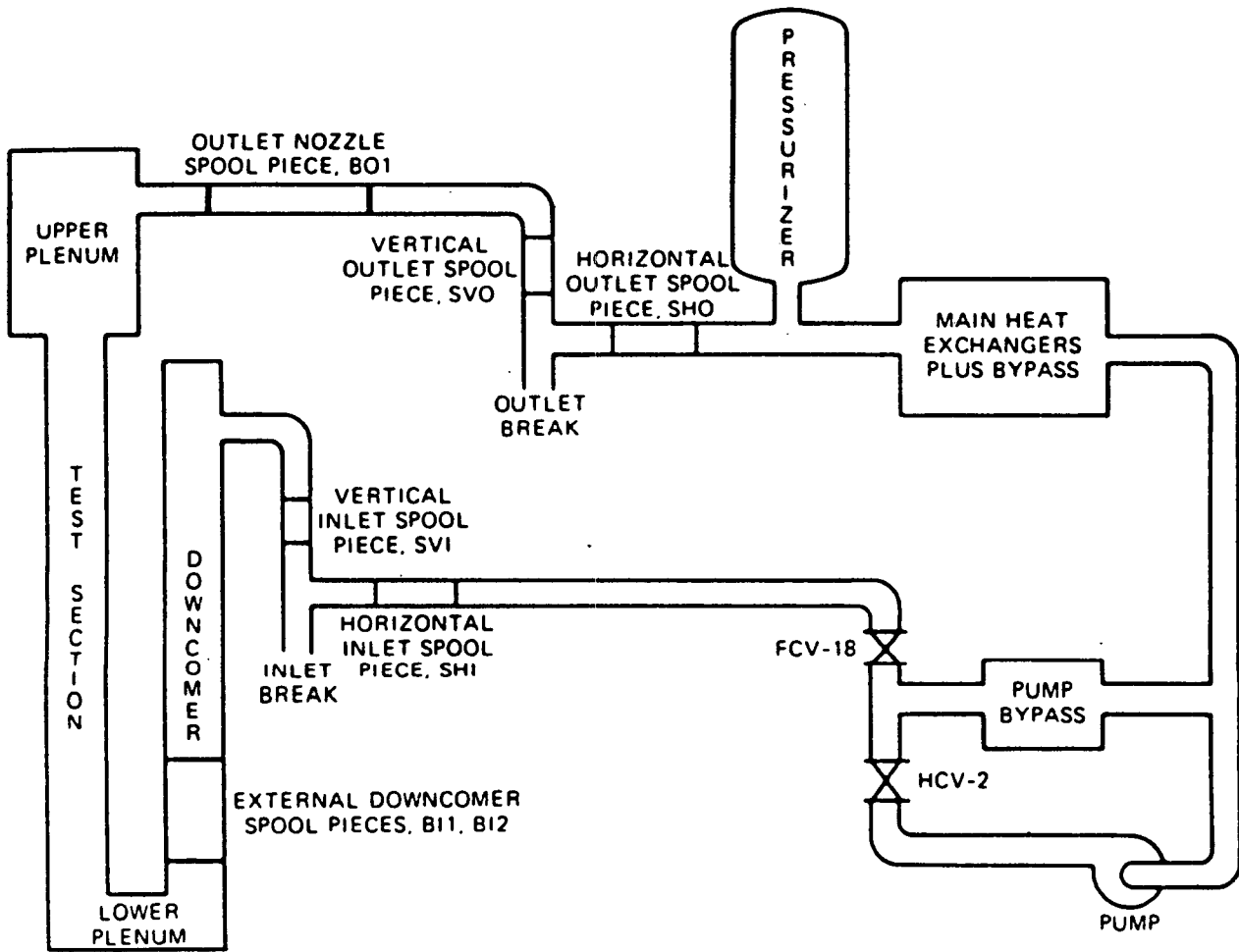


Figure A.15-2 Schematic of THTF loop

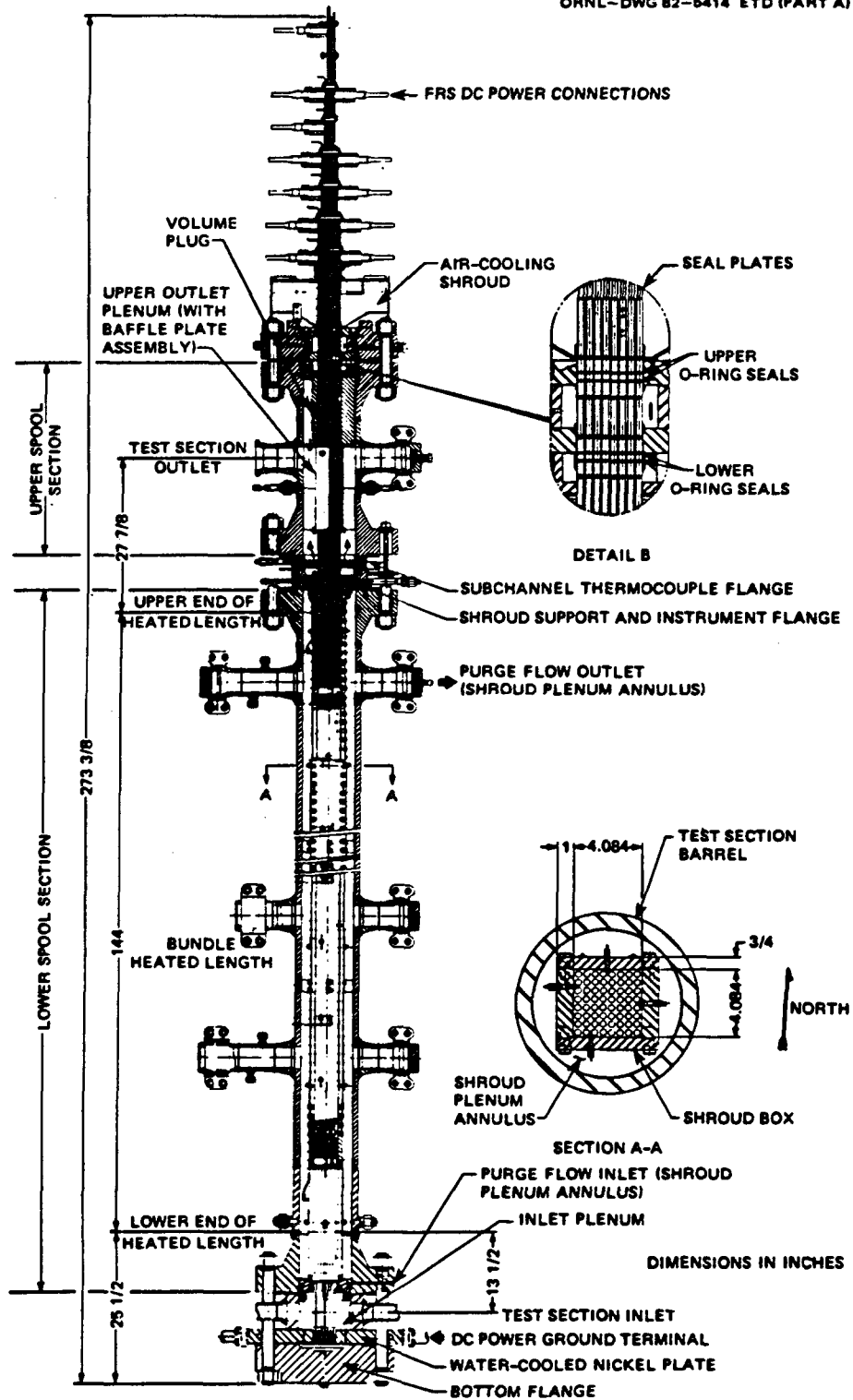


Figure A.15-3 Bundle and rod cross sections

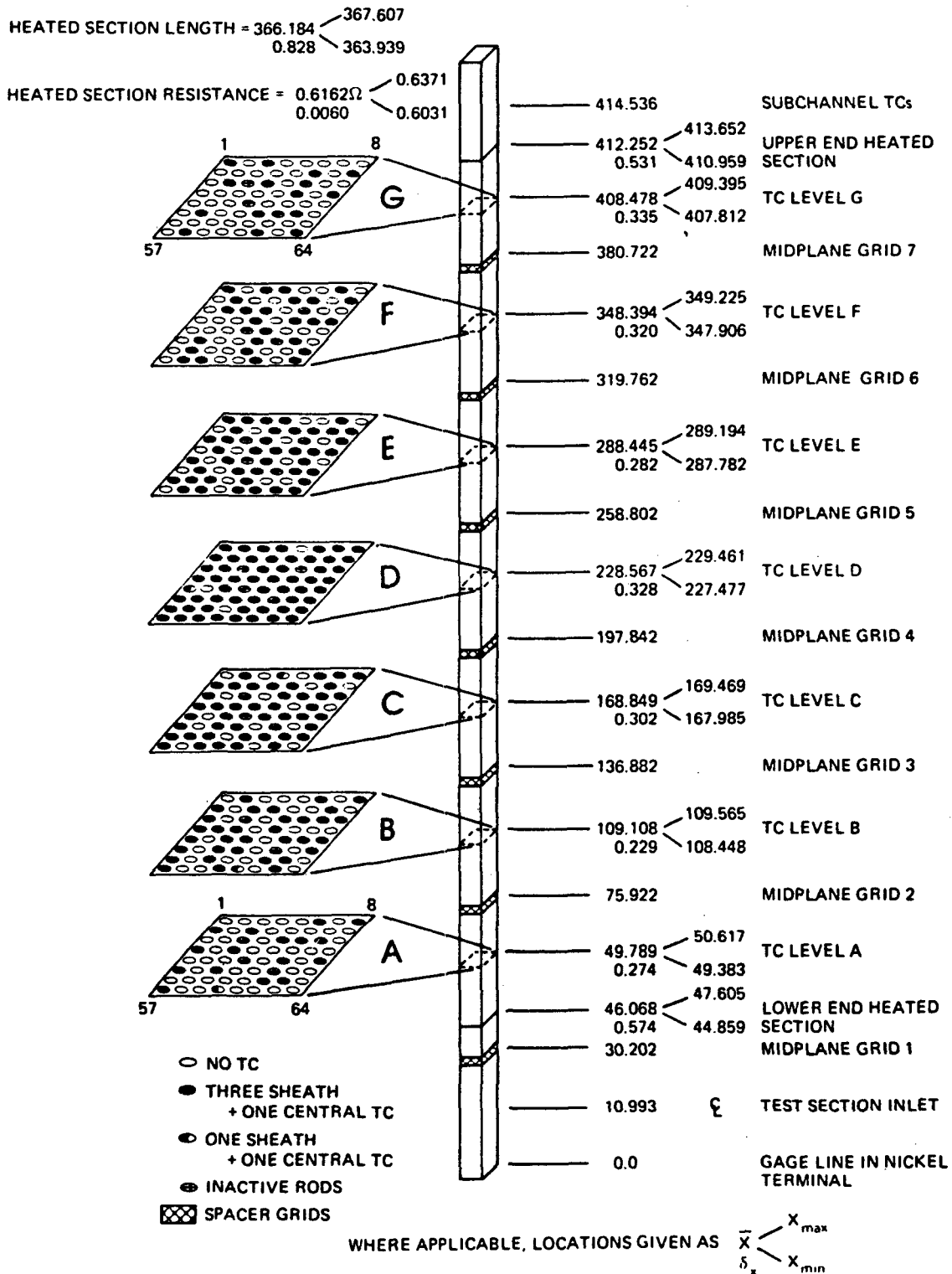
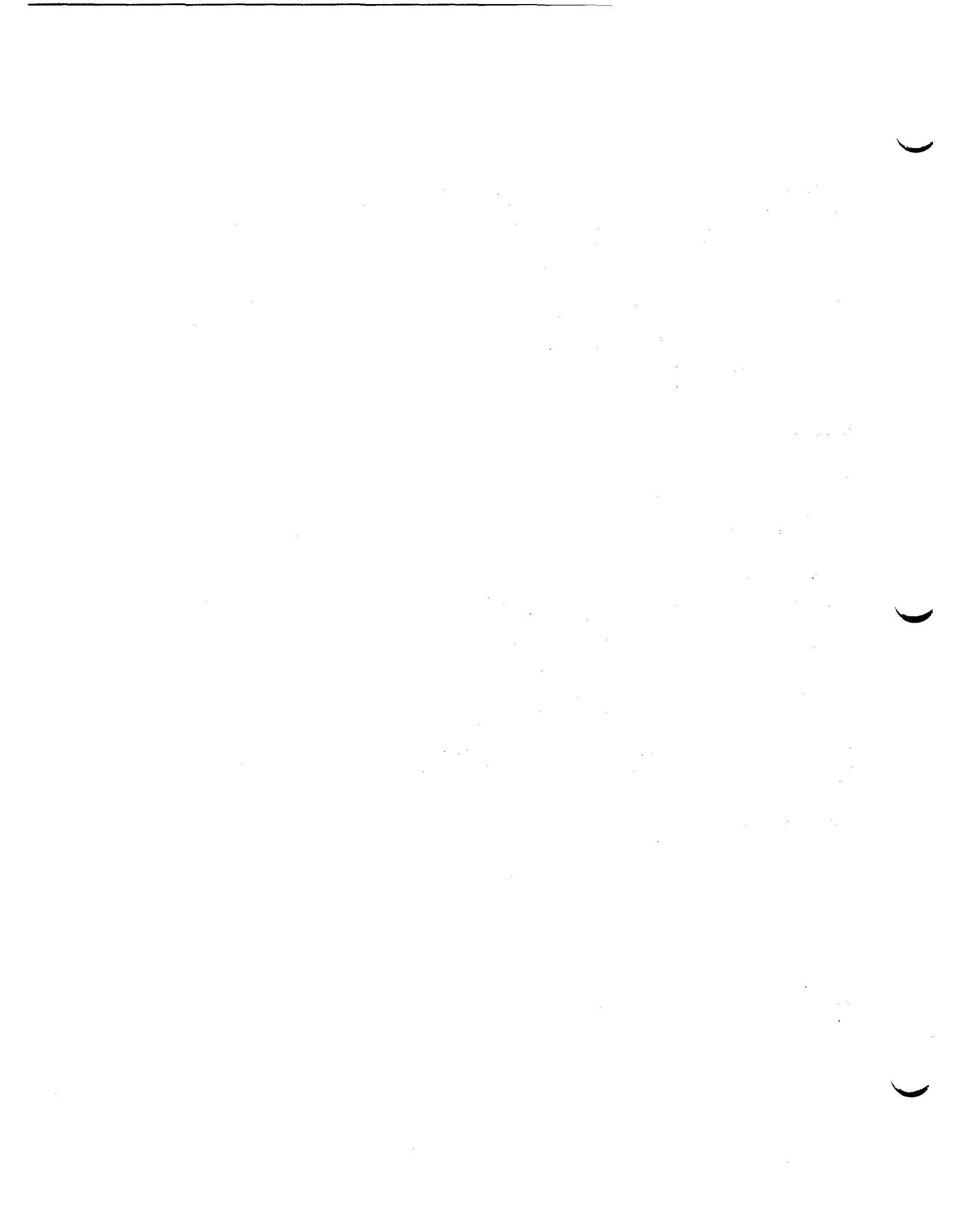


Figure A.15-4 Spacer grid and thermocouple locations within the THTF bundle  
 Note: dimensions are in centimeters



## A.16 BOILING WATER REACTOR FULL INTEGRAL SIMULATION TEST FACILITY

The Full Integral Simulation Test (FIST) Facility is an upgrade of the TLTA (see Appendix A.9) to eliminate the inherent scaling compromises identified in previous BWR blowdown programs and allow more realistic simulation of LOCAs from break initiation through reflood as well as simulation of transient events involving loss of inventory, multiple system failures, and power transients.\*

This facility was jointly sponsored by and is owned by the U.S. Nuclear Regulatory Commission, the Electric Power Research Institute, and the General Electric Co. (Ref. A.16-1). All planned testing in this facility has been completed and the facility is being maintained. However, the facility bundle was damaged in the last test series and certain instrumentation has been removed for storage. The facility is located at the General Electric Co. site in San Jose, California.

### Description

Figure A.16-1 is a schematic of the FIST test facility, a detailed description of which is given in Reference A.16-2. It features full-height scaling of the vessel and all internal components, a realistic core configuration, accurately scaled components and volumes, operating ECC systems, and a heated feedwater system that provides the capability of limited steady-state operation.

### Pressure Vessel

FIST is an outdoor insulated carbon steel facility. The 64-ft-high test vessel has a volume of 180 gal, which represents very closely the BWR to FIST scale factor of 624 to 1. It is designed for a pressure of 1325 psia at 600°F.

In addition to the main vessel, FIST has a side arm that provides an external downcomer in which two full-height jet pumps are housed and from which flow is taken to two recirculation loop pumps and returned as drive flow for the jet pumps. The jet pumps are the units from TLTA, modified to full height with a scaled tailpipe diameter. The TLTA units were used because of their known characteristics and capability to provide FIST-scaled core flow. The lower plenum houses a simulated guide tube.

The main vessel contains the rest of the scaled volume of the lower plenum, the guide tube region, the bundle/channel, the bypass, the steam separator, a dryer mockup, and the steam dome. This division of the vessel permits a scaled cross-sectional area in the downcomer so that the normal water level is at full reactor height, thereby providing a realistic simulation of level transients and natural circulation conditions.

---

\*The FIST facility is intended to investigate only the thermal hydraulic phenomena associated with a programmed power transient. No simulation of nuclear feedback is possible.

## Core Region

The bundle and bypass regions are composed of several prototypical BWR components, including the fuel support and side entry orifice, the lower tieplate base, and a BWR/6 zircaloy channel housing the rod bundle. Leakage paths in the BWR from the guide tube, lower plenum, and bundle into the bypass are all simulated in FIST. The bundle consists of 62 heater rods and 2 water rods. The heater rod diameters and pitch are the same as those in the BWR. The axial power profile is a 150-in.-long chopped cosine using skin-heated rods.

The heater rods have the same basic design as those used in the TLTA (Ref. A.16-3). While the TLTA design used a ceramic-lined stainless steel channel and a separate bypass region, the FIST bundle uses a typical BWR Zircaloy channel that is physically and thermally in contact with the bypass region, thereby allowing for more realistic bundle-to-bypass heat transfer. More realistic bundle inlet and outlet components are also used, as shown in Figures A.16-2 and -3.

The FIST facility uses the TLTA power supply, which is capable of delivering a maximum power of about 7 MW to the bundle. This is sufficient for the transients that are initiated from the core average bundle power (4.64 MW), as well as the LOCA tests, which require a maximum of 6.49 MW to simulate the peak power bundle in the core.

Pressurization power transients are predicted to result in a peak surface heat flux of about 150% of the initial value, and the use of direct surface heaters requires the bundle power supply to approximate this same transient. The 7-MW capability is sufficient for simulating these core average power transients, since the overpower condition is based on a core average initial power of 4.64 MW.

The FIST heater bundle axial and local power distributions are shown in Figures A.16-4 and -5. Sensitivity analyses on variations in both axial and local power distributions indicate that these represent the limiting conditions with respect to predicted peak cladding temperature during a hypothetical design basis accident (Ref A.16-3).

## Recirculation System

The FIST facility includes two complete independent recirculation loops as well as blowdown lines to simulate a break in one of the loops. Pump inertia is adjusted for each loop to achieve a core flow coastdown that is characteristic of the reference BWR.

## Heated Feedwater System

A heated feedwater system capable of delivering makeup water at BWR rated temperature and scaled flow is included in the FIST facility to allow for simulation of BWR operating transients. More specifically, the system allows steady-state operating conditions for up to 5 minutes at the core average bundle power of 4.64 MW. It also provides the characteristic downcomer temperature gradients necessary for simulating slow-loss-of-inventory events and natural circulation conditions.

## Safety/Relief Valves

The 16 BWR-6 safety/relief valves (SRVs) are simulated in FIST through the use of five valves corresponding to the five functional groups of SRVs in the BWR. The discharge flow from each simulated SRV group is set using flow orifices.

## ECCS Simulation

High-pressure core spray, low pressure core spray, and low pressure coolant injection systems are simulated in the FIST design using the same techniques proven in the TLTA under the BD/ECC Program (Ref. A.16-3). Simulation of the automatic depressurization system (ADS) is accomplished using the simulated SRV that normally represents the BWR SRV group with the highest setpoint. The associated flow orifice matches the scaled ADS flow.

## Reactor Core Isolation Cooling System

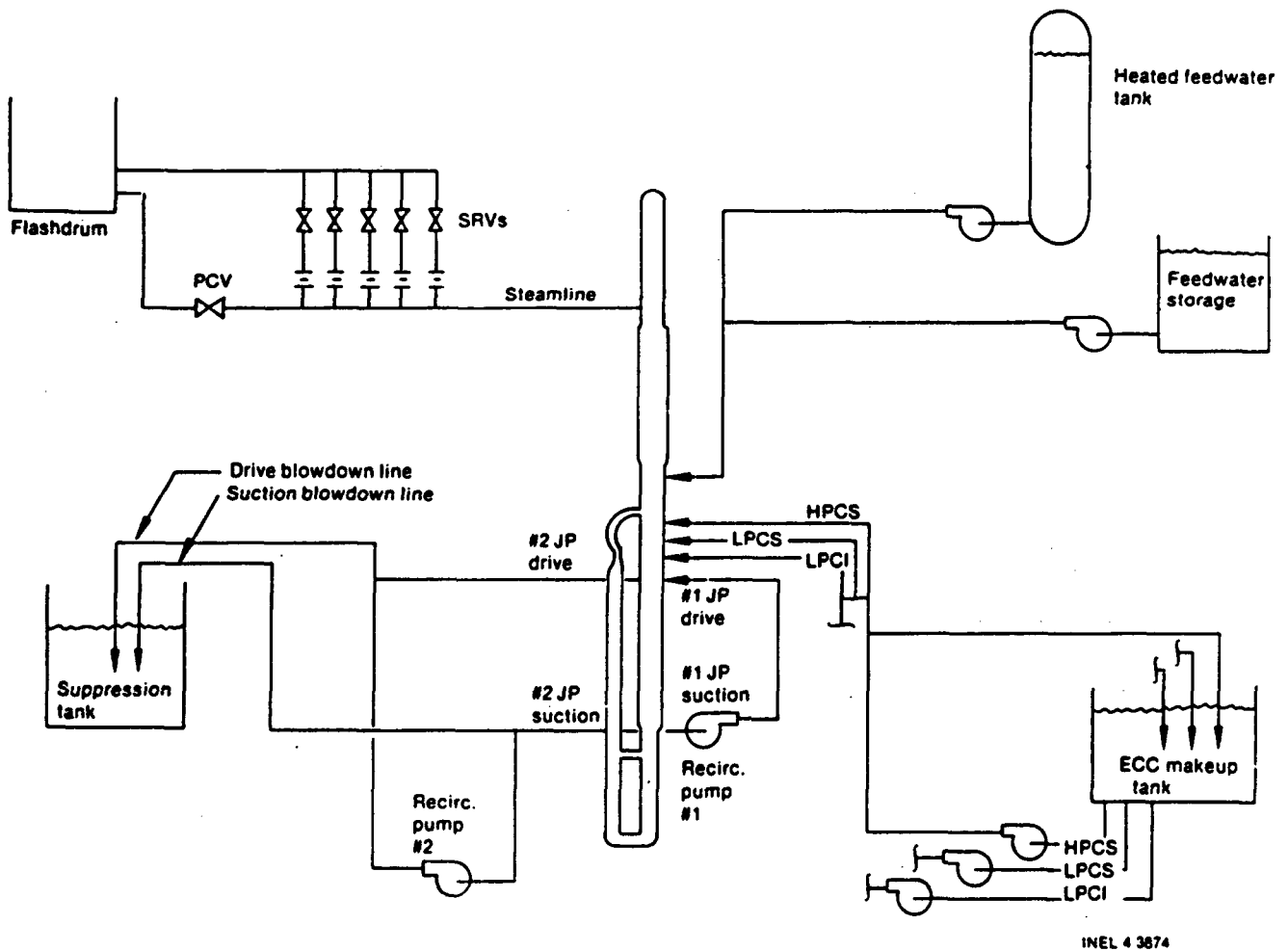
The simulation of operational transients in which non-safety-grade systems are assumed to function requires simulation of the reactor core isolation cooling (RCIC) system. This is accomplished in the FIST facility by injecting the scaled RCIC flow through the feedwater inlet, as this is typical of most BWRs. A separate flow control valve is supplied for this purpose.

## Instrumentation

There are 426 experimental measurements planned for the first test, of which 30% are differential pressure, 26% are heater rod temperatures, 19% are fluid temperatures, and 10% are void fraction. There are 8 calibrated flow measuring instruments within the test vessel and 14 flow orifices in incoming and outgoing lines. A minicomputer-based data acquisition system is used to store test data directly on magnetic tape. The system's output is used to establish whether or not test acceptance criteria are satisfied and to provide a data tape for further data processing on the INEL computer where record data for each test is finally stored.

## REFERENCES

- A.16-1 Contract No. NRC-04-76-251, Modification No. 11 "BWR FIST Program," GE, EPRI, NRC, April 1981.
- A.16-2 A.G. Stephens, "BWR Full Integral Simulation Test (FIST) Program Facility Description Report," NUREG/CR-2576, Sept 1984.
- A.16-3 W. J. Letzring et al., "BWR Blowdown/Emergency Core Cooling Program Preliminary Facility Description Report for the BD/ECC1A Test Phase," GEAP-23592, General Electric Company, December 1977.



INEL 4 3874

Figure A.16-1 Schematic of BWR FIST facility

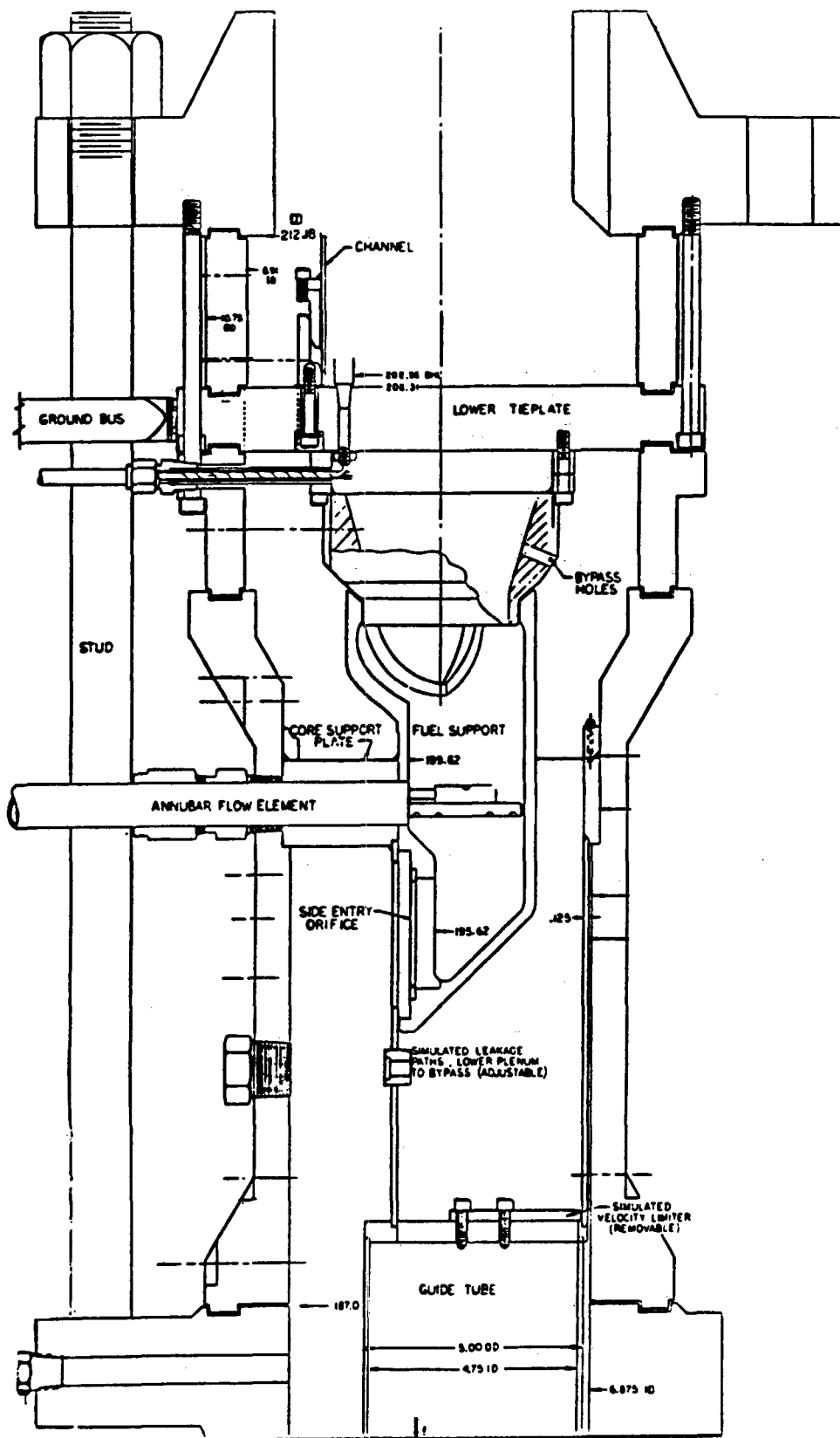


Figure A.16-2 FIST bundle inlet region and lower tie plate/electrode

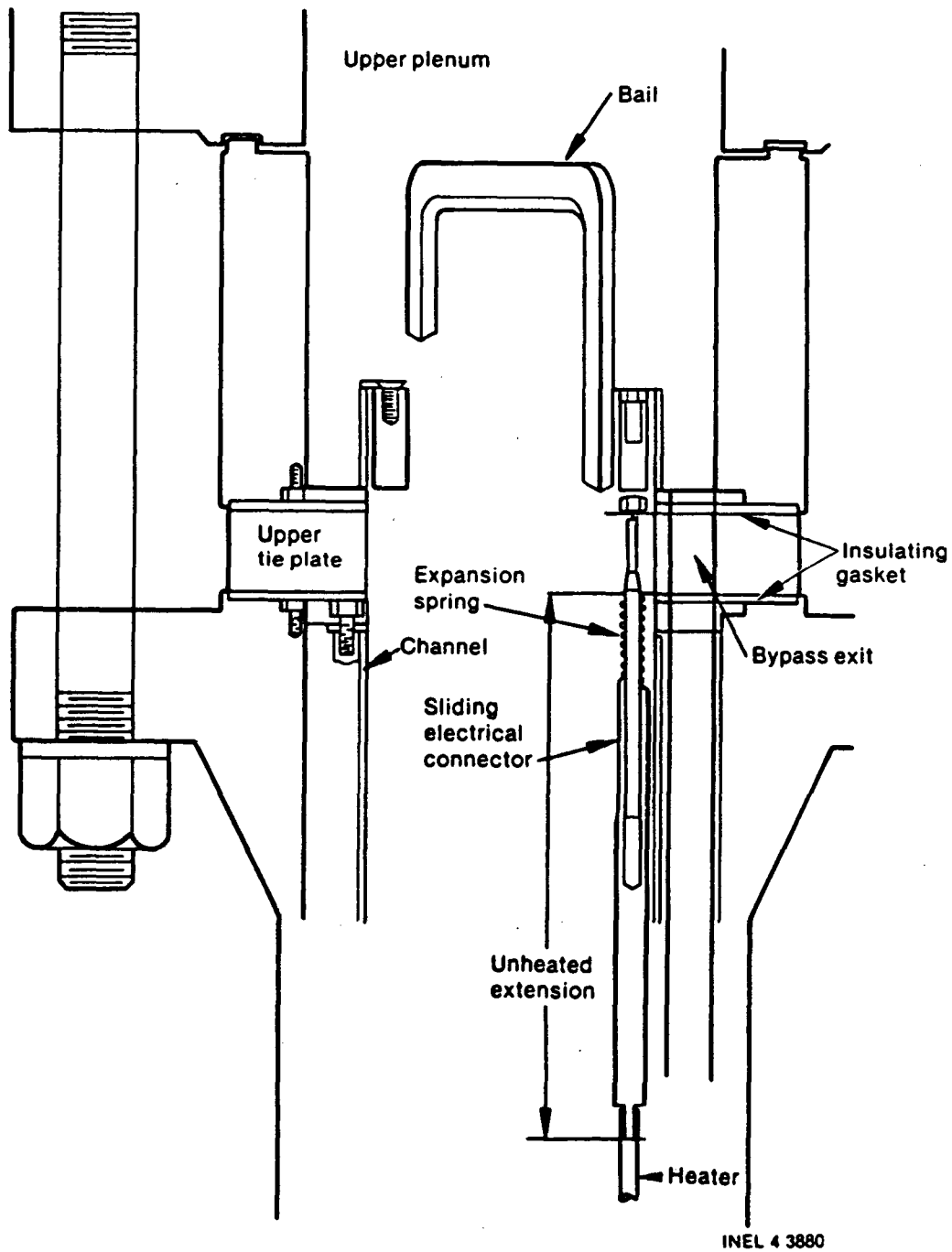
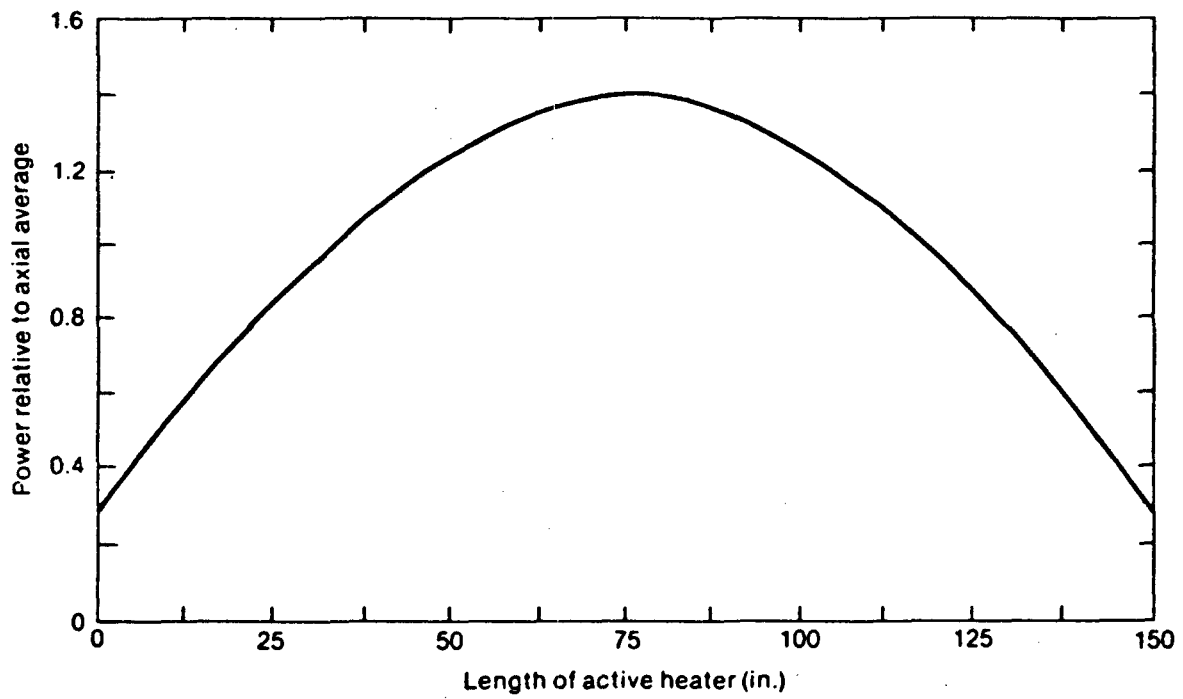
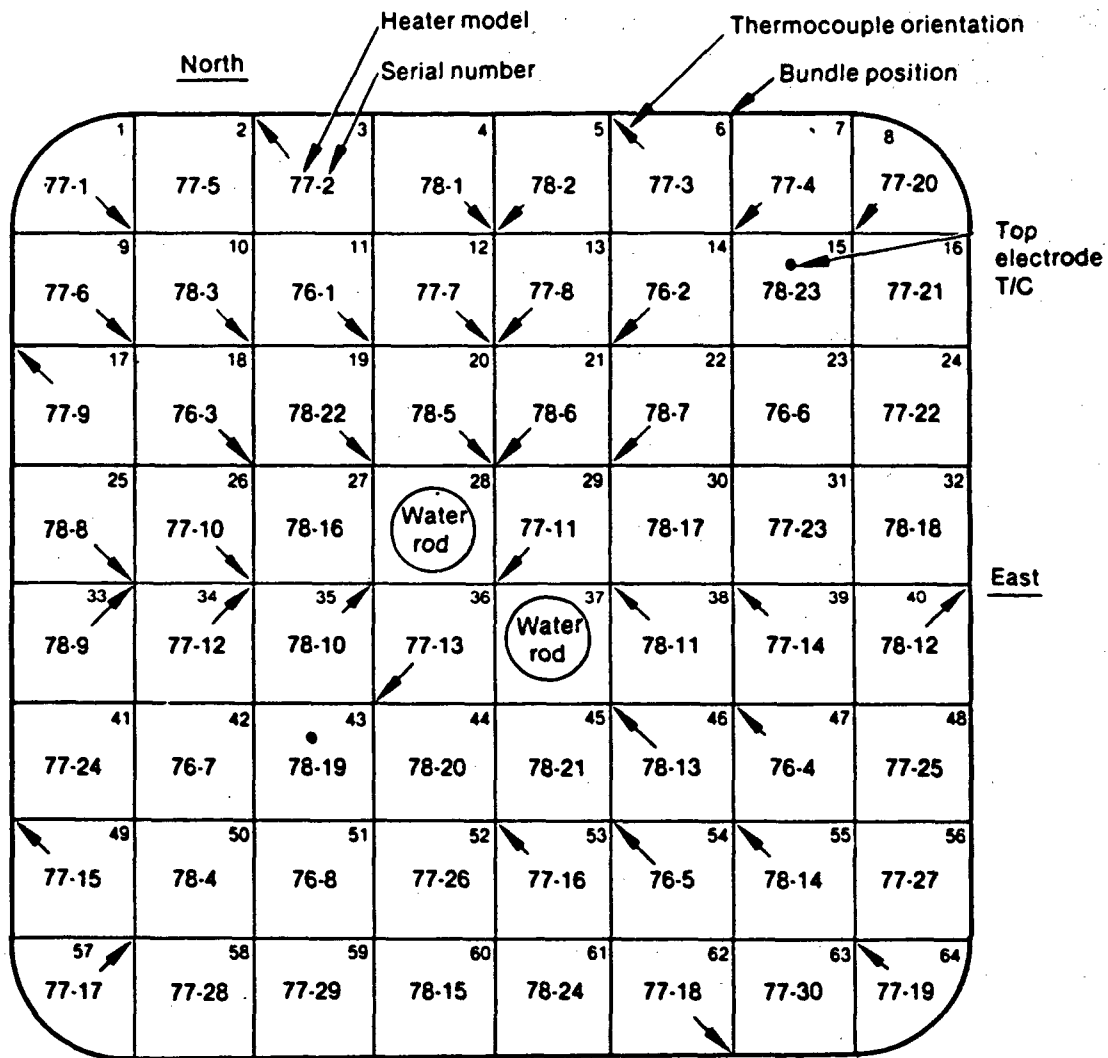


Figure A.16-3 FIST Bundle Outlet Region and Upper Tie Plate/Electrode



INEL 4 3898

Figure A.16-4 FIST Axial Power Profile



Plan view from above  
INEL 4 3903

Rod Heater Model 76 Power Factor = 1.04  
 Rod Heater Model 77 Power Factor = 1.01  
 Rod Heater Model 78 Power Factor = 0.97

Figure A.16-5 FIST Local Power Profile

## A.17 UPPER PLENUM TEST FACILITY

The Upper Plenum Test Facility (UPTF) is located in Mannheim, Federal Republic of Germany, at the site of the Grosskraftwerk Mannheim coal-fired power station. This facility is supported by the Ministry for Research and Technology. At the time of this writing, UPTF was in the final stages of construction and commissioning, was in the final stages of construction and commissioning, and no official tests had been run. UPTF is one of three test facilities included in the trilateral 2D/3D Program. (The other facilities are the Cylindrical Core Test Facility and the Slab Core Test Facility in Japan.) The NRC provided advanced instrumentation for installation in UPTF and computer analysis in support of the testing. The UPTF is a full-scale simulation of a 1300 MWe German Kraftwerk Union PWR, specifically the Grafenrheinfeld plant. An overall view of UPTF is shown in Figure A.17-1.

The UPTF primary reactor vessel is full scale and includes precise geometric simulations of the upper plenum, core barrel and core shroud, downcomer, coolant loop nozzles, and the upper one meter of the core. The simulated fuel rods in the upper core are unheated. The lower 75 percent of the core is replaced by a core simulator injection system, which is designed to inject steam and water in the amounts and distribution that would be generated in the core during reflood (Figure A.17-2). The lower plenum contains the piping leading up to the core simulator injection system. The upper plenum contains a full complement of internals at full scale and in an arrangement duplicating the reference PWR.

The UPTF includes four primary coolant loops. Hot- and cold-leg piping are full scale. The steam generators are replaced by simulators that are steam/water separators. Each simulator also includes a steam injection system to "replace" the separated water stream with a steam flow that would normally be created by vaporization in the steam generator. The four primary coolant pumps are simulated by resistances. The pump simulators are adjustable and can be closed completely when it is desired to conduct single-loop separate-effect studies. One of the primary coolant loops has controllable break valves that can be used to simulate a partial or full offset break in the hot- or cold-leg piping. Special high-capacity steam/water separators are included downstream of the break. Figure A.17-3 shows an overall flow diagram for UPTF, and Table A.17-1 summarizes its major features.

The UPTF is designed principally to test the upper core and upper plenum behavior during the end of blowdown, refill, and reflood phases of a large-break LOCA. Downcomer effects, particularly the bypass of ECC injected through the cold legs during end of blowdown and refill, will also be investigated. About half of the planned 30-test matrix will cover combined injection ECC (hot leg and cold leg injection) which is typical of German PWRs. The other half will cover cold leg injection conditions typical of U.S. PWRs. Separate special tests covering the fluid/fluid mixing during a postulated pressurized thermal shock event and the hot leg countercurrent flow during the reflux cooling mode of a postulated small-break LOCA are also included in the matrix.

Table A.17-1 Summary of major features of UPTF

---

**PRIMARY VESSEL**

---

General

Height: 13.5 m  
 Inside Diameter: 4.865 m  
 Downcomer Gap: 250 mm  
 Design Pressure: 22 bar  
 Design Temperature: 220°C

Core

No. Heated/unheated rods: 0/49408  
 Rod O.D.: 10.7 mm  
 Rod Pitch: 14.3 mm  
 Heated Length: N/A  
 Axial Peaking Factor: N/A

Downcomer

Area: 3.62 m<sup>2</sup>  
 Height (Bottom of LP to Cold Leg Nozzle): 9.2 m

Lower Plenum

Volume: 23.9 m<sup>3</sup>  
 Structures: Piping

Upper Plenum

Volume: 43 m<sup>3</sup>  
 Structures: Full Scale

---



---

**PRIMARY LOOPS**

---

Piping

No. Loops: 4  
 Hot Leg Flow Area: 0.44 m<sup>2</sup>  
 Cold Leg Flow Area: 0.44 m<sup>2</sup>

Steam Generators

Number: 4  
 Type: Steam/Water Separator  
 No. Tubes: N/A  
 Tube O.D./I.D.: N/A  
 Tube Length: N/A  
 Secondary Pressure: N/A

Pumps

No.: 4  
 Type: Simulated by Resistance

Break

Location: Cold/Hot Leg  
 Type: Variable up to 100% Offset

Pressurizer

No.: None  
 Location:

---



---

**ECC SYSTEMS**

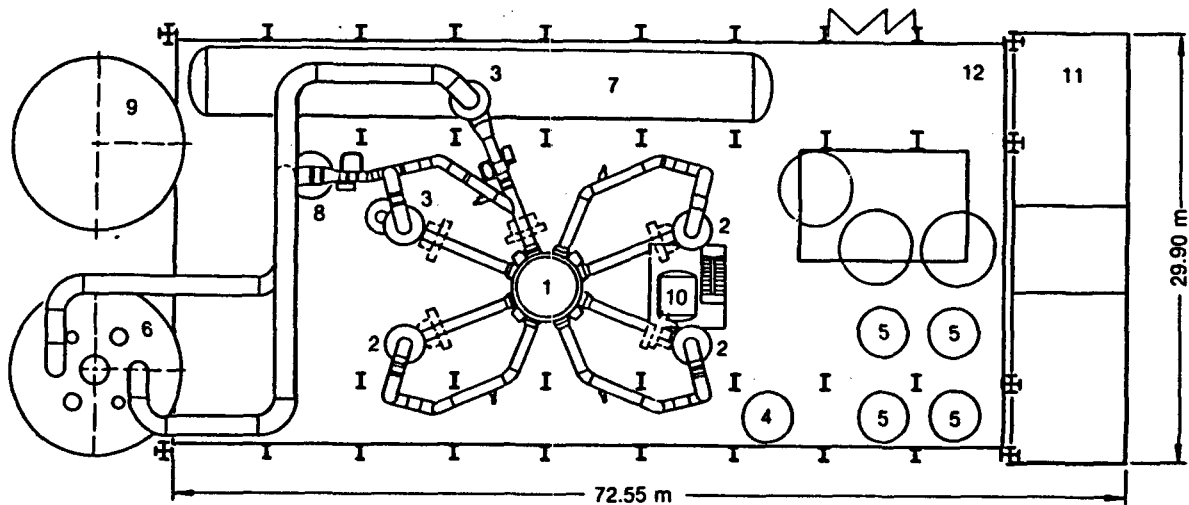
---

Injection Locations

- Cold Leg
- Hot Leg
- Downcomer

Injection Sources

- Accumulator
  - LPCI
-



- |  |                         |                         |
|--|-------------------------|-------------------------|
| 1 Test vessel                            | 5 Accumulators          | 9 Water collecting tank |
| 2 Steam generator simulator, intact loop | 6 Containment simulator | 10 Drainage tank        |
| 3 Water separator, broken loop           | 7 Ruth storage tank     | 11 Switchgear building  |
| 4 Hot water storage tank                 | 8 N <sub>2</sub> -tank  | 12 Test building        |

6 4118

Figure A.17-1 Top view of the Upper Plenum Test Facility

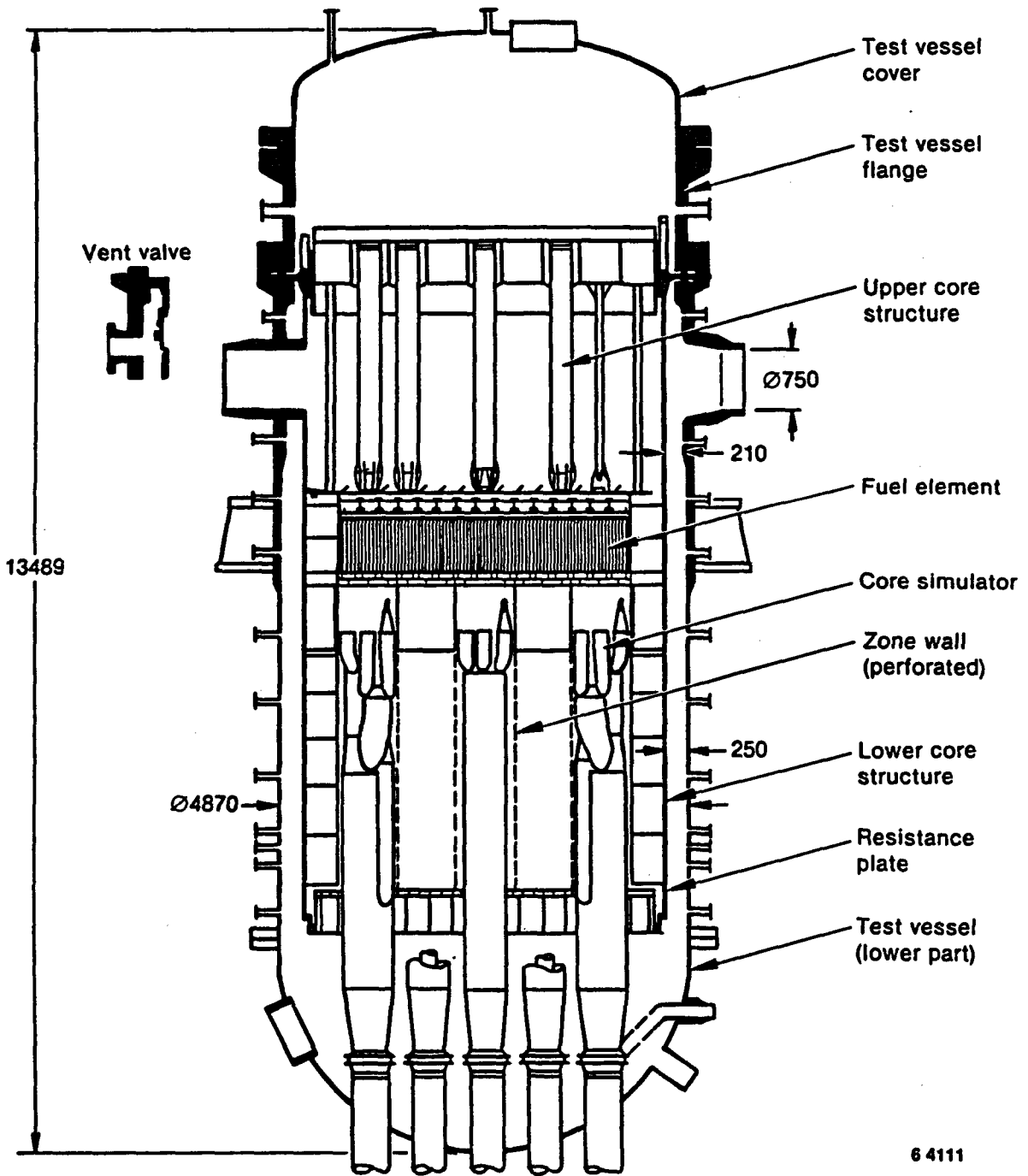
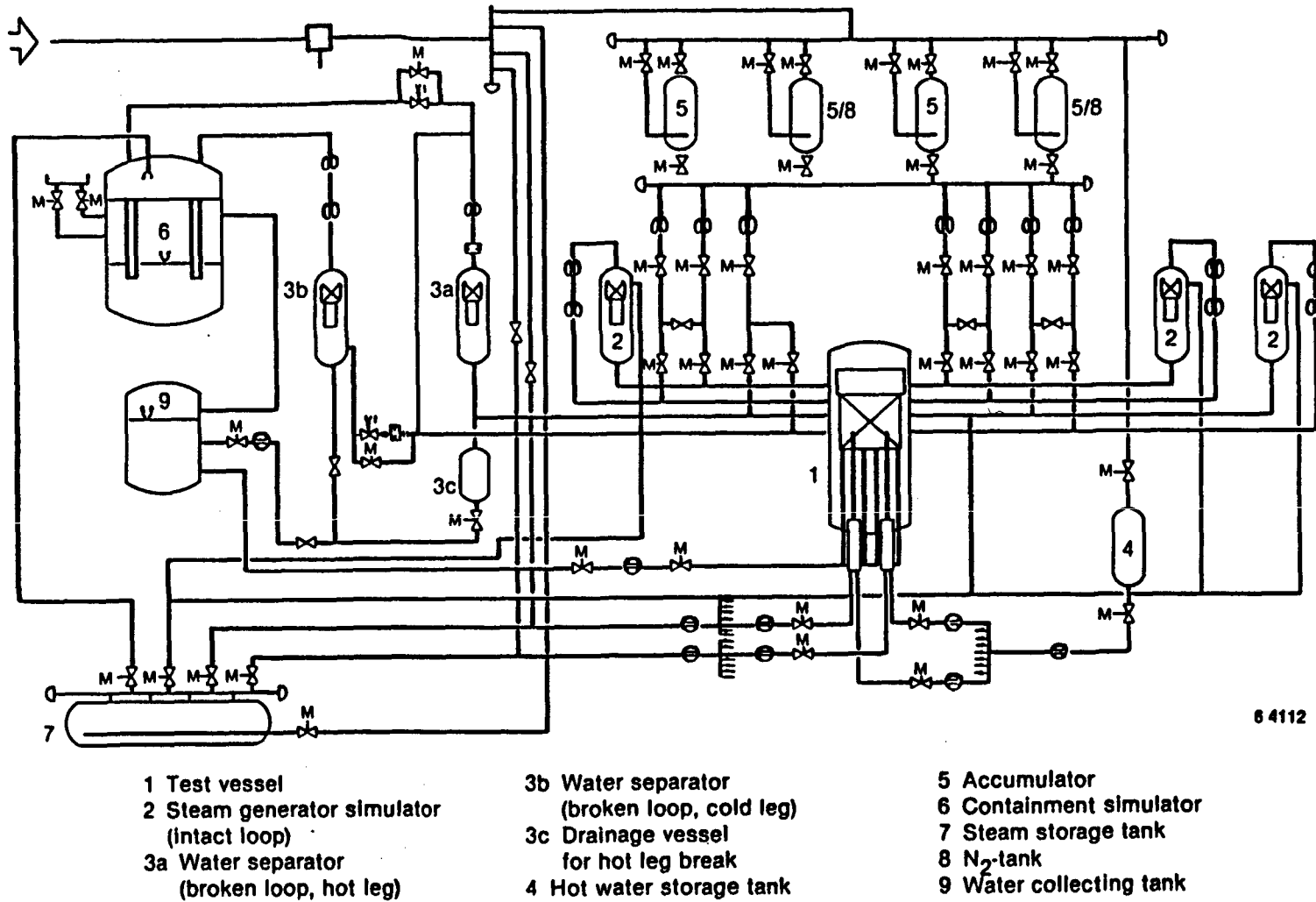


Figure A.17-2 Upper Plenum Test Facility pressure vessel and internals



6 4112

Figure A.17-3 Flow diagram for the Upper Plenum Test Facility



## A.18 CREARE ECC/CORE STEAM FLOW EXPERIMENTS

As part of NRC's effort to evaluate the effectiveness of ECCS design, CREARE Incorporated was contracted to design, build and operate five small-scale facilities. The types of experiments were generally the same at each facility, but the scale sizes were different in order to test the scaling theories that would be used to extend the data to full-size plants. The five facilities are:

1. 1/30-scale transparent facility
2. 1/30-scale countercurrent flow facility
3. 1/15-scale countercurrent flow facility
4. 1/15-scale planar facility
5. 1/5-scale countercurrent flow facility

The primary phenomenon examined with these tests was countercurrent core steam/ECCS fluid flow in the downcomer. The tests simulated a cold leg break in a PWR at various pressures, flow rates, and steam/water temperatures. Some of the facilities had special capabilities in order to perform blowdown tests, visualization studies, or hot-wall delay tests. Each of these facilities is described in the following sections.

Table A.18-1 compares the 1/30-scale (transparent), the 1/15-scale and the 1/5-scale facilities to a typical PWR.

### A.18.1 1/30-Scale Transparent Facility

Figure A.18-1 is a schematic of the 1/30-scale transparent facility. The following identifies the facility dimensions and capabilities.

<u>Test Vessel</u>	<u>Dimensions</u> (inches)
- cold leg inside diameters	1.0
- annulus gap size	0.25
- upper annulus height	6.0
- downcomer length	9.0
- lower plenum depth	21.0
- core barrel inner diameter	1.0
- vessel inner diameter	5.95
- core barrel outer diameter	5.95
- average annulus circumference	17.9
- hot legs	none

### Instrumentation

<u>Parameter</u>	<u>Device</u>
- cold leg fluid flow rate	rotameter
- cold leg fluid temperature	thermocouples
- steam flow rates	orifice/manometer
- air flow rate	rotameter
- lower plenum pressure	pressure transducer
- water delivery timing	stopwatch

## Plant

cold leg fluid flow rates	20 gpm
cold leg fluid temperatures	205°F (max)
pressure	30 psia (max)
steam supply	120 psig

## Facility Capabilities

- models countercurrent core steam/ECCS water flow in the downcomer region
- models countercurrent core steam/ECCS water flow in presence and noncondensibles
- permits visualization of downcomer oscillations during ECC injection

### A.18.2 1/30-Scale Countercurrent Flow Test Facility

Figure A.18-2 is a schematic of the 1/30-scale countercurrent test vessel. The following identifies the facility dimensions and capabilities.

#### Overall Characteristics

cold leg fluid flow rates	20 gpm
pressure	30 psia (max)
cold leg fluid temperatures	208°F (max)
steam supply	120 psig

#### Test Vessel

	<u>Dimensions</u> (inches)
Cold Leg Inside Diameter	1.0
Hot Leg Simulator Diameter	1.5
Gap Size	0.267, 0.502
Upper Annulus Height	3
Downcomer Length	9
Lower Plenum Depth	24
Core Barrel Inner Diameter	4.24, 3.75
Vessel Inner Diameter	6.14
Core Barrel Outer Diameter	5.60, 5.13
Average Annulus Circumference	18.4, 17.7

#### Facility Capabilities

- models countercurrent core steam/ECCS water flow during cold leg break
- permits testing of various annulus gap sizes at 1/30 scale

### A.18.3 1/15-Scale High-Pressure Cylindrical Facility

Figures A.18-3 and A.18-4 are schematics of the 1/15-scale high pressure cylindrical test configuration and vessel geometry. The following identifies the facility dimensions and capabilities.

## Overall Characteristics

### Geometry

Intact Cold Legs:	3
Hot legs:	4
Cold Leg Diameter (ID):	1.875 in.
Hot Leg Diameter (OD):	3.00 in.
Injection Pipe Diameter (ID):	0.625 in
Injection Angle:	60°
Downcomer Gap:	0.5, 1.0 in.
Downcomer Length (below cold leg centerline):	18, 48 in.
Vessel Length:	29.75, 59.75 in.
Vessel Inside Diameter:	11.5 in.
Lower Plenum Radius:	5.75 in.
Average Annulus Circumference:	34.6, 33 in.

### Flow Rates

Water Flow Per Cold Leg (Max):	100 gpm
Water Flow Total (Max):	300 gpm
Steam Flow Per Cold Leg (Max):	1 lb/sec
Steam Flow in Core (Max):	3 lb/sec
Steam Flow Total (Max):	3 lb/sec

### Temperatures

Steam:	212-340°F
Injected Water:	60-212°F
Wall:	70-600°F

### Pressure

Vessel Design Pressure:	600 psia
Facility Design Pressure:	150 psia
System Operating Pressure:	125 psia

### Facility Capability

- models countercurrent core steam/ECC water flow during old leg breaks
- permits testing of various annulus gap sizes and downcomer lengths at high pressure (Figure A.18-5)
- capability of performing blowdown studies (Lower plenum fluid flashing following cold leg break)
- capable of multiple ECC temperatures to determine affect of subcooling

#### A.18.4 1/15-Scale Planar Facility

Figures A.18-6 through A.18-8 are schematics of the 1/15-scale planar facility and fluid flow paths. The following identifies the facility dimensions and capabilities.

## Overall Characteristics

### Geometry

Intact Cold legs:	1 to 3
Hot Legs:	0 to 4
Cold Leg Diameter (ID):	1.875 in.
Hot Leg Diameter (OD):	3.0 in
Injection Pipe Diameter (ID):	0.613 in.
Injection Angle:	60°
Downcomer Gap:	0.2 to 2 in.
Downcomer Length:	18 in.
Downcomer Width:	36 in.

### Flow Rates

Maximum Water Flow per Cold Leg:	100 gpm
Maximum Total Water Flow Rate:	300 gpm
Maximum Steam Flow per Cold Leg:	60 lbm/min
Maximum Core Steam Flow Rate:	180 lbm/min
Maximum Total Steam Flow Rate:	180 lbm/min

### Temperatures

Steam Temperature:	212 to 300°F
Water Temperature:	50 to 212°F
Water Subcooling:	0 to 160°F
Wall Temperature:	70 to 600°F

### Facility Capability

- models countercurrent core steam/ECC water flow during cold leg breaks
- superheated wall capability to evaluate hot wall delay effect on ECC penetration into the lower plenum
- cold leg steam capability to determine how ECC injection mixing in a steam filled cold leg affects ECC penetration into the lower plenum
- facility can model three types of flow baffles in the downcomer to determine effects on ECC penetration into the lower plenum

Table A.18-2 describes the combination of tests performed:

#### A.18.5 1/5-Scale Countercurrent Flow Facility

Figure A.18-9 is a schematic of the 1/5-scale vessel. The following identifies the facility dimensions and capabilities.

## Overall Characteristics

### Geometry

	<u>Dimensions</u> (inches)
Gap Size	1.5 ± 0.050
Average Annulus Circumference	105.6 ± 0.2
Vessel ID	35.125 ± 0.050
Downcomer Length	54
Intact Cold Leg ID	5.8
Broken Cold Leg ID	17.2
Cold Leg Break sizes	1.0, 4.0, 6.0
Plenum Volume	33.2 cubic feet

### Flow Rates

ECC	0-1500 gpm
Countercurrent Core Steam	0-5.5 lbm/s

### Temperature

ECC	60-200°F
-----	----------

### Pressure

System	0-200 psia
Separator tank	15 psia

### Facility Capability

- models countercurrent core steam/ECC water flow during cold leg breaks
- capability of performing blowdown studies (Lower plenum fluid flashing following cold leg break) (Figure A.18-10)
- capable of multiple ECC fluid temperatures to determine effect of subcooling on ECC penetration to lower plenum

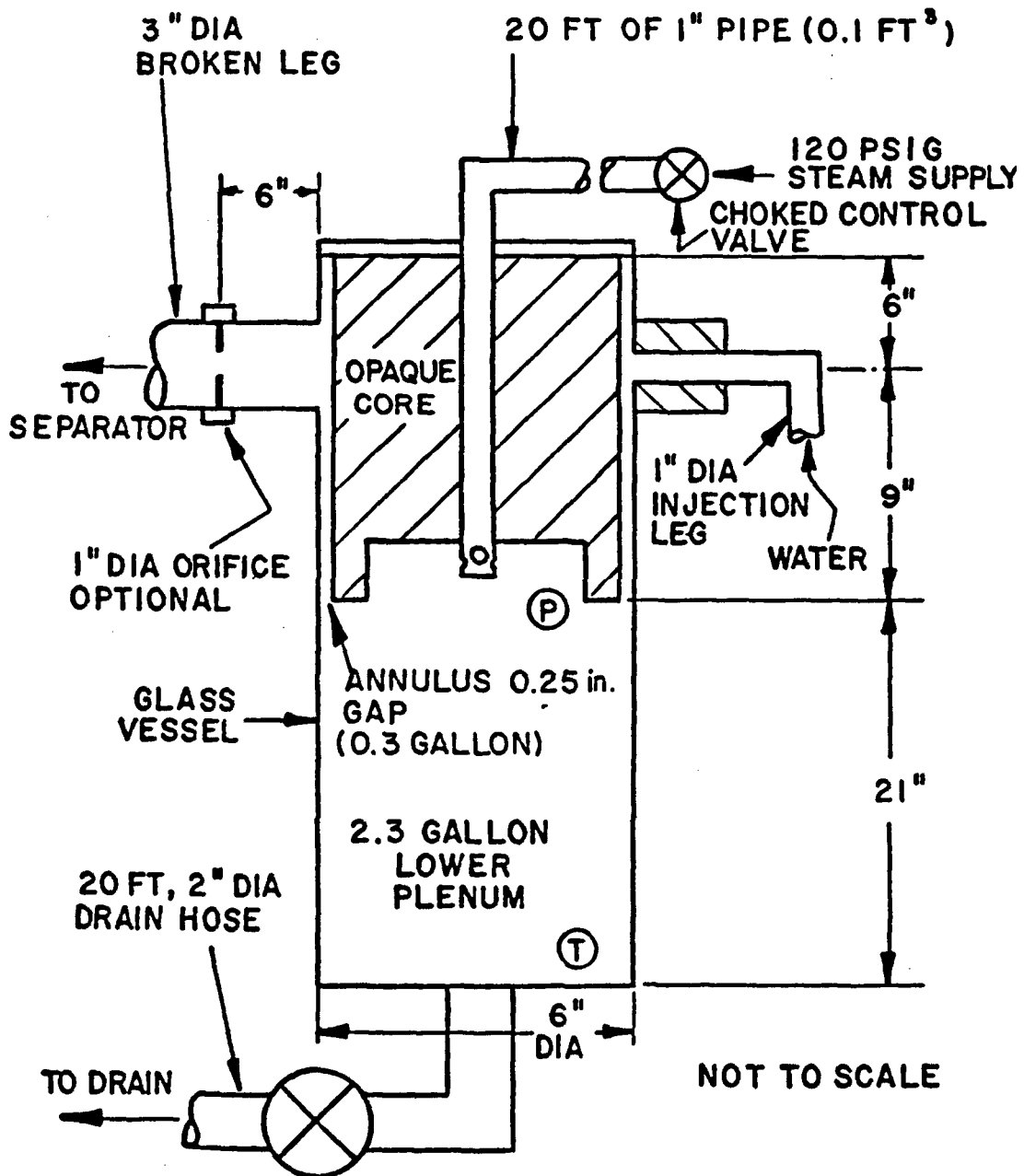


Figure A.18-1 1/30-scale transparent facility

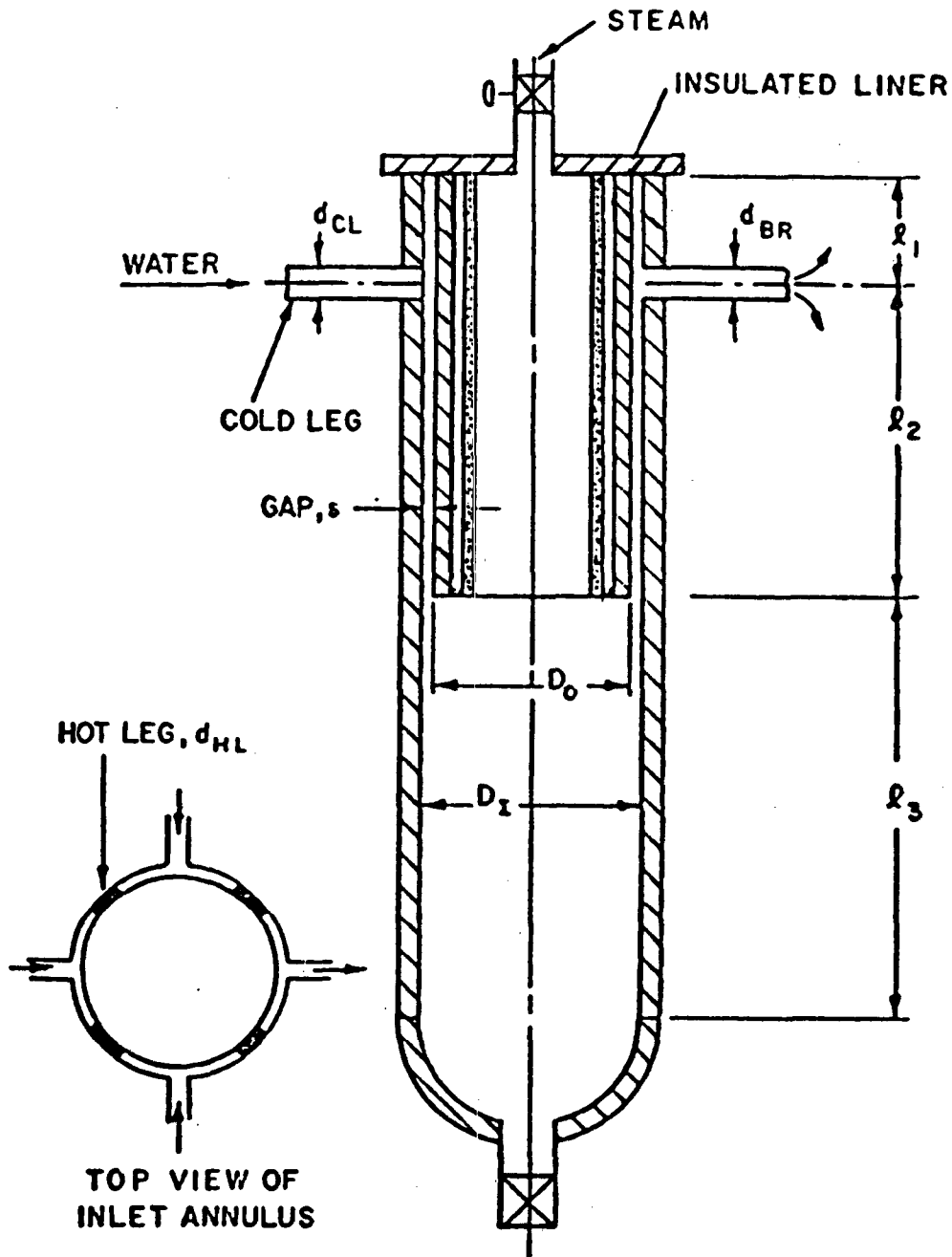


Figure A.18-2 Schematic of vessel geometry used for 1/30-scale countercurrent flow tests

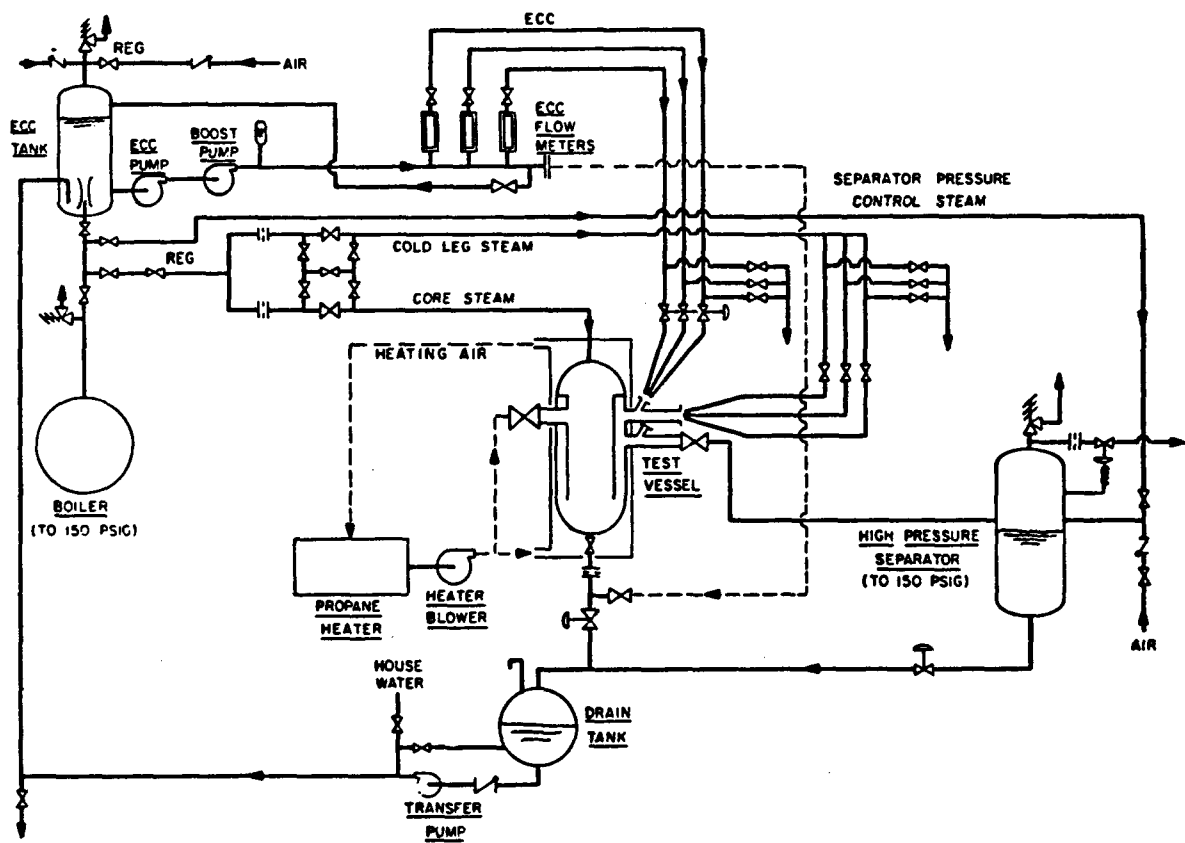


Figure A.18-3 Flow schematic for CREARE 1/15-scale high-pressure cylindrical vessel and facility

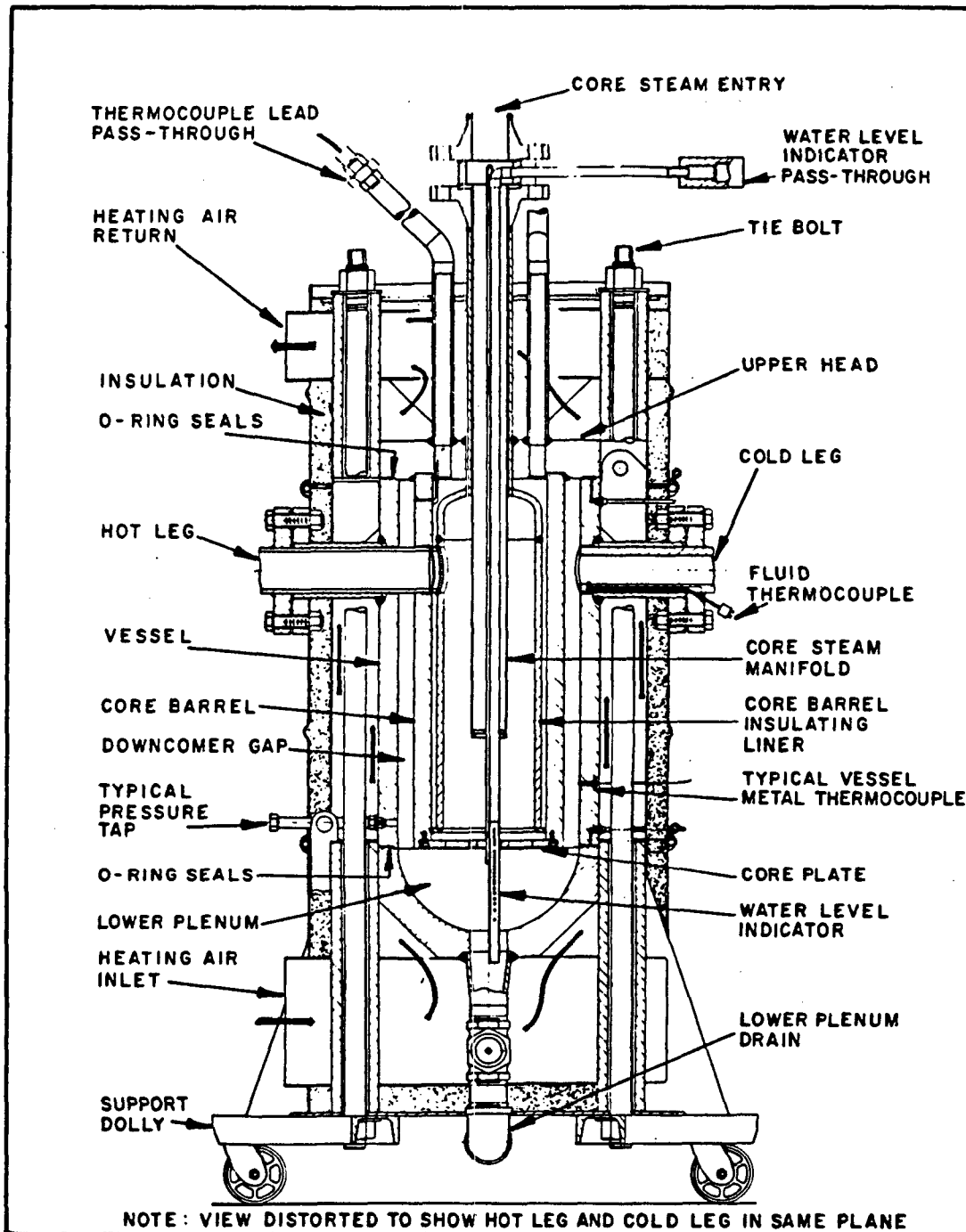


Figure A.18-4 Cutaway view of CREARE 1/15-scale high-pressure cylindrical vessel

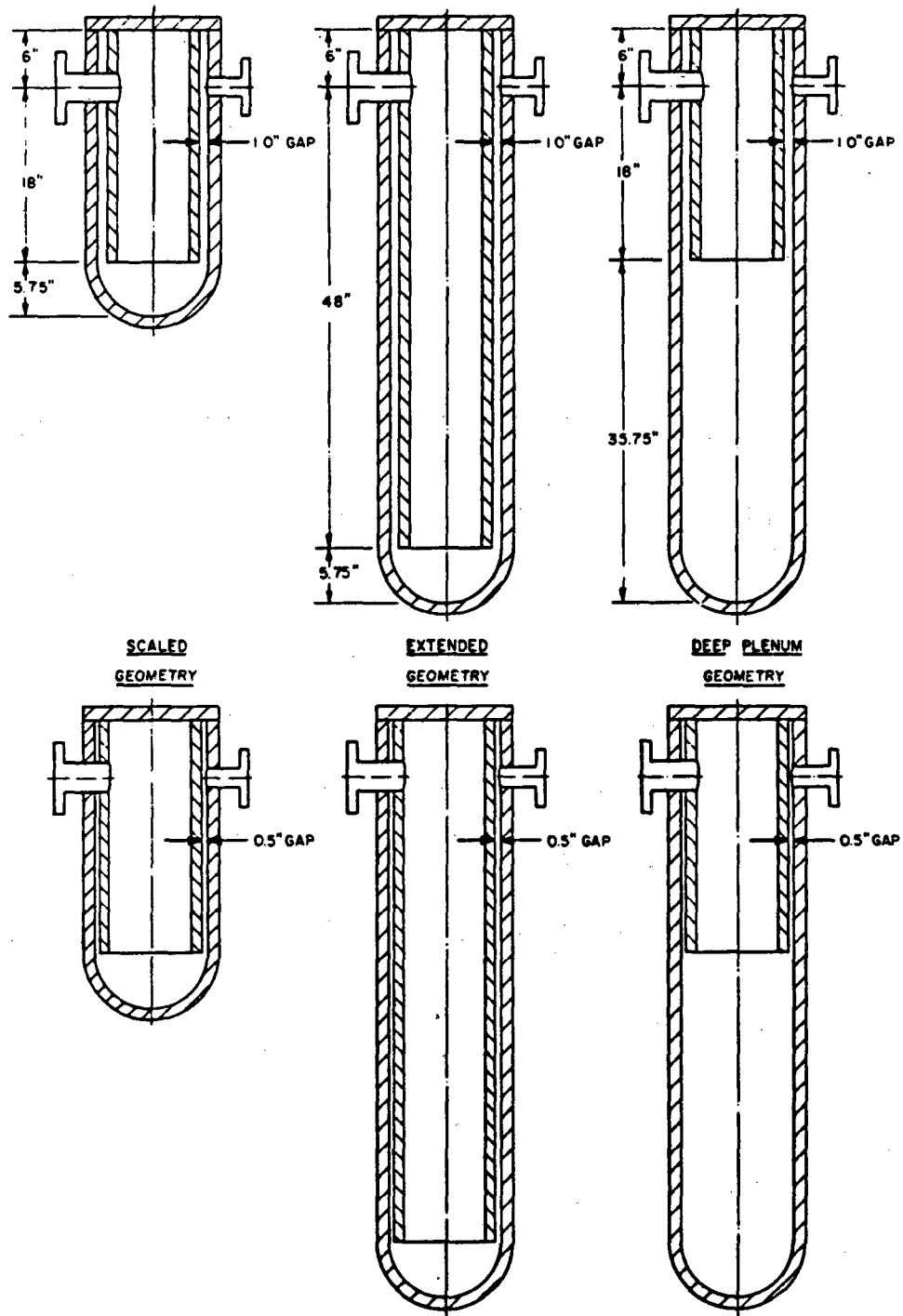


Figure A.18-5 Six geometrical configurations of gap size, vessel length, and plenum depth possible with CREARE 1/15-scale vessel

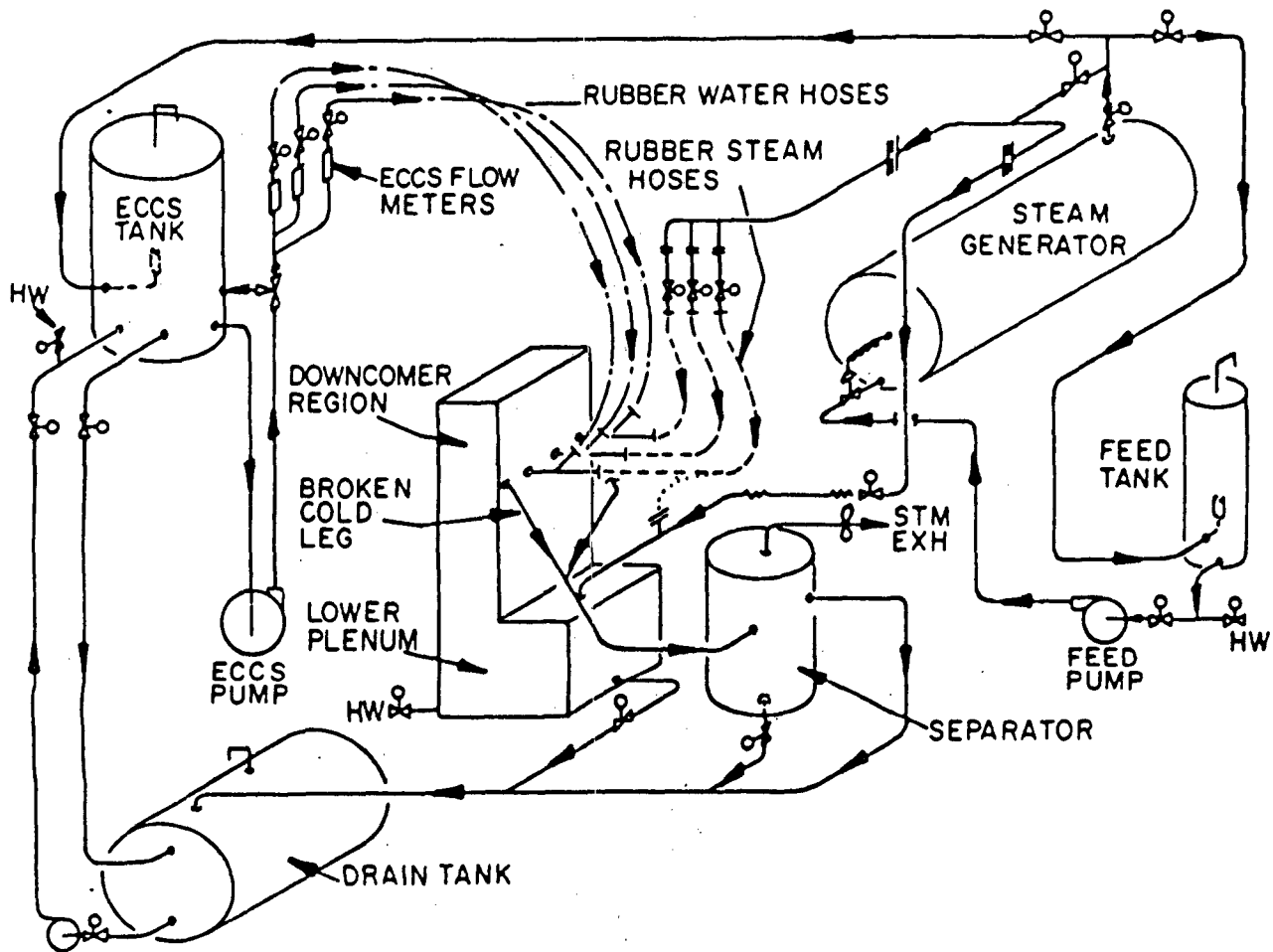


Figure A.18-6 Fluid flow paths in 1/15-scale CREARE planar facility

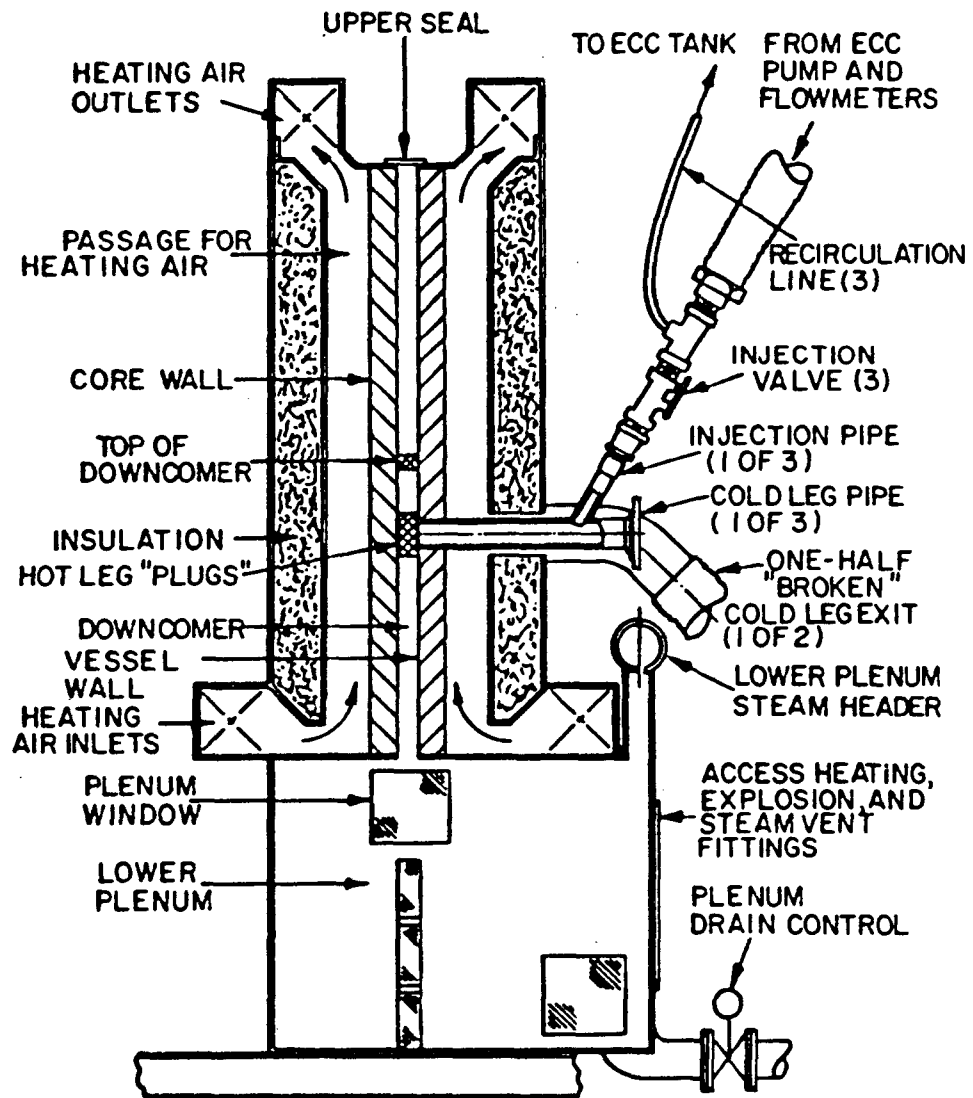


Figure A.18-7 Schematic cross section of CREARE planar test apparatus

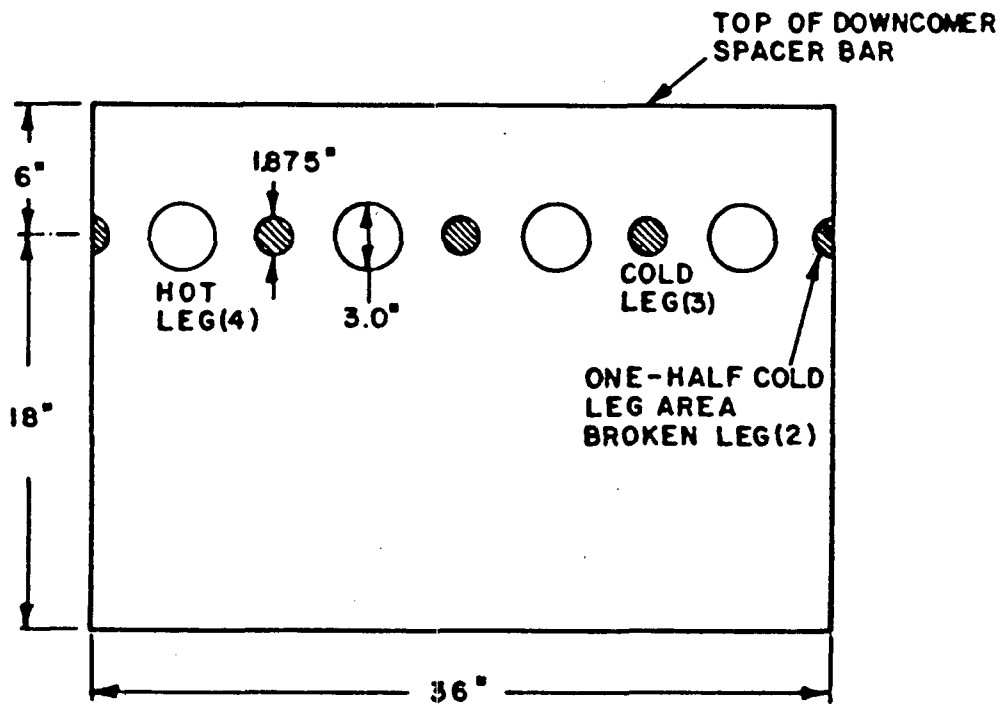


Figure A.18-8 Hot and cold leg arrangement in downcomer of 1/15-scale apparatus

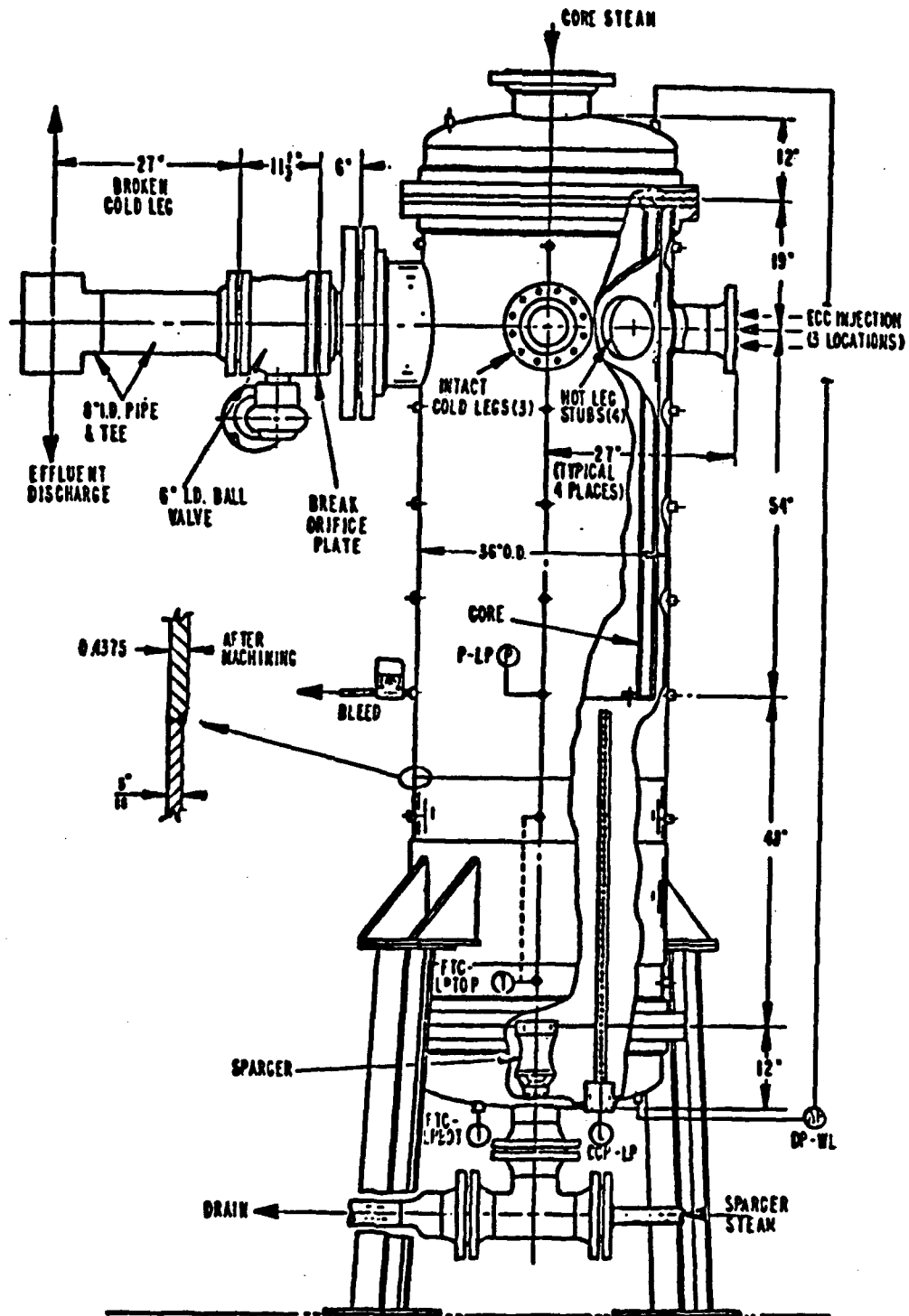


Figure A.18-9 Drawing of CREARE 1/5-scale vessel

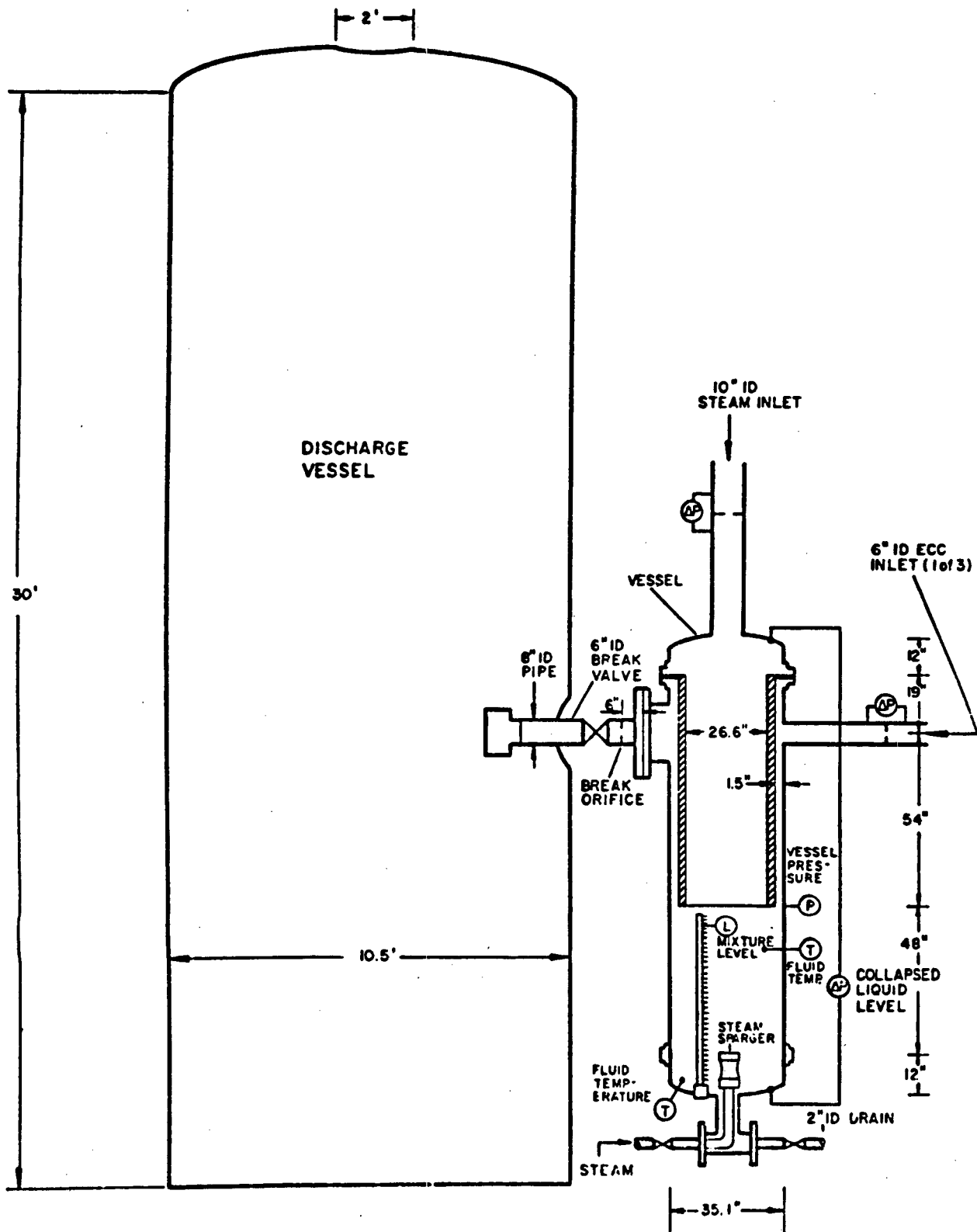


Figure A.18-10 Drawing of 1/5-scale facility for flashing experiments

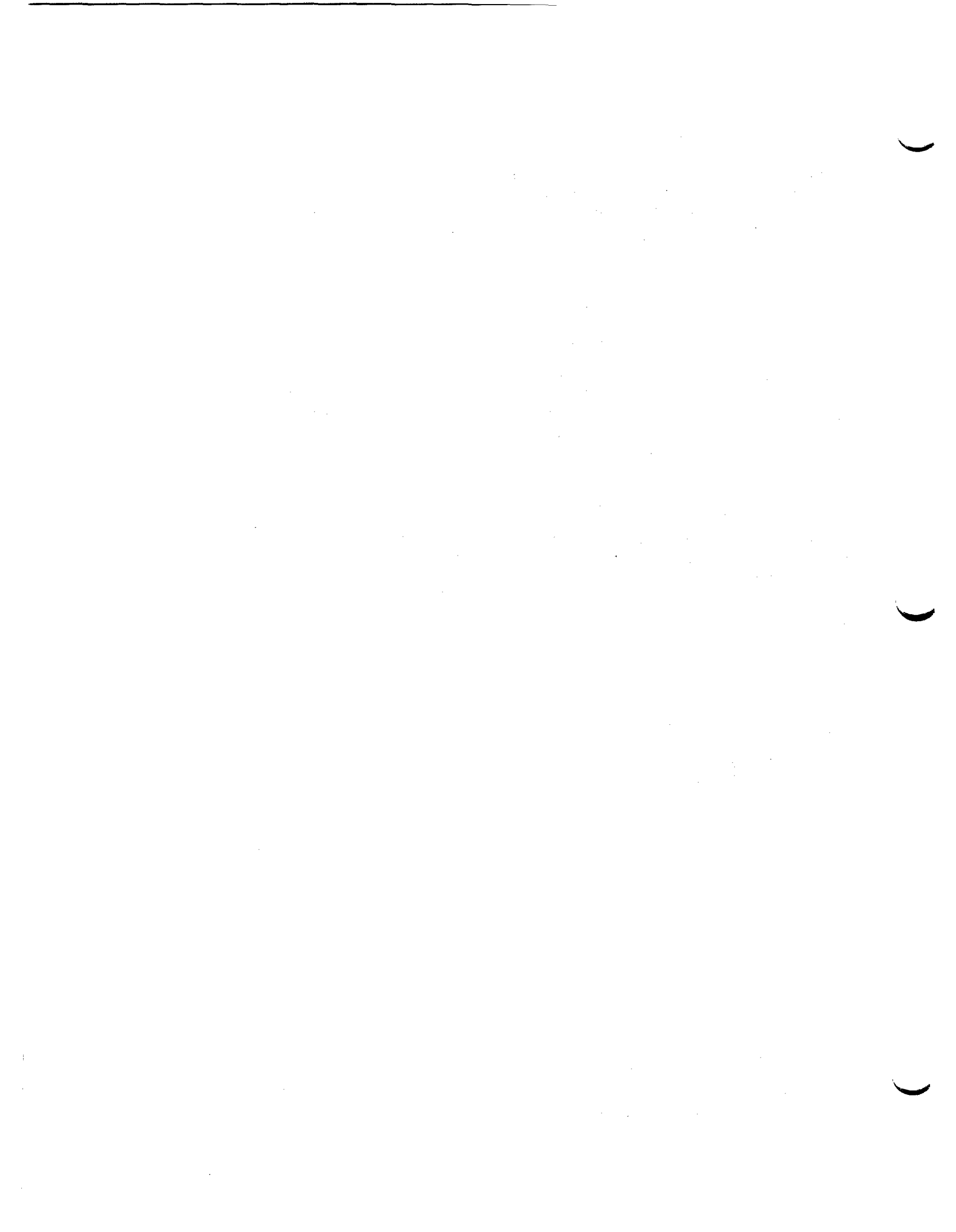
Table A.18-1 Parametric comparison of scale model experiments with typical PWR conditions

Parameter	PWR	1/5-Scale	1/15-Scale	1/30-Scale
Break Area/Plenum Volume [ $A_b/V_{LP}$ (1/ft)]	$3.5 \times 10^{-3}$	$0.16 \times 10^{-3}$ $5.9 \times 10^{-3}$	$0.16 \times 10^{-3}$ $14 \times 10^{-3}$	$1.0 \times 10^{-3}$ to $36 \times 10^{-3}$
Time to Fill Plenum [ $V_{LP}/O_{fin}$ (sec)]	10.5	9.6-58 (17.3)*	9.5-57 (17.1)	12.2-49 (14.7)
ECC Flow Rate [ $J_{fin}^*$ ]	0.10	0.02-0.18	0.02-0.19	0.02-0.12
ECC Flow Rate [ $K_{fin}^*$ ]	7.3	0-6.0	0-3.4	0-1.7
<u>Annulus Gap Size</u> Vessel Diameter	0.058	0.043	0.043	0.042
<u>Downcomer Volume</u> Plenum Volume	1.0	0.20	0.12, 0.90	0.09

\*Nominal Value at  $J_{fin}^* = 0.10$ .

Table A.18-2 Combinations of parameters tested in the CREARE Planar Facility

Test Name	Superheated Wall	Counter-current Core Steam Flow	Cold Leg Steam Flow	Baffles
1. Superheated Wall (no steam)	x			
2. Countercurrent Flow		x		
3. Countercurrent Flow with Cold Leg Steam		x	x	
4. Cold Leg Steam			x	
5. Superheated Wall, Countercurrent Flow	x	x		
6. Superheated Wall, Countercurrent Flow with Baffles	x	x	x	
7. Countercurrent Flow with Baffles		x		x
8. Superheated Wall, Countercurrent Flow with Baffles	x	x		x
9. Superheated Wall with Baffles	x			x
10. Superheated Wall, Countercurrent and Cold Leg Steam Flow with Baffles	x	x	x	x



## A.19 BATTELLE COLUMBUS LABORATORY ECC/CORE STEAM FLOW EXPERIMENTS

Battelle Columbus Laboratory (BCL) designed, built and operated three experiment facilities as part of the NRC's ECC bypass program. The tests performed in each of these facilities were similar, but the scale size was different in order to assess the suitability of various scaling theories. The three facilities were:

1. 1/15-scale transparent vessel
2. 1/15-scale 60 psi model
3. 2/15-scale low pressure facility

The primary phenomenon studied with these facilities was countercurrent core steam/ECC fluid flow in the downcomer during a PWR cold leg break. The tests were performed at various pressures, ECC flow rates and steam-water temperatures. In addition, the 2/15-scale model included the effect of vessel superheat on ECC penetration into the downcomer. The following sections describe each of these three facilities.

### A.19.1 1/15-Scale Transparent Vessel

Figures A.19-1 and A.19-2 are schematics of the 1/15-scale transparent vessel and fluid flow paths. The following identifies the facility dimensions and capabilities.

#### Overall Characteristics

##### Geometry

4-loop	90° arrangement
Cold leg diameter (I.D.)	2.0 in.
Injection pipe diameter (I.D.)	0.63 in.
Downcomer gap	1.2 in.
Vessel inside diameter	12.1 in.
Core barrel length	20.5 in.

##### Temperatures

Injected water	200°F max.
Injected water subcooling	0-170°F

##### Pressures

System	Atmospheric
Steam supply	90 psig

##### Facility Capability

- models countercurrent core steam/ECCS water flow in the downcomer region
- permits visualization of downcomer fluid behavior during ECC injection
- models a 4-loop PWR
- variable injection temperature permits examination of subcooling effect
- cold leg steam capability

### A.19.2 1/15-Scale 60-psi Vessel Model

Figures A.19-3 and A.19-4 are schematics of the 1/15-scale (60 psi) test vessel and flow configuration. The following identifies the facility dimensions and capabilities.

#### Overall Characteristics

##### Geometry

4-loop	90°, 60°-120°
Cold leg diameter (I.D.)	2.1 in.
Injection pipe (I.D.)	0.63 in.
Downcomer gap	1.2 in.
Vessel (I.D.)	12.1 in.
Core barrel length	20.5 in.

##### Flow Rates

ECC flows	75 gpm (max.)
-----------	---------------

##### Temperatures

ECC subcooling	100-270°F
----------------	-----------

##### Pressures

System	75 psia (max.)
--------	----------------

##### Facility Capabilities

- direct downcomer injection - available
- cold leg steam
- variable ECC subcooling
- models countercurrent core steam/ECC water flows in the downcomer region
- models a four-loop PWR with variable cold leg arrangements (Figure A.19-5)

### A.19.3 2/15-Scale low-pressure facility

Figure A.19-6 is a schematic of the 2/15-scale test vessel. The following identifies the facility's dimensions and capabilities.

#### Overall Characteristics

##### Geometry

4-loop	60°-120°
Cold leg (I.D.)	7.6 in.
Cold leg insert (I.D.)	4.0 in.
Injection pipe (I.D.)	1.27 in.
Injection angle	60°, 90°
Vessel (I.D.)	24.35 in.
Core barrel length	45 in.
Downcomer gap	1.23 in.

### Flow Rates

Steam supply	8.3 lbm/s
ECC injections	575 gpm

### Temperatures

ECC	40°-200°F
Hot wall heating	550°F max.

### Pressures

Steam supply	85 psig
System pressure	250 psia

### Facility Capabilities

- models a 4-loop PWR
- models countercurrent core steam/ECCS water flow in the downcomer region
- variable injection temperature permits examination of subcooling effect
- hot wall heaters for ECC delay measurements
- variable ECC injection angles
- cold leg steam
- system pressure up to 250 psia

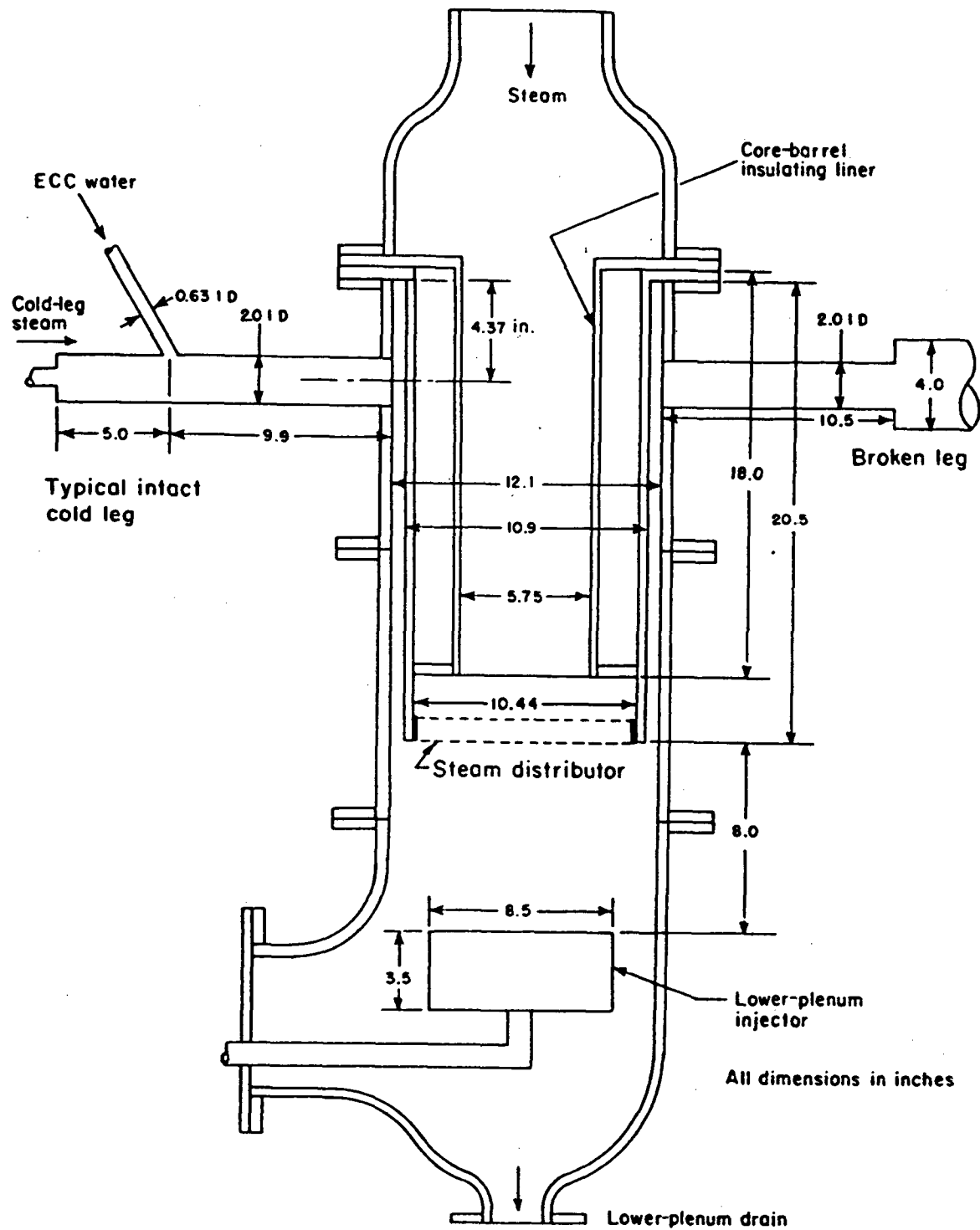


Figure A.19-1 Schematic of BCL 1/15-scale transparent vessel model

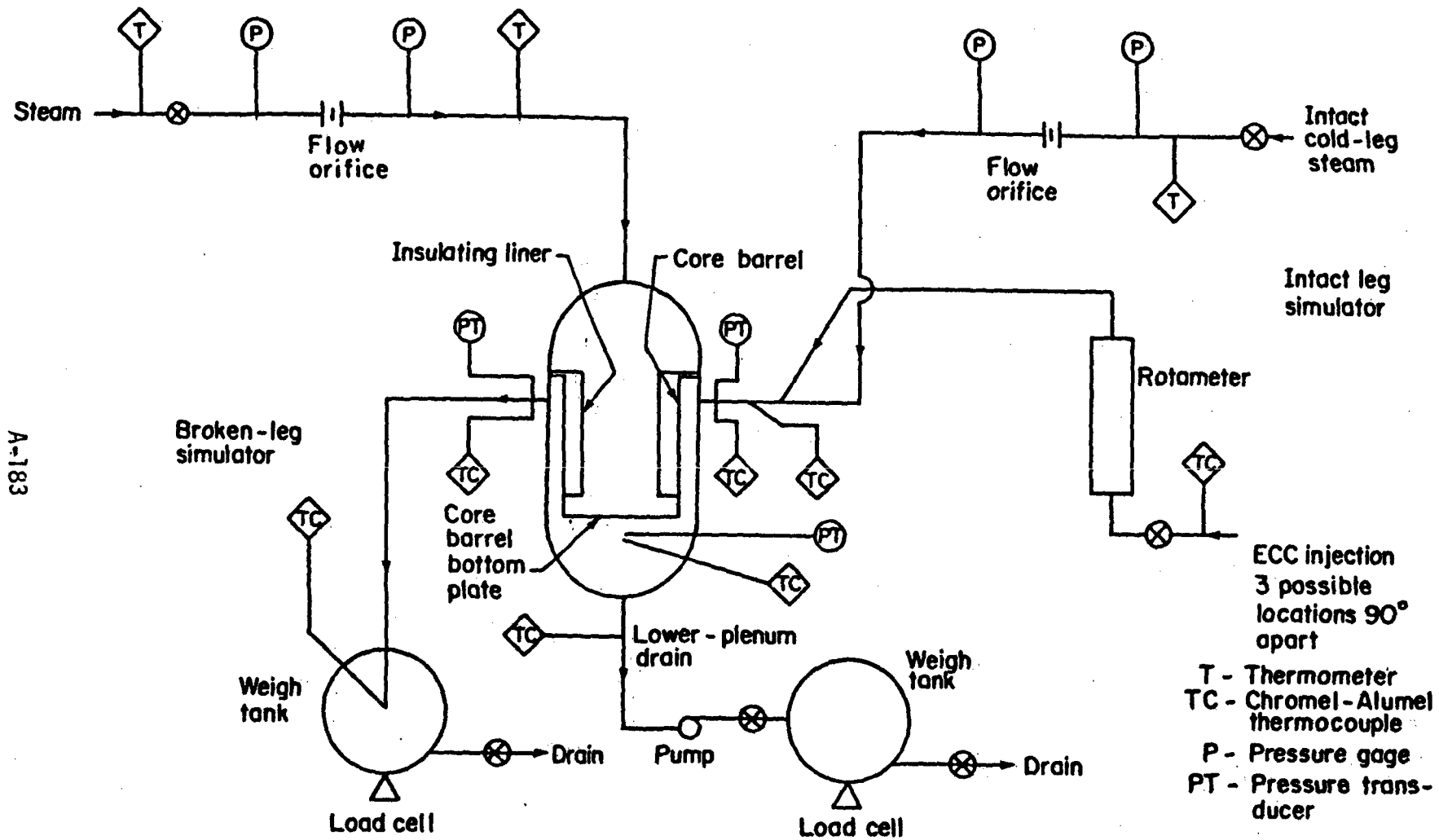


Figure A.19-2 Schematic of BCL transparent vessel facility

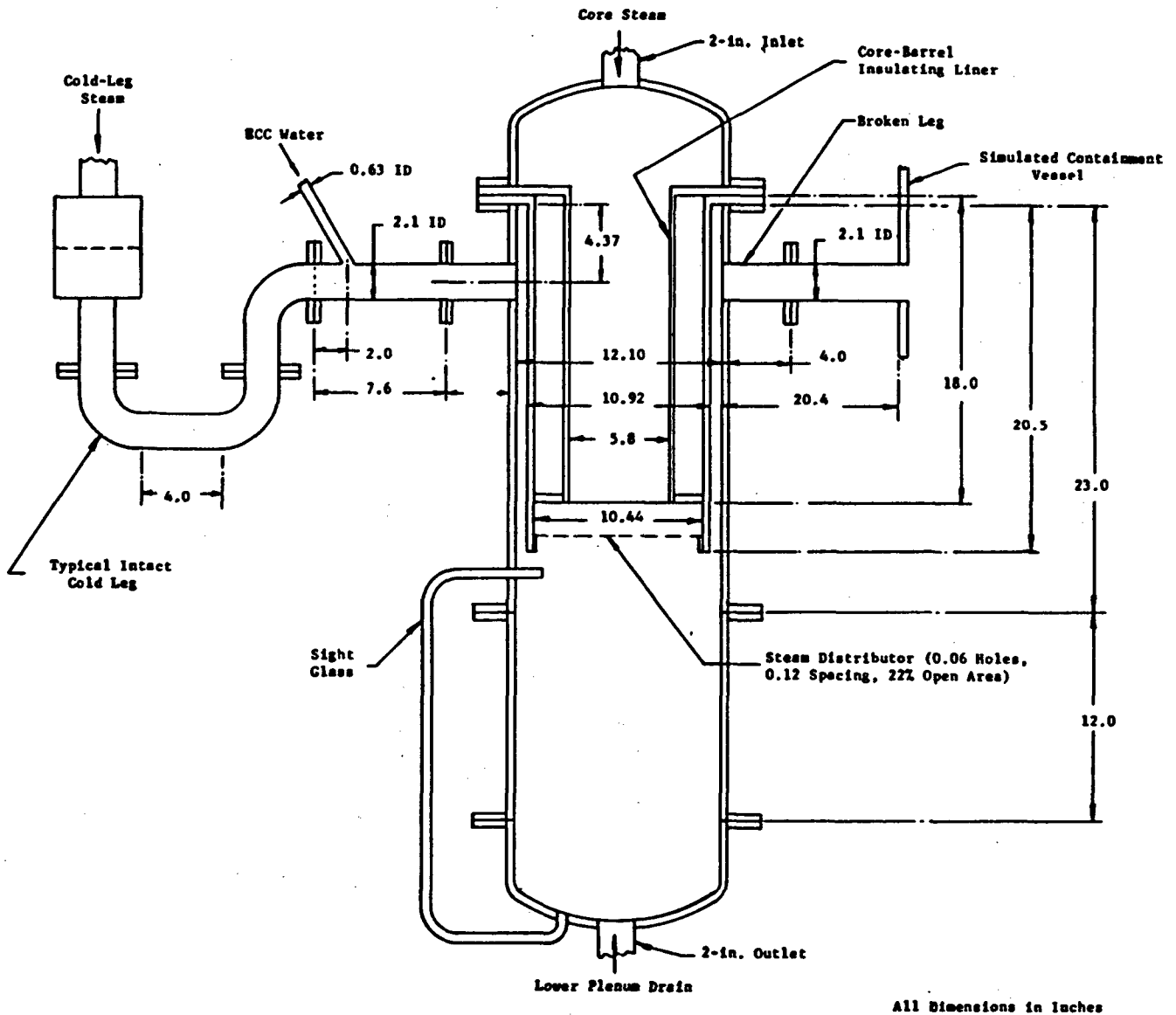


Figure A.19-3 Schematic of BCL 1/15-scale 60 psi vessel model

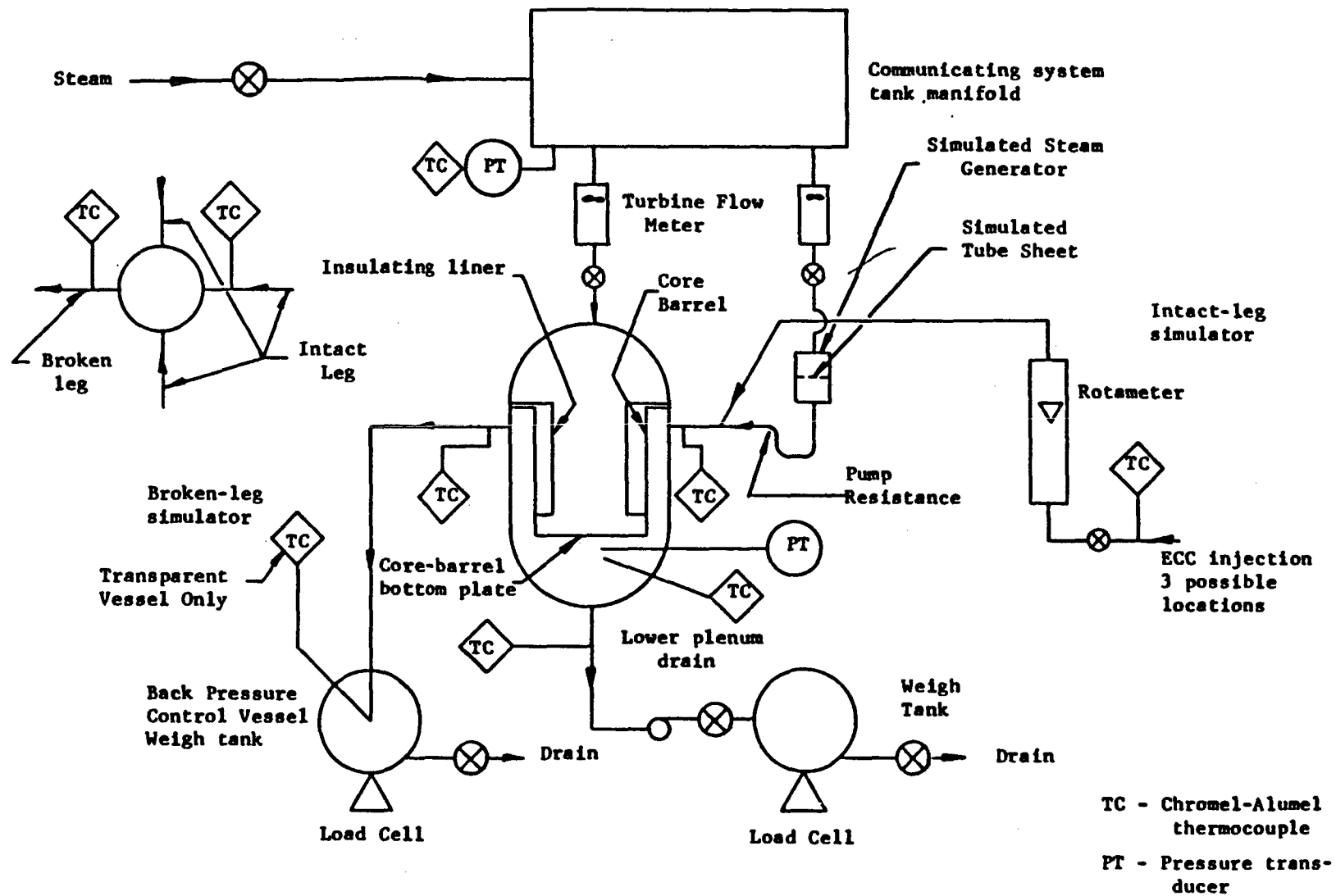


Figure A.19-4 Schematic of flow configuration for BCL 1/15-scale model

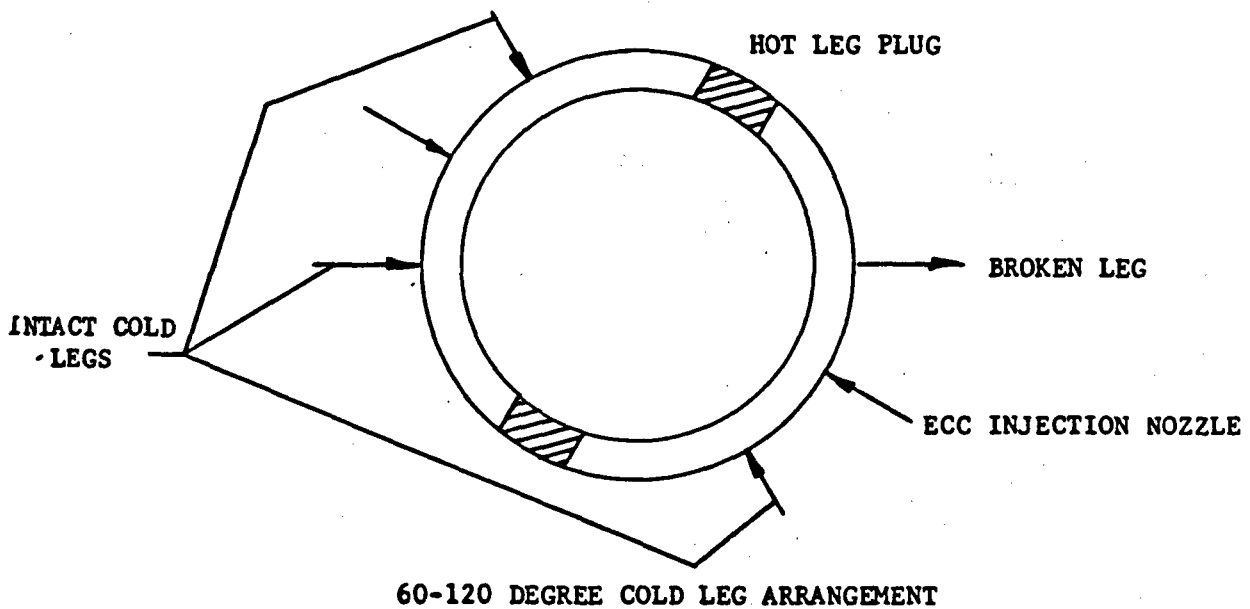
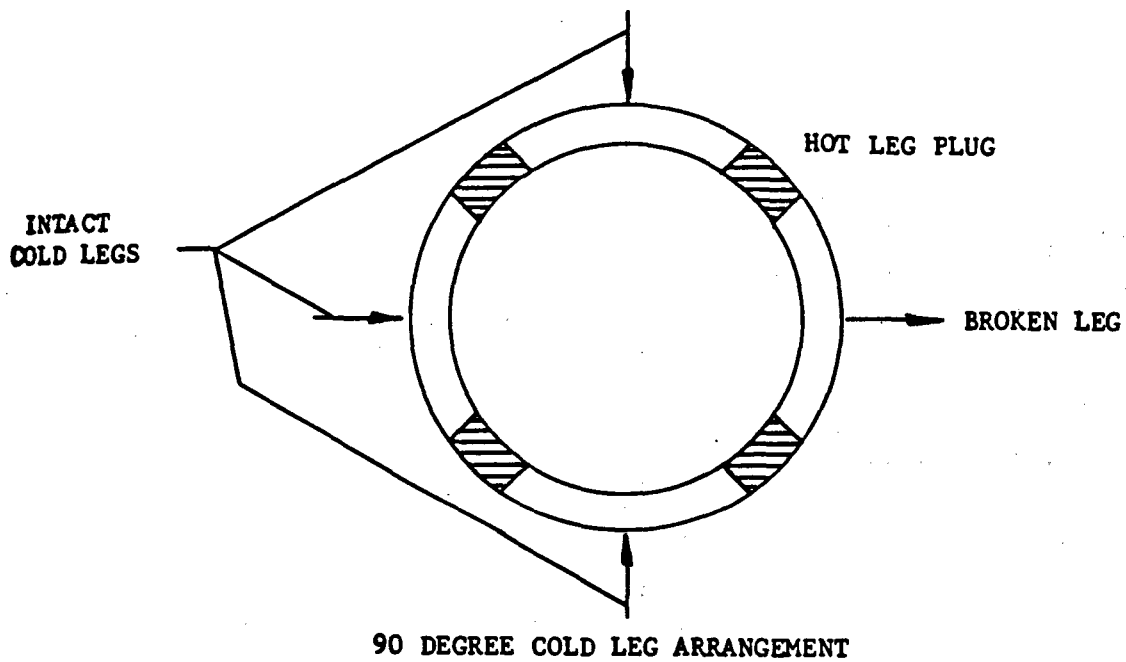


Figure A.19-5 Comparison of cold leg arrangements in the 1/15-scale model vessels





## A.20 POWER BURST FACILITY

The Power Burst Facility (PBF) located at the Idaho National Engineering Laboratory is extremely versatile. The experiment program for the PBF is structured to provide relevant and pertinent data necessary to (1) develop and assess computer models needed for licensing analysis, (2) confirm the adequacy of specific NRC licensing regulations that are designed to ensure plant safety with respect to specific accident conditions, (3) help resolve unanswered safety issues and provide a data base from which new regulations can be established, and (4) indicate where new or revised regulations may be appropriate.

The PBF reactor and the associated test loop is capable of simulating reactivity-initiated accidents (RIA), power-cooling-mismatch accidents (PCM), anticipated transients with and without scram (ATWS), loss-of-coolant accidents (LOCA), and severe fuel damage accidents (SFD) using clusters of up to 32 test fuel rods. The PBF has an integral experiment program that includes test requirements, pretest predictions, and safety analysis; design, fabrication, and assembly of test hardware and instrumented test fuel rods; data acquisition, reduction, and processing; posttest analysis and postirradiation examination; and final test reporting.

During the PBF experiments, measurements of coolant conditions, cladding and fuel temperatures, internal rod pressure, and rod elongation data are recorded on magnetic tape using a computer-controlled data acquisition and reduction system that can accommodate up to 287 data channels. A very sophisticated fission product detection system makes it possible to determine the time-dependent release of fission products during accident simulation tests that result in cladding failure. Pre- and posttest computer code calculations are performed for comparison with the measured data and the data obtained from extensive post-irradiation examinations performed in the INEL hot cells.

An overview description is given in Reference A.20-1 with specific detail on the design and operating characteristics of the driver core, test loop, fission product detection system, data systems, and test train assembly facility that make the testing ability of the PBF unique and versatile.

The Power Burst Facility (PBF) was designed to provide experimental data for the development and verification of computer programs used to calculate the behavior of typical power reactor fuel rods under normal, off-normal, and accident conditions. These light water reactor safety tests are performed in the PBF by testing single rods and clusters of test fuel rods in a central test space in the core.

The facility consists of an open tank reactor vessel; canal; driver core region with an active length of 3 ft (0.9 m); central flux trap region containing an in-pile tube in which the test fuel is located; and a pressurized water flow loop that permits control of the test fuel rod coolant flow rate, temperature, and pressure within typical PWR levels. The open top reactor vessel provides access for installation and removal of test hardware. The canal is used for transfer and temporary storage of PBF reactor fuel and test fuel assemblies. Through the use of high-speed valves, the in-pile tube portion of the loop can be rapidly depressurized in a manner similar to that which would occur in a light water reactor during a postulated loss-of-coolant accident.

The PBF core is approximately a right-circular annulus, 52 in. (1.3 m) in diameter and 36 in. (0.9 m) high, enclosing a centrally located vertical test space 8.25 in. (0.21 m) in diameter. The PBF reactor core can be operated in three modes: (a) a steady-state mode with power levels up to 28 MW, (b) a natural power burst mode which yields reactor periods as short as 1.0 ms and peak powers as large as 270 GW, and (c) a shaped burst mode. Table A.20-1 provides details of the experimental capabilities.

The PBF LOCA test program consists of a series of four tests, with the different cladding peak temperatures planned for each test shown in Figure A.20-1. The different cladding temperatures of 1070, 1190, and 1350 K are attained by varying the rod power history. The three temperatures are the points of (a) maximum ductility of  $\alpha$ -phase zircaloy cladding, (b) minimum ductility in the  $\alpha$  -  $\beta$ -phase transition, and (c) maximum ductility of  $\beta$ -phase zircaloy cladding. Each test is being conducted with four test rods, two of which are internally pressurized to values representative of newly fabricated PWR fuel rods and two of which are internally pressurized to values representative of high burnup fuel rods. One of each type of pressurized rod was previously irradiated in the Saxton reactor to between 10,000 and 16,000 Mwd/MTM.

The programmatic tests in PBF are divided into seven different test series, which are described below.

1. The Power-Cooling-mismatch (PCM) Test Series provided in-pile experimental data on the behavior of single, pressurized water reactor (PWR) type fuel rods as well as measurements of fuel rod interactions and failure propagation, if any, in rod clusters during PCM conditions; e.g., during a decrease in coolant flow or in a slight overpower condition.
2. The Irradiation Effects (IE) Test Series evaluated the behavior of irradiated fuel rods under PCM conditions. Test fuel rods in this series were made from various treatments of irradiated and unirradiated cladding and fuel components.
3. The Gap Conductance (GC) Test Series provided data used in determining the effects of fuel design parameters (such as gap size, fill gas, and fuel density) on the magnitude of fuel-cladding gap conductance.
4. The Loss-of-Coolant Accident (LOCA) Test Series measured the thermal, mechanical, chemical, and internal gas pressure response of both irradiated and unirradiated fuel rods during each major phase of a variety of LOCA situations.
5. The Reactivity Initiated Accident (RIA) Test Series determined threshold energy limits for incipient fuel rod failure and prompt fuel dispersal for test environments typical of power reactor conditions. Of particular interest was the behavior of irradiated fuel rods under RIA conditions.

6. The PBF/Loss-of-Fluid Test (LOFT) Lead Rod Test Series evaluated the anticipated behavior of the LOFT core during the LOFT Power Ascension Tests.
7. The Operational Transient (OPTRAN) Test Series evaluated BWR fuel behavior under severe operational transient conditions.

Tests were conducted with typical PWR-type fuel rods; however, the fuel stack length was only 0.91 m and the enrichment was higher than normal PWR enrichments. The rod plenum volume was scaled in proportion to the active length. Each rod was surrounded by an individual flow shroud and symmetrically placed within a test train in an environment typical of PWR coolant pressures, temperatures, and flow. A cross section of the fuel rods, flow shrouds, and test train is shown in Figure A.20-2.

The PBF loop and blowdown system is illustrated in Figure A.20-3. The tests consisted of a preblowdown power calibration and decay heat buildup, blowdown (coolant depressurization), and test termination with a quench. The system conditions at the initiation of blowdown were an inlet temperature of 590 K, a system pressure of 15.5 MPa, and a rod average power of about 46 kW/m. Test conduct began with the isolation of the in-pile tube from the PBF loop, and then opening of quick-actuating cold leg blowdown valves to initiate a blowdown similar to a hypothetical PWR double-ended cold leg break. The break planes were formed in converging-diverging nozzles with throats sized to control the blowdown flow and depressurization rates. The ejected coolant and fission products carried from the fuel were collected in a blowdown tank. The axial power profile along the fuel rods was shaped with the power flattened in the center third of the active fuel length. The uniform power in this region provided conditions that are typical of a PWR was controlled during blowdown by the PBF transient rods as was programmed to follow a power function determined in pretest calculations. This power was required for additional heating of the test rods to reach and maintain target temperatures. A quench and reflood system for cooling the cladding was used to terminate each test.

The instrumentation associated with the fuel rods consisted of (a) cladding surface thermocouples, (b) a plenum thermocouple and pressure transducer to measure plenum temperature and rod internal pressure, (c) a linear variable differential transformer (LVDT) to measure the fuel rod axial elongation, (d) seven self-powered neutron detectors spaced along the active fuel length to measure the neutron flux during blowdown, (e) three self-powered gamma detectors spaced along the active fuel length to measure gamma flux during blowdown, and (f) an aluminum-cobalt alloy flux wire located on each flow shroud to provide the time-integrated axial power distribution in the test rods. The instrumentation associated with each fuel rod flow shroud consisted of (a) two turbine flowmeters, one located at the shroud inlet and one at the exit, to measure the coolant volumetric flow; (b) thermocouples mounted in the coolant flow stream to measure coolant bulk temperature at the flow shroud inlet and exit; (c) differential thermocouples to measure the coolant temperature increase through the flow shroud; and (d) three flow shroud and coolant thermocouples axially spaced along the shroud to measure the coolant conditions.

REFERENCE

- A.20-1 "Final Safety Analysis Report for the Power Burst Facility, Parts 1 and 2," ANCR-1011, July 1971.

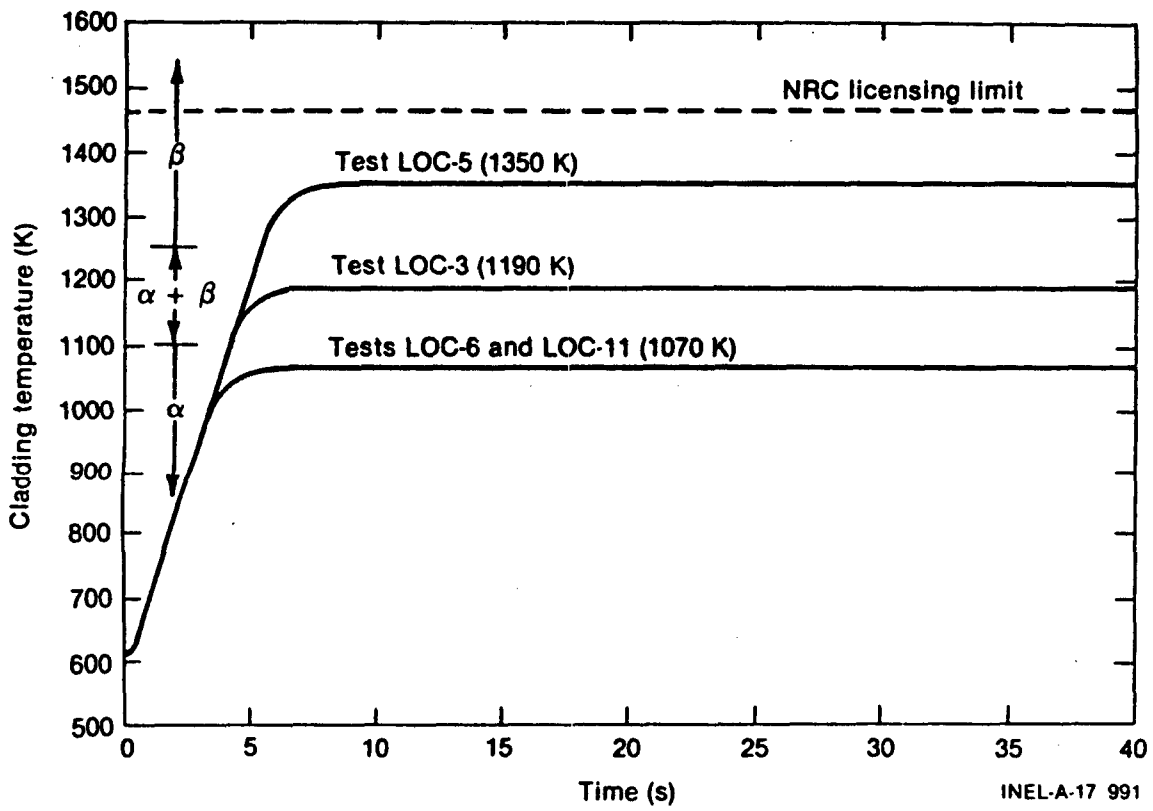


Figure A.20-1 PBF LOCA program target cladding temperature histories

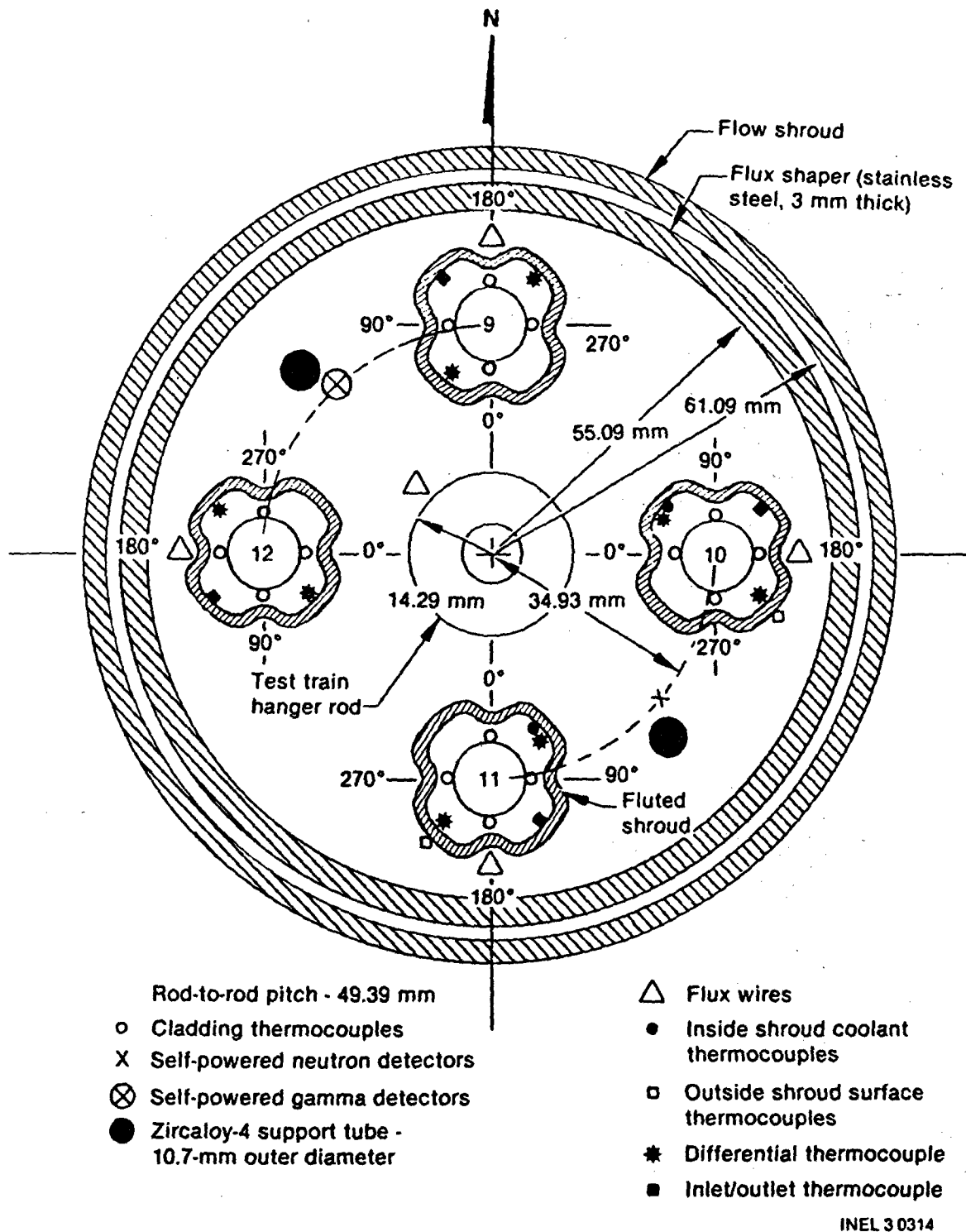
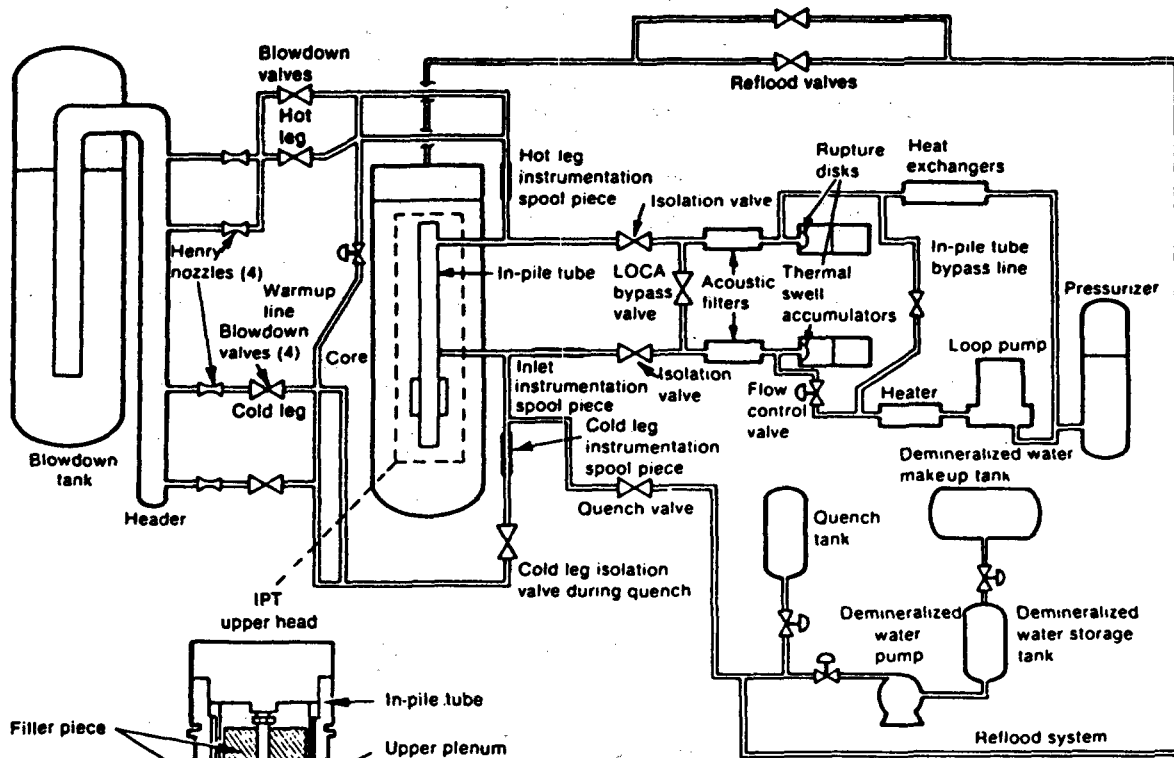


Figure A.20-2 PBF/LOCA fuel train orientation



INEL 2 1057

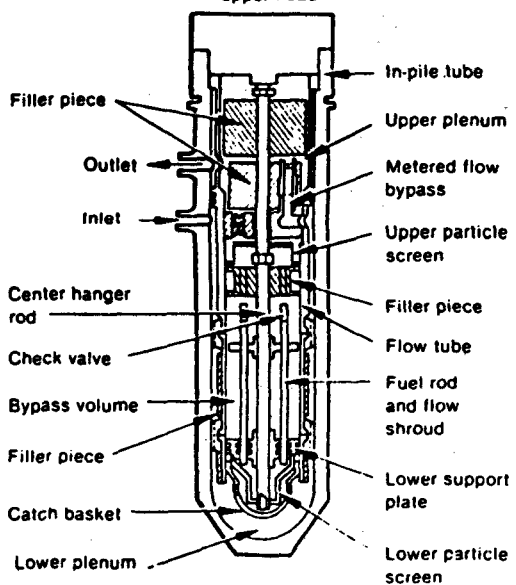


Figure A.20-3 PBF LOCA test system

Table A.20-1 Experimental envelope for operation of PBF

**TABLE I  
EXPERIMENTAL ENVELOPE FOR OPERATION OF PBF**

PARAMETER OR VARIABLE	DESIGN CAPABILITIES AND/OR LIMITS
Maximum core steady power	28 MW
Maximum core power in shaped burst	1000 MW
Maximum core power in natural burst	270 GW nominal for design burst[a]
Peak neutron flux in IPT	$\approx 7 \times 10^{17}$ nv at 270 GW
Maximum duration for steady power operation	48 hours
Maximum power for initiation of shaped burst	100 kW
Maximum power for initiation of natural burst	28 MW nominal
Maximum core fuel temperature for steady power operation	2573 K (4171°F) nominal at 28 MW
Maximum core fuel temperature for burst operation	2623 K (4261°F) without coupling; 2733 K (4460°F) with coupling
Maximum core fuel enthalpy for steady power operation	7451 MJ/m <sup>3</sup> (1780 cal/cm <sup>3</sup> ) nominal at 28 MW
Maximum core fuel enthalpy for burst operation	8539 MJ/m <sup>3</sup> (2040 cal/cm <sup>3</sup> ) without coupling; 10,318 MJ/m <sup>3</sup> (2465 cal/cm <sup>3</sup> ) with coupling
Maximum reactivity insertion for natural burst operation	4.60\$ nominal for design burst
Maximum transient rod speed for natural burst operation	9.52 m/s (375 in./s)
Maximum transient rod speed for shaped burst or steady power operation	0.51 m/s (20 in./s)
Minimum asymptotic period for natural burst operation	1.0 ms for design burst
Maximum energy release for natural burst operation	1350 MJ nominal for design burst; 1750 MJ nominal for design burst with coupling
Maximum experiment fission power	2 MW
Maximum experiment Pu inventory	147 g (5.2 oz)
Maximum fission product inventory in test fuels	That resulting at end of following operation history: 2 MW for 558 days, 42 days decay time; 2 MW for 48 hours, 7 days decay time
Maximum loop operating temperature	616 K (650°F)
Maximum loop operating pressure	15.6 MPa (2250 psig)
Maximum transient source pressure within in-pile tube	51.7 MPa (7500 psi)

[a] Design burst is defined as the natural burst initiated from zero power that results in 8539 MJ/m<sup>3</sup> (2040 cal/cm<sup>3</sup>) at the core hot spot. Nominally, this requires a 1.0 ms period burst initiated by a 4.60\$ reactivity step, with an energy generation of 1350 MJ.

## A.21 NRU FACILITIES

The Nuclear Reactor Universal (NRU) facility at Chalk River, Ontario, Canada, has been operated by Atomic Energy of Canada, Ltd. (AECL) as a research and isotope production facility since 1958. The reactor underwent significant modifications between 1972 and 1974, including a change from natural uranium to fully enriched uranium fuel.

The tank-type NRU reactor is moderated, cooled, and reflected by heavy water. The core consists of 227 pressure tubes, of which approximately 83 are occupied by fueled subassemblies, and 16 by control rods; 3 are attached to permanent experiment loops. Each fuel subassembly consists of 12 uranium/aluminum alloy rods clad with aluminum. The uranium is enriched to 93%. The rods are arranged nine in an outer circle and three in an inner circle within an aluminum flow tube with an outside diameter of 52.5 mm (2.1 in.). Characteristics of the NRU are summarized in Table A.21-1.

The principal advantage of the NRU facility is the relatively long active fuel length of 2.74 m (108 in.) and the high flux. Also, the NRU reactor has experiment loops capable of testing multirod bundles. The principal disadvantage results from the fact that the loop pressure is lower than that of a PWR and the capability for blowdown does not presently exist.

The LOCA simulations in the NRU are described in Reference A.21-1. Test conditions are summarized in Table A.21-2.

### REFERENCES

- A.21-1 C. R. Hann et al., "Program Plan: LOCA Simulations in the National Research Universal (NRU) Reactor," July 1979.
- A.21-2 M. D. Freshley et al., "Coolant Boilaway and Damage Progression Testing in NRU," presentation to USNRC staff, Washington, DC, March 8, 1983.

Table A.21-1 Characteristics of NRU

Type	Heterogeneous, thermal, tank type
Power, MW	135
Moderator	Heavy water
Reactor Coolant	Heavy water
Fuel	12 uranium/aluminum alloy rods clad with aluminum in a 52.5 mm O.D. aluminum flow tube
Enrichment, %	93
Thermal flux, n/cm <sup>2</sup> sec	$1.4 \times 10^{14}$
Fast <sub>2</sub> flux, n/cm <sup>2</sup> sec (E>0.1 MeV)	$1.3 \times 10^{13}$
Active fuel length, m (in.)	2.74 (108)
Inlet temperature, °C (°F)	37 (100)
Pressure, MPa (psi)	0.65(94)
Flow, m <sup>3</sup> /s (gpm)	2.6 (42,000)
Control	Control rods Regulating rods Safety rods

Table A.21-2 Test conditions for the NRU LOCA simulation program

<u>PARAMETER</u>	<u>TH-1</u>	<u>MT-1</u>	<u>MT-2.2</u>	<u>TH-2.14</u>	<u>TH-3.03</u>	<u>MT-3.06</u>	<u>MT-4.04</u>
Two-phase flow during rupture	Does not apply	Yes	Yes	Does not apply	Does not apply	Yes	No
Reflood delay time, s	10-80	32	36	7	7	9	57
Average time to rupture, s	Does not apply	70	65	Does not apply	Does not apply	133	55
Reflood rate, cm/s(in./s)	2.0-27.2 (0.8-10.7)	5.3 (2.1)	1.3-13.7 (0.5-5.4)	1.3-5.1 (0.5-2.0)	1.0-5.6 (0.4-2.2)	1.0-5.6 (0.4-2.2)	0-5.1 (0-2.0)
Average rod power, kW/ft	~0.36	0.39	0.39	0.37	0.35	0.39	0.37
Test duration, <sup>a</sup> min	<6	3.2	4.7	5.5	6.5	4.5	18.7

<sup>a</sup>Time from steam off to reactor trip.



## A.22 TWO-PHASE FLOW LOOP

The LOFT Two-Phase Flow Loop (Ref. A.22-1) was designed and built at INEL to duplicate a representative portion of the flow combinations expected in the primary piping in LOFT during a typical loss-of-coolant experiment (LOCE). The loop is designed for steady-state conditions and contains adequate reference instruments to calibrate the LOFT instruments. The loop shown schematically in Figure A.22-1 consists of four large steam supply vessels that produce steam by controlled flashing, a moisture separator, a diesel-driven centrifugal pump, a steam separator, a two-phase mixing section, a steam metering section, a water metering section, a two-phase flow mixing section, and associated pressure and flow control valves.

A small high-pressure boiler (10.35 MPa and 3.7 MW) is used to fill, heat, and pressurize the steam supply vessels. Steam is bled from the steam supply vessels through the mixer, where it mixes with water. The two-phase mixture flows through the test section to the steam separator. Steam is vented from the steam separator through a pressure control valve. The water is continuously recirculated by the pump. Two-phase flow conditions can be maintained at constant pressure and temperature until the pressure in the vessels can no longer drive the steam through the system (approximately four minutes at maximum steam flow conditions).

The system is capable of supplying the following ranges of conditions:

Fluid Flows:	Steam, 2.5 to 25 kg/s Water, 42 to 420 kg/s
Pressure:	2 to 6 MPa
Temperature:	212 to 275°C.

Measurements from the facility can be monitored from a central data acquisition system. This system is a 64-channel digital recording system with analog-tape-recording backup.

The digital system is equipped with a Neff 620 data acquisition system that converts analog input signals to digital form for processing by a ModComp II/45 computer. The signal conditioning system provides the input conditioning required for Type K thermocouples, bridge pressure transducers, and resistance temperature detector (RTD) devices.

### REFERENCE

- A.22-1 C. L. Nalezny, "Final Design Report for the LOFT Two-Phase Flow Calibration Loop," EG&G Idaho, November 1980.

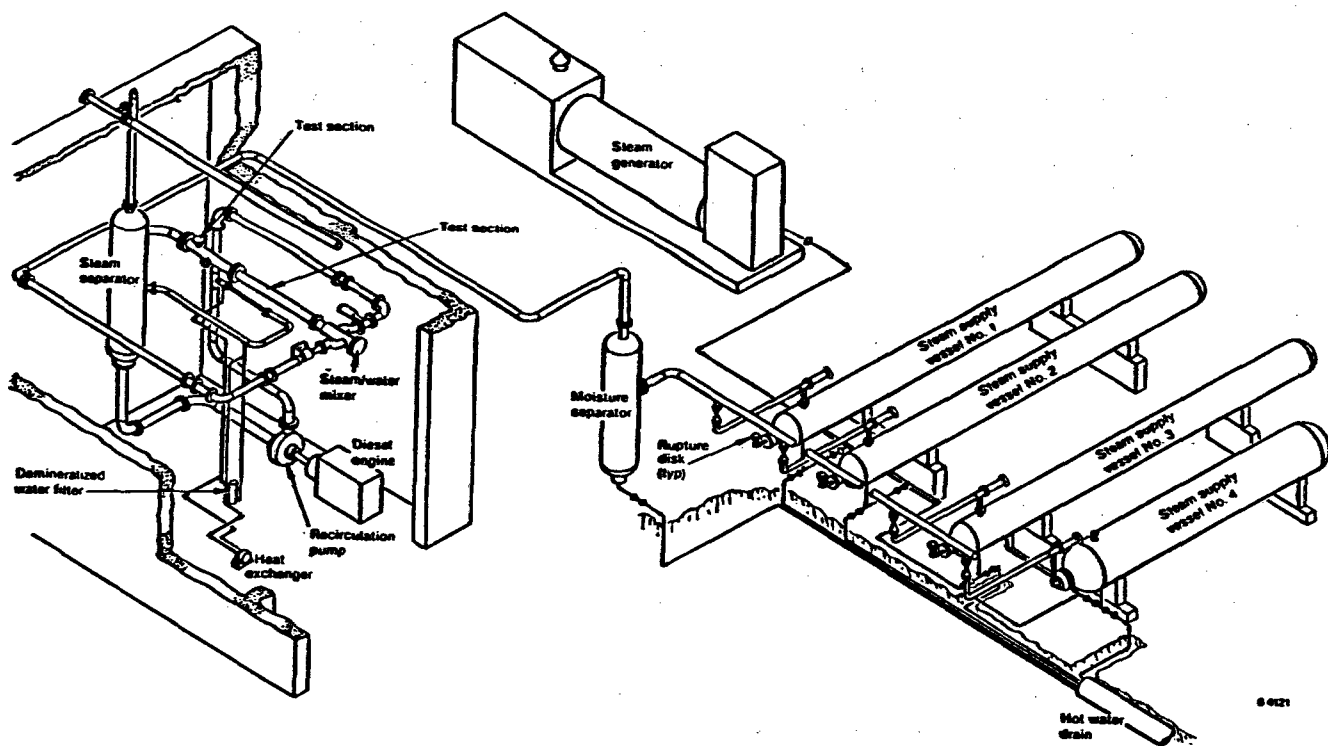


Figure A.22-1 Diagram of Two-Phase Flow Loop

## A.23 30° STEAM SECTOR TEST FACILITY

The 30° Steam Sector Test Facility (SSTF) was located at GE's gas turbine/jet engine installation in Lynn, Massachusetts. Facility construction was initiated in 1977, and testing was conducted by GE in 1979. As part of the CCFL/Refill-Reflood program with the NRC, the Electric Power Research Institute, and GE, the existing SSTF was upgraded to perform transient LOCA simulation tests. The SSTF configuration is depicted in Figures A.23-1 and -2. Details of the facility design are included in Reference A.23-1. The facility was demolished following completion of the CCFL/Refill-Reflood program.

### Internals

The facility internals provided an accurate representation of the reference BWR/6-218 (624 bundle) reactor through the use of prototypical hardware and geometry. The upper plenum was a full-scale mockup of a 30° sector of the reference upper plenum with accurate simulation of the geometric shape and the shroud head curvature and height. Standpipes simulating the steam separators extended up from the shroud head. The upper and lower core-spray spargers were full-scale mockups of 30° sectors of the reference BWR/6-218 HPCS and LPCS spargers with regard to size, curvature, location, and nozzles. An LPCS lower header representative of BWR/4,5 design could also be installed in the upper plenum to simulate earlier core-spray designs. The core region simulation included both mock fuel bundles and bypass region. The core region was full scale in cross section but was a 30° sector. It contained 42 complete bundles and 16 partial bundles with removable cover plates and baffles to simulate the 30° boundary within the partial bundle. The bundles used production-version hardware for channel, channel fasteners and spacer, upper tieplate, lower tieplate, and finger springs. Simulated fuel rods were included in both the upper and lower tieplate regions. The upper fuel rod simulation included production-version expansion springs, end pins, locking tab washers, hexagon nuts, and one fuel-rod spacer. A steam injection tube was provided in each bundle below the upper rods to deliver the channel steam from the steam distribution manifold located outside the 30° shroud wall. A weir-tube measuring device was provided in selected bundles above the lower rods to measure the liquid flow. The bypass region flow area was simulated. It included dummy control rods mounted on production-version fuel-support castings. Leakage and flow path simulation between bundle, bypass, upper plenum, lower plenum, and guide tube were ensured by using production-version hardware in conjunction with accurate representations of the top fuel guide and core plate. Twelve volume-scaled guide-tube regions were provided (one for each of the 12 centrally located side-entry fuel supports). The lower plenum volume represented the scaled volume of the reference lower plenum region outside the guide tubes.

Two simulated (non-functioning) jet pumps scaled on the basis of BWR equivalent single-phase flow resistance connected the lower plenum to the annulus. The jet pump lengths were scaled to compensate for the fact that the core is fore-shortened. The annulus region was scaled on a volumetric basis with regard to the reference BWR/6-218.

LPCI lines passed through the annulus to inject ECC flow into the core shroud for simulating BWR/6 LPCI. By modifying the LPCI internal piping, ECC liquid could also be injected into the top of the jet pumps to simulate BWR/4 LPCI.

A blowdown pipe connected to the outer wall of the annulus simulated the BWR recirculation line outlet and (under transient LOCA simulation tests) directed the blowdown mixture past a flow-restricting nozzle (simulating the reactor break area) to the blowdown suppression tank.

A volumetrically scaled steam dome region completed the BWR simulation. The steam dome was formed by partitioning the volume between the test section internals and the excess volume\* of the pressure vessel.

### Pressure Vessel

The SSTF pressure vessel (14 ft in inside diameter and 27 ft in inside height) served as a pressure envelope for the 30° sector internals. The vessel was designed with numerous nozzles and penetrations to permit attaching the various process lines that service the internals and to provide routing for the various instrumentation lines and cables. The vessel was surrounded by service platforms and walkways and was serviced by a traveling overhead crane.

### Facility Services

The SSTF was located in the central region of an existing turbine hall in which the necessary process equipment and loop hardware had been installed to provide the required services to the facility. A steam supply of 130,000 lbm/hr at 150 psia and 388°F was available.

Water was supplied to the facility from a 10,000-gallon condensate tank and retained in an 18,000-gallon supply tank that was part of the ECCS water supply and recirculation loop. The temperature of the water in the tank could be controlled by recirculating through a 500-gpm heat exchanger loop. Water from the lower plenum of the test section could be pumped back to the supply tank via a single-pass heat exchanger unit, recirculated to the top of the upper plenum, or circulated through the LPCI systems to accommodate both separate-effect and transient-test operation needs. The ECCS supply system provided flow representative of the reference BWR/6-218 reactor. The system consisted of three 600-gpm pumps connected in parallel and one 2400-gpm booster pump to provide up to 2400 gpm at 150 psia to the 10-in. main ECCS header. This main header in turn supplied a 6-in. HPCS line with up to 533 gpm and an 8-in. LPCI line with up to 1333 gpm. A secondary water drainage system provided drainage capability for the guide tube and annulus regions of the test section for control of initial mass inventory during transient tests.

A vessel blowdown system consisting of a blowdown line (with removable flow restricting nozzle), quick-opening valve, flash tank, and suppression/containment tank managed the blowdown effluents during transient LOCA simulation tests.

Onsite data acquisition/data reduction was provided by a Hewlett Packard processor with a 400-channel input signal capacity.

\*Vessel free volume in excess of the BWR-scaled value.

## Vapor Injection Simulation

Adiabatic steam injection was provided in the core, guide tubes, and lower plenum of the test section to simulate/augment liquid flashing and bundle steam generation during separate-effect and transient LOCA simulation tests, and to set initial void and mass distribution conditions representative of that predicted for the reference reactor at the initiation of the tests. Control of the injected steam flow was by automatic systems capable of providing steady-state injection rates or programmed injection transients.

## Measurement System

The measurement system developed for the SSTF emphasized a global measurement approach within the test system rather than a high concentration of detailed localized measurements. The specific measurements provided in the SSTF were divided into five categories:

1. Mass and energy input and discharge from the test vessel.
  - a. ECCS inputs (LPCI, LPCS, HPCS)
  - b. injected steam inputs to steam dome, core, guide tube/bypass, and lower plenum
  - c. vessel steam discharge
  - d. vessel blowdown mass discharge
  - e. lower plenum liquid discharge
2. Mass history ( $\Delta P$ ) and liquid levels (conductivity probes) in internal test section regions.
  - a. upper plenum at three radial locations
  - b. six fuel bundles of the core sector
  - c. bypass at four radial locations
  - d. one jet pump
  - e. lower plenum at three locations
3. Internal flows through the following paths.
  - a. liquid downflow through six fuel bundles (weir tubes)
  - b. vapor updraft indication through three standpipes ( $\Delta P$ )
  - c. reverse flow through each jet pump ( $\Delta P$ )

4. Internal pressure and differential pressure strings.
  - a. vessel pressure
  - b. differential pressure across three standpipes
  - c. upper plenum pressure
  - d. upper plenum axial pressure differential at three radial locations
  - e. upper plenum radial pressure differential at bottom of the upper plenum
  - f. bypass axial pressure differential at four radial locations
  - g. bypass radial pressure distribution string at one axial location
  - h. axial differential pressure across annulus
  - i. differential pressure across one jet pump
  - j. differential pressure across core support plate
  - k. lower plenum pressure
  - l. lower plenum axial differential pressure at three locations
  - m. axial differential pressure across four guide tubes
  - n. differential pressure between four guide tubes and the lower plenum
  - o. differential pressure across the excess volume diaphragm
5. System temperatures.
  - a. temperature of all liquid and vapor inputs and discharges
  - b. temperature above six and below all 58 upper tie plates
  - c. temperature profile in six bundles
  - d. jet pump fluid temperature
  - e. fluid temperature above and below six and below six additional side-entry orifices
  - f. upper plenum temperature distribution
  - g. lower plenum temperature distribution

- h. bypass temperature distribution
- i. miscellaneous surface temperatures within the test vessel

REFERENCE

A.23-1 J. E. Barton et al., "BWR Refill-Reflood Program; Task 4.4-30° SSTF; Description Document, "NUREG/CR-2133, General Electric Company, May 1982.

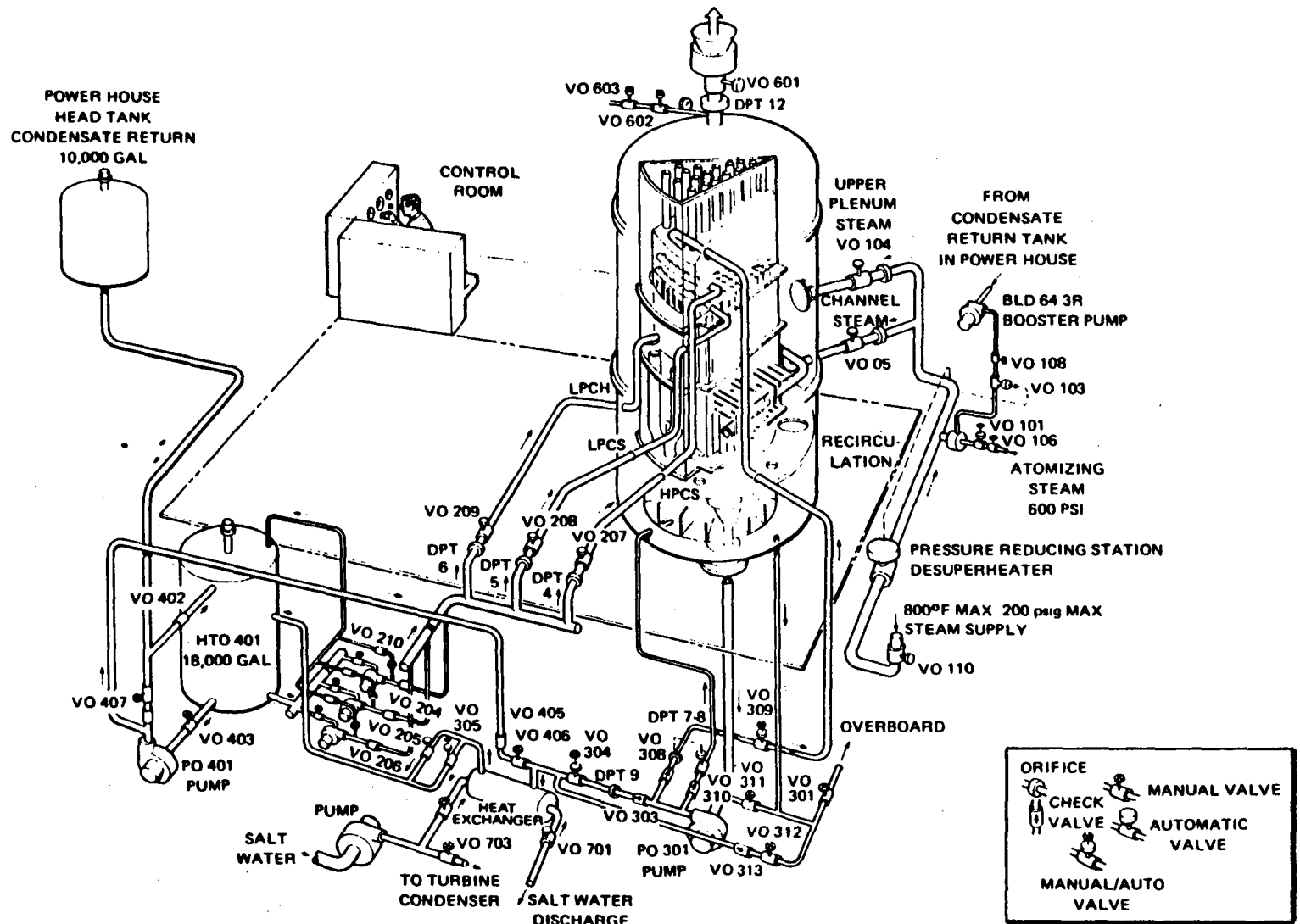


Figure A.23-1 30° steam sector test facility

A-209

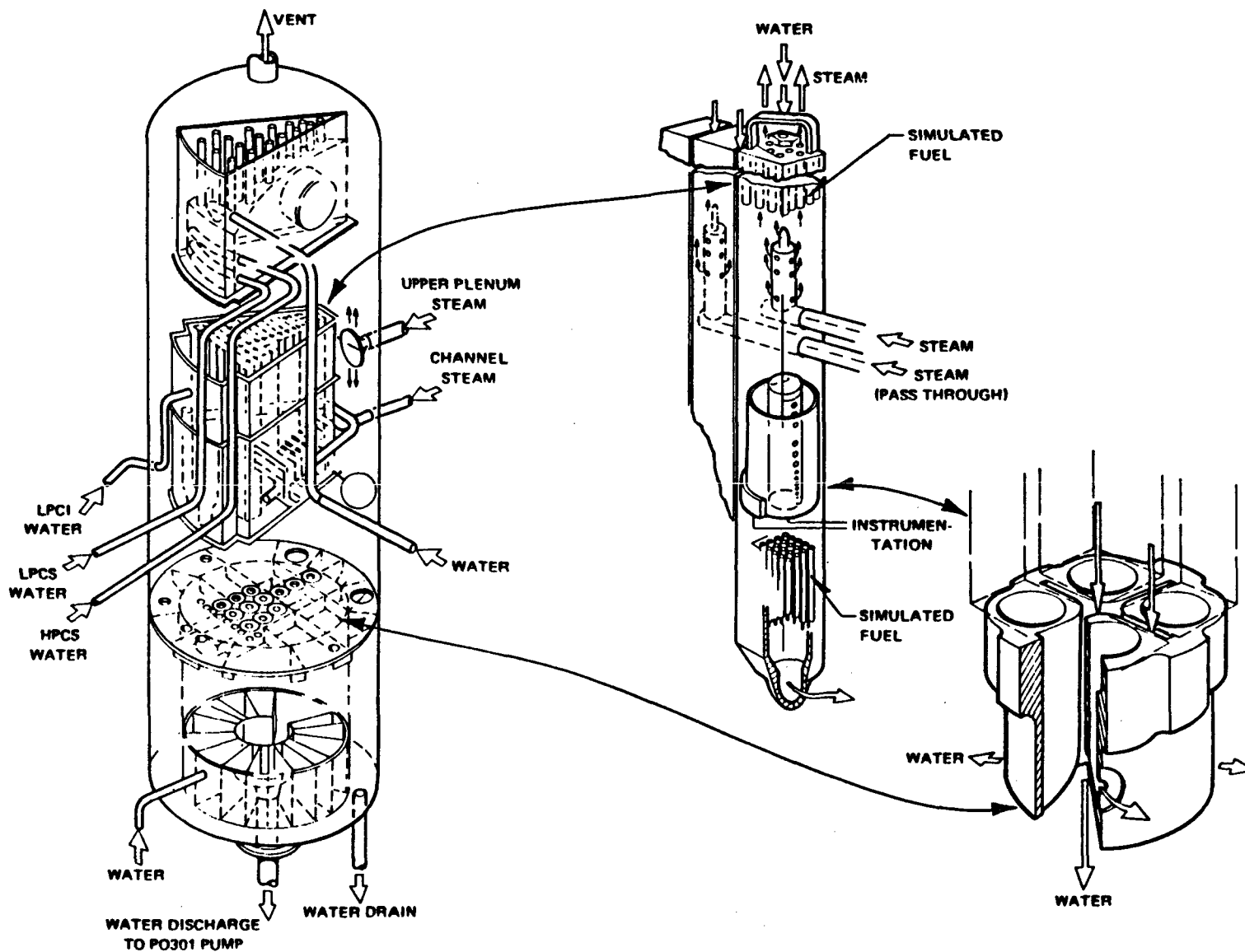
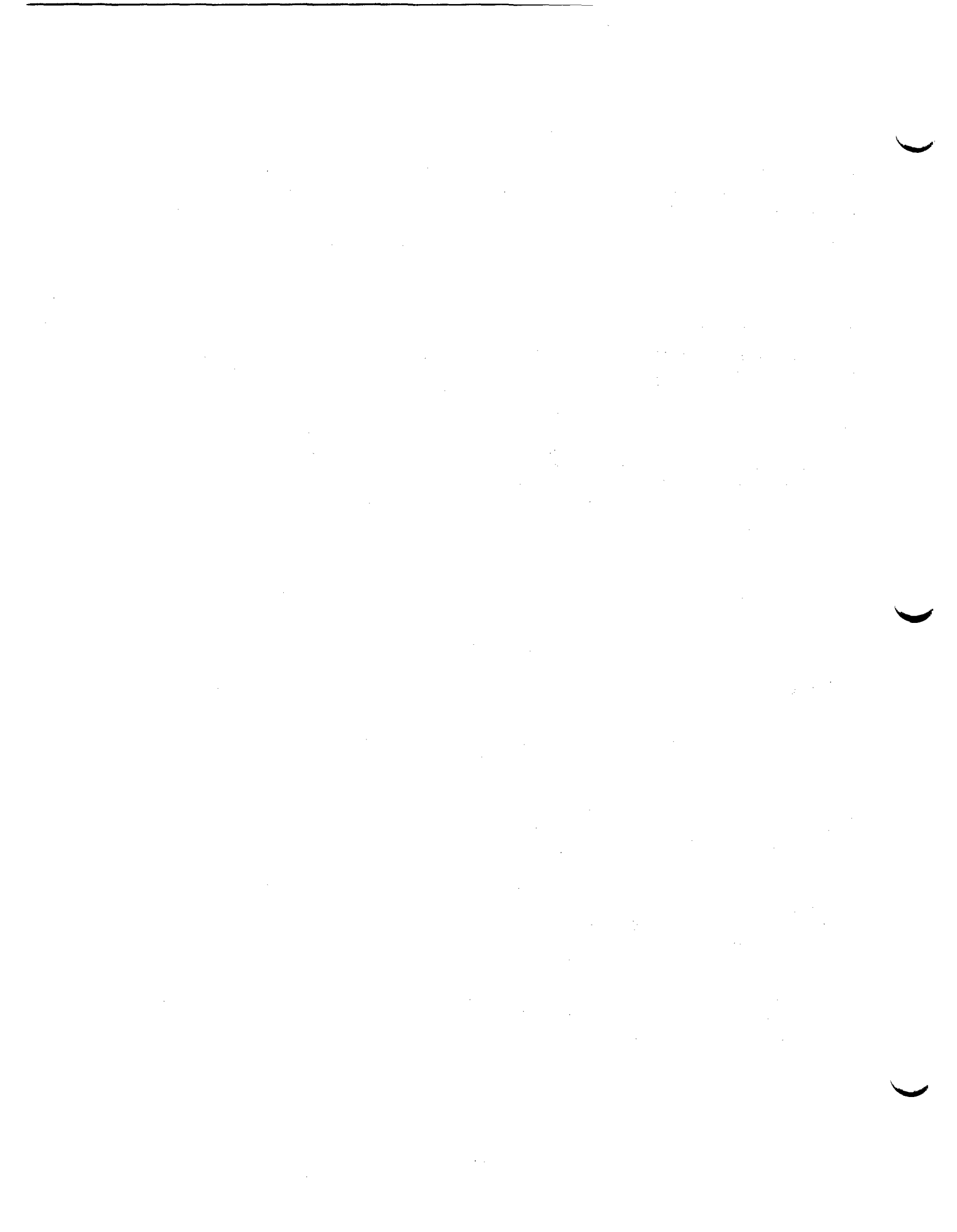


Figure A.23-2 30° steam sector test section



## A.24 ONCE-THROUGH INTEGRAL SYSTEM (OTIS)

The Once-Through Integral System (OTIS) program testing was sponsored by the Nuclear Regulatory Commission (NRC), the Babcock and Wilcox Owners Group (BWOOG), Babcock and Wilcox (B&W), and the Electric Power Research Institute (EPRI). The facility was a one-loop representation of raised-loop reactor systems of the B&W design. The purpose of the facility was to generate integral system data for post-small break loss-of-coolant accident (SBLOCA) to verify computer codes used for reactor safety analyses.

### Facility Description

The general arrangement of the major components and systems of the facility is shown in Figure A.24-1. The loop consisted of one 19-tube Once-Through Steam Generator (OTSG), a simulated reactor, a pressurizer, a single hot leg, and a single cold leg. Reactor decay heat, following a scram, was simulated in the test loop by electrical heaters in the reactor vessel. No pump was included on the main primary loop, but a pump in an isolatable cold leg bypass line was available to provide forced primary flow. The test loop was full raised-loop plant elevation, approximately 95 feet high, and shortened in the horizontal plane (to approximately 6 feet) to maintain approximately volumetric scaling.

Other primary loop components included a reactor vessel vent valve (RVVV), pressurizer pilot-operated relief valve (PORV) or safeties, and a hot leg high point vent (HPV). Auxiliary systems were available for scaled pressure injection (HPI), controlled primary leaks in both the two-phase and single-phase region, a secondary forced circulation system for providing auxiliary feedwater (AFW) to the OTSG, steam piping and pressure control, a cleanup system for the secondary loop, and gas addition for the primary loop.

### Scaling

The details of scaling considerations are presented in Reference A.24.1. The four scaling criteria used to configure OTIS, in order of priority, were (a) elevations, (b) post SBLOCA flow phenomena, (c) volumes and (d) irrecoverable pressure loss characteristics.

SBLOCA fluid behavior is typically buoyancy driven; therefore, full elevation modeling was assigned first priority. To obtain flow phenomena in the test loop as close to plant-typical as possible, the governing phenomena were determined, evaluated, and accommodated as second priority in the scaling criteria. Volumetric scaling of the loop components was generally possible, but was assigned third priority. The last major scaling criterion was the loop irrecoverable pressure losses. When the other scaling consideration were accommodated, irrecoverable losses were adjusted to plant-typical by the inclusion of flow restrictors in expected single-phase water locations of the loop.

OTIS power and volume scaling originated with the size of the model OTSG. The model OTSG contained nineteen full-length and plant-typical tubes, which represented the 16013 tubes in each of the two steam generators used in the 205-fuel

assembly plants. Therefore, the dominant power and volume scaling in the loop resulted in a scaling factor of 1686. The distance between secondary faces of the lower and upper tubesheets in the 19-tubes OTSG was full length as shown in Figure A.24-2. Auxiliary feedwater nozzles were located in the model steam generator at two elevations. The tubesheet thicknesses in the model OTSG were not plant-typical, and the model inlet and outlet plenums were reduced. Therefore, the hot leg-to-steam generator inlet and steam generator-to-cold leg lengths were atypical. Piping extensions between the steam generator inlet and exit plenums were used to retain plant-typical elevations.

The hot leg inside diameter was scaled to preserve Froude number, and thus, the ratio of fluid inertial-to-buoyancy forces. This criterion was invoked to approximately preserve two-phase flow regimes and reflooding phenomenon according to certain correlations. Scaling with Froude number resulted in a hot leg diameter twice that indicated by ideal volumetric scaling. Although this added approximately 20% to the ideal system (total loop) volume, this choice of hot leg inside diameter was considered most likely to avoid the whole-pipe slugging behavior which has been observed in other scaled SBLOCA test facilities.

The spillover elevation of the plant hot leg U-bend was retained in OTIS by matching the elevation of the bottom (inside) of the plant and model hot leg u-bend pipes. The radius of the U-bend obtained exact volumetric scaling of this component.

The pressurizer in OTIS was volume and elevation scaled. The elevation of the bottom of the pressurizer was plant typical, as was the spillover elevation of the pressurizer surge line. The centerline elevation of the hot leg-to-pressurizer surge connection matched that of the plant.

An electrically heated reactor vessel provided heat input to the primary fluid to simulate reactor decay heat levels up to 8% of scaled full power. Based on a plant power rating of 3600 Mwt, 1% of scaled full power in OTIS was 21.4 kW. The model core heat input capacity was 180 kW. OTIS primary flow scaling obtained 1% of scaled full flow = 0.259 lbm/s; on the secondary side, 1% of scaled full secondary flow = 0.0265 lbm/s. These conversion factors are discussed in more detail in the OTIS Test Specification (Ref. A.24.1).

The annular downcomer of the plant reactor vessel was simulated by a single external downcomer in OTIS. The spillover elevation in the horizontal run at the bottom of the model downcomer corresponded to the elevation of the uppermost flow hole in the plant lower plenum cylinder. The OTIS reactor vessel consisted of three regions: a lower plenum, a heated section, and an upper and top plenum. The center of the heated length of the model core corresponded to the center of the active fuel length in the plant core. (The model heated length was half of full scale). The core region of the model reactor vessel contained excess volume due to construction constraints; therefore, to maintain the total reactor vessel scaled volume, the reactor vessel was shorter than plant-typical. Non-flow lengths were sacrificed to maintain the reactor vessel scaled volume.

The center of the cold leg-to-downcomer connection in OTIS matched the cold leg-to-reactor vessel nozzle centerline in the plant. Similarly, the center of the hot leg-to-upper plenum connection in OTIS corresponded to the reactor

vessel-to-hot leg nozzle centerline in the plant. The model cold leg did not contain an in-loop pump, since OTIS was designed to simulate the natural circulation phases of an SBLOCA. Upstream of the reactor coolant pump spillover point, a flange was provided in the cold leg piping to admit a flow restrictor which simulated the irrecoverable pressure loss characteristic of a stalled reactor coolant pump rotor. The model cold leg originated at the lower plenum of the 19-tube OTSG and extended downward to match the spillunder elevation of the plant cold leg. The highest point in the cold leg (the spillover into the sloping cold leg discharge line) matched the reactor coolant pump spillover elevation in the plant. Because horizontal distances were shortened in OTIS, the slope of the cold leg discharge line was atypically large.

OTIS atypicalities are summarized as follows:

- OTIS was predominantly a vertical system, due to the shortened horizontal distances and small cross sections of the various components such as steam generator and reactor vessel. Therefore, OTIS was inherently a one-dimensional model.
- Because of the small size of the piping used in OTIS, the ratio of loop wall surface to fluid volume was approximately 20 times that of the plant. Therefore, the fluid and wall-surface temperatures were much more closely coupled than those of a plant.
- In high-pressure models, the ratio of metal volume to fluid volume increases as the model is made smaller. In OTIS, the ratio of metal volume to fluid volume was approximately twice that of the plant.

The pipe surface-to-fluid volume ratio atypically results in higher heat losses in the scaled facilities than in the plants. The effect was minimized by using both guard heaters and passive insulation on the model piping. Guard heating was used for the OTIS hot leg, pressurizer, surgeline, and reactor vessel upper head.

The OTIS secondary system provided the steam generator secondary inventory and those fluid boundary conditions which affect SBLOCA phenomena. These included the steam generator level, AFW flow rate, and steam pressure control systems.

The OTIS instrumentation included pressure and differential-pressure measurements; thermocouple (TC) and resistance temperature detector (RTD) measurements of fluid, metal, and insulation temperatures; level and phase indications by optical-ports and conductivity probes as well as by differential pressures; and pitot tubes and flowmeters for measurements of flow rates in the loop. In addition to these measurements, the following loop boundary conditions were metered: HPI, HPV (hot leg and RV), (controlled) leak, PORV, secondary steam and feed flow rates. Noncondensable gas (NCG) injections were controlled and metered; NCG discharges with the two-phase primary effluent streams were measured; and the aggregate primary effluent was cooled and collected for integrated metering. OTIS instrumentation consisted of approximately 250 channels of data which were processed by a high-speed data acquisition system. The data acquisition rate could be either event-actuated, or adjusted by the loop operator to acquire and store a full set of data as often as every 5 seconds.

## Features

OTIS consisted of a closed primary loop, closed secondary loop, and several auxiliary systems. A general arrangement showing the relationship of the key components of these systems is shown in Figure A.24-3. In this section the key features of these systems will be discussed. The key features are:

- Multiple leak location,
- Gas addition capability,
- Guard heating,
- Scaled high pressure injection (HPI),
- Simulated reactor vessel vent valve (RVVV),
- OTSG level control,
- Automatic cooldown,
- High and low auxiliary feedwater addition.

Multiple leak locations were present in OTIS to allow a controlled SBLOC. Controlled leaks were located at the bottom of the lower plenum of the reactor vessel, at the top of the top plenum of the reactor vessel, in the cold leg upstream of the simulated reactor coolant pump (RCP) spillover, in the cold leg downstream of the RCP spillover, a high point vent (HPV) at the top of the hot leg U-bend (HLUB), and a simulated pilot operated relief valve (PORV) at the top of the pressurizer. Leak flow was controlled by an orifice located just downstream of the leak site. The leak flow control orifice was located in a 5/8" diameter tube as shown in Figure A.24-4 to form the leak flow control orifice assembly. Scaled leaks in the range of 10 cm<sup>2</sup> and 15 cm<sup>2</sup> were tested in the single phase regions (cold leg leaks), while ~10 cm<sup>2</sup> scaled leaks were tested at the PORV. The actual diameter of the scaled leak was obtained from the ideal volume scaling factor of 1686. Thus a scaled leak of 10 cm<sup>2</sup> has a diameter of 0.034 inches in OTIS.

To preclude leakage from the loop, sealed stem valves were used, where possible. Additionally, all instrument fittings in the reactor coolant system, above the top of the core heaters were sealed welded. A helium leak check was performed to ensure that the loop was leak tight.

As a result of the large surface area to fluid volume ratio, heat loss in the OTIS loop was proportionally greater than that in the plant. To minimize this effect, guard heaters were used along the hot leg piping, pressurizer, pressurizer surge line, and the reactor vessel upper and top plenums. The objective of the guard heating system was to provide heat to the components in an amount equal to heat loss of that component to ambient. A layer of control insulation, approximately 1/2" thick, enclosed by a thin shell of stainless steel lagging, was placed over the pipe sections to be guard heated. The heater tapes were spirally wrapped over the lagging material, covering nearly 100% of the pipe section. Two layers of passive insulation then covered the guard heaters. The heaters were controlled based on thermocouples located on the pipe OD and at a point mid-way into the control insulation. Tests were performed to evaluate the heat loss from the OTIS loop and to characterize the operation of the guard heaters.

Two high pressure injection (HPI) locations were provided one at the cold leg low point, upstream of the simulated RCP spillover, the other in the downward sloping cold leg, downstream of the simulated RCP spillover. A scaled HPI flow

provided by a positive displacement pump. The flow into the loop was controlled to simulate the plant scaled head-flow curve. In OTIS, HPI flow was direct exclusively to the cold leg discharge piping.

The reactor vessel vent valve (RVVV) was simulated by a single pipe extending from the upper and top plenum of the reactor vessel to the external downcomer. The pipe elevation matched the spillover elevation of the plant RVVV. A pneumatically-operated, automatically-controlled valve was located in the pipe. The valve was controlled to open and close when the differential pressure between the reactor vessel and downcomer reached preset values. A vertically oriented slit orifice in the pipe, downstream of the valve, set the flow through the simulated vent valve.

The secondary loop consisted of the 19-tube OTSG, steam piping, a water cooled condenser, hot well, feedwater pump, feedwater heater, and feedwater piping. The secondary side simulation of the modeled plant was limited to the steam generator and the elevation of the auxiliary feedwater (AFW) inlets. Additionally, several control functions were used to simulate plant performance. These included:

- continuous level (inventory) control
- band level control
- steam pressure control
- automatic cooldown

The secondary loop could operate at steam pressures of approximately 200 to 1200 psia. Steam pressure was automatically controlled by a steam control valve, based on a signal from the steam pressure transmitter. In addition to automatic steam pressure control, the steam pressure could be controlled to decrease at a pre-programmed rate. This feature allowed the simulation of a plant-operator-controlled cooldown. The desired cooldown rate was keyed into the controller as a series of linear segments of pressure and time. When activated, the steam pressure control valve modulated to obtain the stipulated depressurization.

Auxiliary feedwater addition could be made at either of two locations in the steam generator - a high feed elevation, typical of the B&W domestic plants, and at a low elevation. The AFW nozzle at each elevation could be configured for maximum wetting or minimum wetting of the steam generator tubes. The two configurations, allows comparison of the effects of a spray pattern on heat transfer (typical of the outer rows of tubes near the AFW nozzles in the plant), with the effects of pool heat transfer (typical of the large majority of tubes that are away from the AFW nozzles in the plant).

### Tests Conducted

A total of 13 tests in three categories (1) a benchmark test, (2) 10 single variable tests, and (3) two composite tests conducted by an operator versed in plant procedures were conducted in OTIS. The 10 single-variables tests consisted of seven SBLOCA transients, an HPI-PORV (feed-and-bleed) cooldown, and two natural circulation cooldowns. Each of the seven SBLOCA transients varied a single major boundary conditions from the conditions of the nominal test.

Two additional tests were conducted to investigate effects of guard heater and pressurizer isolation at test initiation. Details of tests are given in Reference A.24.2.

References

- A.24.1 OTIS Design Requirements: OTIS design considerations, supplements GERDA design requirements, B&W Document No. 51-1149127-00, Babcock & Wilcox, Lynchburg, Virginia.
- A.24.2 OTIS Final Report, NUREG/CR-4567, September 1986, Babcock & Wilcox, Lynchburg, Virginia.

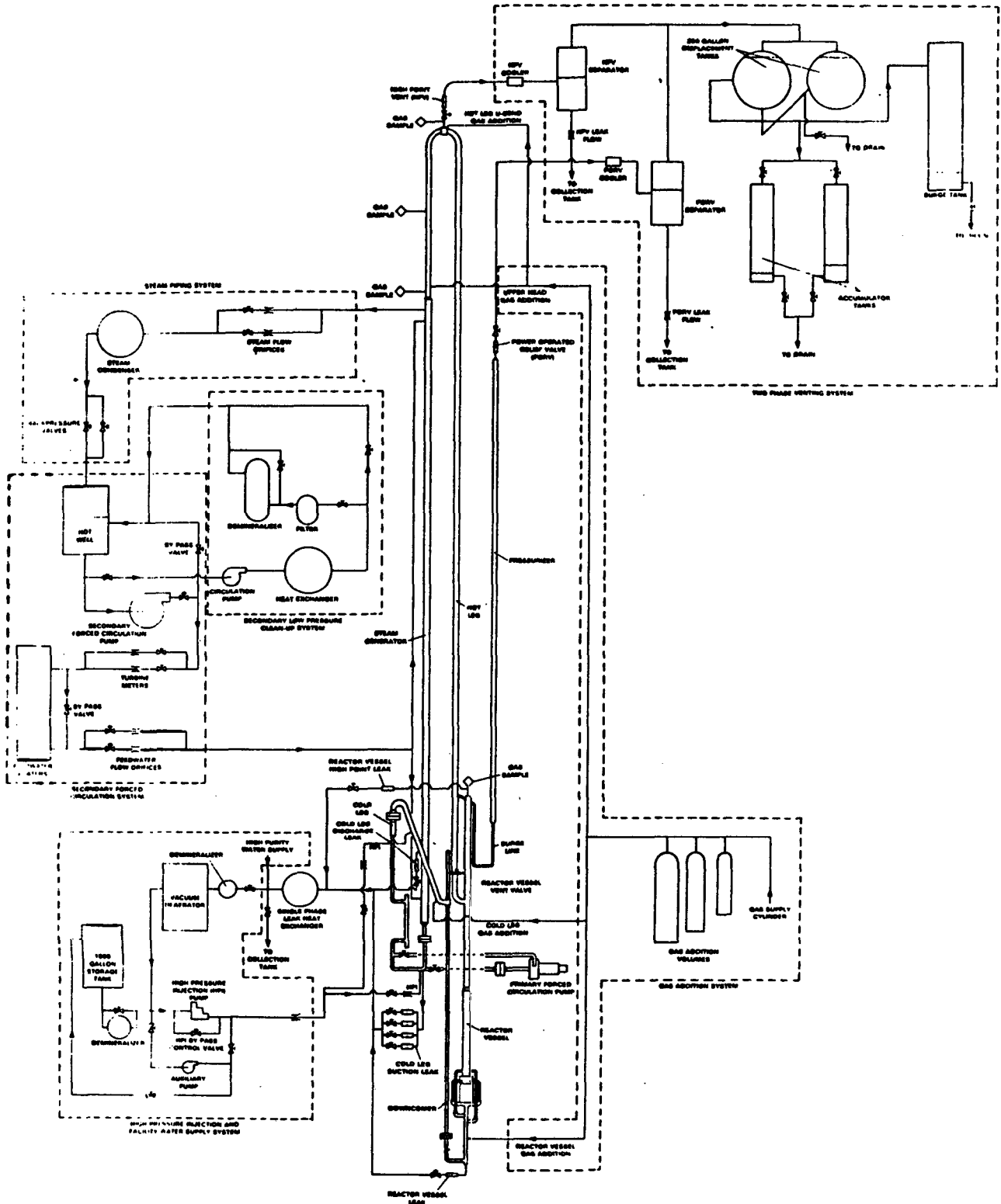
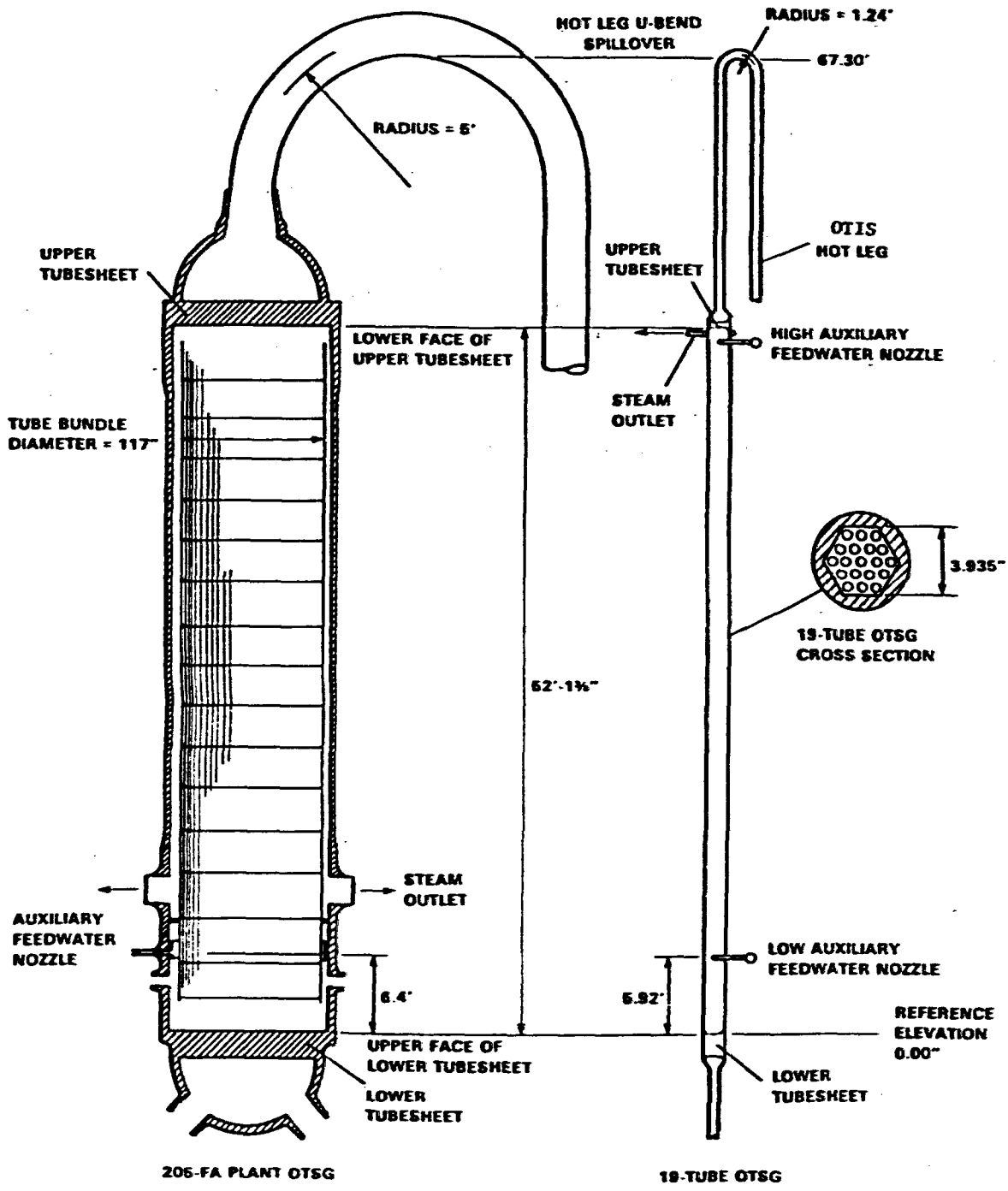


Figure A.24.1 OTIS Test Facility



NOTE: COMPONENTS ARE DRAWN TO SCALE IN ELEVATION; PIPE DIAMETERS ARE EXAGGERATED FOR CLARITY

Figure A.24.2 Comparison of Full-Size 205-FA Plant OTSG to 19-tube OTSG of OTIS

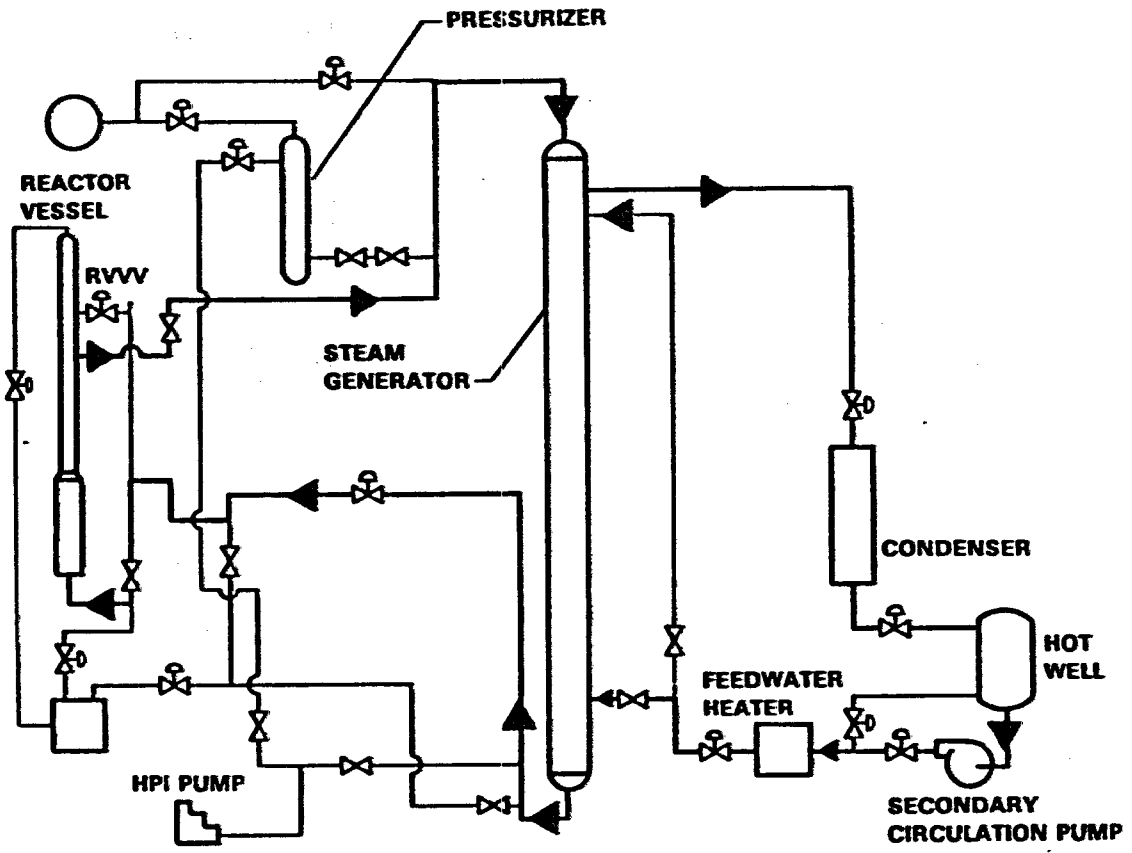


Figure A.24.3 OTIS General Arrangement

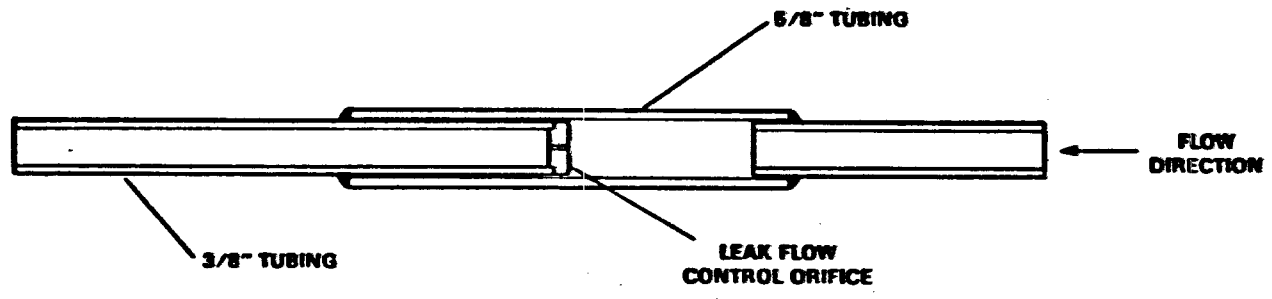


Figure A.24.4 Leak Flow Control Orifice Assembly



## A.25 MARVIKEN

The Marviken full-scale CFT (Critical Flow Test) program was conducted between mid-1977 and December 1979 as a multinational project at the Marviken Power Station in Sweden. The 27 CFT experiments obtained critical mass flow rate data for short pipes of large diameter in the subcooled and low quality regions under steady and quasi-steady state conditions. The CFT Program was financed by the Forsogsanlaeg Riso (Denmark), the Kernforschungszentrum Karlsruhe GmbH (Federal Republic of Germany), the Technical Research Centre of Finland (Finland), the Commissariat a l'Energie Atomique and the Electricite de France (France), N.V tot Keuring van Electrotechnische Materialen (the Netherlands), the Institutt for Atomenergi (Norway), Studsvik Energiteknik AB (Sweden), the Electric Power Research Institute and the United States Nuclear Regulatory Commission (USA).

Although extensive critical mass flow testing had been conducted with small scale nozzle geometries prior to the CFT program, no data were available to allow researchers to determine whether conclusions based on small-scale results and phenomena observed there were applicable to full scale pipe geometries found in operating nuclear power stations. Thus the CFT Program sought to provide the data necessary to form a link between the available small-scale data and existing operational hardware.

The tests were conducted by discharging water and steam-water mixtures from a full-sized reactor vessel through a large diameter discharge pipe that supplied the flow to the test nozzle. The nine test nozzle geometries all had rounded entrances followed by a nominally 200, 300 or 500mm constant diameter cross-section. The nozzles ranged in length from 166 to 1809mm.

Most tests were conducted with a nominal initial steam dome pressure of 5 MPa (4 MPa for one test) and with the water initially subcooled between 50°C and 1°C (with respect to the steam dome pressure). The water oxygen content was approximately the same for all tests, but it was decreased by a factor of 140 with respect to a reference test in order to determine the effect of the water air content on the critical mass flow rate.

The vessel, discharge pipe, and nozzle were instrumented to determine the test behavior and to provide a basis for evaluating the stagnation conditions and mass fluxes at the nozzle inlet. The instrumentation readings were recorded using a pulse code modulation system. Data error limits were evaluated for all measurements.

### TEST FACILITY DESCRIPTION

A vertical cross-sectional view of the test facility is shown in Figure A.25-1. The major components of the facility are:

- a. The pressure vessel: net volume =  $425\text{m}^3$ , maximum design pressure = 5.75 MPa, and maximum design temperature = 272°C.
- b. The discharge pipe: consisting of the ball valve and pipe spools which house the instrumentation upstream of the test nozzle.

- c. The test nozzles and rupture disc assemblies: a set of nozzles of specified lengths and diameters to which the rupture disc assemblies were attached.
- d. The containment and exhaust pipes: consisting of the drywell (net volume = 1934 m<sup>3</sup>), the wetwell (net volume = 2144 m<sup>3</sup>), the fuel element transport hall (net volume = 303 m<sup>3</sup>), the ground level 3.2m diameter exhaust pipe and the upper 0.4m diameter exhaust pipe.

#### TEST NOZZLES AND RUPTURE DISC ASSEMBLIES

The CFT program was conducted using nozzles with nominal diameters of 200 to 500mm and L/D's (length to diameter ratios) from 0.3 to 3.7. Nozzles in this range were chosen to provide full scale critical flow data for operational nuclear plants. It was acknowledged early in the CFT program that nozzle diameters larger than 500mm could not be tested due to equipment constraints. Nozzle diameters less than 500mm were chosen to allow extrapolation to larger diameters and to provide data in a range between existing data and the 500mm CFT data. The range in nozzle L/D's was selected so as to provide data for short pipes only (i.e., L/D's approximately equal to 4 or less).

Each test nozzle consisted of a rounded inlet, having a radius of curvature equal to the nozzle radius, followed tangentially by a cylindrical section. The inlet radius of curvature was defined as a compromise between all the possible alternatives which could be suggested as a representative inlet pipe section in a nuclear power plant. Each nozzle was bolted to the lower pipe spool. The nozzle outlet was equipped with an assembly containing two rupture discs installed in carrier rings, held in position by a ring fastener. The diameter of the discs was dependent on the test nozzle.

The first 12 critical flow tests were performed using test nozzles with flared outlets combined with rupture disc assemblies and flared ring fasteners. However, midway through the CFT program, concern was expressed because it was suspected that the fluid could not expand freely in the flared outlets downstream of the constant diameter test section. It was therefore decided to modify the nozzles and the rupture disc assemblies to obtain a constant flow area. Because constant diameter nozzle/rupture disc assemblies were not immediately available, Tests 13 and 14 were conducted with the constant diameter test nozzle with 200mm diameter and L/D = 3.0 and 400mm diameter rupture disc assembly. Finally, Tests 15 through 27 were conducted using a constant diameter test nozzle section, formed in part by the rupture disc assemblies and the straight ring fastener.

#### TEST MATRIX DESCRIPTION

The tests conducted during the CFT program are listed in Table A.25-1 according to increasing nozzle size and increasing subcooling. The objective of each test is summarized in Reference A.25.1. In general, the test matrix was constructed to define a test envelope with inlet conditions ranging from at least 30°C subcooled to low quality saturation for each nozzle. Tests conducted with water subcooled 15°C or more would give saturated data at pressures below 4.5 MPa, whereas tests with less than 5°C subcooling would

give some saturated data at pressures greater than 4.5 MPa (usually as high as 4.8 MPa).

#### SUMMARY OF TEST PROCEDURE

The test procedure was designed to obtain the specified initial steam dome pressure and fluid temperature profile. The first step in test preparation was to fill the vessel with deionized water. With the vessel full, the integrity of the rupture discs was checked. Instrumentation sense lines were also bled to ensure that all air was removed. Water was then drained from the system until the specified elevation (at room temperature) was reached. The water was heated in three warm-up stages by circulating water from the bottom of the vessel through an external electric heater and reintroducing it into the vessel steam dome. The water from the heater was reintroduced along with other water also taken from the bottom of the vessel, but injected into the steam dome through a set of spray nozzles.

#### REFERENCE

A.25-1 The Marviken Full Scale Critical Flow Tests, NUREG/CR-2671, May 1982.

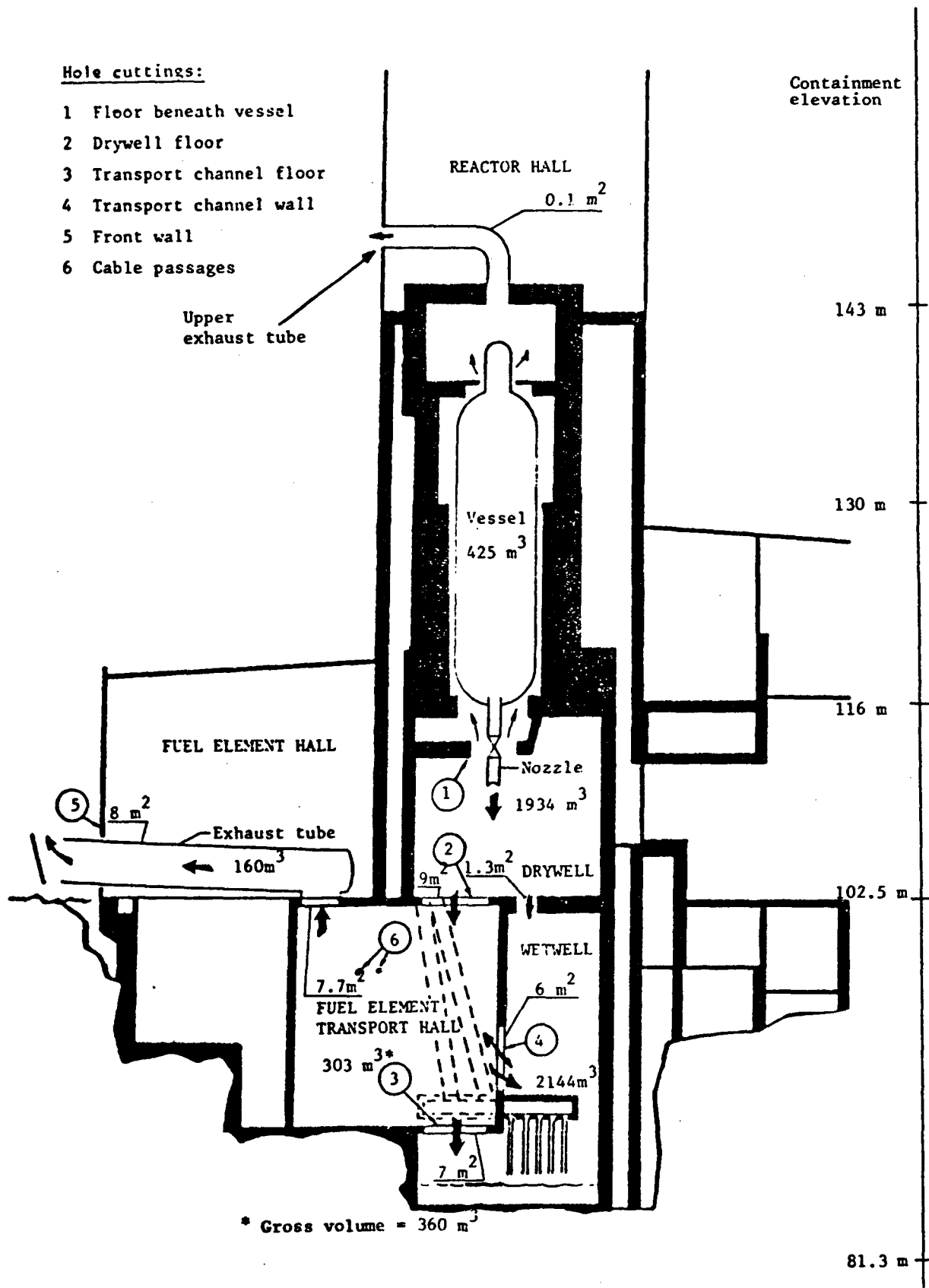


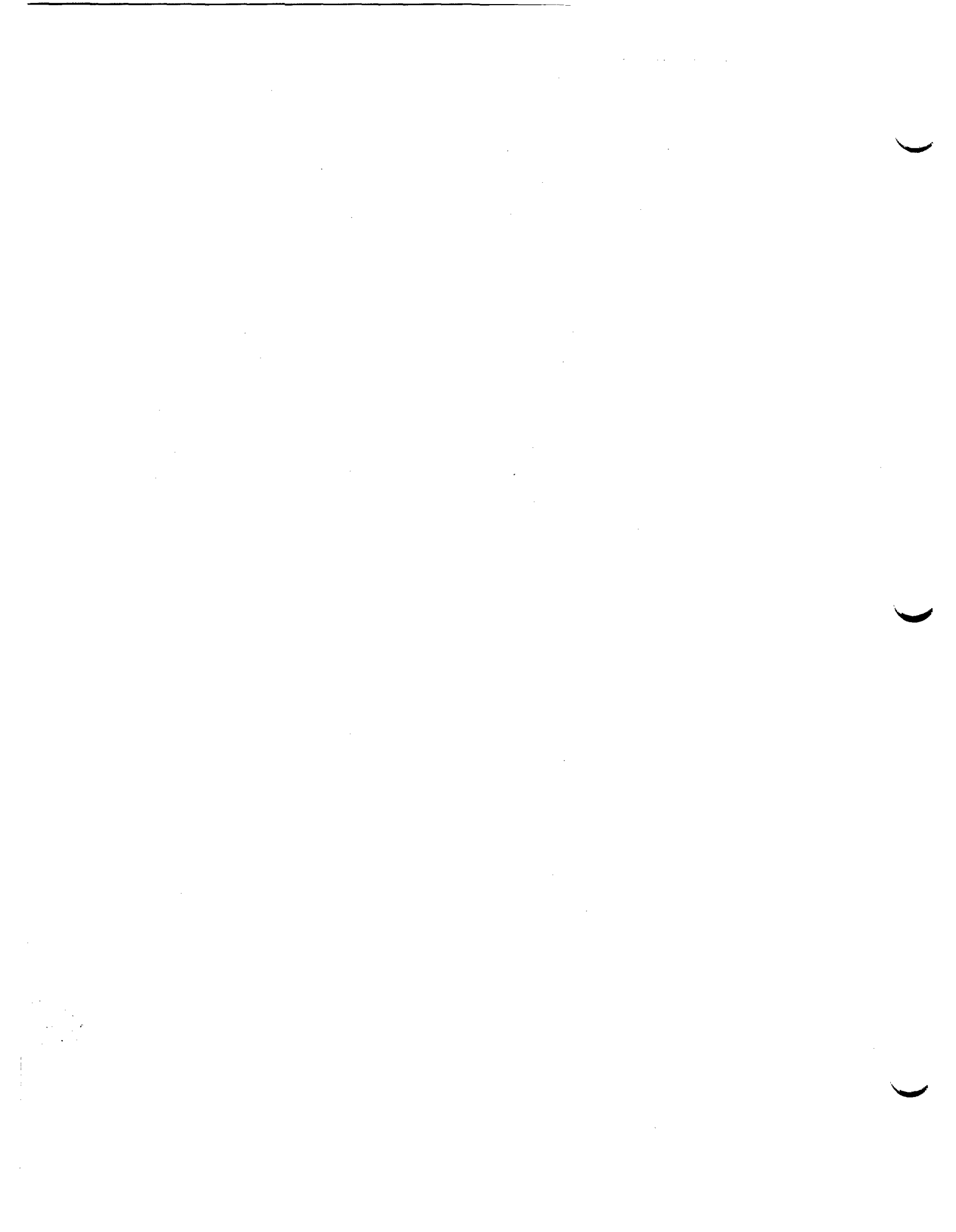
Figure A.25-1 Maryiken facility diagram, showing flow paths during a critical flow test

Table A.25-1 Summary of the CFT program test objectives

Nozzle Diameter ~ mm	L/D	Nominal* Subcooling ~ °C	Test Category	Test No	Test Objective
200	3.0	<5 30	III	14	Envelope definition
			I	13	Envelope definition
300	1.0	15 30	I	7	Envelope definition
			I	6	Envelope definition
300	1.7	<5 30	III	25	Envelope definition
			II	26	Envelope definition
300	3.0	15 30 30	I	1	Envelope definition
			I	2	Envelope definition
			I	12	Repeatability cf: Test 2
300	3.7	<5 30 30	III	19	Envelope definition
			I	18	Envelope definition
			II	17	Examine effect of new initial temp. profile cf: Test 18
500	0.3	<5 30	III	23	Envelope definition
			II	24	Envelope definition
500	1.5	<5 30 30	III	20	Envelope definition
			II	21	Envelope definition
			II	27	Examine effect of decreased water air content cf: Test 21
		II	22	Envelope definition	
500	3.6	30	I	16	Examine effect of nozzle geometry change cf: Test 11
		30	II	15	Examine effect of new initial temp profile cf: Test 16
509	3.1	30	I	5 <sup>+</sup>	Envelope definition
		<5	III	9	Envelope definition
		<5	III	10	Repeatability cf: Test 9
		15	I	3	Envelope definition
		30	I	4	Envelope definition
		30	I	8	Repeatability cf: Test 4
30	I	11	Repeatability and also examine data at nozzle exit in rupture disc assembly cf: Test 8		

\* All tests performed at initial nominal steam dome pressures = 5 MPa except test 5.

+ Initial steam dome pressure = 4 MPa.



---

# R E P O R T S U M M A R Y

---

<b>SUBJECTS</b>	Safety analysis / Analysis and testing	
<b>TOPICS</b>	Safety analysis Loss-of-coolant accidents Emergency core cooling systems	Test data BWR PWR
<b>AUDIENCE</b>	Safety managers and analysts / R&D engineers, scientists, and designers	

---

## **EPRI R&D Contributions to the Technical Basis for Revision of ECCS Rules**

Creating more realistic standards for the design of future nuclear plants could streamline the units and cut utility costs. This summary of EPRI projects dealing with LOCA phenomena and ECCS methodology shows how research is building a sound technical basis for revising the current guidelines.

---

<b>BACKGROUND</b>	Nuclear reactors have emergency core cooling systems (ECCSs) that are designed for operation in the event of a loss-of-coolant accident (LOCA). In the early 1970s, NRC established guidelines for evaluating the performance of these systems. The guidelines, stated in Appendix K of 10CFR50, are based on the understanding of fuel behavior and two-phase thermal hydraulics that prevailed at that time. As a result, they have a number of built-in conservatisms.
<b>OBJECTIVE</b>	To summarize the EPRI research that has yielded an improved understanding of LOCA phenomena and appropriate ECCS design.
<b>APPROACH</b>	The project team compiled and summarized all EPRI-sponsored research concerning LOCA phenomena and ECCS methodology conducted over the past 10 years. The various types of work documented include experiments, analyses, computer code development, and code assessment efforts.
<b>RESULTS</b>	<p>The results of EPRI research efforts when added to those of other studies show that the existing ECCS guidelines are overly conservative and that some of their assumptions are nonphysical. The research also provides much of the technical basis needed to set new requirements. This summary covers EPRI projects dealing with</p> <ul style="list-style-type: none"><li>• Two-phase critical flow</li><li>• Blowdown heat transfer</li><li>• Reflood heat transfer</li><li>• ECCS flow distribution</li><li>• Reactor coolant pump performance</li><li>• Core uncovering</li></ul>

---

- 
- Steam generator performance
  - Decay heat
  - Metal-water reaction
  - Fuel rod performance

Also described are EPRI projects of a fundamental nature and projects in computer code development and verification.

---

**EPRI PERSPECTIVE**

Using a more realistic ECCS methodology can save an estimated \$50 to \$100 million per plant for advanced LWRs. Such a methodology also allows greater flexibility in the operation of existing plants. It would permit better fuel-cycle planning and leave more margin for loadings that minimize neutron flux at the vessel wall and extend plant life. This report summarizes EPRI-sponsored work in an important area of nuclear plant improvement.

---

**PROJECT**

EPRI Project Manager: V. K. Chexal  
Nuclear Power Division

---

For further information on EPRI research programs, call  
EPRI Technical Information Specialists (415) 855-2411.

**EPRI R&D Contributions to the Technical  
Basis for Revision of ECCS Rules**

---

**NP-4146-SR**

**Special Report, July 1985**

**Prepared by**

**V. K. Chexal  
R. Duffey  
J. Horowitz**

**Generic Safety Analysis Program  
Safety Control and Testing Program  
Nuclear Power Division**

**Electric Power Research Institute  
3412 Hillview Avenue  
Palo Alto, California 94304**

## ORDERING INFORMATION

Requests for copies of this report should be directed to Research Reports Center (RRC), Box 50490, Palo Alto, CA 94303, (415) 965-4081. There is no charge for reports requested by EPRI member utilities and affiliates, U.S. utility associations, U.S. government agencies (federal, state, and local), media, and foreign organizations with which EPRI has an information exchange agreement. On request, RRC will send a catalog of EPRI reports.

Copyright © 1985 Electric Power Research Institute, Inc. All rights reserved.

## NOTICE

This report was prepared by the Electric Power Research Institute, Inc. (EPRI). Neither EPRI, members of EPRI, nor any person acting on their behalf: (a) makes any warranty, express or implied, with respect to the use of any information, apparatus, method, or process disclosed in this report or that such use may not infringe privately owned rights; or (b) assumes any liabilities with respect to the use of, or for damages resulting from the use of, any information, apparatus, method, or process disclosed in this report.

APPENDIX B

EPRI R&D Contributions to the Technical  
Basis for Revision of ECCS Rule

EPRI NP-4146-SR





Electric Power  
Research Institute

September 19, 1986

William Beckner  
Reactor System Branch  
Division of Reactor Safety Research  
U.S. Nuclear Regulatory Commission  
Washington, DV 20555

Dear Mr. Beckner:

EPRI is pleased to grant the NRC permission to reprint the following EPRI report as an appendix to "Compendium of ECCS Research for Realistic LOCA Analysis," NUREG-1230:

EPRI NP-4146-SR, "EPRI R&D Contributions to the Technical Basis for Revisions of ECCS Rules," July 1985.

Please acknowledge EPRI as the source in the following manner:

Copyright © 1985, Electric Power Research Institute, NP-4146-SR, "EPRI R&D Contributions to the Technical Basis for Revisions of ECCS Rules." Reprinted with permission.

If you have any further questions, please contact me at (415) 855-7956.

Most sincerely,

Gina Wickwar  
Technical Publications

cc: Bindi Chexal

/gw



## EPRI FOREWORD

Emergency core cooling systems (ECCSs) of nuclear reactors are designed to mitigate the consequences of large-break and small-break loss-of-coolant accidents (LOCAs). Currently two very different approaches are available to evaluate the performance of ECCS for a design basis LOCA. In the first approach, guidelines established by the NRC and stated in Appendix K of 10CFR50 are followed. These guidelines are based on the understanding of fuel behavior and two-phase thermal hydraulics of the early seventies. The guidelines have built-in conservatisms, such as higher decay power and subtraction of all the injected coolant during the blowdown phase from the primary system inventory, permitting the return to nucleate boiling only in the reflood phase, etc. These guidelines are primarily used for licensing purposes. Various studies during the last 12 years have shown that this approach is very conservative, and many guidelines are nonphysical. In the second approach, the latest technology of fuel behavior and two-phase flow is used as the basis for evaluating ECCS performance. Best-estimate codes, such as TRAC-PWR, TRAC-BWR, and RELAP5, are used to predict most probable plant conditions during the simulation of the transient. This provides a sound technical basis for an improved ECCS methodology.

There is a consensus in the nuclear industry, as well as recognition within the NRC staff, that the LOCA model requirements have many conservative provisions that could be made more realistic, while still retaining adequate conservatism. Applying a realistic ECCS methodology in the design of a future nuclear power plant could reduce plant complexity, capital cost, and operating cost.

This report summarizes all the EPRI research (more than \$50 million) that has helped show that Appendix K is conservative and that allows quantification of that conservatism. Research experiments, computer code development, and code assessment efforts funded by EPRI are documented. This work also serves as part of the EPRI

program on ECCS methodology to develop an appropriate set of analysis requirements to be used for future plants. The other activities under way in this program are to

- Review currently available best-estimate models and correlations to model phenomena that govern the course of large-break and small-break LOCA and to recommend appropriate correlations
- Assess the sensitivity of peak-fuel-clad temperature to delays in starting diesel generators using best-estimate as well as realistic evaluation models
- Determine the differences in the hardware requirements associated with ECCS equipment if the equipment were designed using realistic methods instead of the current conservative methods

It is estimated that using a realistic ECCS methodology can save \$50 to \$100 million per plant for advanced LWRs. However, this methodology can also be used by existing plant owners for significant operational flexibility. It would allow better fuel-cycle planning and leave more margin for loadings that minimize neutron flux at the reactor vessel wall. (This could be very important for plant life extension.) For these reasons, the ECCS methodology topic is considered to be a significant plant improvement topic.

V. K. Chexal, Project Manager  
Nuclear Power Division

## ABSTRACT

EPRI research efforts over the last ten years in the area of ECCS methodology are summarized. The results when added to those of the NRC and others provide a technical basis to show that the regulatory requirements in 10CFR50 Appendix K, are very conservative. In addition, these research efforts allow quantification of that conservatism. The research experiments, computer code development, and code assessment efforts funded by EPRI or cofunded with others are described.



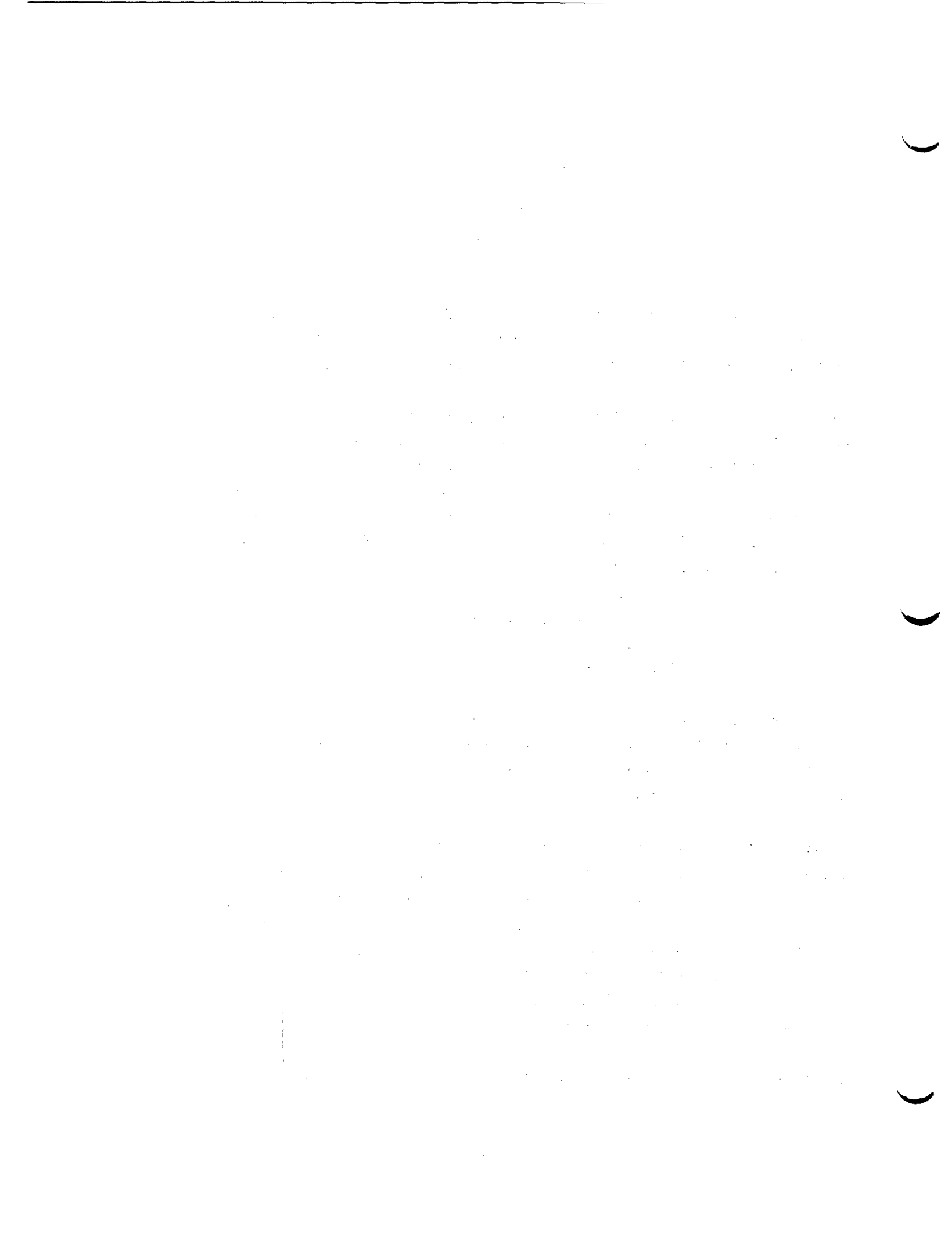
## ACKNOWLEDGMENTS

The authors wish to note the contributions of L. Agee, J. Chao, D. Franklin, P. Kalra, J. Kim, J. Lang, G. Lellouche, M. Merilo, H. Ocken, F. Rahn, J. Santucci, A. Singh, B. Sun and J. Sursock.



## CONTENTS

<u>Section</u>	<u>Page</u>
1 TWO PHASE CRITICAL FLOW	1-1
2 BLOWDOWN HEAT TRANSFER	2-1
3. REFLOOD HEAT TRANSFER	3-1
3.1 Single Tube Reflood Heat Transfer	3-1
3.2 Small Bundle Reflood Heat Transfer	3-2
3.3 Large Bundle Reflood Heat Transfer	3-4
3.4 Combined Bottom and Top Reflooding	3-5
4 ECC FLOW DISTRIBUTION	4-1
5 REACTOR COOLANT PUMPS	5-1
6 CORE UNCOVERING	6-1
7 STEAM GENERATORS	7-1
7.1 Steam Generator Modeling	7-1
7.2 Natural Circulation System Tests	7-3
7.3 Single Tube Studies	7-4
8 DECAY HEAT	8-1
9 METAL WATER REACTION AND FUEL ROD PERFORMANCE	9-1
10 FUNDAMENTAL STUDIES	10-1
10.1 Heat Transfer	10-1
10.2 Critical Heat Flux	10-2
10.3 Counter Current Flow Limit	10-4
10.4 Two-Phase Flow	10-5
10.5 Mixing	10-6
11 COMPUTER CODE DEVELOPMENT	11-1
11.1 EPRI Support of NRC Code Development	11-1
11.2 RETRAN	11-2



## Section 1

### TWO PHASE CRITICAL FLOW

An important aspect of LWR safety analysis is the capability to predict the maximum (or critical) mass flow rate from a break or leak in the primary system. EPRI has funded both experimental and analytical studies in this area.

In the experimental area a series of tests were conducted in the Marviken Full Scale facility. These tests were conducted between mid-1977 and December 1979 as a multinational project at the Marviken Power Station in Sweden. A total of 27 tests were conducted by discharging water and steam mixtures from a full-sized reactor vessel through a large-diameter discharge pipe that supplied the flow to the test nozzle. Nine test nozzle geometries were tested; all had rounded entrances followed by a nominal constant-diameter cross-section. All tests except one were initiated with a stagnation pressure of 750 psia and with the water initially subcooled. The 27 critical flow experiments, together with the test procedures, equipment, and evaluation techniques, are presented in a set of reports consisting of 35 volumes (1).

These tests provided the data necessary to enhance the current understanding and predictive capabilities of critical flow models used in reactor safety analyses and thereby to predict more accurately the margin of safety. During the early stages of a blowdown, the water is saturated or slightly subcooled, and during depressurization it may become saturated. Parametric trends observed in the Marviken data can be categorized basically under two different conditions-- subcooled and saturated stagnation conditions. Under subcooled conditions, the critical mass flux increases with decreasing test section length for length-to-diameter ratios less than 1.5 and is relatively insensitive to length for length-to-diameter ratios greater than 1.5. Comparison of the Marviken data at equivalent subcooled stagnation conditions showed no significant effect of diameter. Under saturated conditions, there is a trend of decreasing mass flux with increasing test-section length, but the variation is small and within experimental error limits. Comparison of the data at equivalent saturated stagnation conditions showed an increase in critical mass flux with smaller

diameter nozzles. A decrease in the initial dissolved air content had no observable effect on the nozzle mass flux.

In the analytical area, several of the existing two-phase critical flow models were evaluated against the Marviken data (2, 3). The data were analyzed by determining the observed parametric effects of subcooling, nozzle diameter, and length on critical flow and comparing these trends against various two-phase critical flow models; e.g., homogeneous equilibrium model (HEM), Moody, Henry-Fauske, Burnell, Ardon, and Richter models.

Comparison against the Marviken data shows that the currently applied models--the Henry-Fauske model in the subcooled flow regime and the Moody slip model in the saturated regime--generally overpredict the flow data, indicating a significant flow rate margin which is important for both accident analyses and plant design. HEM can predict fairly well the Marviken critical flow data for subcooled stagnation conditions and length-to-diameter ratios greater than 1.5. The Henry-Fauske model is also able to predict much of the data if the nonequilibrium parameter is varied according to the stagnation pressure and nozzle geometry. Critical flow predictions by the two-fluid models in general and Richter's model in particular were the most successful in predicting the entire range of Marviken data. Recommendations are made to improve the predictive capabilities of the two-fluid critical flow models that are similar in formulation to those studied in this project.

Parametric trends from the Marviken data show that under subcooled conditions, critical mass flux increases with decreasing test-section length for length-to-diameter ratios of less than 1.5. Under equivalent subcooled stagnation conditions, diameter does not seem to have any significant effect on critical flow. Under saturated stagnation conditions, there is a trend of decreasing mass flux with increasing test-section length.

At one time there was not a single adequate model for critical flow that considered subcooled upstream conditions or thermal nonequilibrium and that was valid for a variety of geometric configurations. An improved critical flow model was developed specifically focused on the subcooled behavior that is especially important for operational transients and small breaks (4). The model was designed to be developed in a form that could be utilized by a large-system analysis code like RETRAN.

A simplified nonequilibrium flashing model was developed. The model, which is applicable especially to rapidly decreasing pressures along the flow path, assumes that water has to be superheated (or decompressed) a prescribed amount before it starts to flash into steam and that, at a given local pressure below the decompression pressure, enough steam will be formed to bring the water superheat down to the decompression amount. In addition, the flow is assumed to be homogeneous; i.e., the steam and liquid velocities are equal. Finally, an isentropic process is employed to calculate the nonequilibrium steam quality and the critical flow rate.

A key element of the model is the liquid-decompression pressure drop or superheat employed in the model. It is shown to be similar to the semiempirical correlation of Alamgir and Lienhard, and a slight modification to their expression is developed. Overall good agreement is obtained with the large-scale Marviken tests and most small-scale experiments.

#### REFERENCES

1. Electric Power Research Institute. The Marviken Full Scale Critical Flow Tests Volume 1: Summary Report, NP-2370, May 1982.
2. Abdollahian, D., et al. Critical Flow Data Review and Analysis, NP-2192, Electric Power Research Institute, January 1982.
3. Abdollahian, D., et al. Comparison of Selected Two-Phase Critical Flow Models with Data from the Marviken Critical Flow Tests, presented at the 7th International Heat Transfer Conference, Munchen, Federal Republic of Germany, September 1982.
4. Levy, S. and Abdollahian, D. Homogeneous Nonequilibrium Critical Flow Model, NP-2503, Electric Power Research Institute, July 1982.



11

## Section 2

### BLOWDOWN HEAT TRANSFER

The early thermal-hydraulic behavior of the coolant in the reactor core has a very strong influence on the peak clad temperature reached during a large-break loss-of-coolant accident. EPRI has sponsored a program of experimental and analytical efforts to investigate blowdown heat transfer and CHF for both PWRs and BWRs.

Transient critical heat flux (CHF) behavior has been studied under conditions typical of those in the first few seconds following a postulated large-break LOCA in a PWR (1, 2). A total of 25 tests were run in a 5 x 5 square rod array with a heated length of 12 feet. The rod design was typical of 15 x 15 type PWR.

The primary focus of the testing was to obtain a data base, for transient CHF in a rod bundle cooled by water, that was amenable to model development efforts. A single controlled parameter variation approach was utilized for 21 of the 25 tests. The parameters varied included pressure, pressure decay rate, flow, flow decay rate, flow direction, power, inlet temperature, and initial system pressure. These parameters were selected to bound the values calculated to occur during a large-break PWR LOCA.

Three tests were performed to evaluate specific CHF theories based on simple voiding and spontaneous nucleation. One natural blowdown system effects test was run to obtain data to verify any correlations developed from the single-parameter effects tests. These test data have been reduced to provide local fluid conditions inside the test bundle on both a bundle average (MAYU 4) and a subchannel (COBRA IV) basis. Calculations of the times to critical heat flux were made using the reduced data and compared to the measured CHF times. As a result of these comparisons, it appears that the currently available transient CHF correlations tend to overpredict the extent of CHF within the test section.

A qualitative review of the CHF predictions by the bundle average and subchannel methods indicates that the extent of CHF was better predicted by the subchannel methodology. However, the overall accuracy of the initial time to CHF predictions

was similar for both methods. A comparison of the fluid conditions at initial CHF shows that the bundle average analysis generally calculates higher enthalpy and lower mass velocity than the subchannel analysis.

In order to obtain blowdown heat transfer data for BWRs, an experimental program was conducted (3). This program, jointly funded by the NRC, EPRI and GE, was carried out in a scaled test apparatus to study the system performance and thermal response characteristics of BWRs under the postulated loss-of-coolant accident (LOCA) conditions.

Effects of various configuration changes (from BWR/4 to BWR/6 simulations) on the system performance were investigated. The test results show that the system depressurization during the blowdown phase is insensitive to the bundle lattice (8x8 versus 7x7) and bundle power, but strongly affected by the break size. The elevations of the jet pump suction and exit are shown to have an affect on the system performance particularly during and after the lower plenum flashing. The bundle heatup is found to be dependent on the bundle power as expected. The peak cladding temperatures observed in the 8x8 bundle were substantially lower than in the case of the 7x7 bundle.

The system performance and key event during the LOCA transient were identified. The code predictions show (1) faster depressurization after 20 seconds, (2) lower cladding temperature for the first 30 seconds, and (3) higher mass accumulation in the lower plenum and guide tube bypass region. The data comparison indicates the limitations of the phenomenological models used in the transient calculations such as counter current flooding limit, rewet-in-the bundle, etc.

The test data are used to provide a basis not only for evaluating the BDHT phenomena but also for the future blowdown/emergency core cooling system interaction experiments. In addition, these test results are utilized to evaluate the predictions performed with the analytical codes. Further studies on specific phenomenologically based models are recommended. The improved phenomenological understanding can be utilized to develop more accurate and realistic predictions of the system thermal-hydraulic blowdown response and bundle heat transfer performance.

Further BWR tests were conducted to obtain a physical understanding of the system thermal hydraulic and bundle heat transfer responses during a LOCA simulation, and to provide a data base for evaluating the models and assumptions used in BWR

analyses (4). To meet these objectives, 14 tests were conducted under this test phase: 11 tests simulated a large break LOCA; two tests simulated a small break LOCA; and one test series simulated low-flow, core uncover heat transfer (5, 6). The significant findings from the large break test series are:

1. Counter-current flow limitation conditions of the inlet delay bundle uncover during the early period of the LOCA transient and therefore allow dissipation of most of the bundle-stored heat.
2. Steam condensation at the top of the bundle due to subcooled ECC injection results in CCFL breakdown, causing an early inventory drainage through the core and therefore enhancing the core-cooling process.
3. The bundle power variation effects on the system response are not significant.
4. The ECC injection is very effective in mitigating the thermal transients by keeping peak cladding temperature much lower than the conservation estimates.

The data are useful for assessing best-estimate codes for BWR systems.

#### REFERENCES

1. McIntyre, B. A., and Volpenhein, E. C. Full-Scale Controlled Transient Heat Transfer Tests Data Analysis Report, NP-2547, Electric Power Research Institute, August 1982.
2. McIntyre, B. A., and Merilo, M. "Controlled Transient CHF Tests in a 5X5 Rod Bundle Under Loss-Of-Coolant Accident Conditions," Heat Transfer 1982, Proceedings of the Seventh International Heat Transfer Conference, Munich, Federal Republic of Germany, edited by U. Grigul, E. Hahne, K. Stephan and J. Straub, 1982.
3. Hwang, W. S., et al. BWR 64-Rod Bundle Blowdown Heat Transfer, NP-1720, Electric Power Research Institute, February 1981.
4. Lee, L. S., Sozzi, G. L., and Allison, S. A. BWR Large-Break Simulation Tests, Volumes 1-2, NUREG/CR-2229, GEAP-24962-1, NP-1783, U.S. Nuclear Regulatory Commission, General Electric Company, and Electric Power Research Institute, 1982.
5. S. P. Kalra, Editor. BWR Transient Response, NP-2224-SR, Electric Power Research Institute, January 1982.
6. Hwang, W. S., Alamgir, M., and Sutherland, W. A. BWR Full Integral Simulation Test: Phase 1 Results, NUREG/CR-3711, GEAP-30496, NP-3602, U.S. Nuclear Regulatory Commission, General Electric Company, and Electric Power Research Institute.



### Section 3

#### REFLOOD HEAT TRANSFER

Reflood heat transfer is one of the important emergency core cooling mechanisms for light water reactors during the design basis loss-of-coolant accident (LOCA). Extensive large-scale experiments have been conducted worldwide in recent years to investigate the heat transfer effectiveness during simulated LOCA reflood conditions. Simultaneously, extensive analytical and experimental investigations have been made to enhance the fundamental understanding of the thermal-hydraulic phenomena occurring during the reflooding process.

The EPRI sponsored work (completed or in progress) in this area can be listed under four categories: single tube tests, small scale bundle tests, full scale bundle tests, and combined injection tests.

#### 3.1 SINGLE TUBE REFLOOD HEAT TRANSFER

An experimental program (1, 2) was undertaken to provide physical insight into the transient phenomena that govern the reflooding progress. The objective was to determine accurately quench front propagation, heat transfer coefficients, and characteristics of the effluent as a function of pressure and several other important variables.

An electrically heated 12-foot vertical tube simulating a single-core flow channel was employed with wall temperatures and injection rates chosen to bound the possible core reflood conditions. Experiments were conducted under system pressures of 1, 2, and 3 atmospheres simulated conditions expected in a large-break loss-of-coolant accident.

These experiments show that reflooding of a hot tube is accelerated by increasing the system pressure. The magnitude of the change depends on the inlet feed velocity and the initial tube wall temperature and is most noticeable for low velocities and high wall temperatures. The effect of pressure on collapsed liquid levels is smaller, suggesting that the accelerated quenching may be due to a greater amount of precursory cooling by two-phase flow. The results compare

favorably to those of other experiments on the reflooding of single tubes and bundles.

After the single tube data were obtained, an analytical program (3) was undertaken to develop models/correlations to predict the thermal-hydraulic performance under reflooding conditions of a single tube.

A mechanistic, best-estimate, "local-conditions" model of a fuel rod and its associated flow channel undergoing bottom reflooding was developed and a computer code written. The code can also be used to predict reflooding of internally cooled tubular test sections. The initial state of the rod or tube wall, the system pressure, and the variations in time of the reflooding rate, of the inlet coolant temperature, and of the power generation are inputs to the code. The local flow conditions are first determined all along the channel, and then heat transfer is calculated according to these local conditions.

Prediction of a limited number of single tube experimental reflooding runs by the code showed very good agreement with measured wall temperature histories at a number of axial locations. Additional model verification is obtained by comparing predicted and measured quench front propagation. Good agreement was typical of the comparisons made. Finally, the liquid and total carry-over rates out of the test section were well predicted, confirming the validity of the hydrodynamic models used in the code.

### 3.2 SMALL BUNDLE REFLOOD HEAT TRANSFER

An experimental effort was undertaken (4) to investigate the quenching and heat transfer behavior of Zircaloy cladding. This was necessary because in a number of instances reflooding heat transfer data and correlations were derived from experiments using steel-clad bundles. However, the thermal properties of steel are significantly different from Zircaloy cladding, and this particularly manifests itself in the quenching behavior. Since the position of the quench front is a reference point for the development of the post-dryout and film boiling heat transfer, it is important to estimate correctly its velocity and position. The thermal stresses on quenching are also important for estimating fuel rod integrity. These experiments show that Zircaloy cladding quenches faster than stainless steel cladding (up to twice as fast in a Zircaloy-clad bundle and 1.3 times as fast in a mixed bundle containing both steel- and Zircaloy-clad rods). This translates to an increase of up to 20% in core reflood rate for postulated accident conditions.

More recent work (5) has been performed in order to investigate:

- high-temperature (1000°C) quenching behavior of Zircaloy, including bundle failure modes, and the
- effect of clad deformation on the cooling of bundles.

The major objective was the development of correlations for the local quenching speed, the wall temperature or quenching, and the vapor-blanketed surface heat removal. The influence of the local flow variables was also determined in order to translate the results for reactor use.

A 4-rod Zircaloy bundle was tested. Both an undeformed as well as a deformed bundle were quenched. The experiments and subsequent data analysis show that:

1. Correlations used to predict the local quenching rate accurately predict the data.
2. Enhancements occur in heat transfer downstream of blockages which offset the loss of cooling due to flow diversion around the blockages.
3. The failure modes of a successively heated and quenched bundle are shown to be from cracking due to oxidation embrittlement.

These data were used in model development for analyzing blockage effects in large PWR cores during core recovery or reflooding in both small- and large-break transients which deplete the reactor inventory.

Additionally, an analytical investigation (6) was undertaken to investigate the interaction between reactor coolant heat transfer and cladding swelling in LWR LOCA analysis. This study was intended as an effort to gain understanding about physically realistic phenomena that occur under hypothesized LOCA conditions. Current licensing and realistic LOCA analysis methodologies do not account for these interactive effects.

COBRA is a computer code capable of calculating the rod temperatures and thermal-hydraulic conditions of the coolant in the reactor core. It was modified (6) by adding a gap conductance model, an axial gas flow model, and a cladding deformation model (based on the DILATE code). The axial gas flow model was checked against experimental data. The methodology was assessed against the German experiment that provided the most demanding test of the coupled fuel behavior and thermal-hydraulic aspects of the developed methodology. A

sensitivity study was conducted to perform parametric calculations for a typical U.S. design fuel rod.

The results of this study showed that in increased coolant flow delays cladding swelling and shifts the location of swelling in the direction of coolant flow. The difference between the reactor coolant pressure and the local fuel rod internal gas pressure acts as the driving force that causes swelling. A gap between the fuel and cladding of 25  $\mu\text{m}$  was calculated to produce an axial pressure gradient in the fuel rod. This implies that the local swelling driving force, as currently calculated, is overestimated and is probably conservative, that is, the amount of flow blockage affecting core coolability will tend to be overestimated. Since this study was done with a single rod, the potentially important effect of adjacent rods on the thermal-hydraulic and fuel behavior response was not evaluated. However, the single rod analysis demonstrated the temperature sensitivity of the Zircaloy swelling process and the effect of reactor coolant heat transfer on deformation.

### 3.3 LARGE BUNDLE REFLOOD HEAT TRANSFER

EPRI, NRC, and Westinghouse have cosponsored the FLECHT SEASET (Full-Length Emergency Core Cooling Heat Transfer--Separate-Effects And System-Effects Tests) program. It is a multi-facility five-year test and analysis program. The overall objective of this program was to provide experimental heat transfer and two-phase flow data in simulated PWR geometries for postulated conditions of reflooding, core boiloff, and natural circulation. The test parameters covered a spectrum of conditions that encompass both the best-estimate and current licensing calculations. The test bundle simulated a full-length portion of PWR cores with fuel rod geometry typified by a Westinghouse 17 x 17 assembly design.

The program consisted of two major subprograms, each with experimentation and analysis efforts: (1) the flow blockage subprogram to address safety and licensing requirements for steam cooling and the flow blockage effects and (2) the system effects subprogram to examine system and bundle reflood response for a postulated LOCA. Both subprograms had the flexibility to address small-break core uncover and natural circulation phenomena. The FLECHT SEASET Program has been conducted in several phases as described.

In the first test series (7) data on an unblocked 21 rod bundle was obtained. The tests consisted of forced and gravity reflood experiments and steam cooling tests, using electrical heater rods to simulate current nuclear fuel arrays of PWR. Data

obtained include rod clad temperatures, turnaround and quench times, heat transfer coefficients, inlet flooding rates, overall mass balance, differential pressures and calculated void fractions in the test section, thimble wall and steam temperatures, and exhaust steam and liquid carryover rates.

The next series, (8) tests were performed on a 21 rod blocked bundle. Six different bundles were tested. Steam cooling and hydraulic characteristics tests were conducted. These tests were utilized to determine effects of various flow blockage configurations (shapes and distributions) on reflooding behavior, to aid in development/assessment of computational models in predicting reflooding behavior of blocked bundles, and to screen flow blockage configurations for the 163-rod flow blockage bundle tests.

After the completion of these small bundle tests, large bundle tests were performed on unblocked and blocked bundles.

The unblocked tests on a 161-rod bundle (9) added considerable data and information about reflood thermal hydraulics. A new heat transfer correlation was been developed and shown to predict the FLECHT SEASET data as well as the older FLECHT data. A method was developed to calculate steam quality just above the quench front. Improved models for estimating effluence rate and preliminary exploration of the transition zone above the quench front were discussed. Droplet size and velocity data deduced from high-speed movies taken during the tests have led to better understanding of these parameters. A model has been proposed to predict the onset of droplet entrainment, and an analytical expression to predict critical void fraction developed.

The 163-rod blocked bundle tests (10) produced extensive thermal and hydraulic data from both forced and gravity reflood tests. The data, which covered a wide range of thermal and hydraulic conditions, provided a basis for assessing the flow-blockage models developed from 21-rod bundle test data (8). Peak rod temperatures in the downstream of the blocked islands were lower than the corresponding rod temperatures in a 161-rod unblocked bundle for all conditions tested (9), confirming the enhancement of heat transfer due to blockages.

#### 3.4 COMBINED BOTTOM AND TOP REFLOODING

In addition to the PWR reflooding heat transfer work already described, EPRI performed an experimental study of combined reflooding (11). System performance and thermohydraulic response to simultaneous bottom and top water injection were

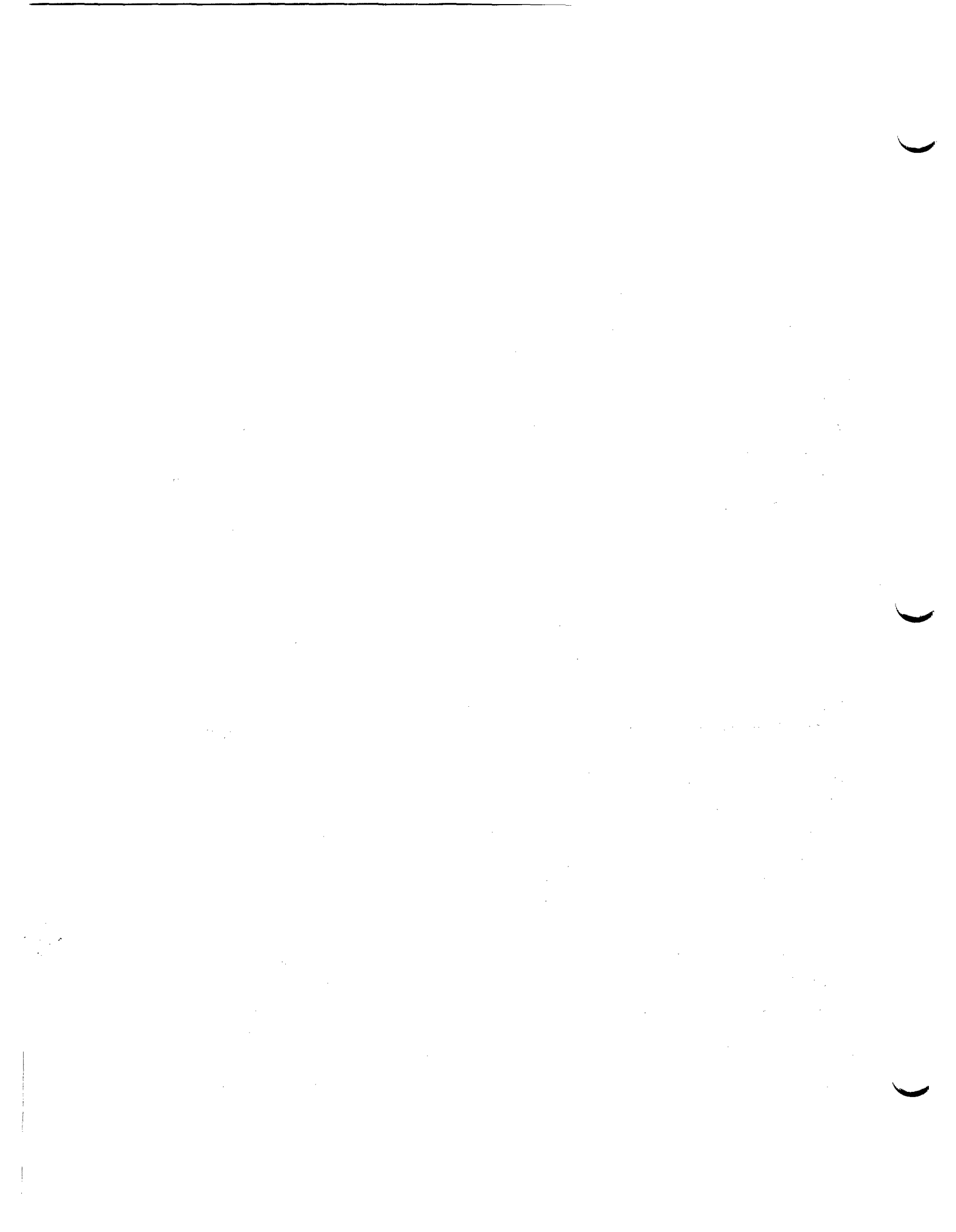
investigated in a 3x3 rod bundle reflood test facility. An extensive series of tests, encompassing both simple bottom and combined injection reflooding, were carried out. A number of phenomena governing the thermodynamic coupling between the bottom reflood updraft and the top deluge were identified. Counter current flow limiting phenomena hindered the penetration of water from inventory in the upper plenum into the bundle section. Condensation phenomena in the upper plenum and in the venting pipework characterized the thermohydraulic response of the bundle to simultaneous bottom and top water injection.

Two stages were clearly identified during the reflooding transient with combined injection: (1) pressure-controlled stage followed by a (2) condensation controlled stage. Furthermore, an inverted density profile characterized the void distribution in the upper plenum during the condensation controlled stage. The experimental results were found to be in good agreement with the theoretical analysis which used the homogeneous two phase flow model to correlate the vent line pressure drop to reflooding performance. In addition, the effect of upper tie-plate open flow area on reflooding phenomena and air-water flooding experiments for the upper tie plate region were also carried out.

#### REFERENCES

1. Seban, R., et al. UC-B Reflood Program: Experimental Data Report, NP-743, Electric Power Research Institute, April 1978.
2. Seban, R. A. Reflooding of a Vertical Tube at 1, 2, and 3 Atmospheres, NP-3191, Electric Power Research Institute, July 1983.
3. Arrieta, L., and Yadigaroglu, G. Analytical Model for Bottom Reflooding Heat Transfer in Light Water Reactors (The UCFLOOD Code), NP-756, Electric Power Research Institute, August 1978.
4. Dhir, V. K., and Catton, I. Reflood Experiments with a 4-Rod Bundle, NP-1277, Electric Power Research Institute, December 1979.
5. Drucker, M., and Dhir, V. K. Effects of High Temperature and Flow Blockage on the Reflood Behavior of a 4-Rod Bundle, NP-2122, Electric Power Research Institute, November 1981.
6. Rowe, D. S. An Investigation of Interaction Between Heat Transfer and Cladding Swelling in Light Water Reactor LOCA Analysis, NP-1210, Electric Power Research Institute, November 1979.
7. Loftus, M. J., et al. PWR FLECHT SEASET Unblocked Bundle, Forced and Gravity Reflood Test Data Report, Volume 1, EPRI NP-1459, FLECHT SEASET Program Report No. 7, NUREG/CR-1532, WCAP-9699, 1981.

8. Loftus, M. J., et al. PWR FLECHT SEASET 21-Rod Bundle Flow Blockage Task Data and Analysis Report, Volume 1, EPRI NP-2014, FLECHT SEASET Program Report No. 11, NUREG/CR-2444, WCAP-9992, 1982.
9. Lee, N., et al. PWR FLECHT SEASET Unblocked Bundle, Forced and Gravity Reflood Task Data Evaluation and Analysis Report, EPRI NP-2013, FLECHT SEASET Program Report No. 10, NUREG/CR-2256, WCAP-9891.
10. Loftus, M. S. et al. PWR FLECHT SEASET: 163 Rod Bundle Flow-Blockage Task Data Report, NP-3268s, Electric Power Research Institute, June 15, 1984.
11. Chon, W. Y., et al. Effects of Upper Plenum Steam Condensation Phenomena on Heat Transfer in a Rod Bundle, NP-1332, Electric Power Research Institute, February 1980.
12. Dhiv, V. K., Duffey, R. B., and Catton, I., Quenching on a Zircaloy Rod Bundle, Journal of Heat Transfer, Vol. 103, No. 2, May 1981.
13. Singh, et al. The Effect of Thermal Diffusion and Gap Conductance on Quench Velocity During Bottom Reflooding of Rod Bundles, to be presented at the 3rd International Conference on Reactor Thermal Hydraulics, Newport, Rhode Island, October 15-18, 1985.
14. Rust et al. Effects of Fuel Rod Simulator Geometry on Reflood Behavior Following a Loss of Coolant Accident, to be presented at the National Heat Transfer Conference, Denver, Colorado, 1985.



Section 4  
ECC FLOW DISTRIBUTION

EPRI has sponsored a large program to obtain test data and to develop thermal/hydraulic models which will represent the steam/water interactions expected in a PWR cold leg during a postulated LOCA (1). This program is comprised of two major test series: 1/14-scale tests and 1/3-scale tests. The 1/14-scale series covered thermal/hydraulic conditions typical of blowdown, reflood with accumulator injection water flows, and reflood with safety-pump injection water flows. The 1/3-scale tests covered the range of parameters addressed in the 1/14-scale tests, except blow down, and the test parameter range was expanded to include post-reflood conditions. The primary information desired from the reflood tests was the pressure drop which occurred across the steam/water mixing zone, whereas for the post-reflood tests the primary interest was in the degree of mixing which occurred in the simulated cold leg.

The 1/3-scale tests, as well as the 1/14-scale tests, were intended to be conducted as steady-state separate-effects tests. Initially in the 1/14-scale program, pressure and flow oscillations made it difficult to decouple the test section from the rest of the facility. This decoupling was ultimately accomplished in the 1/14-scale tests by installing large test-section inlet and outlet surge tanks and by using a high-head injection-water pump. These features provided steady, small but controllable steam driving forces in spite of oscillations in the test section. These features also provided steady fluid conditions at the flow-measuring points. The same procedure was followed for the 1/3-scale tests except that the isolation of the test section from the steam supply was not as good as in the 1/14-scale tests.

The 1/3-scale steam/water mixing results confirm the 1/14-scale data as well as other steam/water mixing tests, indicating that complete plugging of the cold leg piping does not occur with the accumulator injection operation during reflood. Complete condensation of the cold leg steam flow occurs at accumulator injection flow rates which result in an effective vent path for the cold leg steam flow. It is also observed that as the injection angle is decreased from 90 to 45°, the

measured pressure drop in the mixing zone becomes increasingly negative due to the jet pump action of the injected water. This effect was also observed in the 1/14-scale and other tests. When sufficient water was available to condense all the reflow steam and fill the cold leg pipe, an oscillating flow regime was established in the cold leg. The 1/3-scale oscillations were similar to the 1/14-scale oscillations except that their frequency was approximately a factor of two lower than the 1/14-scale test frequencies.

Several comparisons are made between the 1/14-scale and 1/3-scale data to determine if any scale effects are evident. These comparisons are complicated by the fact that the flow boundary conditions were somewhat different for the two tests series. Considering the testing differences, when all the 1/14- and 1/3-scale data are compared for accumulator injection velocities, the 1/3-scale data show more scatter from the one-dimensional steady flow momentum model than do the 1/14-scale data. A significant effort was made to examine these differences by conducting several repeat tests. It is observed that the data are repeatable but that apparently the resulting measured pressure drop is dependent on how one reaches the final conditions for a measurement, i.e. two seemingly identical initial fluid conditions can give different pressure drop readings. However, for model comparison purposes, if a larger uncertainty band is used to represent all the data, it will encompass differences observed between the 1/3- and 1/14-scale data. In the 1/14-scale report, an upper bound limit of 0.5 psia was used as an addition to the one-dimensional momentum model prediction to represent all the 1/14-scale data. If all the data now on hand are considered, an upper bound limit of +1.0 psia defines a range that covers 78 percent of the 1/3-scale data.

The injection of air into the accumulator injection water is examined to see its effect on the measured test section pressure drop. Air injection was not an explicit test parameter but rather it was investigated as an on-off effect. Taken as a whole, the injection of air does not change the average difference between the predicted one-dimensional momentum model and the measured pressure drop data. The average differences between the data and one-dimensional momentum model are nearly the same whether air is injected or not.

As was seen in the 1/14-scale tests, the safety-pumped injection flow rates in the 1/3-scale tests result in a two-phase effluent leaving the test section. The test section effluent is steady, not exhibiting the low frequency pulsations characteristic of the accumulator injection flows. The slip flow pressure drop prediction for the 1/14-scale flow was modified to account for the quality effect on the slip

ratio. Incorporation of this into the one-dimensional slip flow pressure drop prediction correlates both the 1/3-scale and 1/14-scale injection flow data, again indicating no significant scale effect. From this absence of significant scale effect, it is concluded that this slip flow model approach does predict the average cold leg pressure drop for the safety-pump injection velocity range.

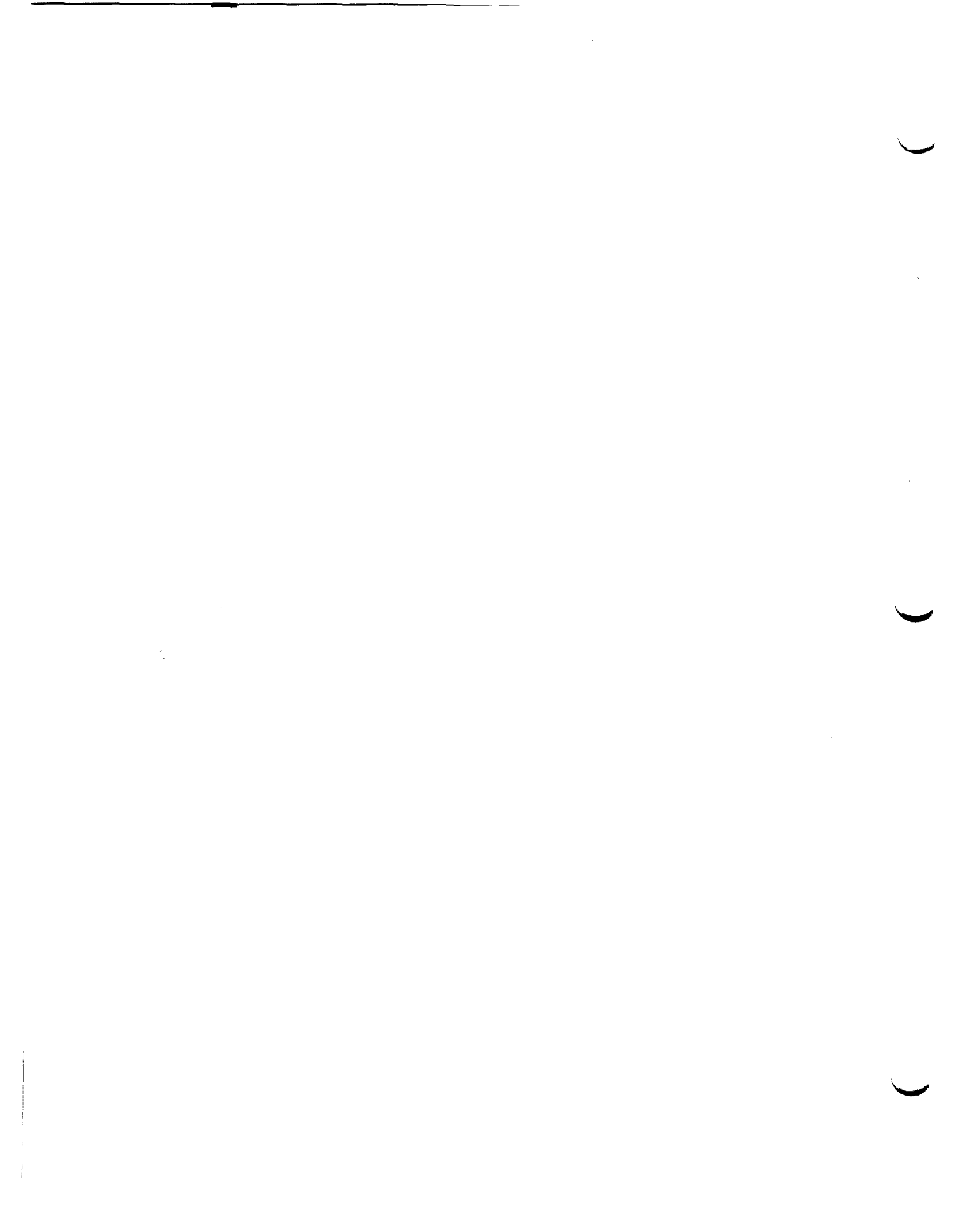
The post-reflood data indicate that mixing occurred very rapidly and, with few exceptions, the steam and water reached thermodynamic equilibrium with 6 to 8 diameters downstream of the injection point. All tests show that thermodynamic equilibrium was reached at 10 diameters downstream of the injection zone. The flow regime inferred from the temperature data appears to be stratified for the 1/3-scale post-reflood cases.

In summary, the 1/3- and 1/14-scale steam/water mixing reports provide data, a calculational model, and discussion of the phenomena observed in the steam/water mixing process. The calculational model presented predicts the time-averaged measured pressure drop across the mixing zone for both accumulator and pumped injection rates for both sets of data.

EPRI also sponsored a small scale test designed to provide flow visualization of potential annulus-flow instability mechanisms that may arise in future scale model tests. A preliminary examination of available data was the initial step followed by scoping tests to evaluate the possibility of periodic slug delivery to the lower plenum; slug delivery was present under certain conditions. A transparent model was then constructed to aid in the observation of such instability mechanisms; however, major distortions were necessary to study counter-current flow behavior as a separate effect. The experimental observations of the flow behavior are described for the two loop model.

#### REFERENCES

1. Lilly, G. P. and Hochreiter, L. E. Mixing of Emergency Core Cooling Water With Steam: 1/3-Scale Test and Summary, EPRI 294-2, Electric Power Research Institute, June 1975.
2. Rothe, P. H., et al. A Preliminary Study of Annulus ECC Flow Oscillations, NP-0839, Electric Power Research Institute, August 1978.



## Section 5

### REACTOR COOLANT PUMPS

Analyses of a postulated LOCA include predicted core flow and broken loop pump overspeed, both of which are dependent on the performance characteristics of the reactor-coolant pumps. The pump in the broken leg pipe directly affects the rate of system depressurization by retarding blowdown flow, and the remaining pumps affect the flow rates and distribution throughout the system. Pump analytical models generally in use for LOCA calculations employ homologous flow relationships to derive head and torque behavior in the two phase flow regimes, and an empirical head degradation factor based on limited experimental information is commonly used.

The EPRI Pump Two-Phase Performance Program was performed to improve and advance LWR safety technology. The overall objectives of this pump program were to:

- Obtain and evaluate steady-state and transient single- and two-phase data
- Develop analytical model(s) based on empirical steady-state data
- Obtain sufficient data on pump characteristics under two-phase transient blowdown conditions to aid evaluation of pump overspeed and flywheel integrity
- Improve understanding of phenomenological pump two-phase behavior, scaling relationships, and media effects on pump performance.

To accomplish these objectives EPRI has performed several projects both analytical and experimental. These experiments were done on various fluids and at various scales to provide an extensive data base.

A fundamental, analytical and experimental study (1) was performed to develop a model to predict pump two-phase performance for steady-state and transient conditions, assuming that pump geometry and normal single-phase operating characteristics are known. The original objective was to develop an analytical model based mainly on first principles. However, due to the unavailability of

detailed pump performance measurements of high quality during the contract period, the analytic modeling had to become more empirical. As a further consequence, the model was not tried out on and compared with actual pump two-phase performance data.

In parallel with the above work, another small-scale study was performed (2). In this work, data were obtained on single and two-phase air/water and steam/water performance of a relatively high specific speed pump. These data are compared with those acquired from tests on the lower specific speed Semiscale pump to better understand the mechanism of performance degradation with increasing void fraction.

The study revealed that scaling down the size of the pump while maintaining the same design specific speed produces very similar performance characteristics both in single and two-phase flows. Effects due to size and operating speed were not discernible within the range of test conditions and within experimental uncertainties. System pressure appears to affect the rate of degradation as a function of void fraction.

The report includes a survey of the existing two-phase pump performance correlations. A new correlation was developed from the data produced as well as from data from other parts of the EPRI program (3, 4 described below).

A much larger scale test was performed to obtain sufficient steady-state and transient two-phase empirical data to substantiate and ultimately improve the reactor coolant pump analytical model currently used for LOCA analysis. A one-fifth scale pump, which geometrically models a reactor coolant pump, was tested in steady-state runs with single- and two-phase mixtures of water and steam over ranges of operating conditions representative of postulated loss-of-coolant accidents. Transient tests were also run to evaluate the applicability of the steady-state-based calculational models to transient conditions.

The pump data base collected in this project is considered sufficiently large and diverse to cover a significant range of pump performance of primary importance to LOCA analysis. Evaluation of the test results indicates that pump head and torque degrade significantly under two-phase flow conditions. Pump free-wheeling speed (pump motor power off) is closely coupled to the volumetric flow rate through the pump during a blowdown transient. The maximum free-wheeling speed observed was nearly twice the rated speed for a discharge break equal to the flow area of the

pump. For smaller size discharge breaks, the peak speed observed was less than twice the rated speed. With electric power to the pump drive motor on throughout the blowdown, however, the pump speed was maintained at an almost constant value.

In order to obtain further insight in the two-phase performance of large reactor pumps, air-water testing of a 1/3 scale pump was performed (4). Data from this test was analyzed, and from this data a two-phase homologous curve pump performance model was developed. This model was incorporated into a computer code, which is used to solve the evolution of system hydrodynamics and core power generation during the blowdown phase of a loss-of-coolant accident (5). Peak cladding temperature calculations were performed for several break sizes and configurations using this pump model. The results of these calculations were compared to previously calculated results obtained using the same code but one that used a pump model developed from the Semiscale data. The newly calculated peak cladding temperatures were essentially the same as those obtained previously.

Pump overspeed calculations were also performed using the air-water pump model. The use of a discharge coefficient of 0.6 resulted in a peak speed of 3007 rpm, 253% of rated speed, for an 8.55-ft<sup>2</sup> double-ended break in the pump discharge piping. This result agrees reasonably well with the overspeed calculation performed in 1973 which did not include pump head or torque degradation as a function of void fraction. Therefore, it appears that overspeed calculations are relatively unaffected by the use of the two-phase pump model. These models and their deficiencies were reviewed, various parameters that could significantly affect two-phase pump behavior were identified and discussed, and future requirements in analytical modeling of two-phase pump performance were recommended in (8).

Based on the recommendation of (8), a study was performed to develop an analytic model to predict the pump performance under two-phase flow conditions without relying primarily on empiricisms that have plagued the modeling approaches in the past (6, 7). Based on the one dimensional control volume method, an analytical method has been developed to determine the performance of pumps operating under two-phase flow conditions. The analytical method has incorporated pump geometry, void fraction, flow slippage and flow regime into the basic formula, but neglected the compressibility and condensation effects. During the course of model development, it has been found that the head degradation is mainly caused by higher acceleration on liquid phase and deceleration on gas phase than in the case of single-phase flows. The numerical results for head and torque degradations

were obtained with the model and favorably compared with the test data of air/water two-phase flow pumps of (4) (1/3 scale) and (2) (1/20 scale). Physical phenomena occurring inside the pump under two-phase flow conditions and their possible mechanisms were explained based on flow visualization tests in an air-water pump (9).

#### REFERENCES

1. Wilson, D. G., Chan, T, and Manzano-Ruiz, J. Analytical Models and Experimental Studies of Centrifugal-Pump Performance in Two-Phase Flow, NP-677, Electric Power Research Institute, May 1979.
2. Kamath, P. S., and Swift, W. L. Two-Phase Performance of Scale Models of a Primary Coolant Pump, NP-2578, Electric Power Research Institute, September 1982.
3. Kennedy, W. G., et al. Pump Two-Phase Performance Program. Volume 1: Summary and Conclusions. NP-1556, Electric Power Research Institute, September 1980.
4. Winks, R. W. One-Third Sclae Air-Water Pump Program Test Program and Pump Performance, NP-135, Electric Power Research Institute, July 1977.
5. Cudlin, J. J. 1/3 Scale Air-Water Pump Program, Analytical Pump Performance Model, NP-160, Electric Power Research Institute, October 1977.
6. Furuya, O. Development of an Analytic Model to Determine Pump Performance Under Two-Phase Flow Conditions, NP-3519, Electric Power Research Institute, May 1984.
7. Furuya, O. An Analytical Model for Prediction of Two-Phase (Noncondensable) Flow Pump Performance, Journal of Fluids Engineering, Vol. 107, No. 1, March 1985.
8. Kim, J. H. "Perspectives on Two-Phase Flow Pump Modeling for Nuclear Reactor Safety Analysis", Cavitation and Multiphase Flow Forum-1983, edited by J. W. Hoyt, ASME, June 1983.
9. Kim, J. H., Duffey, R. B., and Belloni, P. "On Centrifugal Pump Head Degradation in Two-Phase Flow", accepted for presentation at the Symposium on Design Methods for Two-Phase Flow in Turbomachinery, ASME Fluids Engineering Division Conference, Albuquerque, June 1985.

## Section 6

### CORE UNCOVERING

The safety system design and the licensing of nuclear power plants require that there be a provision for sufficient heat removal from the reactor core in the event of a loss of coolant accident or other transients. EPRI has done a considerable amount of work in this area simulating both BWR and PWR bundles.

In the BWR area, EPRI has funded projects (jointly with NRC and GE) on BWR blowdown/emergency core cooling (1, 2, 3, 4, 5, 6) and BWR refill and reflood thermal hydraulics to respond to the LOCA issue. The overall objectives of this program were (1) the BWR system behavior following small break to large break loss of coolant accident including countercurrent flooding limitations (CCFL) with or without ECCS, (2) natural circulation, (3) separate-effect tests, and (4) BWR analysis model development and qualifications.

Tests were performed on a 8 x 8 bundle typical of current BWRs. The test results show (1) the importance of CCFL at the side-entry orifice of the core inlet as it provides effective cooling in the bundle by limiting the mass inventory drainage to the lower plenum, (2) HPCS injection assist in maintaining the inventory in the bundle by reducing system pressure due to enhanced steam condensation, (3) rapid reflooding of the fuel channels by ECC systems during blowdown transients over the range of interest. Tests also demonstrate beneficial effects of multichannel interaction, which provides faster heat removal through early liquid drainage into the peripheral bundles and the bypass and hence early reflooding of the core. The BWR TRAC code has been assessed to provide a best-estimate model for BWR evaluations. A large data base has been generated for validation of BWR TRAC, so that it provides an improved method for realistically quantifying the BWR safety margins.

The primary use of these results is therefore in demonstrating the effectiveness of ECC systems and hence eliminating licensing uncertainties by providing capability for accurate BWR LOCA analysis methods and economic payoff for operating reactors.

In the PWR area, a similar program called FLECHT SEASET (Full-Length Emergency Core Cooling Heat Transfer - Separate-Effects Tests and System-Effects Tests) has been completed (7). Areas of technical concern addressed included reflooding (large-break LOCA), core uncover (small break LOCA) and natural circulation (long term cooling). The program was jointly sponsored by EPRI, NRC and Westinghouse. The test parameters covered a spectrum of conditions that encompassed both the best-estimate and current licensing calculations. The test bundle simulated a full-length portion of PWR cores with fuel rod geometry typified by a W 17 x 17 assembly design. A series of forced convection steam cooling tests at low Reynolds numbers and bundle boil-off tests were conducted.

The forced convection heat transfer data obtained in the FLECHT SEASET program permitted development of an improved heat transfer correlation for the low Reynolds number region for rod bundle geometries. The data obtained also permitted comparisons of rod bundle geometry data with conventional forced convection heat transfer correlations which have been derived from conventional pipe flow heat transfer experiments. The new correlation was found to give higher heat transfer than the conventional Dittus-Boelter correlation in the low Reynolds number region. At higher Reynolds numbers, the data begin to merge with the Dittus-Boelter correlation.

The significant data scatter shown by the results of the bundle boiloff tests prevented correlation of the heat transfer data. However, comparisons were made with the Yeh void fraction model; agreement was shown. Comparing the Reynolds and Grashof numbers with other literature indicated that the flow in the rod bundle was always in a forced convection mode even at very low Reynolds numbers, well within the laminar regime.

Tests were also run using a 336-rod bundle of typical PWR geometry to obtain data on heat transfer above the two phase mixture level under the core uncover conditions of a simulated small-break LOCA. The purpose of this work was to analyze the heat transfer data obtained above the froth level of a 336-rod bundle in core uncover tests, to compare these data with the existing correlations, and to recommend a heat transfer correlation which can be used to compute the cladding temperature of the reactor fuel rods during core uncover in a postulated loss-of-coolant accident (LOCA) under small-break conditions.

It was concluded that much of the reduced heat transfer coefficient data using the steam temperature as a sink temperature were unreliable, probably because of the

wetting of the steam probes, as indicated by the abnormal behavior of steam temperature data. For this reason, an alternative approach was adopted.

The alternative approach consists of using existing correlations to compute the temperatures of heater rods and steam, and comparing the calculated rod temperatures with data. It was found that the calculated temperature was relatively insensitive to the correlation used at large distances from the froth level. Therefore, the calculated temperature difference between the rod and the steam was used as a criterion for obtaining a best correlation and modifying the correlation.

The correlations evaluated in this program were the Dittus-Boelter correlation, the Oak Ridge National Laboratory (ORNL) correlation, the McEligot correlation, and the correlation derived from the FLECHT SEASET steam cooling tests. This comparison showed that, in general, a modified form of the FLECHT SEASET steam cooling correlation performed best in predicting rod and vapor temperature.

EPRI also sponsored a small scale program in order to obtain core uncover data (5). This was done by transiently boiling dry a 3- x 3-rod bundle. The location of the two-phase mixture level, bundle heat transfer, and liquid inventory were measured. The effects of injecting cold water at the top of the bundle were also studied.

These new tests are consistent with other data in that a steady uncover process occurs. Higher bundle powers naturally give faster boiloff rates. The effect of cold water injection into the top of the bundle increased the heat removal.

#### REFERENCES

1. Seedy, D. S., and Muralidhoran, R. BWR Low-Flow Bundle Uncovery Test and Analysis, NP-1781, NUREG/CR-2231, GEAP-24964, Electric Power Research Institute, U.S. Nuclear Regulatory Commission, and General Electric Company.
2. Sutherland, W. A., Barton, J. E., and Findlay, J. A. BWR Refill-Reflood Program Single Heated Bundle Tests, NP-2372, NUREG/CR-2001, GEAP-24936, Electric Power Research Institute, U. S. Nuclear Regulatory Commission, and General Electric Company.
3. Findlay, J. A. BWR Refill-Reflood Program CCFL-Refill System Effects Tests (30° Sector)-Evaluation of Parallel Channel Phenomena, NP-2373, NUREG/CR-2566, GEAP-22044, Electric Power Research Institute, U. S. Nuclear Regulatory Commission, and General Electric Company.

4. Schumacher, D. G., Eckert, T., Findlay, J. A. BWR Refill-Reflood Program Test Results: CCFL-Refill System-Effects (30° Sector), NP-2374, NUREG/CR-2568, GEAP-22046, Electric Power Research Institute, U. S. Nuclear Regulatory Commission, and General Electric Company.
5. Hwang, W. S., et al. BWR Full Integral Simulation Test: Phase 1 Results. NP-3602, Electric Power Research Institute, March 1985.
6. Myers, L. L. BWR Refill-Reflood Program: Final Report. NP-3093, Electric Power Research Institute, April 1984.
7. Yeh, H. C., et al. Heat Transfer Above the Two Phase Mixture Level Under Core Uncovery Conditions in a 336-Rod Bundle. NP-2161, Electric Power Research Institute, December 1981.
8. Chon, W. Y., et al. Uncovery Boiloff Transients in a 3- x 3-Rod Bundle. NP-2121, Electric Power Research Institute, November 1981.

## Section 7

### STEAM GENERATORS

EPRI has conducted an extensive amount of steam generator modeling work. This work has been both experimental, analytical and covers both U-tube and once-through steam generators.

#### 7.1 STEAM GENERATOR MODELING

The flow distribution within various steam generator components governs heat transfer phenomena and heat rejection capability. Yet, to evaluate fully the thermal-hydraulic performance of steam generators, researchers need a large data base representing dynamic conditions. To obtain this data, EPRI sponsored research (1).

- To provide a data base for validating steam generator codes.
- To evaluate steam generator response under off-normal conditions.

Researchers first designed and built a 1/7-scale-model steam generator with an integral downcomer, heated U-tube bundle riser, unheated riser section, and separator. A spectrum of steady-state experiments were performed to evaluate facility performance and a range of transient experiments to simulate loss of feed and primary and steam line breaks. The thermal-hydraulic parameters on each transient test were monitored using a high-speed data acquisition system. High-speed movies of the transients were taken for identification of flow regimes. Analytic predictions for selected transients--using the three-dimensional thermal-hydraulics code ATHOS--were compared with available data to evaluate code prediction capabilities.

The steady-state experiments conducted in the project provided system performance characteristics--namely, dependence of circulation ratio on inlet conditions and overall primary-to-secondary heat transfer for given downcomer mass flux and level. These experiments formed the basis for extensive transient response tests. A parametric study of the test data was conducted, and a large data base was developed, using fluid-to-fluid (Freon-to-water) modeling. Comparisons of the

ATHOS predictions for certain transients with test data showed good agreement for most parameters monitored.

In order to extend this work to larger steam generators, EPRI participated in a joint program (2) to conduct a series of full-height prototypical simulation experiments to test U-tube steam generator response to selected transient conditions. Objectives of this program were

- To perform a scaling analysis of a model boiler facility to assess its capabilities for simulating PWR U-tube steam generator transients under accident conditions.
- To plan a test series that would provide a data base to help qualify best-estimate safety methods.

Project engineers performed a scaling analysis of the 52-tube, full-height Westinghouse model boiler (MB-2) facility, which operates under prototypical steam generator conditions. The scaling analysis of the 6-MW test facility was undertaken to determine how closely the MB-2 response resembled that of a full-scale facility to three simulated steam generator accidents: a steam line break (SLB), a steam generator tube rupture (SGTR), and a loss-of-feedwater (LOF) transient. Instrumentation and modifications were identified to ensure that MB-2 tests would provide the data base necessary for qualifying best-estimate safety methods.

The scaling analysis revealed some deviations from a full-scale boiler response and identified test-facility modifications that would be required for proper simulation of the SLB, SGTR, and LOF accident scenarios.

In addition to the above experimental work, EPRI has sponsored an extensive program to develop a PWR steam generator computer code with best-estimate predictive capability for determining nuclear steam generator and power plant responses under transient conditions (3, 4, 5, 6).

The investigators assessed numerical modeling methods and empirical correlations for various heat transfer regimes in steam generators for use in developing new models. A numerical solution was achieved by use of an extended implicit

continuous-fluid Eulerian (EICE) method, which was developed in this project. The EICE method takes into account both fluid compressibility and heating effects during steam generator transients.

The EICE method uses a two-step iterative approach to obtain the time-dependent solution of fluid conservation equations, which are fully coupled with the equation of state. The modeling concept includes a single-fluid, two-phase slip flow model applicable to steam generators. The result is a one-dimensional, dynamic computer code that can simulate thermal behavior of both once-through and U-tube steam generators. The code can interface with system codes and can include other component models of a PWR system.

## 7.2 NATURAL CIRCULATION SYSTEM TESTS

EPRI has sponsored one test program and cosponsored another to study the natural circulation mode of steam generator operation. Specifically, these programs were designed to generate experimental data for estimating heat transfer coefficients and flow regimes involved in natural circulation cooling modes in PWRs, and to demonstrate the effectiveness of natural circulation in removing decay heat from a PWR core under small-break LOCA conditions.

In the first program (7), researchers conducted a series of natural circulation tests in the FLECHT SEASET test facility, a 1/307-scale model (by volume) modified to provide a low-pressure, closed-loop simulation of a four-loop PWR. Natural circulation and reflux condensation cooling experiments were run using electrically heated rods to simulate nuclear core arrays of current PWR designs. After steady-state single-phase, two-phase, and reflux condensation cooling modes were established, researchers measured the corresponding flow and heat transfer characteristics.

The tests showed that stable cooling can be achieved in a PWR with less than a full primary system. Performance during the single-phase tests was as expected, and the power flow relationships served to verify published calculational methods. Cooling remained stable during cold leg, upper plenum, and noncondensable gas injections. A large thermal stratification--as much as 11°C (20°F) temperature difference--was observed to exist between the top and bottom of the hot leg.

The two-phase test showed a peak flow at a lower system inventory--about 85%--than found in previous tests. Injecting noncondensable gas during two-phase circulation acted to pressurize the primary system.

Analysis of the steam generator heat transfer data yielded results that gave the overall heat transfer coefficient, as well as the local heat flux distribution. Heat flux calculations verified that the bottom four feet of the steam generator are most active as a heat sink.

In the second program (8, 9, 10, 11) tests were performed on systems modeling: TMI-with its once-through steam generators, and one-loop, two-loop, three-loop, and four-loop U-tube steam generator plants.

The main result of these tests was that decay heat in the "core" of this test facility can be successfully removed by either single-phase or two-phase natural circulation or by reflux boiling. The differences among these three states are the amounts of water in the primary system.

Other results were:

- The primary-temperature signatures during single-phase natural circulation are unsteady. Large temperature fluctuations, on the order of 50°F (30°C), were recorded.
- Two-phase natural circulation flow is unsteady, as reflected in the primary-temperature fluctuations. The existence of more than one set of temperature signatures suggests that different modes of two-phase natural circulation occur under different system conditions.
- Allowing boiling in the secondary does not significantly affect the primary system's operation until the secondary level drops to about 25% of the tube height. At that point, large pressure and temperature variations are experienced in the primary system.
- In transient tests, such as small-break LOCAs or noncondensable gas injections, the gross responses of the system, such as the primary pressure, exhibited the expected behaviors.

### 7.3 SINGLE TUBE STUDIES

In addition to the loop tests, EPRI sponsored a program to investigate the heat transfer during reflux condensation. This area is of interest because if a small-break loss-of-coolant accident should result in a substantial loss of primary coolant in a PWR, the plant operator might need to remove decay heat through the reflux condensation process. In that process, steam generated in the reactor vessel would condense on the steam generator tube walls and then run back to the vessel in a countercurrent flow. The many factors that may affect this heat transfer process include interfacial shear, waviness, and the presence of

noncondensable gases. These factors have not usually been incorporated in simulation models.

The reflux condensation program was divided into two parts. The first part was to develop empirical information about the reflux condensation process in inverted U-tubes that will serve as input for analytic models (12). The second was to develop a comprehensive analytic model for heat transfer during reflux condensation that is supported by experimental data (13).

In the first program, the mechanisms governing heat removal and liquid holdup in a closed-loop, transparent test apparatus were systematically studied. The apparatus used prototypical tube sizes and scaled the steam and liquid flow rates to preserve conditions typical of a LOCA. Because of these features, one could actually observe the types of flow that occur in an inverted U-tube when vapor is condensing in the tubes. The pressure and temperature variations were monitored so as to derive the basic characteristics of the flow regimes involved.

Using different steam and liquid velocities, three types of flow regimes were identified and characterized. These regimes will serve as bases for analytic models. The first regime, reflux condensation, is a counterflow of steam and water in the riser. The second is natural circulation, a concurrent flow of steam and water over the U-bend in the steam generator tube. The third regime is an oscillatory mode in which there is a periodic accumulation of water above the two-phase condensation region followed by dumping of the liquid column over the U-bend. The formation of this liquid column may induce core uncovering.

In the second program, a thermosiphon was used to reproduce reflux condensation conditions in a controlled environment and measure key parameters. The closed system was flexible enough to allow the use of different working fluids under a variety of thermophysical conditions. Film condensation was studied to determine the effects of subcooling, fluid acceleration, and vapor drag. Also investigated was the interfacial shear that resulted from vapor flow, as well as wave effects and the effect of noncondensable gases present in the system. An analytic model based on the well-known Nusselt condensation theory was developed, adding the all-important effects of the wavy liquid film structure, interfacial shear, and noncondensable gases.

Study results indicated that the Nusselt solution for film condensation does not explain the reflux condensation phenomenon satisfactorily. The data base

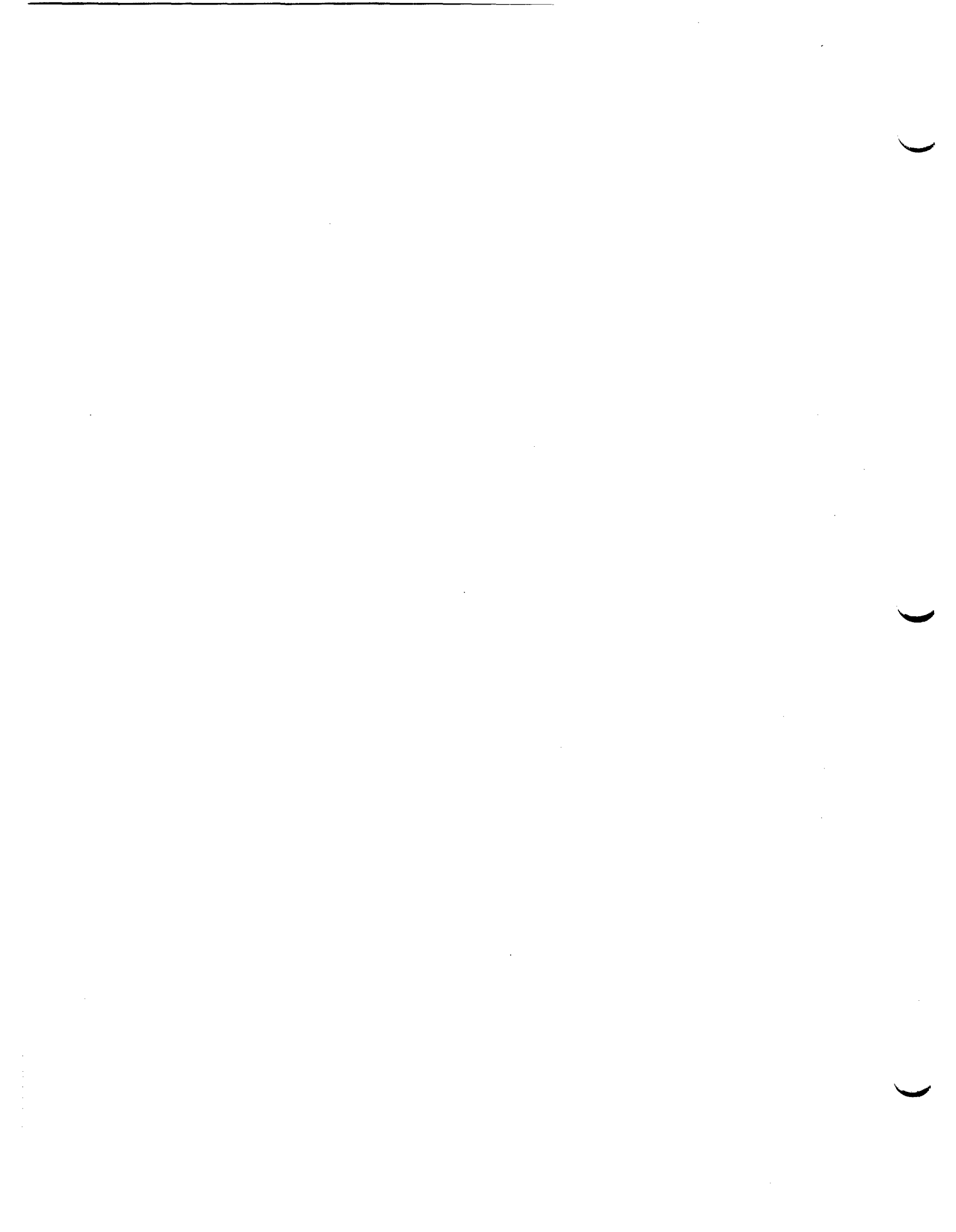
developed during this work includes valuable information regarding the heat transfer process, which the study demonstrated to have substantial impact on analysis of decay heat removal following loss-of-coolant accidents. The data was used in deriving an improved analytic model for reflux condensation.

In addition, a brief list of refereed papers is provided in references 14 to 24.

#### REFERENCES

1. Adams, G., Wolfe, K, and McGovern, D. Transient Simulation Studies for PWR U-Tube Steam Generators, NP-3412, Electric Power Research Institute, March 1984.
2. Young, M. Y., et al. Prototypical Steam Generator Transient Testing Program: Test Plan/Scaling Analysis, NP-3494, Electric Power Research Institute, September 1984.
3. Lee, J. C., et al. Transient Modeling of Steam Generators in Nuclear Power Plants: Computer Code, TRANSG-01, NP-1368, Electric Power Research Institute, March, 1980.
4. Lee, J. C., et al. Review of Transient Modeling of Steam Generator Units in Nuclear Power Plants, NP-1576, Electric Power Research Institute, October 1980.
5. Lee, J. C., et al. Simplified Models for Transient Analysis of Nuclear Steam Generators, NP-1772, Electric Power Research Institute, April 1981.
6. Lee, J. C., et al. TransG-01: A Computer Code for Transient Analysis of Nuclear Steam Generators, NP-3394-CCM, Electric Power Research Institute, January 1984.
7. Hochreiter, L. E., et al. PWR FLECHT SEASET Systems-Effects Natural Circulation and Reflux Condensation Data Evaluation and Analysis Report, NP-3497, Electric Power Research Institute, February 1985.
8. Kiang, R. L. Two-Phase Natural Circulation Experiments in a Test Facility Modeled After Three Mile Island Unit-2, NP-2069, Electric Power Research Institute, October 1981.
9. Jeuck, P. R., III, and Kiang, R. L. Natural Circulation Experiments in a UTSG Four-Loop Test Facility, NP-2615, Electric Power Research Institute, September 1982.
10. Kiang, R. L., Jeuck, P. R., III, and Eid, J. C. Decay Heat Removal Experiments in a UTSG Two-Loop Test Facility, NP-2621, Electric Power Research Institute, September 1982.
11. Kiang, R. L., Jeuck, P. R. and Eid, J. C. Decay Heat Removal Experiments in a U-Tube Steam Generator One-Loop Test Facility, NP-3472, Electric Power Research Institute, May 1984.
12. Nguyen, Q., and Banerjee, S. Experimental Data Report on Condensation in a Single Inverted U-Tube, NP-3471, Electric Power Research Institute, May 1984.

13. Tien, C. L., et al. Reflux Condensation in a Closed Tube, NP-3732, Electric Power Research Institute, October 1984.
14. Kalra, S. P., Srikantiah, G. S., Singh, A., and Duffey, R. B. Steam Generator Safety and Thermal-Hydraulic Research at EPRI, Proceedings Specialist Meeting on Steam Generator Problems, Stockholm, Sweden, October 1-5-, 1984.
15. Kalra, S. P. "On the Natural Circulating PWR U-Tube Steam Generators - Experiments and Analysis", Proceedings of International Center for Heat and Mass Transfer Seminar on Advancement in Heat Exchange, Dubrovnik, Yugoslavia, September 7-12, 1981, Hemisphere Publishing Corp., Washington, D.C., 1982.
16. Kalra, S. P. Dynamic Thermal-Hydraulic Behavior of PWR U-Tube Steam Generators-Simulation Experiments and Analysis, EPRI-NP-1837-SR, Electric Power Research Institute, 1981.
17. Kalra, S. P., and Ahmad, S. Y. "Critical Heat Flux Measurements in a Vertical Multi-Element Segmented Cluster", Fluid Flow and Heat Transfer Over Rod in Tube Bundles, Proceedings of the Winter Annual Meeting of the American Society of Mechanical Engineers, New York, December 2-7, 1979, pp 171-180, S. C. Yao and P. A. Pfund (Eds.), American Society of Mechanical Engineers, New York, 1979.
18. Kalra, S. P., Adams, G., Duffey, R. B., Lapson, W., and Lundberg, R. "Experimental Simulation Studies of PWR U-Tube Steam Generators", Boiler Dynamics and Control in Nuclear Power Stations, Proceedings of the Second International Conference held in Bournemouth, October 23-25, 1979, pp. 9-76, British Nuclear Energy Society, London, 1980.
19. Kalra, S. P., Duffey, R. B., and Adams, G. "Loss of Feed Water Transients in PWR U-Tube Steam Generators: Simulation Experiments and Analysis", Heat Transfer-Orlando 1980, R. P. Stein (Ed.), AIChE Symp. Ser. 199, 76: 36-44, 1980.
20. Kalra, S. P., and Adams, G. Thermal-Hydraulic of Steam Line Break Transients in Thermal Reactors-Simulation Experiments, Trans. Am. Nucl. Soc. 35:297-298, 1980.
21. Kalra, S. P., and Adams, G. On the Transient Thermal-Hydraulic Behavior of U-Tube Boiler During Feed Line Break, presented at ASME-JSME Thermal Engineering Conference, Honolulu, Hawaii, March 20-19, 1983.
22. Kalra, S. P., and Adams, G. System Heat Transfer Effects in Natural Circulating U-Tube Steam Generators During Primary Flow Transients, ASME Paper 82-NE-11, American Society of Mechanical Engineers, New York, 1982.
23. Kalra, S. , Yao, L. S., and Davis, W. E. R. Flow Behavior in a Static Vane Centrifugal Separator-Simulation Experiments and Analysis, presented at ASME/ANS/AIChE Second International Topical Meeting on Nuclear Reactor Thermal Hydraulics, Santa Barbara, California, January 11-14, 1983.
24. Lee, J. C., Akcasu, A. Z., and Duderstadt, J. J. Simplified Models for Transient Analysis of Nuclear Steam Generators, Interim Report (Research Project 684-1), NP-1772, Electric Power Research Institute, April 1981.



Section 8  
DECAY HEAT

In 1971, the American Nuclear Society Standards Subcommittee 5 (ANS-5) proposed the adoption of a standard entitled "Decay Energy Release Rates Following Shutdown for Uranium-Fueled Thermal Reactors." By virtue of NRC requirements, it is now specified as part of the ECCS evaluation models, with the heat generation rate from the radioactive decay of fission isotopes assumed to be equal to 1.2 times the values appearing in the standard. The factor 1.2 appears to be based on the uncertainty quoted in the standard for short cooling times. Subsequent experimental and computational work has lowered the magnitude of the decay heat values at short times after reactor shutdown and has significantly reduced its uncertainty. As a result, another decay heat standard has been developed and approved by ANS-5 and has been issued. EPRI along with NRC and others has sponsored some of the work necessary to produce the new, more accurate standard.

EPRI has sponsored two studies to determine the decay heat from the the fission products of  $^{235}\text{U}$  (1, 2). In the first study, the absorbable components of the fission-product decay heat from thermal-neutron fission of  $^{235}\text{U}$  have been measured in the 1 to  $10^5$  second time range for a one-day (86,400 second) irradiation time. The systematic uncertainty of the measurement is 2.4%, with statistical uncertainties of 2% at 1 second, increasing to about 4% at  $10^5$  seconds. The measurements were made using a "nuclear calorimeter" which is based on a large (4000 liter) liquid scintillator. The uranium irradiations were made by a water-moderated  $^{252}\text{Cf}$  source. A rapid pneumatic system transferred the irradiated sample to the scintillator.

In the second study, a calorimetric measurement of decay heat power of  $^{235}\text{U}$  fission products has been made using a fast response calorimeter in the cooling time range from 10 to  $10^5$  seconds. The calorimeter is based on measurement of the rate of change of energy stored in a mercury absorber together with measurement of heat flow through a thermopile. Agreement between the measured values and summation calculations is good in the cooling time range from 500 to  $10^4$  seconds. At earlier times the potential accuracy of the instrument was not realized; the

average of measured results is higher than predicted by up to 17%. The estimated uncertainty of the measurement is 3.4% (one sigma) from 400 to  $10^4$  seconds and rises to 22.7% at 11 seconds.

As part of this study, an analytical method of determining the decay heat from the nuclear input data was developed (3). A method for the solution of the system of ordinary differential equations for the concentration, activity, and decay heat of fission products is presented that is based upon a digital computer evaluation of the exact solution of the system expressed in recursive form.

The system of coupled differential equations describes the rate of change of the concentration of fission products resulting from direct production in fission, radioactive decay, and neutron absorption for 818 different nuclides. The decay heat is obtained by summing over the beta and gamma energies of each radioactive nuclide. The input nuclear data consists of fission yields, half-lives, branching ratios, and average energies of beta particles and gamma rays.

A computer program was written for the evaluation of these recursive concentration expressions and for the calculation of individual and total decay power. The program makes use of averaged data for fission products resulting from the thermal and fast spectrum fissioning of  $^{235}\text{U}$ ,  $^{239}\text{U}$ ,  $^{239}\text{Pu}$ ,  $^{241}\text{Pu}$  and  $^{232}\text{Th}$  based on the ENDF/B-IV nuclear data file. The output of the computer program is a summary table giving the total decay power of all the nuclides combined and also separately the total beta and total gamma power. The contribution of the present work over previous methods of computing decay heat by large codes in so-called "summation calculations," consists in treating the effect of neutron absorption and the elimination of singular coefficients in an exact fashion without approximations.

EPRI also sponsored research to determine the decay heat contribution of  $^{239}\text{Pu}$  (4, 5, 6). Emphasis was given to the  $^{239}\text{Pu}$  results because a large fraction of the fissions in high exposure fuel is due to  $^{239}\text{Pu}$ . In order to remove some remaining experimental discrepancies and to provide data for checking the so-called "summation" calculations used to predict decay power under specific reactor operating conditions, spectral (i.e., energy) measurements were also obtained.

EPRI has also sponsored research into spatial deposition of gamma ray energy in the core of nuclear reactors following shutdown. This work is intended to provide a benchmarked tool for use in safety analyses in the postulated event of LOCA.

Present NRC regulations state that, in the case of such an unlikely event as a LOCA, certain important safety margins must be demonstrated, including the peak cladding temperature of the fuel and the amount of H<sub>2</sub> produced to radiolysis in the coolant. The peak cladding problem is of concern in the short time frame (i.e., 10<sup>3</sup> seconds) following reactor shutdown in a LOCA analysis, while for H<sub>2</sub> radiolysis, the time frame of interest is days and weeks.

An experimental study was undertaken to produce a precise and readily interpretable description of the distribution of absorbed energy in a LWR fuel element (7). A mock-up was constructed consisting of a 10x10 matrix of cladding tubes two feet long and loaded with depleted UO<sub>2</sub> to form fuel pins. Internal dimensions were such that the mock-up simulated precisely a section of a PWR fuel element. Some measurements were also made in a configuration which simulated a typical BWR fuel element.

Monoisotopic sources were inserted between the fuel pellets in the center of the assembly. Measurements were made with sources of <sup>60</sup>Co, <sup>137</sup>Cs, and <sup>51</sup>Cr, whose gamma radiations were typical of major fission product sources. Lithium fluoride thermoluminescent dosimeters (TLDs) were selected as the detectors. A large number of data points have been measured, with an average standard deviation of 6%. These data are useful in determining the spatial distribution of the absorption of fission product gamma ray energy around regions of high local power density following the shutdown of a nuclear reactor.

A companion study (8), developed a computational methodology to investigate actinide and fission product gamma ray effects in a post-LOCA situation. Specifically, gamma ray source strengths from ORIGEN are coupled with Monte Carlo transport results to predict the gamma ray heat redistribution (for a transient non-flooded case) and gamma ray energy deposition in water (for the long term hydrolysis of water in a flooded case). The transport calculations are performed with the SAM-CE code making use of its extended combinatorial geometry capability. This enables the reactor core to be modeled in great detail including individual fuel pins, control rods, water holes, etc. Subsequently, the methodology was applied to representative PWR and BWR plants (Oconee and Nine Mile Points, respectively). It was found that the NRC guidelines for both gamma ray heat redistribution and deposition in water were conservative. The methodology as it now exists may be applied to other LWR plants.

## REFERENCES

1. Friesenhahn, S. J., et al.  $^{235}\text{U}$  Fission Product Decay Heat from 1 to  $10^5$  Seconds, NP-280, Electric Power Research Institute, Palo Alto, California, February 1976.
2. Schrock, V. E., et al. A Calorimetric Measurement of Decay Heat from  $^{235}\text{U}$  Fission Products from 10 to  $10^5$  Seconds, NP-616, Volume 1, Electric Power Research Institute, Palo Alto, California, February 1978.
3. Grossman, L. M., and Stein, W. The Calculation of the Decay Heat of Fission Products from Exact Relations, NP-616, Volume 2, Electric Power Research Institute, Palo Alto, California, February 1978.
4. Dickens, J. K., and McConnell, J. W. Fissions Determination in  $^{239}\text{Pu}$  Sample, NP-997, Electric Power Research Institute, Palo Alto, California, February 1979.
5. Friesenhahn, S. J., and Lurie, N. A. Measurements of  $^{239}\text{Pu}$  and  $^{235}\text{U}$  Fission Product Decay Power from 1 to  $10^5$  Seconds, NP-998, Electric Power Research Institute, Palo Alto, California, September 1979.
6. Friesenhahn, S. J., and Lurie, N. A. Measurements of  $^{235}\text{U}$  and  $^{239}\text{Pu}$  Fission Product Decay Spectra, NP-999, Electric Power Research Institute, Palo Alto, California, December 1979.
7. Bass, R. B., and Johnson, W. R. Spatial Distribution of Fission Product Gamma-Ray Energy Deposition in Light Water Reactor Fuel Elements, NP-672, Volume 1, Electric Power Research Institute, Palo Alto, California, April 1978.
8. Steinberg, H., Lichtenstein, H., and Cohen, M. O. An Analysis of Post LOCA Gamma Ray Effects in Representative Light Water Reactors, NP-425, Volume 1, Electric Power Research Institute, December 1976.

## Section 9

### METAL WATER REACTION AND FUEL ROD PERFORMANCE

The exothermic reaction between the Zircaloy clad in steam at high temperatures is important during a LOCA because heat is added to the system, and also because resulting clad swelling and failure could impede reflood heat transfer. EPRI has sponsored several programs to establish a credible technical basis establishing the Zircaloy-water rate reaction and the impact of the resulting reaction on the system behavior during a LOCA.

Under contract to EPRI (1), a large number of tests in the GLEEBLE loop to study the oxidation kinetics of Zircaloy in steam in the temperature range 1200-1800°F were performed. Additional tests verified the Baker-Just data at high temperatures (2200°F). An alternate correlation to the Baker-Just equation was developed. Although conservative, the EPRI correlation is a significant improvement to Baker-Just since its data set covers not only high temperatures, but also lower temperatures, which are more relevant to ECCS calculations. Relative to Baker-Just, the EPRI data and correlation yield oxidation rates that are 1.8 times less than Baker-Just at 2200°F. In addition, the EPRI correlation is found to be conservative by a factor of 4 due to the influence of preoxidation films and anisothermal conditions (4).

A computer code was written to characterize the oxidation of Zircaloy in steam in the range of 1200-2700°F for both isothermal and transient oxidizing conditions. Accurate predictions have been demonstrated for conditions representative of LOCAs in LWRs.

EPRI also took part in a joint program to investigate cladding properties during a LOCA (2). There were four tasks performed.

- Zircaloy material properties as a function of oxygen content
- evaluation of relative ID/OD oxidation of cladding during LOCA

- transient deformation and rupture characteristics of cladding during LOCA
- mechanical deformation of cladding during LOCA

Evaluation of material properties is significant since the cladding deformation process is both time- dependent and path-dependent (i.e. different paths taken for temperature as a function of time and relative pressure as a function of time can change the strain at failure significantly (for example for 4% to 40%). Previous analysis relied on final-strain-at burst data for conditions found in LOCA.

The EPRI work developed "fundamental" data and "proof test" data for a path-dependent cladding deformation analysis model.

Among the major conclusions: (a) the anisotropic behavior of Zircaloy was found to be significant at temperatures below 1500°F, and of little consequence above 1500°F; (b) oxygen effects influence strongly the strength of the cladding at high temperatures, and the uniform and maximum strain at failure.

The data and the analytical and experimental techniques developed can be used for best estimate materials performance predictions during LOCA.

EPRI is also taking part in the Halden Reactor Project which has been performing experiments that help to validate the large body of out-of-pile data with reactor experiments. Oxidation during blowdown and reflood conditions were simulated in in-pile rigs. Clad temperatures, heat-transfer coefficients, and clad-ballooning data were collected on nuclear fuel rods. These data were compared to similar data obtained with electrically heated rods. The tests are significant since validation of out-of-pile data is necessary to minimize uncertainty in ECCS evaluation models.

This project is scheduled for completion in mid-1985.

#### REFERENCES

1. Biederman, R. P. A Study of Zircaloy 4 Steam Oxidation Reaction Kinetics, NP-0225, Electric Power Research Institute, September 1976.
2. Mohr, C. L. Transient Deformation Properties of Zircaloy for LOCA Simulation, NP-0526, Electric Power Research Institute, May 1980.
3. Vik, T. J. Status Report, September-December, 1984, Halden Project Report, HP-690, February 15, 1985.
4. H. Ocken. An Improved Evaluation Model for Zircaloy Oxidation, Nuclear Technology, Vol. 47, February 1980.



## Section 10

### FUNDAMENTAL STUDIES

EPRI has conducted many studies of the phenomena occurring during a LOCA in order to obtain basic information about the physical processes. These studies have been grouped into broad areas, and will be discussed below.

#### 10.1 HEAT TRANSFER

A study was made to develop improved analytical methods capable of predicting the rewetting of a hot surface during reflood (1). An analytical one-dimensional conduction model was developed for this purpose. A generalized boiling curve is applied to account for the various heat transfer regimes involved in the quenching phenomenon. A non-dimensional velocity is defined, which plays the role of an eigenvalue in the solution of the governing equation and is shown to generalize the applicability of the predicted results for a wide range of experimental conditions. The method is applicable for an arbitrary distribution of heat flux in the sputtering region and does not require the conventional a-priori definition of a rewetting temperature.

Transition boiling is the boiling process between stable film boiling, where vapor blanketing of the fuel rods is maintained, and nucleate boiling, where the rod surfaces are quenched and rewetted. The transition boiling process is often characterized by unsteady temperature and flow fluctuations. Because of the complexity, it remains as the least understood phenomenon in the boiling process.

EPRI cosponsored a project to improve the understanding and better correlate the heat transfer coefficient during transition boiling (2).

Steady-State and transient transition boiling heat transfer tests with water at low pressures were conducted using a loop in which the test sections were heated by hot mercury. These tests were coupled with phenomenological studies. By using the new and more reproducible steady-state heat transfer data, together with previous data from the literature, a revised heat transfer correlation was

developed. The new correlation, which includes a flow effect not previously considered, provides an appreciably better fit of all the data.

Transient heat transfer data in the transition boiling region were obtained in two separate test sections. In both experiments the transient was initiated by a sudden increase of the water flow rate. Comparison of these heat transfer data with the prediction of the new steady-state correlation indicates that the new heat transfer correlation also applies to transient data. The rewetting rates observed were highly dependent on the local void fraction and geometry of the test section. At high void fractions in the annular test section, the rewetting rate was determined by the availability of cooling water to the heated surface.

Phenomenological studies included void fraction measurement, visual and photographic observations and an examination of wall temperature fluctuations. It was found that the relationship between void fraction and quality could be predicted using the drift flux model. The wall temperature fluctuations observed at high mass velocities are believed due to periodic passage vapor slugs. Visual observations showed that the temperature fluctuations at low mass velocities occurred during annular flow and were due to the oscillatory behavior of the liquid film on the heated surface. These oscillations were successfully analyzed using a moving rivulet model.

## 10.2 CRITICAL HEAT FLUX

Critical Heat Flux (CHF) is an important phenomenon which is important in the steady-state reactor design and also for accident analysis. EPRI has sponsored both transient and steady-state experimental and analytical work.

EPRI sponsored work to develop a method of predicting CHF in flow transients (2, 3). This investigation produced a self-consistent physically based procedure for calculating when the vapor blanketing or CHF conditions actually do develop in a constant pressure rapid flow reversal transient. The method used steady state CHF correlations with transient predictions of local fluid conditions and was shown to adequately predict the CHF level, time, and location in high pressure FREON 113 flow reversal transients.

It was suggested that the worst pipe break location in a Pressurized Water Reactor accident from the standpoint of time to CHF is one which causes a flow stagnation point to develop in the core. A simple analysis was presented to show that even

if CHF did not occur, complete voiding of liquid coolant from the core could occur in from one to two seconds under such conditions.

The homogeneous two phase model was shown to be adequate for analysis of rapid flow reversal transients, and a small but versatile computer program was written for either pressure drop forced or inlet flow forced one-dimensional simulation of such complicated constant pressure rapid flow transients.

EPRI also sponsored work to develop and qualify a CHF correlation which can be used today to predict thermal limits in a BWR (4). This correlation was intended to be developed in a form which could be utilized in conjunction with nuclear analysis codes developed by EPRI.

A critical quality-boiling length correlation was generated which includes the effects of rod-to-rod (local) peaking factor, different axial heat flux profiles, pressure, rod diameter and bundle geometry. The CHF data base for this correlation is primarily 16-rod, with heated lengths up to 12 feet, with axially uniform and non-uniform heat flux, in a pressure range from 600 to 1400 psia, and a mass velocity range from 0.25 to  $1.5 \times 10^6$  lb/hr ft<sup>2</sup>. The correlation predicts the critical power of the test data used to create the correlation with a standard deviation of 5.5%, and a mean value of 0.9948. When all applicable BWR CHF data are compared to the correlation, it predicts the test bundle critical power with a standard deviation of 7.5%, with a mean value of 1.0295.

EPRI also sponsored an effort to develop a generalized subchannel CHF correlation from the Columbia University CHF data base (5, 6). The COBRA-IIIC code was used to develop a correlation based on local fluid properties. The correlation covers PWR and BWR normal operating conditions as well as LOCA conditions. This correlation was developed utilizing 3607 CHF data points from 65 test sections simulating PWR and BWR fuel assemblies. The data covered wide parameter ranges (pressure: 200-2450 psia; mass flux:  $0.2-4.1 \times 10^6$  lbs/hr-ft<sup>2</sup>; quality: -0.25-00.75). The correlation predicted the source data with an RMS error of 7.2 percent and an average ratio of 0.995. The effect of cold wall on CHF was determined and appropriate mass flux dependency was incorporated in the correlation. The effect of grid spacers on CHF was investigated and this effect was quantized in terms of the grid loss coefficient. The adequacy of the present CHF correlation in predicting CHF limits in fuel assemblies with non-uniform axial heat flux distribution was evaluated using 933 CHF data points from 23 test sections with eight types of axial heat flux profiles (7). The correlation predicted the non-uniform axial

heat flux data with an RMS error of 8.6 percent and an average ratio of 1.00. A comparison of the present CHF correlation represents significant improvement in predicting CHF over wide range of conditions.

### 10.3 COUNTER CURRENT FLOW LIMIT

EPRI has sponsored a number of studies into the nature of two phase flow phenomena. A large amount of effort has been spent on investigating the Counter Current Flow Limit (CCFL) also called flooding. In particular, two multi-year experimental and analytical research programs were sponsored.

In one program, an effort was made to investigate the relationship between entrainment and CCFL. Both single and multiple path configurations were studied (8, 9). Two-phase countercurrent flows of air and water were run in single-tube and contraction plate-in-tube test sections. Results include data for liquid carry-over rates from 0 to 90% of the liquid injection rates. Flow regimes are described. For these tests, flooding was defined as the onset of significant liquid carry-over (2% or more of the liquid injection rate). The effects of plate geometry, water injection scheme, and liquid surface tension were investigated. Analytic work included a new flooding model that predicts not only the onset of flooding but also the liquid carry-over rate from 0 to 70% of the liquid injection rate for contraction plate tests. For the single-tube tests, the top flooding flow regime was analyzed and a prediction for the onset of top flooding was obtained. In each model, experimental data are required to evaluate two constants in the prediction equations.

In the other research program, air-water and steam-water CCFL tests were performed (10, 11, 12, 13). The results of the air-water tests were well correlated with either the Wallis correlation or a correlation based on the Kutateladze number depending on the tube diameter. The steam-water results were quite different. Depending on the flow rates of steam and water, the water temperature, the test section geometry, and the injection method, the condensation of steam can lead to three distinctive regimes of behavior: no water penetration, complete penetration, and partial penetration (i.e., countercurrent flooding). The result has been compared to similar studies for boiling water reactor (BWR) bundle geometries and showed that the behaviors are essentially the same. The boundaries between the above regimes are defined by the hydrodynamic counterflow limitations of the system and by direct condensation characteristics. Two of the regime boundaries were close to ideal limits:

1. Achievement of thermodynamic equilibrium between steam and water in one of the plenum chambers. If there was excess water, all of the steam condensed; if there was excess steam, the water was heated to saturation.
2. A purely hydrodynamic limitation in agreement with air-water tests in the same facility.

Some regime boundaries varied, depending upon whether the steam or water was turned on first (this determined in which of the plenum chambers condensation would occur). Long transients sometimes occurred when the flow rates were changed, accompanied by oscillations (chugging) of a steam-water interface in the tube and by the violent popping of collapsing steam bubbles.

#### 10.4 TWO-PHASE FLOW

EPRI has sponsored a number of studies of two-phase flow behavior as applied to nuclear safety issues.

Systems that inject subcooled sprays into steam environments function to reduce pressure or eliminate excess heat in localized reactor areas. Examples include pressurizer sprays in PWRs, high-pressure-system injections over reactor cores in BWRs, and auxiliary feedwater injections in the secondary sides of once-through steam generators. The thermal-hydraulic effects produced by such injections--though local--have significant impact on the cooling of a reactor's total primary system.

An analytical study was performed to develop a detailed model of the interaction between subcooled spray droplets and the surrounding vapor field in BWRs (14, 15, 16). The model developed is based on a detailed evaluation of mechanisms affecting the interaction between the liquid drops in the spray and the surrounding vapor. It treats the vapor as a continuous field affected by heat sinks (the droplets). Dimensionless equations describe the evolution of the vapor field, the trajectories of the spray droplets, and the overall shape of the spray. For validation, the model's predictions were compared with experimental data generated earlier in the project on the water flux distribution below a single nozzle in steam at several pressures.

The study results indicate that for practical applications condensation forces dominate the spray droplet trajectories in steam. A computer code was written to describe the vapor flow field and the spray velocities and trajectories.

EPRI sponsored a project designed to determine the significance of multi-dimensional flow effects during reflood (16, 17, 18, 19, 20). To do this, a 1700-pin, scaled reactor core model was built, and measurements were taken of the three-dimensional flow and heat transfer that occurred during core reflooding. These small-scale results agreed with earlier full-scale reflooding studies. The method used to analyze these results included new features of an explicit treatment of the three-dimensional flows and the tracking of two-phase levels. Special correlations were developed that describe the heat transfer and core heat-up. The analytic and numerical solutions incorporating these correlations were then compared.

This work provides the first simple quantitative corroboration of the significance of multidimensional effects on core reflooding. Cross-flow effects are small, and a multidimensional analysis can predict correctly full- and large-scale effects without further fine-tuning. Agreement also exists between a code which was developed during this project and the results of the large USNRC TRAC code. The effects of the spatial core power distribution are such that significant variations in heat removal for the peak-, average-, and low-power assemblies occur. The assemblies are coupled through the core-quenching and hydrostatic head effects.

#### 10.5 MIXING

EPRI has sponsored several projects dealing with fluid mixing both within the core, and as part of the study of ECC bypass and related subjects.

A study was performed to improve fluid flow and heat transfer models for reactor fuel and core analysis by providing experimental data on the mixing and void-fraction characteristics of fuel rod bundles (21). The bundles studied were designed to model PWR fuel.

The results indicated single-phase mixing is smaller than is usually assumed. Two-phase flow conditions did not increase the single-phase mixing coefficient. The mixing results were affected by the bowing of the simulated fuel rods. This bowing resulted in subchannel conditions that were not completely mixed. The results were also affected by flow bypass in the vicinity of grid spacers. Subsequent studies with COBRA were conducted to resolve these problems. Careful consideration should be given to the way two-phase mixing is modeled in subchannel codes. A model that preferentially mixes the coolant seems to give better results.

EPRI also sponsored a project designed to obtain detailed thermal-hydraulic measurements for parallel interconnected channels in the vicinity of flow blockages in models representing portions of nuclear reactor fuel bundles (22, 23, 24). A test section consisting of two interconnected subchannels was used to study the inter-channel mixing and detailed pressure drop characteristics near a blockage that had been placed in one channel. In this stage of the project, the effects of smooth- and sharp-edged blockages with single-phase water as the working fluid were determined.

The study produced detailed experimental data on the mass flow rate and pressure drops in the channels. Upstream of the blockage, the flow diversion occurs over a relatively short distance, whereas downstream the recovery of the diverted flow is a slow process. Except for the large blockage areas, the equalization of pressure between the channels is fairly rapid. The COBRA III-C code adequately described the data for smooth blockages in which up to 60% of one channel was blocked and for sharp-edged blockages in which up to 30% of the channel was blocked. The reflood phase of a postulated design basis accident is important because it can determine the maximum temperature that is ultimately reached. Consequently, a substantial research effort has been devoted to this subject. The refill-reflood program for BWRs and the FLECHT-SEASET program for PWRs address this issue on a large-scale basis. However, small-scale research, such as this project, is also required to support the effort. The present work provides detailed flow information that would be difficult, if not impossible, to obtain in larger experiments. In particular, the results are useful for benchmarking codes that analyze large-scale data. The results of using a two-phase, air-water mixture will be presented in a later report.

#### REFERENCES

1. Chambré, P., and Elias, E. Rewetting Model Using a Generalized Boiling Curve, NP-571, Electric Power Research Institute, Palo Alto, California, October 1977.
2. Weisman, J., et al. Studies of Transition Boiling Heat Transfer with Saturated Water at 1-4 Bar, NP-1899, Electric Power Research Institute, Palo Alto, California, June 1981.
3. Griffith, P. Critical Heat Flux in Flow Reversal Transients, NP-151, Electric Power Research Institute, Palo Alto, California, May 1976.
4. Hench, J. E., and Gillis, J. C. Correlation of Critical Heat Flux Data for Application to Boiling Water Reactor Conditions, NP-1898, Electric Power Research Institute, Palo Alto, California, June 1981.

5. Fighetti, C. F., and Reddy, D. G. Parametric Study of CHF Data. Volume 1: Compilation of Rod Bundle CHF Data Available at the Columbia University Heat Transfer Research Facility, NP-2609, Volume 1, Electric Power Research Institute, Palo Alto, California, September 1982.
6. Fighetti, C. F., Reddy, D. G., and Merilo, M. "Compilation of Critical Heat Flux Data in PWR Fuel Assemblies with Non-Uniform Axial Heat Flux Distribution". Proceedings of the Seventh International Heat Transfer Conference, Munich, West Germany, Volume 5, Hemisphere Publishing Corporation, New York, Washington, London, pp. 447, 1982.
7. Reddy, D. G., Fighetti, C. F., and Merilo, M. "Prediction of Critical Heat Flux in PWR Fuel Assemblies with Non-Uniform Axial Heat Flux Distribution," Proceedings of the Seventh International Heat Transfer Conference, Munich, West Germany, Volume 4, Hemisphere Publishing Corporation, New York, Washington, London, pp. 333, 1982.
8. Liu, C. P., Tein, C. L., and McCarthy, G. E. Flooding in Vertical Gas-Liquid Countercurrent Flow Through Parallel Paths, NP-2262, Electric Power Research Institute, Palo Alto, California, February 1982.
9. Lee, H. M., McCarthy, G. E., and Tein, C. L. Liquid Carry-Over and Entrainment in Air-Water Countercurrent Flooding, NP-2344, Electric Power Research Institute, Palo Alto, California, April 1982.
10. Bharathan, D. Air-Water Countercurrent Annular Flow, NP-1165, Electric Power Research Institute, Palo Alto, California, September 1979.
11. Wallis, G. B., et al. Countercurrent Annular Flow Regimes for Steam and Subcooled Water in a Vertical Tube, NP-1336, Electric Power Research Institute, Palo Alto, California, January 1980.
12. Merilo, M., Colah, M. and Duffey, R. B. "The Condensation Induced Transition from Bubbling to Liquid Downflow in a Turbulent Two-Phase Pool", Non-equilibrium Interfacial Transport Process, 18th National Heat Transfer Conference, San Diego, California, August 6-8, 1979; American Society of Mechanical Engineers, N.Y., N.Y., pp. 53,
13. Sargis, D. A., Khadem, M., and Merilo, M. Correlation and Multidimensional Analysis of Scaled CCFL Breakdown Tests, ASME Journal, 82-WA/HT-9.
14. Crossman, R. K. E., et al. Influence of Vapor Condensation on Subcooled Sprays, NP-3827, Electric Power Research Institute, December 1984.
15. Chan, F. W. K., Chan, R. K. C., and Stuhmiller, J. H. Single Nozzle Spray Distribution Analysis, NP-1344, Electric Power Research Institute.
16. Richter, H. J., and Durkee, G. G. C. BWR Spray Nozzle Performance in Steam Environment, NP-3119, Electric Power Research Institute, May 1983.
17. Catton, I., Ghiaasiaan, S. M., and Duffey, R. "On Multi-Dimensional Thermal-Hydraulics and Two-Phase Phenomena during Quenching of a Nuclear Reactor Core," Natural Convection: Fundamentals and Applications, edited by W. Aung, S. Kakac and R. Viskanto, Hemisphere Publishing Corporation, New York, 1985.
18. Ghiaasiaan, S. M., Catton, I., and Duffey, R. Thermal Hydraulic and Two-Phase Phenomena in Reflooding of Nuclear Reactor Cores, ASME Paper No. 82-FE-1.

19. Ghiaasiaan, S. M., Catton, I., and Duffey, R. B. A Single Channel Reflood Model, ASME Paper No. 82-WA/HT-33.
20. Ghiaasiaan, S. M., and Catton, I. Multidimensional and Two-Phase Flow Effects in PWR Core Reflooding, NP-3474, Electric Power Research Institute, Palo Alto, California, May 1984.
21. Barber, A. R., and Zielke, L. A. Subchannel Thermal Hydraulic Experimental Program (STEP). Volume 1: Mixing in a Pressurized Water Reactor (PWR) Rod Bundle, NP-1493, Electric Power Research Institute, Palo Alto, California, August 1980.
22. Tapucu, A., Gencay, S., and Troche, N. Experimental Study of the Diversion Cross-Flow Caused by Subchannel Blockages, NP-3459, Volume 1, Electric Power Research Institute, April 1984.
23. Gencay, S., Tapucu, A., Troche, N., and Merilo, M. Experimental Study of the Diversion Crossflow Caused by Subchannel Blockages, Journal of Fluids Engineering, Volume 106, December 1984.
24. Tapucu, A., Gencay, S., Troche, N., Merilo, M. Experimental Study of the Diversion Crossflow Caused by Subchannel Blockages, Journal of Fluids Engineering, Volume 106, December 1984.

1

2

3

## Section 11

### COMPUTER CODE DEVELOPMENT

EPRI has sponsored a great deal of code development effort. EPRI has supported the development of NRC codes, and also developed the RETRAN code. Each of these areas will be described.

#### 11.1 EPRI SUPPORT OF NRC CODE DEVELOPMENT

TRAC (Transient Reactor Analysis Code) is a computer code for best estimate analysis for the thermal hydraulic conditions in a reactor system. BWR component models were developed in one study (1). These models are necessary to structure a BWR-version of TRAC. These component models are the jet pump, steam separator, steam dryer, two-phase level tracking model and upper plenum mixing model. These models have been implemented into TRAC-BD2. Also a single channel option has been developed for individual fuel channel analysis following a system response calculation.

As a result of this work, qualified best-estimate models applicable to large LOCAs were developed and added to the BWR version of the TRAC code. The models demonstrated their accuracy in representing the physical phenomena and their ability to handle realistic BWR system interactions.

EPRI also performed a review of the application of TRAC-PD02 code (2). Comparison calculations were made using both the TRAC-P1A and TRAC-PD2 codes to simulate the EPRI-University of California at Berkeley reflood experiments, the FLECHT and FLECHT-SEASET experiments, the Semiscale MOD-1 test S-02-6, and the LOFT 11-4 test. The results indicate that the TRAC-PD2 can satisfactorily model portions of these experimental results.

EPRI has also sponsored work on the RELAP series of codes. RELAP4 and RELAP5 have been used to calculate NRC Standard Problems (3, 4, 5 and 6), to model the Two Loop Test Apparatus Experiments at GE (7), to model the LOFT non-nuclear tests (8), to perform operational transients (9), and to analyze a LOCA combined with a steam generator tube rupture (10).

EPRI also sponsored an effort to perform an impartial evaluation of the RELAP-5 code and to determine its capabilities and applications to various problems (11). These analyses helped to establish RELAP as a computer code suitable for best estimate LOCA calculations.

EPRI has also sponsored work (12) to develop methods for probabilistic quantification of uncertainties and identification of conservatisms in nuclear power plant safety analyses such as those performed for the loss-of-coolant accident (12). The process studies involves the use of best-estimate codes to determine the output distribution induced by input uncertainties. This particular task involved application of methods developed in a previous task to a code for which experimental data were available, and comparison of the experimental data to calculated uncertainty bounds derived from the output distribution. It was concluded that the methods developed provide a reasonable approach to studying the effect of uncertainties in a complex thermal-hydraulic code. Approaches for dealing with each of fit to linear or simple quadratic functions were also evolved.

This work is general in its application to determining the uncertainties of other best-estimate LOCA codes.

## 11.2 RETRAN

EPRI has sponsored the development of the RETRAN computer code (13-21). A versatile and reliable computer program for use in best estimate transient thermal-hydraulic analysis of light water reactor systems. The RETRAN-02 computer program is an extension of the RETRAN-01 program designed to provide analysis capabilities for (1) BWR and PWR transients, (2) small break loss of coolant accidents, (3) balance of plant modeling, and (4) anticipated transients without scram. RETRAN has been used for many different types of analyses. Of interest to this report are comparison of RETRAN results from the LOFT and SEMISCALE tests (22, 23), and the analysis of a small break LOCA (24, 25, 26). RETRAN has also been compared and validated by comparing the calculated results with actual plant transients. Among the transients analyzed are: the Crystal River Incident where a loss of power on an instrumentation bus eventually resulted in a reactor trip and turbine trip (27), the steam generator tube rupture at Prairie Island Unit 1 (28 29), and two LOFT ATWS tests (30).

These sets of calculations demonstrate the adequacy and application of RETRAN to small-break LOCA analysis and other thermal-hydraulic analyses.

#### REFERENCES

1. Alamgir, M. BWR Refill-Reflood Program: Final Report, NP-2377, NUREG/CR-2571, GEAP-22049, Electric Power Research Institute, U. S. Nuclear Regulatory Commission, and General Electric Company, February 1984.
2. Chan, R. K. C. Review and Application of the TRAC-PD2 Computer Code, NP-2826, Electric Power Research Institute, January 1983.
3. Sawtelle, G. R., et al. Comparison of RELAP4 Predictions with Standard Problems 1, 2 and 3, NP-0205, Electric Power Research Institute, November 1976.
4. Moore, K. V., et al. Analysis of GE BWR Blowdown Heat Transfer Program, Test 4906 (AEC Standard Problem Four), EPRI-0280-KR, Electric Power Research Institute, November 1975.
5. Fujita, N., et al. A Prediction of the Semiscale Blowdown Heat Transfer Test S02 8 (NRC Standard Problem Five), NP-0212, Electric Power Research Institute, October 1976.
6. Lyczkowski, R. W., et al. The Development of RELAP/SLIP for the Semiscale Blowdown Heat Transfer Test S-02-6 (NRC Standard Problem 6), NP-0343, Electric Power Research Institute, December 1976.
7. Burrell, N. S., et al. A RELAP4 Analysis of the GE BWR Blowdown Heat Transfer Two Loop Test Apparatus Experiments Tests 4902 4903 4904, NP-0169, Electric Power Research Institute, November 1976.
8. Davis, P. R., et al. Comparison of Experimental Results with Analytical Predictions for LOFT Nonnuclear Tests with Core Simulators, NP-0800, Electric Power Research Institute, May 1978.
9. White, J. R. Response of a B&W Lower Loop Plant to Overcooling Transients Using RELAP5, NSAC-71, Electric Power Research Institute, June 1984.
10. Jensen, R. T. Response of a B&W Plant to SG Tube Ruptures Resulting From a LOCA, NSAC-72, Electric Power Research Institute, July 1984.
11. Trapp, J. A. Descriptive Evaluation of RELAP-5, NP-2361, Electric Power Research Institute, April 1982.
12. Marshall, J. A., et al. Application of Statistical Evaluation Methodology to the RELAP Code, NP-1053, Electric Power Research Institute, April 1979.
13. Moore, K. V., et al. RETRAN a Program for On Dimensional Transient Thermal Hydraulic Analysis of Complex Fluid Flow Systems, NP-0408, Volume 1, Electric Power Research Institute, January 1977.
14. McFadden, J. H., et al. RETRAN-01 A Program for One-Dimensional Transient Thermalhydraulic Analysis of Complex Fluid Flow Systems, NP-2175, Electric Power Research Institute, December 1981.

15. McFadden, J. H., et al. RETRAN-02 A Program for Transient Thermal-Hydraulic Analysis of Complex Fluid Flow Systems, Volume 1: Theory and Numerics, (Revision 2), NP-1850, Volume 1, Electric Power Research Institute, November 1984.
16. McFadden, J. H., et al. RETRAN-02 - A Program for Transient Thermal Hydraulic Analyses of Complex Fluid Flow Systems, NP-1850 CCM-A, Revision 2, Electric Power Research Institute, 1984.
17. Peterson, C. E., Gose, G. C. and McFadden, J. H. RETRAN-02 - A Program for Transient Thermal Hydraulic Analyses of Complex Fluid Flow Systems, Volume 4 Applications, NP-1850 CCM, Volume 4, Electric Power Research Institute, January 1983.
18. Agee, L. J., Editor, Conference Proceedings: First International RETRAN Conference, WS-80-150, Electric Power Research Institute, April 1981.
19. Agee, L. J., Editor, Conference Proceedings: Second International RETRAN Conference, NP-2494-SR, Electric Power Research Institute, July 1982.
20. Agee, L. J., Editor, Conference Proceedings: Third International RETRAN Conference, NP-3803-SR, Electric Power Research Institute, February 1985.
21. Agee, L. J. RETRAN Thermal-Hydraulic Analysis: Theory and Applications, in "Progress in Nuclear Energy," Volume 10, No. 1, pp. 19-67.
22. Feinauer, et al. Comparison of Experimental Results with Analytical Predictions for LOFT Test L2-2, NP-1204, Electric Power Research Institute, November 1979.
23. Sawtelle, G. R. RETRAN Analysis of Semiscale Tests S-02-8 and S-06-4, NP-1373, Volumes 1 and 2, Electric Power Research Institute, March 1980.
24. Clements, T., et al. Analysis of a Hot Leg SBLOCA in a Three-Loop Westinghouse PWR Plant, NSAC-68, Electric Power Research Institute, April 1984.
25. Agee, L. J., and Naser, J. Small Break Loss-of-Coolant Accident Analyses in LWRs, Specialists Meeting, Monterey, California, August 25-27, 1981.
26. Fader, G. B., Calia, C., and Kessler, T. C. Evaluation of RETRAN-02 Capabilities for Small Break LOCA Analysis, NP-2816, Electric Power Research Institute, January 1983.
27. Brown, W., et al. Thermohydraulic Analysis of Crystal River-Unit 3 Incident, NSAC-15, Electric Power Research Institute, June 1981.
28. Chao, J., et al. Using RETRAN-02 and DYNODE-P to Analyze Steam Generator Tube Breaks, NSAC-47, Electric Power Research Institute, May 1982.
29. Peterson, C. E., et al. Response of a W Two-Loop Plant to Steam Generator Tube Ruptures, NSAC-77, Electric Power Research Institute, July 1984.
30. Hendrix, C. E. RETRAN-02 Analysis of LOFT ATWS Experiments, NSAC-78, Electric Power Research Institute, November 1984.

APPENDIX C

INSTRUMENTATION DEVELOPMENT PROGRAM AND RESULTS



## APPENDIX C

### INSTRUMENTATION DEVELOPMENT PROGRAM AND RESULTS

C.1	PURPOSE AND ORGANIZATION OF APPENDIX C .....	C-1
C.2	OVERVIEW .....	C-2
C.3	MEASUREMENT REQUIREMENTS .....	C-2
C.3.1	Model Development .....	C-2
	A. Blowdown Phase .....	C-4
	B. Refill Phase .....	C-4
	C. Reflood Phase .....	C-4
C.3.2	Code Assessment .....	C-5
	A. Blowdown Phase .....	C-5
	B. Refill Phase .....	C-5
	C. Reflood Phase .....	C-5
C.4	DEVELOPMENT PROGRAMS .....	C-6
C.5	RESULTS OF INSTRUMENTATION DEVELOPMENT--CATEGORY I .....	C-6
C.5.1	Dragbody .....	C-6
C.5.2	Turbine Meter.....	C-9
C.5.3	Gamma Densitometer .....	C-9
C.5.4	Conductance Liquid Level Detector .....	C-10
C.5.5	Spool Piece .....	C-10
C.6	RESULTS OF INSTRUMENTATION DEVELOPMENT--CATEGORY II .....	C-14
C.6.1	Impedance Probes .....	C-14
C.6.2	Film Probe .....	C-16
C.6.3	Tie Plate Flow Measurement Package .....	C-21
C.6.4	Other Instruments .....	C-28
C.6.4.1	Pulsed Neutron Activation .....	C-28
C.6.4.2	Steam Superheat Probe .....	C-33
C.6.4.3	Laser Doppler Anemometer .....	C-33
C.6.4.4	Heated or Cooled Thermocouples .....	C-38
C.6.4.5	Optical Liquid Level Detectors .....	C-38
C.7	REFERENCES .....	C-42



## C.1 PURPOSE AND ORGANIZATION OF APPENDIX C

The purpose of this appendix is to describe the instrumentation development efforts that were carried out specifically as a part of the overall LOCA ECCS research. Section 4.4 of this report provides a historical overview of ECC research instrumentation needs and development. As discussed in that section, the bulk of the required instruments for the major experimental programs were based on "conventional" measurement technologies (e.g., thermocouples, pressure and differential pressure cells, orifices, etc.). In most of these cases, though, special efforts were required to "adapt" the technology to the specific applications. An example is clad thermocouples, i.e., thermocouples were a well-established technology at the outset of ECC research, but the installation of thermocouples on the clad surfaces of nuclear and electric rods had to be substantially developed, particularly when all the other requirements of the measurement were considered (e.g., fast response, maintain integrity throughout severe transients, etc.). This "adaptation" of conventional technologies was a major part of the overall instrument development and in general was successful.

In addition to the conventional instruments which were adapted as discussed above, numerous additional measurement technologies were developed for use in ECCS research facilities. These development efforts were entirely in the area of gaining increased local information about two-phase flows, as opposed to relying only on "global" information such as net mass/energy balances. This development proved to be very challenging, primarily because of the inherent nature of two-phase flow (large number of independent hydraulic parameters, high turbulence, possibility of many flow regimes, etc.). Accordingly, the development effort focused on developing sensors which measured specific two-phase flow quantities (e.g., a gamma densitometer measuring void fraction) or "suites" of instruments in very specific geometries which could be used to determine a more complete measurement of the flow (e.g., piping spool piece equipped with multiple instruments).

This appendix describes the instrumentation development program and results and is organized as follows:

- o First, an overview is given of the objectives of the program and the primary experimental facilities which drove the program (Section C.2).
- o Next, a general discussion of the measurement requirements, including the data requirements for different phases of a LOCA is given (Section C.3).
- o An overall discussion of the development program, covering the numerous instruments and contractors involved is presented (Section C.4). The instruments "adapted" from conventional technologies for use in LOCA-ECCS research are identified in this section but are not discussed in detail in this appendix. The "developmental" instruments are identified and divided into two

groups--Categories I and II. Category I consists of those instruments providing reliable, high-priority information which can be meaningfully compared to the predictions of computer codes. Category II consists of those instruments providing useful, supplementary information for model development and insight.

- o Next, the development and results for the Category I instruments are discussed (Section C.5).
- o Finally, the development and results for the Category II instruments are discussed (Section C.6).

## C.2 OVERVIEW

The objectives of the instrument development program were to:

- o Evaluate, modify, and adapt instrumentation to the measurement needs of various separate effects and integral facilities, and
- o Develop new instrumentation to fill in the measurement gaps.

The NRC Reactor Safety Research (RSR) program received responsibility for the instrumentation research and development program in 1976. This program grew and evolved to meet part of the measurement needs of the LOFT Program and most of the measurement requirements of the 2D/3D Program (References C-1, C-2, and C-3).

To meet the measurement requirements, the instrumentation R/D Program gradually evolved into an extensive program involving many national laboratories and universities. In the subsequent sections, the instrumentation needs will be discussed, the RSR Instrumentation R/D Program described; and the results presented.

## C.3 MEASUREMENT REQUIREMENTS

The measurements to be made in the RSR experiments were to meet the needs of model development and code validation (see Table C-1).

In the subsequent sections, the parameters for each of the above categories will be discussed in terms of physical phenomena and locations. For each section, the parameters will be listed according to the important phases encountered during a hypothetical LOCA-ECC event, namely blowdown phase, refill phase and reflood phase.

### C.3.1 Model Development

For model development needs, the physical properties to be measured are usually of a detailed and local nature. The knowledge of these parameters enables researchers and code developers to postulate or verify the thermal-hydraulic models used in the various codes. They can be measured either in separate effects tests or integral tests. If they are

TABLE C-1. INSTRUMENTATION REQUIRED FOR CODE VALIDATION AND MODEL DEVELOPMENT

Parameter	Devices	Development Needed?
Temperature of fluids	Thermocouples	No
Temperature of metal	Thermocouples	No
Temperature of clad	Thermocouples	Rod fabrication Inversion code
Superheat temperature of steam	Shielded thermocouple	Needs development
Pressure of system	Pressure transducer	No
Pressure difference	dp-cells	No
Void fraction	dp-cell String probe Conductance probe $\gamma$ -densitometer PNA RF-densitometer Light-densitometer	No--But for slow transients Yes--New device Yes--New device Yes--Need to improve accuracy Yes--Spatial distribution model Yes--New device Yes--New device
Velocities	Turbine meter Transit time	No--Application in homogeneous flow only Yes--Modeling needed--limited application and range
Film velocity and thickness	Film probe	Yes--New device
Flow rates	Spool piece--combination of dragbody, turbine and $\gamma$ -densitometer	Yes--Each component needs improvement modeling for combined result
Visual	Storz lens Optical probe	Yes--Hardware development Yes--Enhance image
Tie-plate flows	Special package of drag-plate, turbine, dp, and breakthrough detector	Yes--New concept, hardware, modeling, calibration are all needed

measured in integral tests, these parameters can also be used for diagnostic purposes to identify deficiencies in the code. The model development parameters are usually more difficult to measure but not crucial to code validation. Thus, they can be obtained with advanced, developmental type instrumentation. The following are the model development data requirements:

A. Blowdown Phase

- o Rod temperature (for Critical Heat Flux)
- o Core void fraction
- o Break mass flow rate for critical flow
- o Mass flow rate in loop piping
- o Pressure
- o Liquid inventory in reactor coolant system components

B. Refill Phase

- o Mass flow rate in and out of cold and hot legs
- o Liquid inventory and void distribution in downcomer
- o Liquid level in reactor vessel lower plenum

C. Reflood Phase

1. In the core:

- o Liquid level
- o Local fluid temperature, including steam temperature
- o Fluid velocity and void fraction at boundaries, (e.g., reactor vessel nozzles, tie plates, etc.)
- o Heater rod temperature
- o Average void fraction at various levels in the core
- o Droplet size distribution and temperature distribution near grid-spacers and at any flow blockage

2. In the upper plenum:

- o Film thickness and velocity on vertical structures

- o Liquid level
  - o Void fraction and velocity near hot legs
3. Loops:
- o Phase mass flow rate
  - o Pressure drop

### C.3.2 Code Assessment

The code assessment data are used to check the code performance. The primary objective of the LOCA test facilities is to provide code-assessment measurements. These parameters are usually more global in nature to provide information on the state or mass/energy balance of a system or major component. They must be more reliable and accurate than those of the model-development category. Thus, only proven devices are normally used to provide code-assessment measurement.

The following is a list of code assessment parameters:

#### A. Blowdown Phase:

- o Fluid temperature
- o Fluid pressure
- o Cladding temperature
- o Break flow
- o Mass flow rates in the hot and cold legs
- o Fluid inventory in core

#### B. Refill Phase:

- o Mass flow rate in each leg
- o Liquid level in core
- o Fluid temperature
- o Fluid pressure

#### C. Reflood Phase

- o Fluid temperature

- o Clad temperature
- o Pressure
- o Liquid level in core, downcomer and upper plenum
- o Steam mass flow rate leaving core and flowing through each loop
- o Water carryover flow rate to hot legs
- o Pressure drop in primary loops and from primary system to containment
- o Containment pressure
- o Flow rate into the containment
- o Temperature distribution near grid-spacer or blockage

#### C.4 DEVELOPMENT PROGRAMS

To provide measurements of the parameters listed in the previous section, various types of instrumentation were needed. They are listed in Table C-2.

To meet the instrumentation needs, many new transducers had to be developed and existing transducers modified or improved. Many national laboratories and universities participated in the concerted efforts of developing advanced instrumentation for reactor safety research. As discussed above, the instruments grouped as Category I instruments were mainly used. Category II instruments were generally used for model development.

#### C.5 RESULTS OF INSTRUMENTATION DEVELOPMENT--CATEGORY I

The instruments in this category were developed and applied to many RSR sponsored test facilities. The following is a discussion of the development of these instruments.

##### C.5.1 Dragbody (See References C-4 and C-5)

The dragbody measures fluid momentum flux by sensing the force applied to a body held in the flow. The dragbody was originally made in the form of a disk. Later many different forms were designed such as perforated plates or screens covering the whole pipe. These new configurations sampled the momentum flux across the entire flow cross-section in small diameter pipes. In the later models, the dragbody for large pipes was hinged on three points and instrumented with three strain gages (Figure C-1). This improvement was instituted to sense uneven distributions of momentum flux over the pipe cross-section.

TABLE C-2. CATEGORIZATION OF INSTRUMENTS

---

I. Category I--Proven items, for code validation purposes

Drag body

Turbine

$\gamma$ -densitometer

Spool pieces for combination of above

Liquid level detector

II. Category II--Items to be developed, for model development use

Impedance probes

Film probe

Storz lens and optical probe

Superheat steam thermocouples

Pulse neutron activation (PNA)

Laser Doppler anemometry (LDA)

Ultrasonic probes

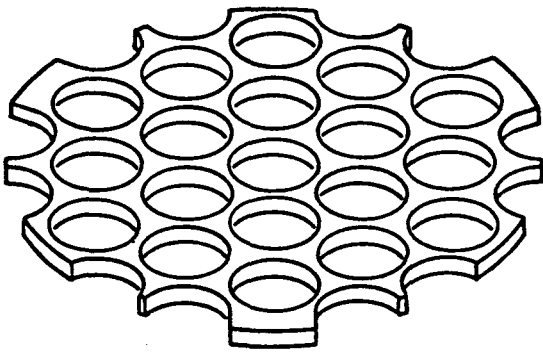
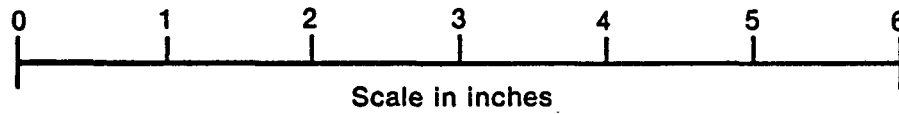
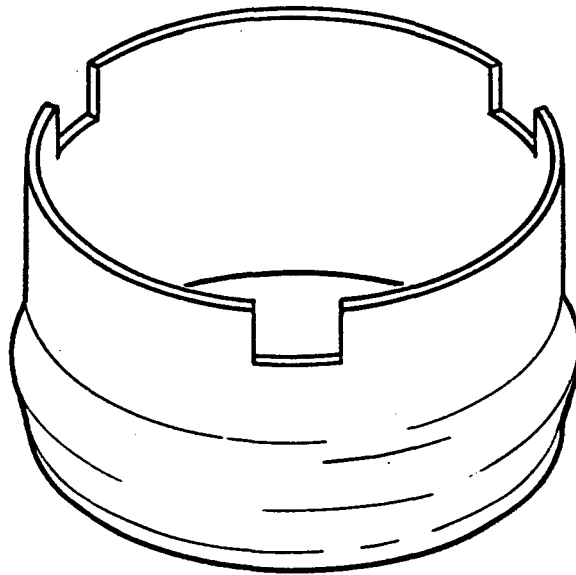
Radio-frequency and visual light densitometers

Heated/cooled thermocouples

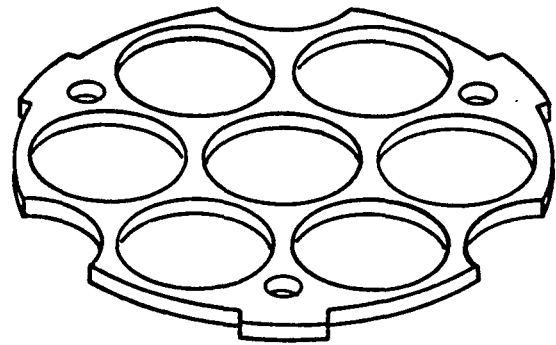
Holography and tomography

Neutron noise analysis

---



$$\frac{A_0}{A_t} = 0.67$$



$$\frac{A_0}{A_t} = 0.77$$

6 2943

Figure C-1. Rigid plate configurations used for design evaluation.

An alternative is to use an array of dragbodies which provide sampling of momentum flux at specific points over the pipe cross-section. By suitably combining the individual dragbody outputs, the average pipe momentum flux can be determined.

### C.5.2 Turbine Meter (See Reference C-6)

The turbine meter measures fluid velocity by sensing the rotational speed of a free-spinning turbine in the flow. The turbine meter has been a standard velocity measurement instrument for single-phase flow. However, when it is used in two-phase flow, the phase separation causes several problems. The major problem is that the two phases can be flowing at different velocities. Another problem is the wearing of bearings under a high temperature steam-water environment since hot dry steam does not lubricate the bearing.

The improvements made on turbines under the RSR instrumentation program are:

- o Development of a turbine flow model which accounts for the different forces acting on the turbine blades.
- o Development of long-wearing bearings to prolong the life of turbines.

As with the dragbody described in Section C.5.1, two types of turbine meters have been used in the various LOCA-ECCS facilities:

- o A "full-flow" turbine which measures the velocity over the entire pipe cross-section.
- o A "turboprobe" which measures the velocity at a specific location in the cross-section.

### C.5.3 Gamma Densitometer (See Reference C-7)

A gamma densitometer measures fluid density by sensing the attenuation of a beam of gamma radiation passing through the fluid. The early interest in reactor safety testing was in large breaks. Correspondingly, the emphasis in fluid density determinations was on fast response measurements, short duration tests, low void fractions, high pressures and more-or-less homogeneous two-phase flow regimes. The densitometers for these measurements were multiple beam, large source strength (20-30 Curie) and high photon energy (662 keV). This allowed the beam to penetrate through the thick stainless steel pipe walls and achieve rapid frequency response (1-10 ms).

As interest expanded into the reflood portion of a postulated accident (and into small-break tests after the TMI incident), emphasis changed to medium pressures, high void fractions, large ratios of liquid to vapor density and much longer tests with lower frequency response needs. Also,

two-phase regimes (such as stratified flow) in horizontal piping runs became important. Longer tests and lower frequency response permitted use of smaller source strengths. Accuracy requirements in high void fraction conditions and measurement requirements in small pipes was the driving force for RSR Instrumentation program development of multiple beam low photon energy densitometers (Figures C-2, C-3). These were facilitated by use of (a) transparent beryllium pressure boundary inserts, and (b) good energy resolution germanium and silicon solid state detectors.

#### C.5.4 Conductance Liquid Level Detector (CLLD)

The conductance liquid level detector (CLLD) is basically a stalk containing an array of electrodes at various elevations. The presence of water at an electrode closes the circuit and thus the distribution of closed or open gaps indicates the water level. An array of CLLDs can be used to measure the three-dimensional steam-water distribution within a region. CLLDs were used in most of the LOCA-ECCS facilities including Semiscale, LOFT, and the Japanese SCTF and CCTF facilities.

#### C.5.5 Spool Piece (See References C-8 through C-10)

A spool piece typically consists of a dragbody, turbine, densitometer, pressure sensor and thermocouple, all mounted in a "spool" of pipe (see Figure C-4). The purpose of a spool piece is to determine two-phase mass flow rates and void fraction. With a spool piece the mass flow rate (M), for homogeneous flow can be calculated in three different ways as follows:

$$\begin{aligned} M_1 &= \rho_d U_t A \\ M_2 &= (\rho U^2)_{db} A / U_t \\ M_3 &= A [(\rho U^2)_{db} \rho_d]^{1/2} \end{aligned}$$

where

$$\begin{aligned} \rho_d &= \text{density from the gamma densitometer measurement} \\ (\rho U^2)_{db} &= \text{momentum flux from the dragbody measurement} \\ U_t &= \text{velocity from the turbine measurement} \\ A &= \text{pipe flow area} \end{aligned}$$

For non-homogeneous flow conditions (e.g., including separation or slip between the phases), an alternate set of equations must be used which properly account for the effects of the individual phase conditions on the responses of the spool piece instruments. Examples of such techniques are discussed in Reference C-4.

Spool pieces using full flow measurements have been made for pipes of up to 20 cm in diameter. For large pipes, it is generally not practical to

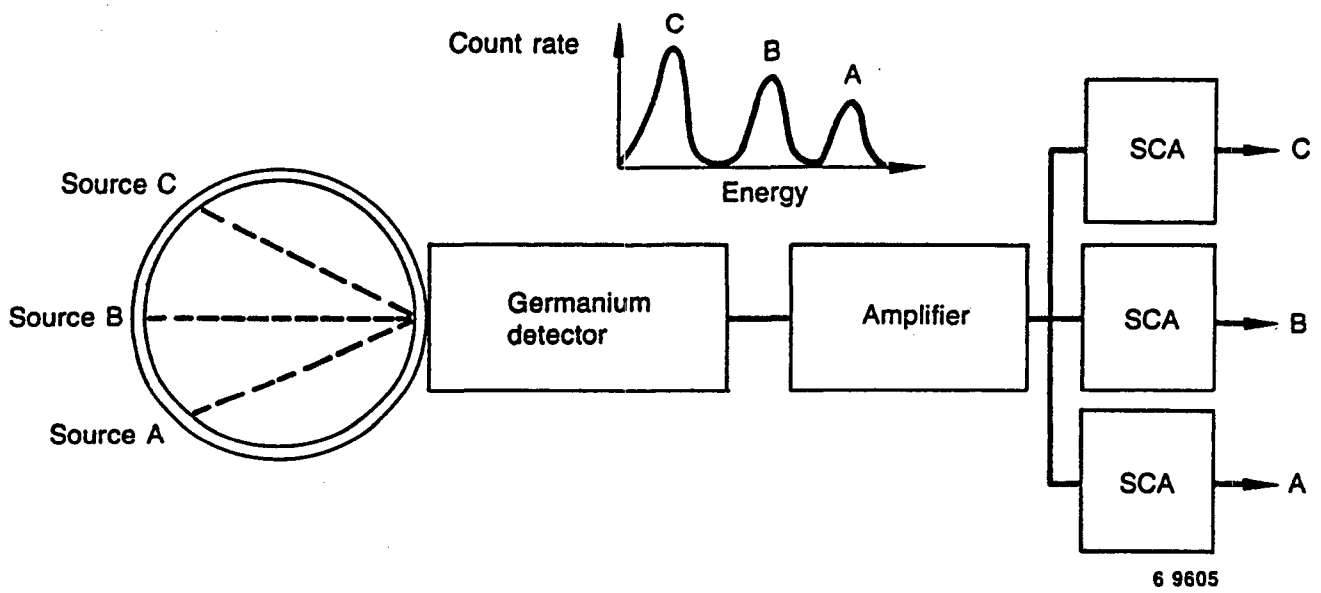
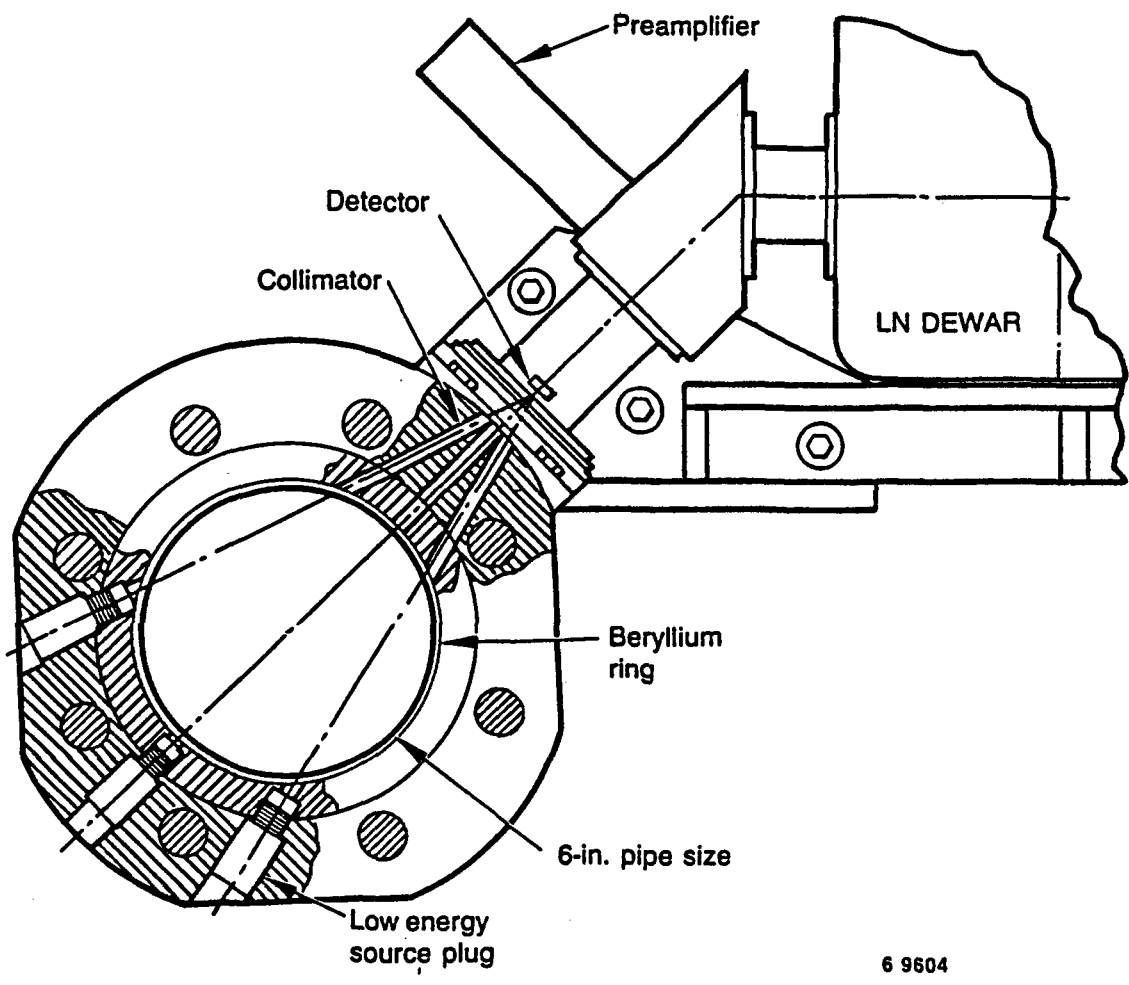
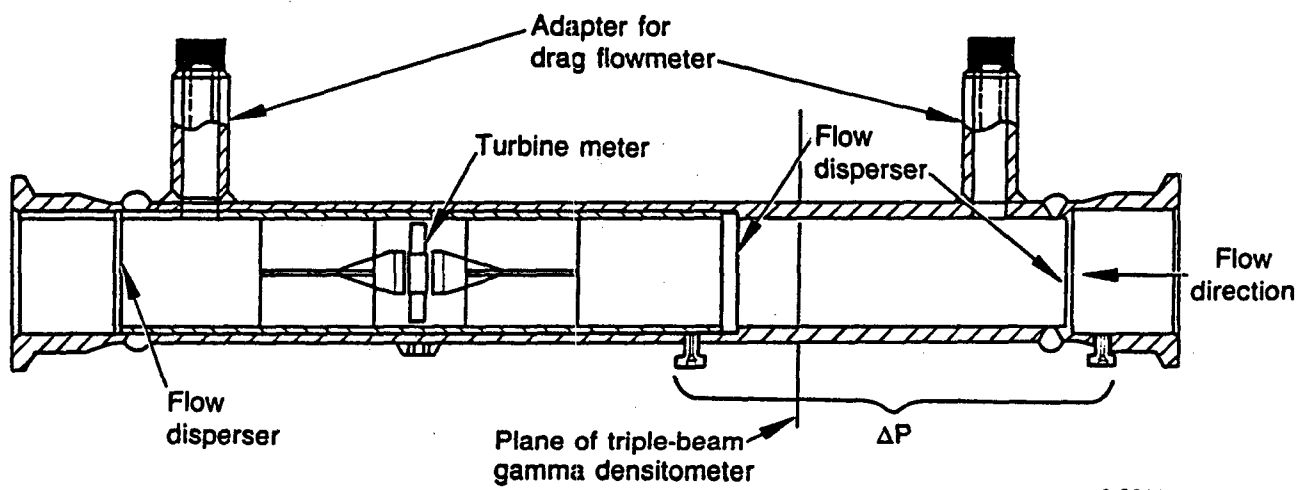


Figure C-2. Low energy densitometer (Semiscale densitometer).



6 9604

Figure C-3. Multisource arrangement.



6 9611

Figure C-4. Instrumented piping spool piece used in air-water testing.

use full flow turbine meters, and drag bodies and arrays or rakes of turbine meters or pitot tubes must be used. For free field measurements, care must always be exercised to ensure correct spatial sampling through proper location of sensors. Another problem with the spool piece is the flow disturbance caused from upstream elbows, upstream sensing devices, or other transducers. The shadow effect is particularly strong if a turbine meter is upstream of a drag screen (or plate). Thus, for bidirectional flow, it is desirable to have a drag screen located on both sides of the turbine meter so that in either flow direction there is always a dragbody upstream of the turbine meter. An additional benefit of having two dragbodies is that additional information on flow velocity can be inferred from cross-correlation of signals from the two sensors and used to check the turbine meter velocity.

## C.6 RESULTS OF INSTRUMENTATION DEVELOPMENT--CATEGORY II

Since the model development for codes requires a great deal of information of local physical parameters, many new measuring techniques and devices had to be developed to meet the need. For developing these instruments, NRC Instrumentation Development Program provided the funding to stimulate the instrumentation community and to enhance the awareness of the importance of flow modeling in addition to hardware development.

Many advanced instrumentation devices and related models were developed. The majority were developed for measuring incore conditions during reflood, with another significant fraction developed for the LOFT application. A third and small fraction were developed by the universities to aid in thermal hydraulic model development. These were used on bench-scale experiments.

### C.6.1 Impedance Probes

(See References C-11 through C-16 and Pages IV.10-1 through 16 and IV.11-1 through 21 of Reference C-3)

The measurement principle of impedance probes is that the impedance between two electrodes in a two-phase medium varies as the void fraction between the electrodes changes. This principle is an extension of the concept used in the conductivity liquid level detectors, which sense a change in impedance in a very small sensing region and infer the presence of either all steam or all water. The sensing regions of impedance probes are somewhat larger than the conductivity liquid level detectors, although the impedance probes are still very local measurements on the scale of LOCA experiments. Figure C-5 shows several different impedance probe configurations developed by ORNL.

Impedance probes were also fabricated in pre-arranged pairs (see flag probes on Figure C-5) with the intent that cross-correlation of the signals between sensors in a pair would yield a local velocity measurement.

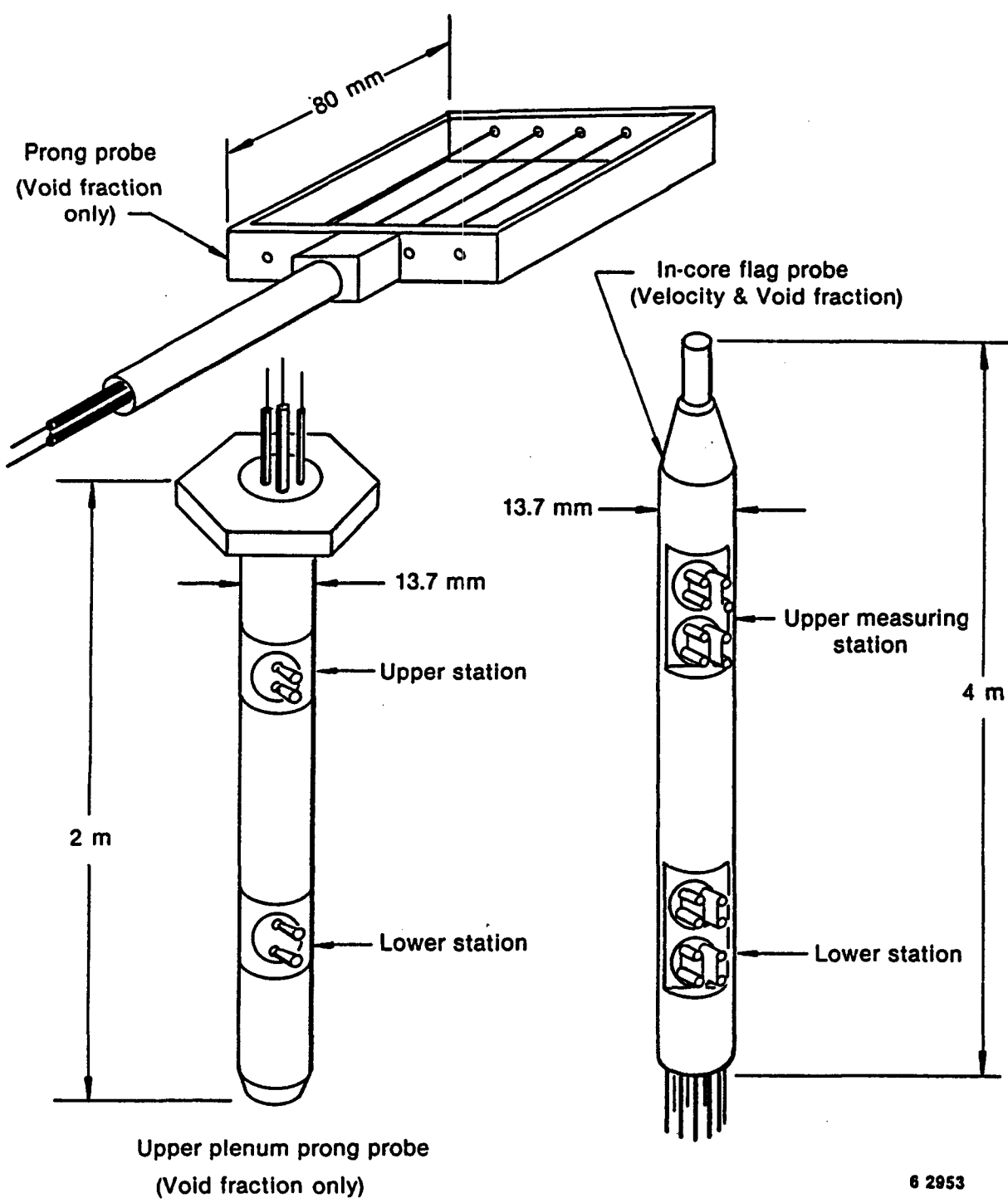


Figure C-5. Three types of impedance probes for use in high temperature environments.

The impedance probe development program was initiated at ORNL in the mid-1970s, primarily to support the 2D/3D Program. The immediate technical challenge of this program was the development of suitable electrical insulators. These electrical insulators had to be:

- o Large in size, compared to previous insulators.
- o Able to withstand severe thermal transients without degrading.
- o Able to be bonded to metal and form part of a pressure boundary.

At the outset of the development program, no existing insulators were suitable. A major early success of the program was the development of a ceramic-metal (cermet) material which fulfilled the requirements.

Impedance probes of the types shown in Figure C-5 were fabricated by ORNL and installed in five major test programs (PKL-II, CCTF-II, SCTF-I, SCTF-II and SCTF-III). At least a fraction of the instruments provided valid data from each of these facilities. The primary results and drawbacks were:

- o The in-core probes suffered from attrition as the number of thermal transients accumulated (Table C-3). Ex-core probes generally survived well.
- o In most cases, the data from prearranged probe pairs was not sufficiently coherent to obtain usable velocity data.
- o The void fraction data had an uncertainty which was not well quantified. This is due to the variety of modeling assumptions (e.g., dispersed or separated regime) which can be made in the data interpretation (Figure C-6).

Figure C-7 shows the ORNL calibration test data for a prong probe which compared the measured void fraction to a gamma densitometer void fraction. Figure C-8 shows PKL-II prong probe data compared to the void fraction determined from a differential pressure measurement in the same region.

#### C.6.2 Film Probes

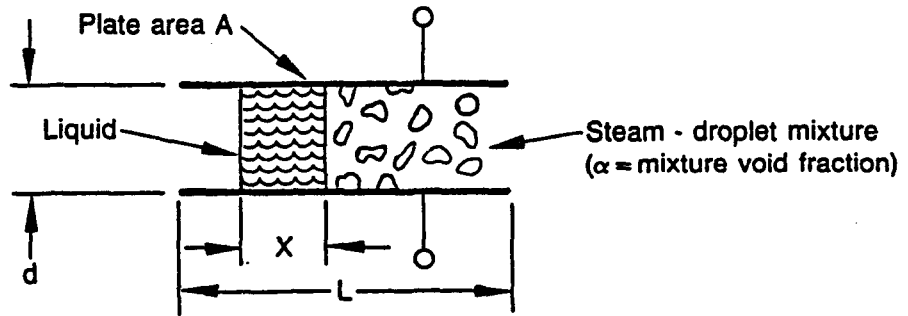
(See Pages I.10-1 through 14 in Reference C-1 and Pages IV.13-1 through 30 of Reference C-3)

The measurement principle of film probes is similar to that of the impedance probes discussed above, i.e., the impedance between two electrodes varies as the fraction of water between the two electrodes changes. By fabricating the two electrodes flush on a surface, the instrument becomes most sensitive to the thickness of a film on the surface. Furthermore, the instrument output can be "normalized" by dividing the conductance between electrodes by the electrode-to-ground

TABLE C-3. SURVIVAL RATE OF ORNL ADVANCED INSTRUMENTATION

<u>Facility</u>	<u>As of</u>	<u>Installed</u>	<u>Good</u>	<u>Marginal</u>	<u>Bad</u>
SCTF-I	4-81	46	23	14	9
	6-81	46	10	4	32
	10-81	46	16	2	28
	12-81	46	6	10	30
	9-82	46	5	11	30
PKL-II	6-82	25	17	0	8
	4-83	25	11	0	14
CCTF-II	3-82	39	33	1	5
	9-82	39	20	5	14
	5-83	39	16	9	14
	10-83	39	15	8	16
SCTF-II	8-83	32	32	0	0
	12-83	32	28.5	2	1.5

Parallel plate admittance can be calculated for various distributions



Admittance relationships

(a) Admittance  $Y_T = G_T + j \omega C_T$   
 Total conductance  $G_T$  and Total capacitance  $C_T$

(b) Capacitance  $C_T = C_l + C_{mix} = \frac{A}{d} \left[ \epsilon_l \left( \frac{X}{L} \right) + \epsilon_{mix} \left( 1 - \frac{X}{L} \right) \right]$

(c) Conductance  $G_T = G_l + G_{mix} = \frac{A}{d} \left[ \sigma_l \left( \frac{X}{L} \right) + \sigma_{mix}^0 \left( 1 - \frac{X}{L} \right) \right]$

(d) Loss angle  $\tan Y = \frac{G}{\omega C_T} = \frac{\sigma_l \left( \frac{X}{L} \right)}{\omega \left[ \epsilon_l \left( \frac{X}{L} \right) + \epsilon_{mix} \left( 1 - \frac{X}{L} \right) \right]}$

(e)  $\epsilon_{mix} = \epsilon_{stm} \left[ \frac{\epsilon_l [1 + n(1 - \alpha_m)] + n \alpha_m \epsilon_{stm}}{\epsilon_l \alpha_m + \epsilon_{stm} (n + 1 - \alpha_m)} \right]$

( $\alpha_m$  = void fraction of dispersed region)

6 9600

Figure C-6. Calculation of fluid mixture admittance for parallel plate electrodes.

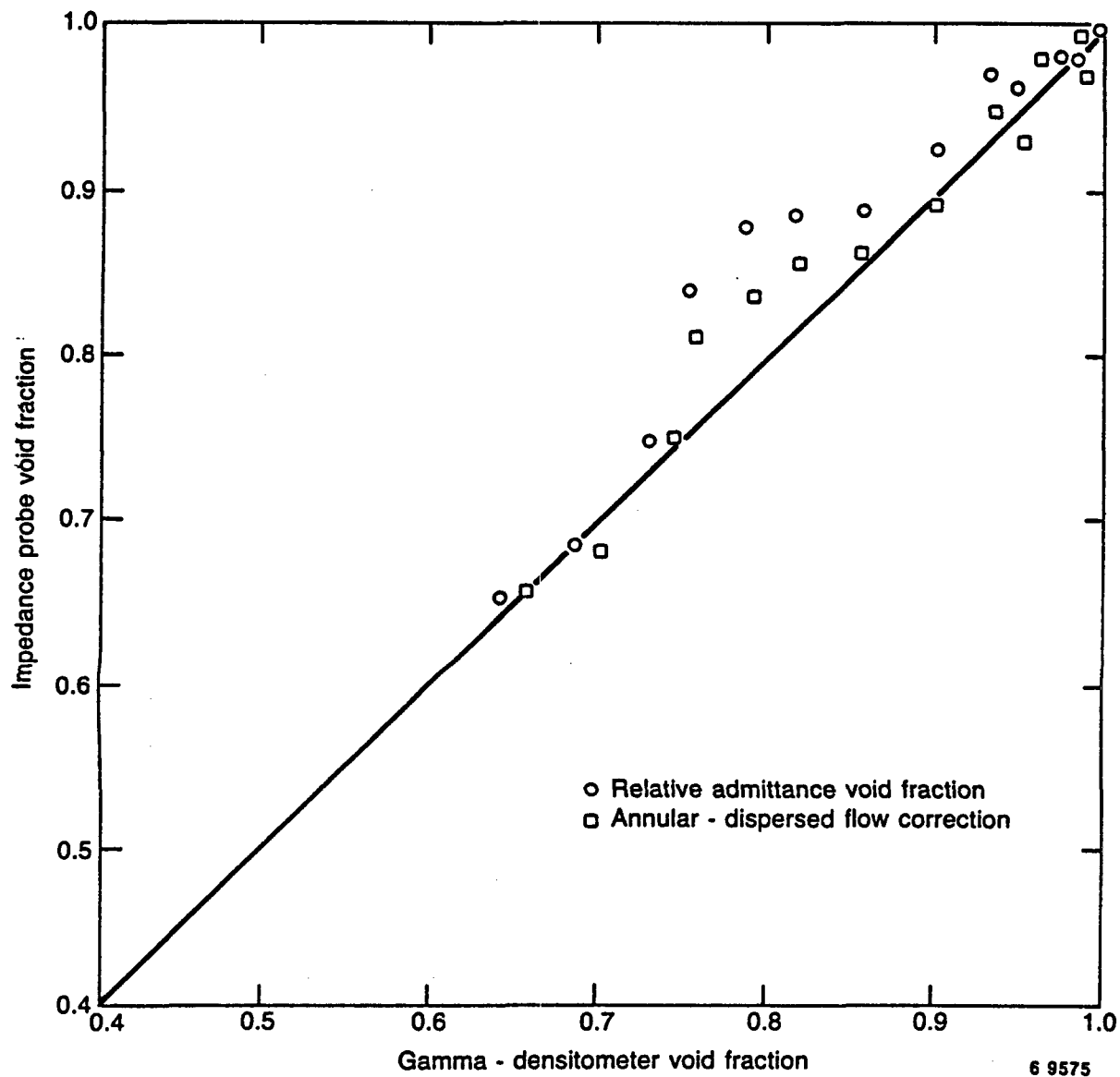


Figure C-7. Prong probe void fraction versus gamma densitometer steam, water tests (T=330°F).

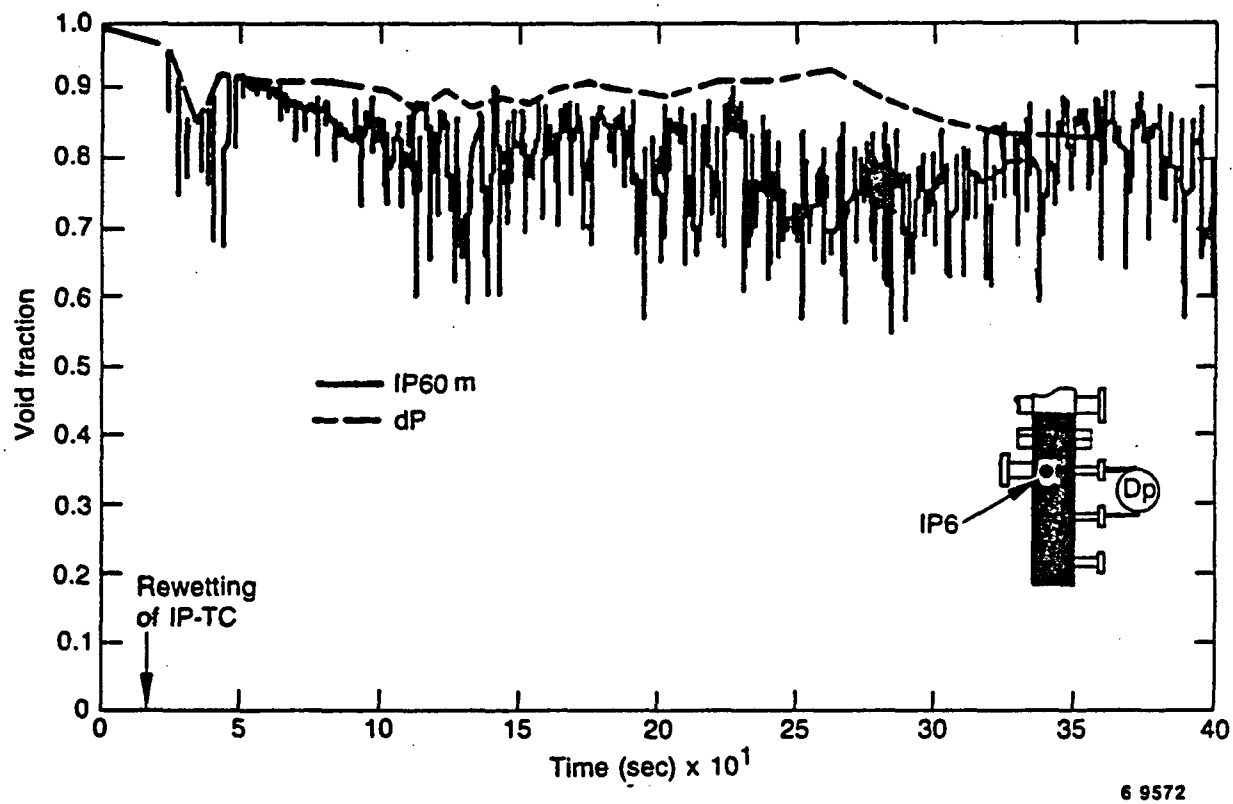


Figure C-8. Comparison of void fraction measurement for in-core prong probe IP6DM and dP transducer during Run PKL.II A.9.

conductance, which tends to remove the effect of water conductivity (temperature) variation. A typical film probe response is shown in Figure C-9, and a typical film probe module is shown in Figure C-10.

As shown in Figure C-10, film probes were fabricated in prearranged pairs, once again with the intent of determining velocity by cross-correlation. Also, a special "electrolysis potential" film velocity probe was developed, which determined velocity by measuring DC current between two flush wall electrodes.

Film probes were developed by ORNL in the same period of time as the impedance probes. The same cermet insulator material was used (see Section C.6.1, above). Film probes were supplied to the same five major programs as impedance probes (PKL-II, CCTF-II, SCTF-I, SCTF-II and SCTF-III). The majority of the instruments provided valid data from each of these facilities. The major findings were:

- o The film thickness sensors provided valid data in the majority of applications. Sensors mounted on in-core rods tended to fail eventually due to severe thermal transients.
- o Data from film probe pairs was not sufficiently coherent to obtain usable velocity data by cross-correlation.
- o The method of obtaining film velocity by the electrolysis potential sensor did not provide meaningful data, mainly because this method is very sensitive to water conductivity, film thickness and film configuration. The method was shown to work in ideal laboratory conditions but useful field data were not obtained.

In general, films on in-vessel vertical surfaces were found to be less than a millimeter to a few millimeters thick. Although film velocity measurements were not made, these film thicknesses are larger than would normally be expected for free-falling gravity films. The larger thickness implies the films being measured were being "held up" by the steam flow.

### C.6.3 Tie Plate Flow Measurement Package (See References C-17 and C-18)

In the 2D/3D reflood tests, it is desirable to know the flow rates across the fuel assembly upper tie plates so that mass balances on the core and upper plenum region can be performed. Since the upper tie plate flow is two-phase, bidirectional and transient in nature, it is very difficult to perform accurate measurements. NRC developed a measurement methodology which used measurements of momentum flux, velocity and void fraction. It was anticipated these measurements would be obtained by, respectively, tie plate differential pressure, turbine meter probe above the tie plate, and collapsed level (differential pressure) above the tie plate. These instruments were essentially fully developed, except it was recognized

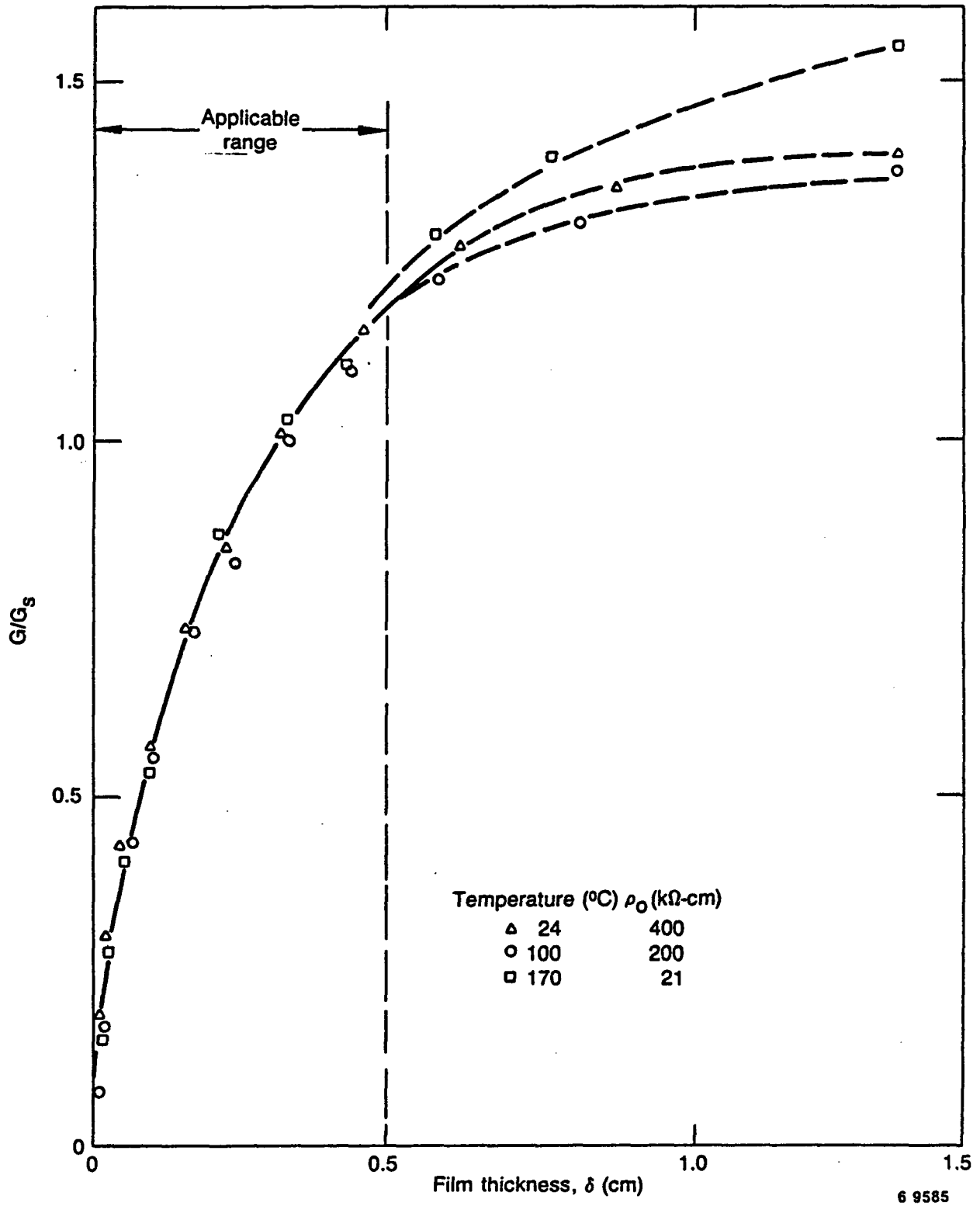
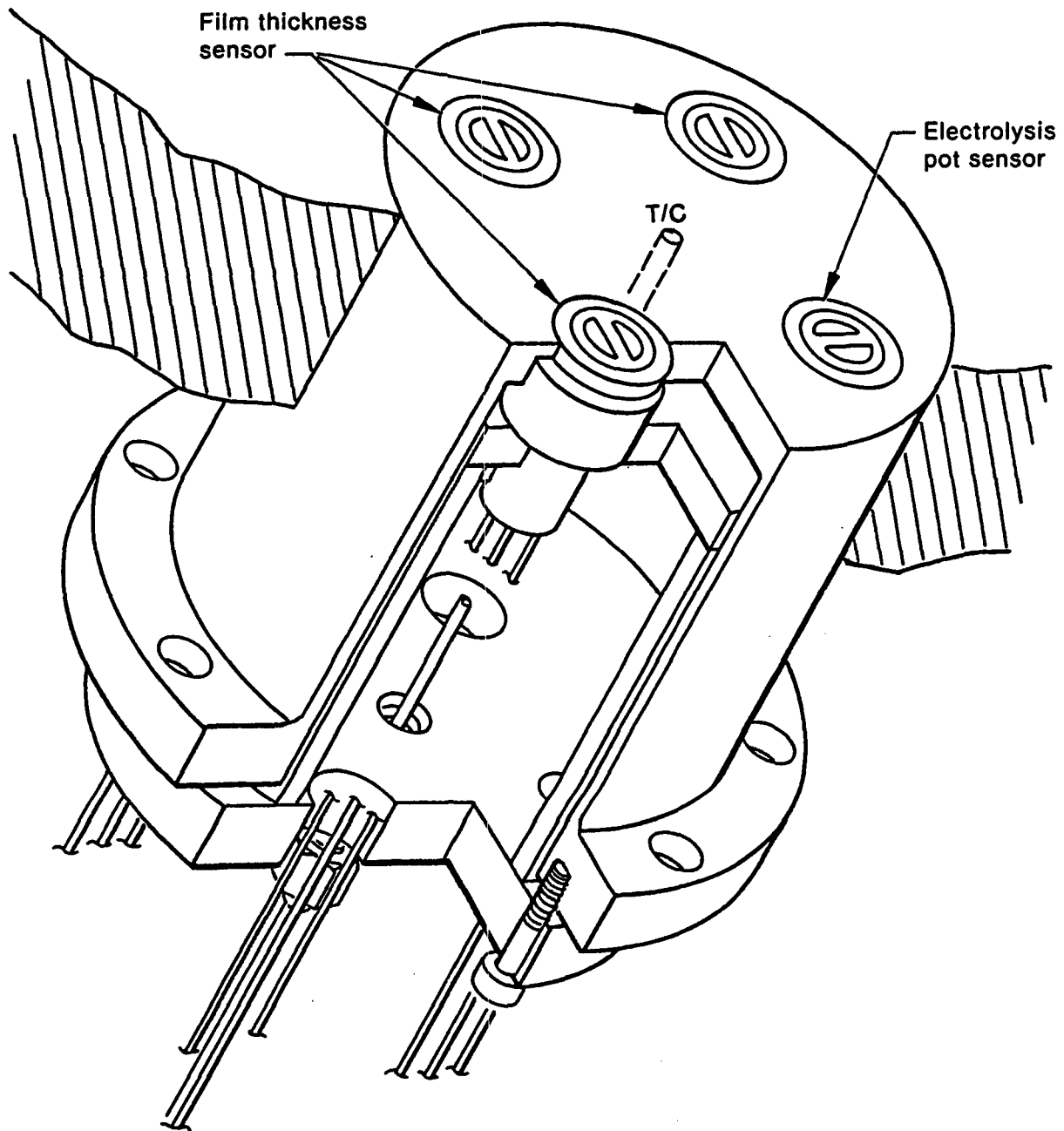


Figure C-9. Variation of conductance ratio with film thickness for probe.



6 2956

Figure C-10. ORNL film probe design for SCTF-1 wall and upper plenum.

there would be special problems in UPTF with differential pressure measurements due to very long tap lines. However, these instruments had not been calibrated in two-phase flow in a tie plate geometry.

ORNL carried out the required instrument development work and calibration tests in two-phase flow. In the area of differential pressure measurements, ORNL developed a long-line, water filled, continuously purged system for use in UPTF. The continuous purging was required because the tap lines passed through hot areas of the facility which would have vaporized the water in the lines. ORNL also identified and developed an improved method for making the tie plate momentum flux measurement in the form of a tie plate dragbody. This instrument involved separating a portion of the tie plate and suspending it in place with a strain gage force transducer (Figure C-11). The advantage of this instrument is that it sampled a significant fraction (70%) of the tie plate area, providing a more steady, reliable measurement than the differential pressure.

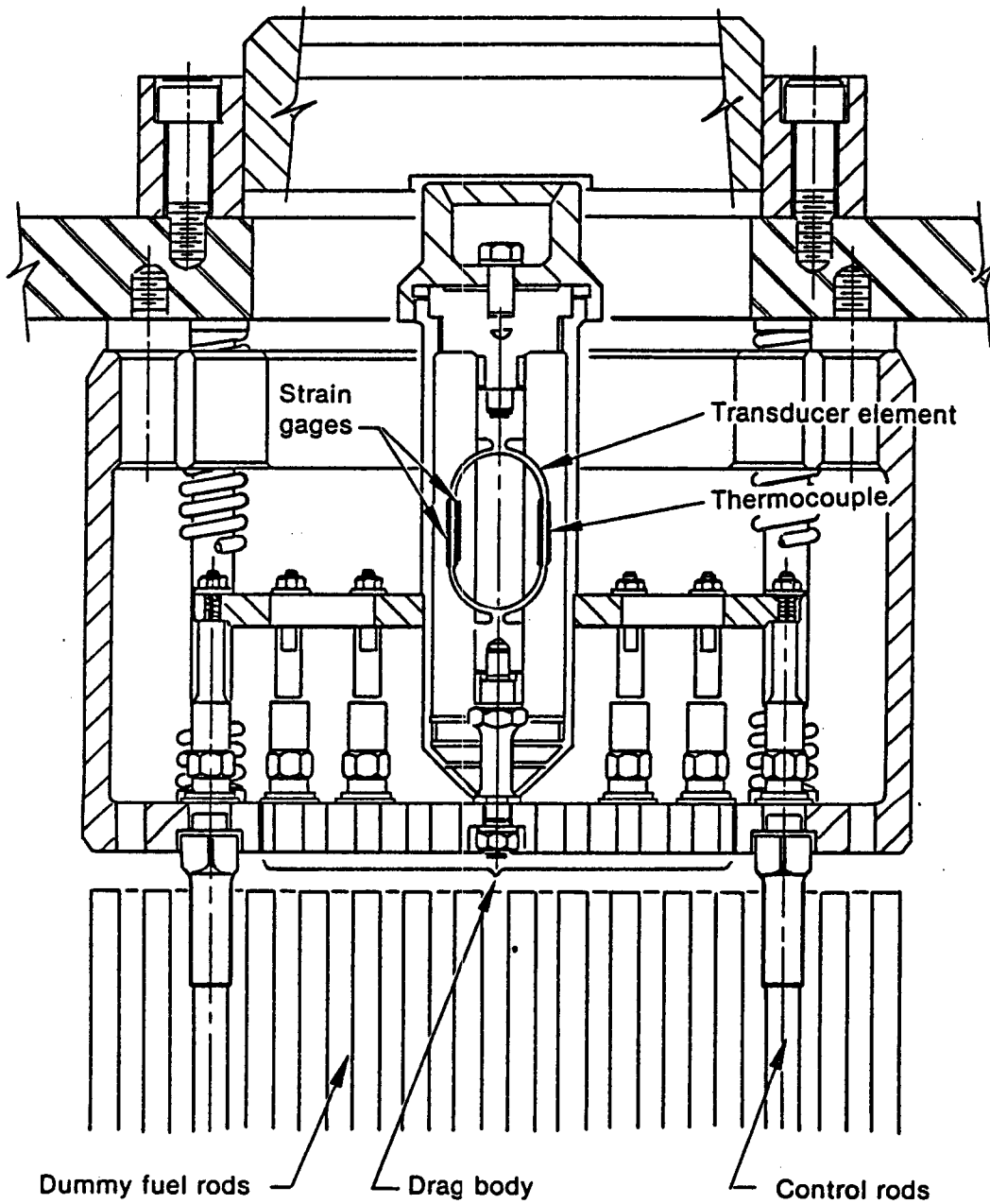
ORNL built two air/water facilities (one bundle and three-bundle) and one steam/water facility (one bundle) for calibrating the tie plate flow instruments. Steady-state calibrations were run in all three facilities and transient tests for verifying the algorithms were run in the steam/water facility. Figures C-12 and C-13 show typical performance data of the dragbody and turbine meter, respectively.

The results of the calibration showed that:

- o For cocurrent upflow, the combination of the dragbody (or differential pressure) and turbine meter gave satisfactory results. The uncertainty was about  $\pm 10\%$ .
- o For low upflows and countercurrent flows, the turbine data were erratic and unusable. A combination of dragbody and collapsed level (differential pressure) above the tie plate gave a method with an uncertainty up to about  $\pm 2$  kg/sec, which was the same order as the flows being measured.
- o For downflow, single-phase water flow was the dominant condition and either the dragbody or differential pressure gave a method with an uncertainty less than  $\pm 10\%$ .

Accordingly, reliable measurements can be obtained if the majority of the test is in the all upflow or all downflow regimes. The intermediate regime is inherently difficult to measure due to the nature of the flow (extremely turbulent, large spatial and temporal fluctuations, etc.). Analysis of transient tests verified high accuracy when this regime was avoided and also confirmed the types of errors obtained when this regime was present.

An extension of the ORNL tie plate work was the development of a small dragbody which could be attached below the tie plate. This dragbody was designed to measure the forces associated with the initiation of liquid



6 2957

Figure C-11. Drag body transducer location relative to end box components.

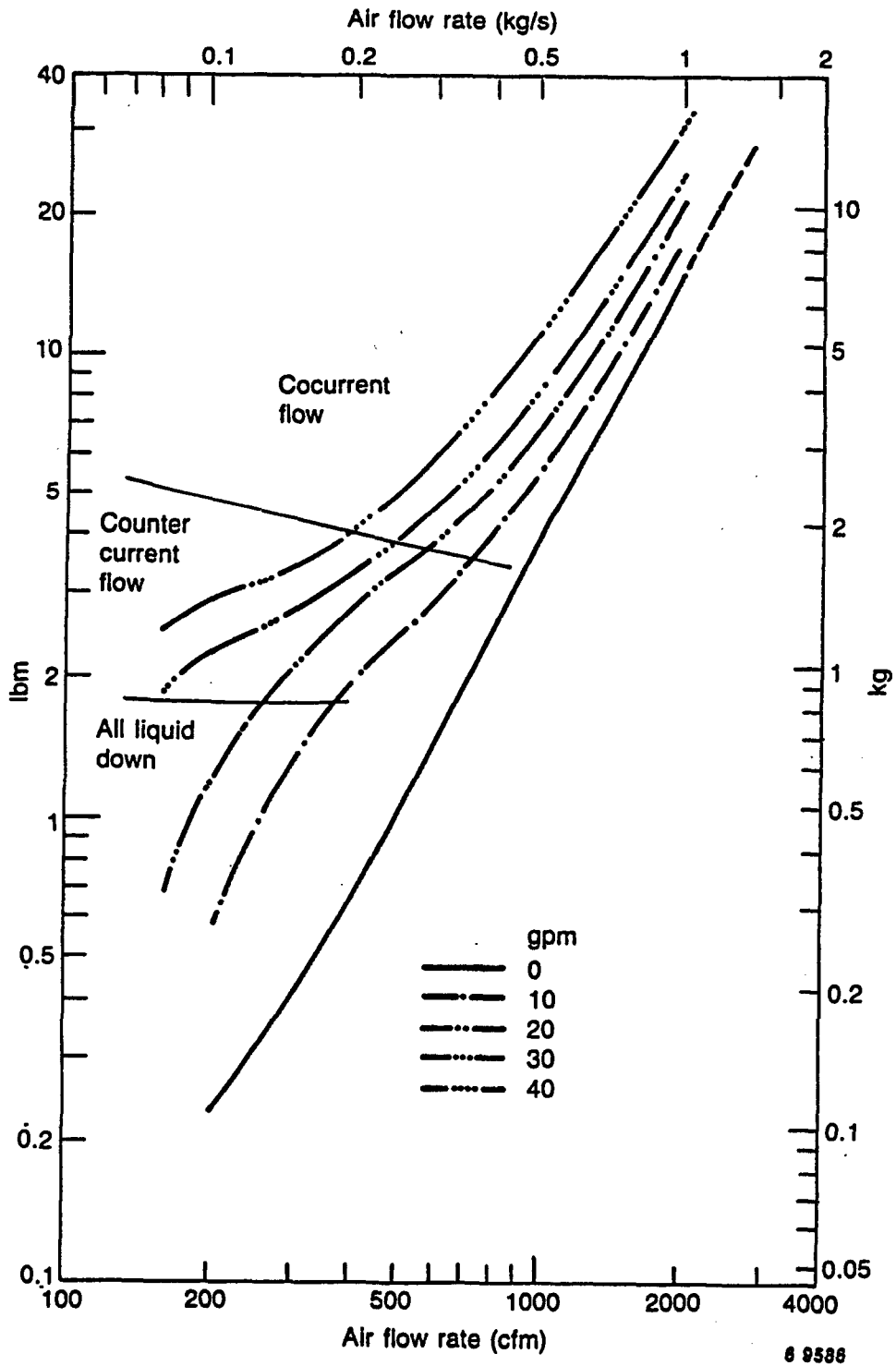


Figure C-12. Performance of tie-plate drag body in air/water loop.

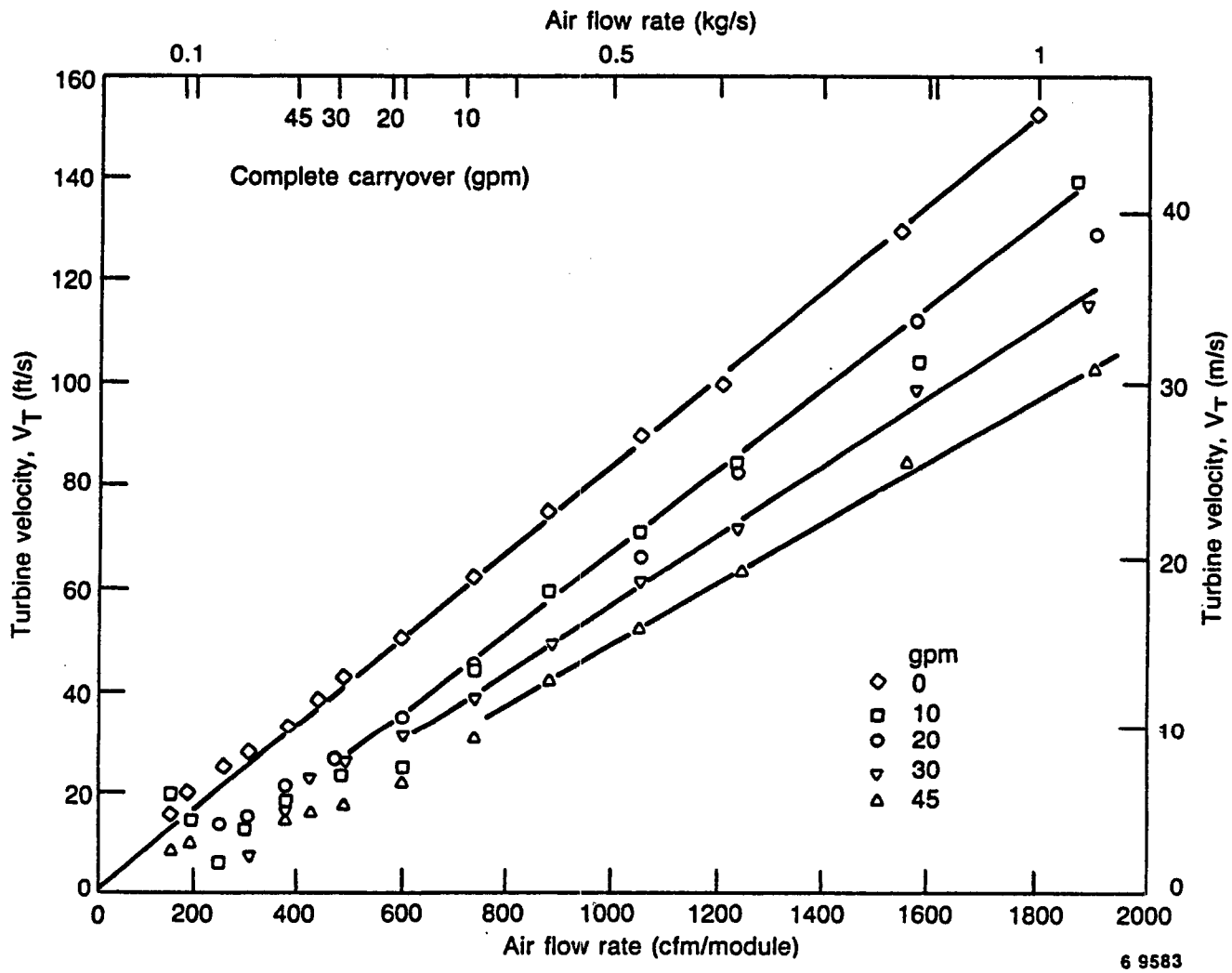


Figure C-13. At high air flow rates, turbine above tie plate responded in a linear fashion to increased air flow rate.

downflow from the upper plenum to the core. This phenomenon is called "breakthrough" and the instrument is called a breakthrough detector (Figure C-14). A strain gage measurement principle was also used in this instrument.

Overall, 36 tie plate flow measurement packages consisting of dragbody, turbine meter probe and collapsed level DP were provided to UPTF, and four of these packages were provided to SCTF. For UPTF, nine tie plate differential pressure measurements were also provided as dragbody backup measurements. Finally, 94 breakthrough detectors were provided to UPTF and two to SCTF.

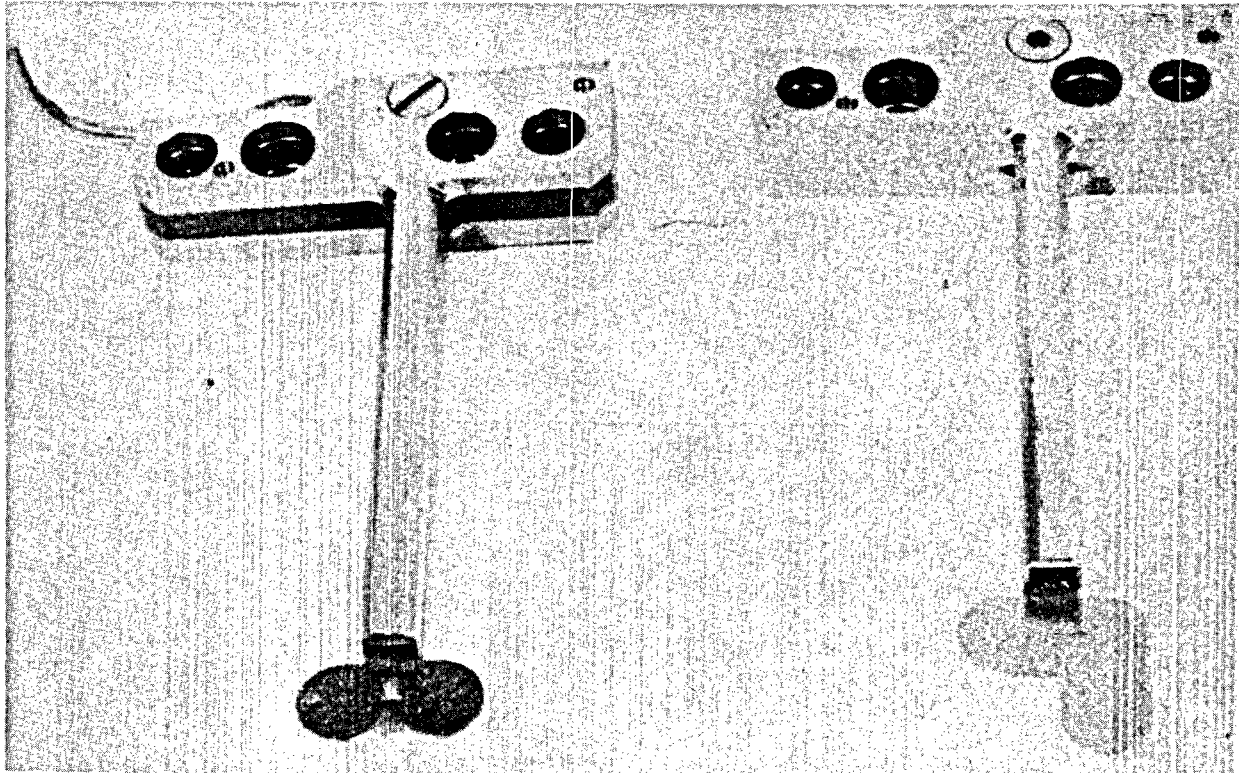
#### C.6.4 Other Instruments

This section provides a description of other instruments which were developed primarily to aid in thermal-hydraulic model development. Descriptions of the instrument measurement techniques along with typical results may be found in References C-1, C-2 and C-3. Summary discussions of measurement techniques and results are provided in the following paragraphs for five instruments which were utilized to a significant extent in the LOCA-ECCS facilities. A list of other instruments which were developed by various program participants but not used in the main LOCA-ECCS facilities is provided in Table C-4.

##### C.6.4.1 Pulsed Neutron Activation (PNA) (See References C-19 through C-21 and Pages IV.1-1 through 37 of Reference C-3)

- A. Description. The pulsed neutron activation (PNA) technique is used to determine the flow velocity of a fluid stream. It utilizes a radioactive tracer which is introduced into the flow stream through activation of the fluid by a neutron source. With water flow, a 14 MeV source is used to activate the oxygen and produce a short-lived isotope of nitrogen. The nitrogen emits a gamma ray with an energy of 6.2 MeV when it decays. The arrival time of the nitrogen tracer is measured by a detector which is located a known distance downstream of the source, as illustrated in Figure C-15. The detector is connected to a multichannel analyzer which stores, in separate time channels, the number of counts registered by the detector during a given time interval following the neutron burst. The velocity of the flow stream is then computed based on the average transit time determined by the multichannel analyzer.
- B. Results. Utilization of the PNA technique in the LOCA-ECCS facilities is described in the following:
  - o In the LOFT facility, the instrument was used to measure the rate of bypass of ECC fluid out the broken cold leg.
  - o In the German PKL facility, the PNA technique was used to measure the flow velocity in the downcomer pipe during the small-break test series. Figure C-16 provides typical

Breakthrough Detector



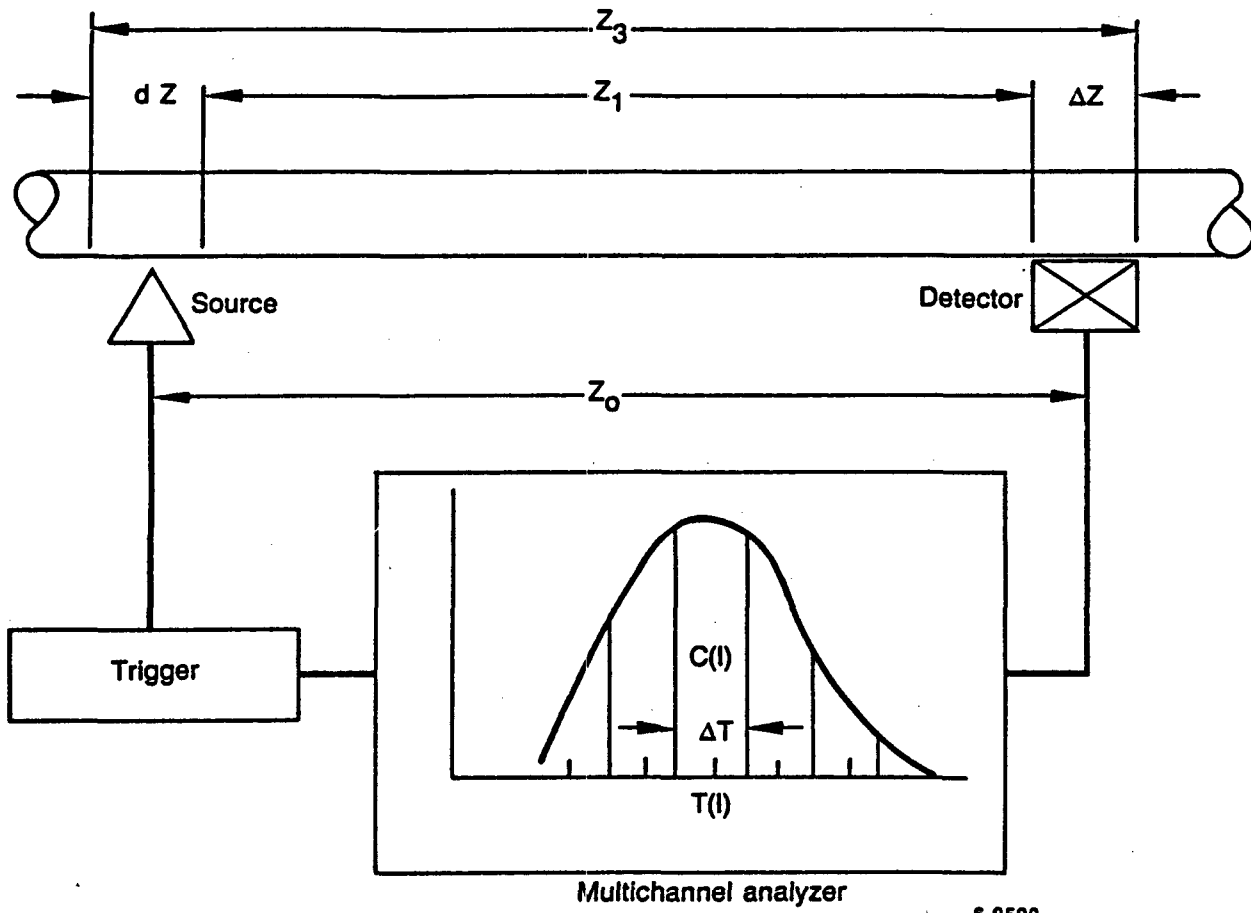
Previous design

Current design

Figure C-14. Break-through detector for tie-plate flow measurement at UPTF.

TABLE C-4. OTHER TWO-PHASE INSTRUMENTS

Instrument	Measurement Type	Reference
Ultrasonic detectors	Two-phase fluid density and thickness of water film	Pages IV.11-1 through 21 of Reference C-3 and Pages I.1-1 through 33 of Reference C-1
Radio-frequency and light attenuation	Void fraction distribution	Pages IV.3-1 through 37 of Reference C-3
Holography and tomography	Three-dimensional two-phase density distribution	Pages IV.6-1 through 40 and V.5-1 through 23 of Reference C-3
Neutronic noise analysis	Two-phase flow regime in reactor fuel assemblies	See Reference C-23 and Pages V.1-1 through 20 of Reference C-3
Storz lens	Two-phase flow visualization	Pages I.8-1 through 18 of Reference C-1



6 9590

Figure C-15. PNA measuring system.

Spacing = 1.105  
Delta time = 0.2  
Start channel = 24  
End channel = 235  
Start counts = 150.91  
End counts = 80.82  
Constant background = 40.41  
Decaying background = 123.6  
Decay constant of background = .02384  
Neutron monitor = 1.1588  
Flow velocity = .034 m/sec

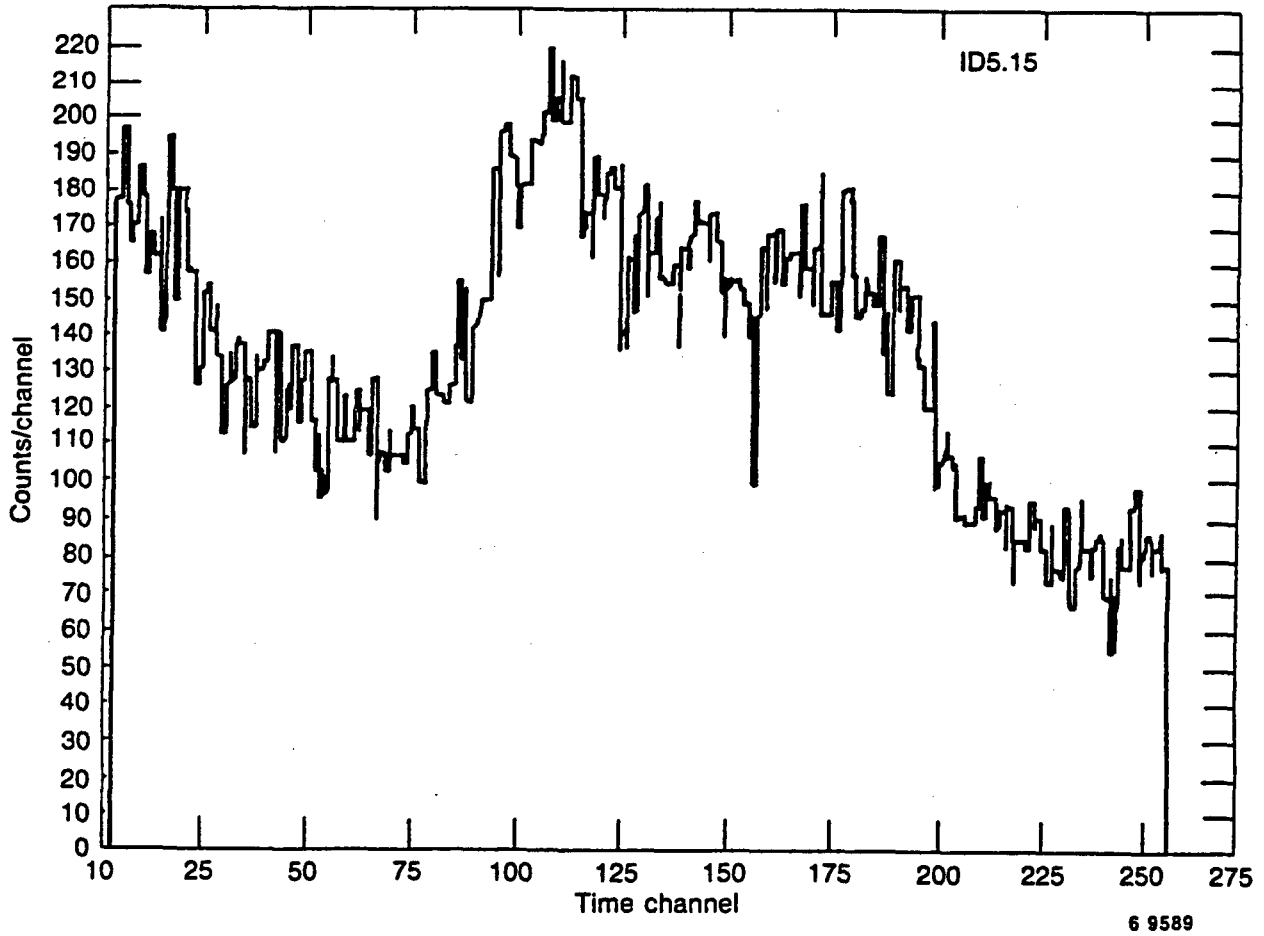


Figure C-16. PKL test data.

results for a PKL test. The multiple peaks in the multichannel analyzer data are indicative of a fluid flow oscillation in the facility downcomer.

C.6.4.2 Steam Superheat Probe (See Pages III.12-1 through 13 in Reference C-2 and Pages IV.4-1 through 17 in Reference C-3)

- A. Description. The steam superheat probe is used to measure the temperature of steam in a mixture of steam and entrained water droplets. The intent of this instrument was to determine the superheat of steam which may be existing in a nonequilibrium mixture (e.g., in the core during reflood). As illustrated in Figure C-17, the probe consists of a small diameter thermocouple which is located in a sampling tube. Steam is aspirated from the test section past the thermocouple. Good accuracy is obtained in measuring the steam temperature since:
- o Because of the direction changes required to flow from the test section into the sampling tube, good separation results between the superheated steam and water droplets and only a small fraction of the droplets enter the sampling tube.
  - o The concentric probe jackets provide good radiation shielding of the thermocouple from the test section wall.
- B. Results. The steam superheat probe was used to measure steam temperature in the Westinghouse FLECHT and FLECHT-SEASET and the JAERI CCTF heated core facilities. Typical transient response of the probe in a development test facility is shown in Figure C-18. Note that the probe correctly indicates a steam temperature which is between the temperatures of the water droplets (i.e.,  $T_{sat}$ ) and the test section wall.

C.6.4.3 Laser Doppler Anemometer (LDA) (See Reference C-22 and Pages IV.5-1 through 36 of Reference C-3)

- A. Description. The laser Doppler anemometer (LDA) is used to measure the water droplet size and velocity distributions in a two-phase dispersed flow mixture. This technique measures the frequency shift between the laser signals incident and reflected from a water droplet and computes the droplet velocity from the Doppler effect. In addition, based on the amplitude of the return signal, the size of the water droplet can be determined. A variety of measurement schemes were developed at SUNY-SB for measurements with small and large droplet flows.
- B. Results. The LDA technique was used by SUNY-SB to measure the water droplet size and velocity distributions upstream and downstream of a simulated fuel assembly tie plate for a dispersed flow regime. The measured distributions are shown in Figures C-19 and C-20 and illustrate the dispersive effects of the tie plate on the steam/droplet mixture.

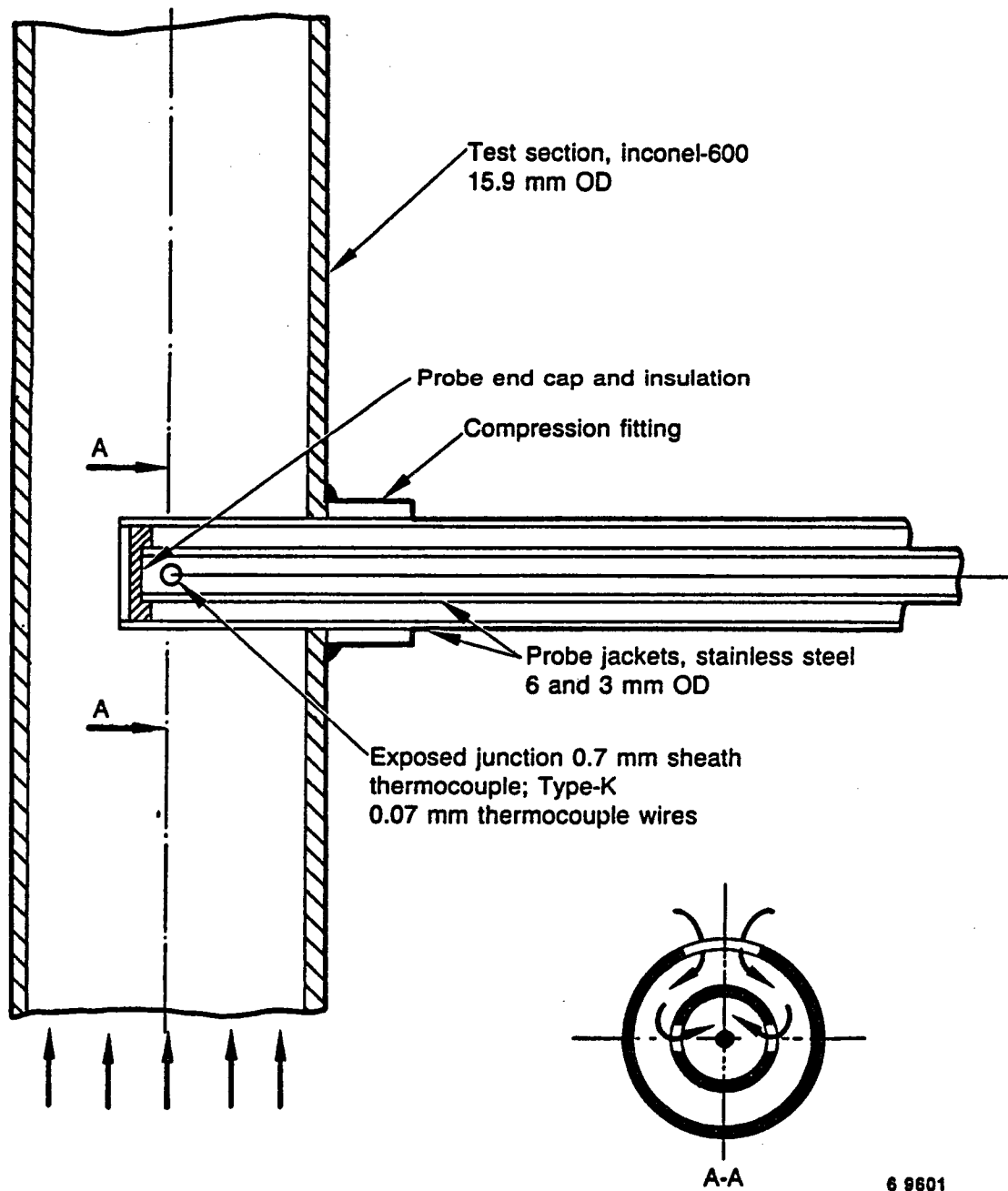


Figure C-17. The vapor probe.

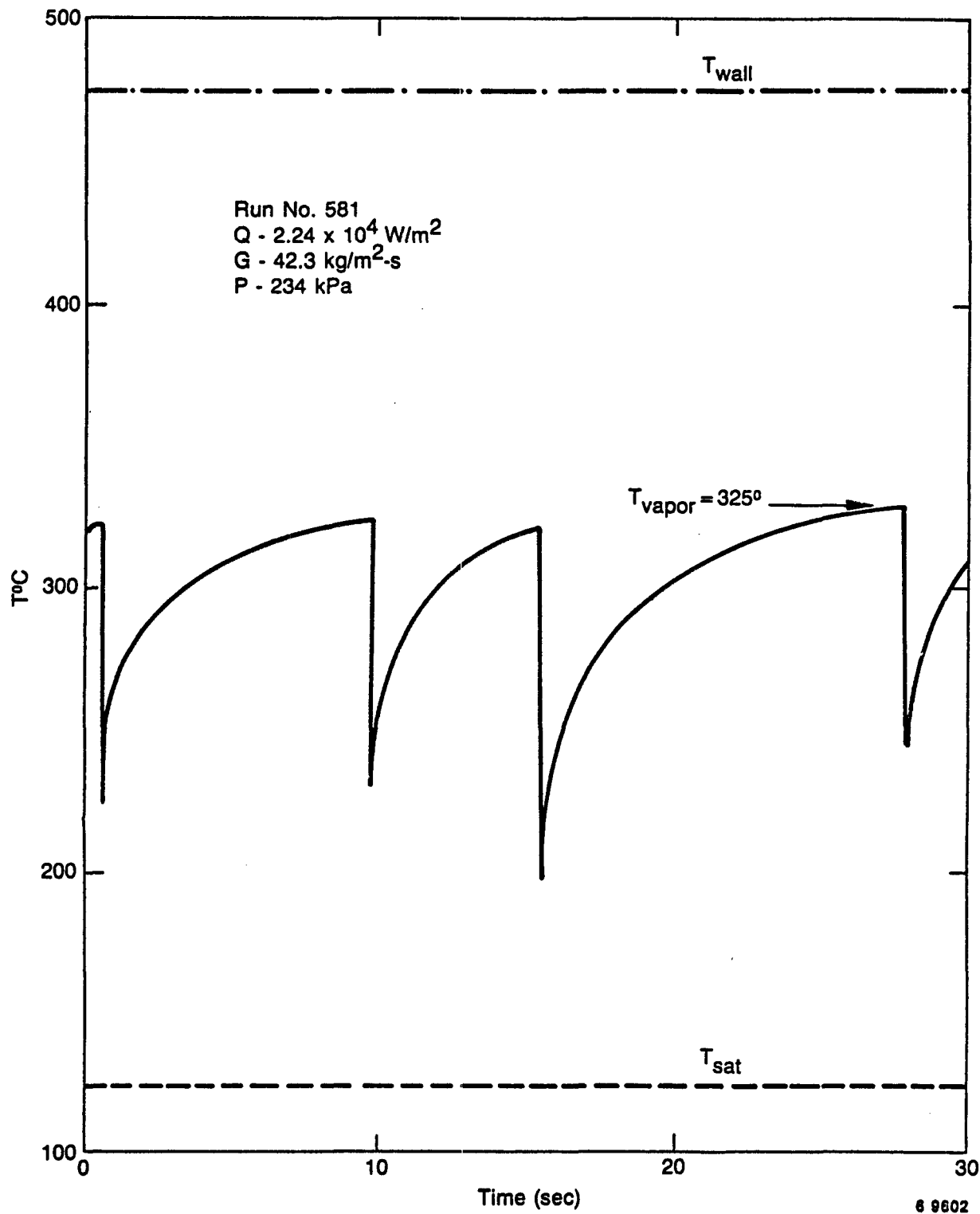


Figure C-18. Transient response of vapor probe for Run 581.

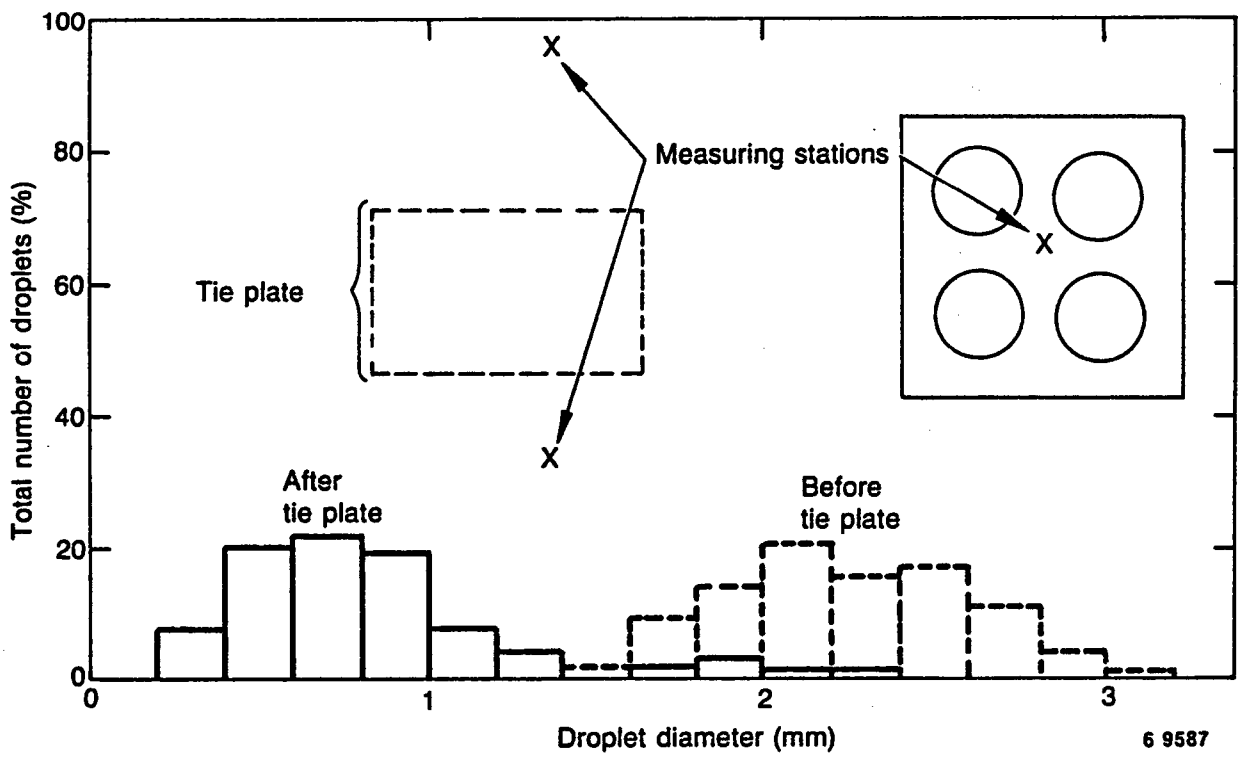


Figure C-19. Droplet size distribution.

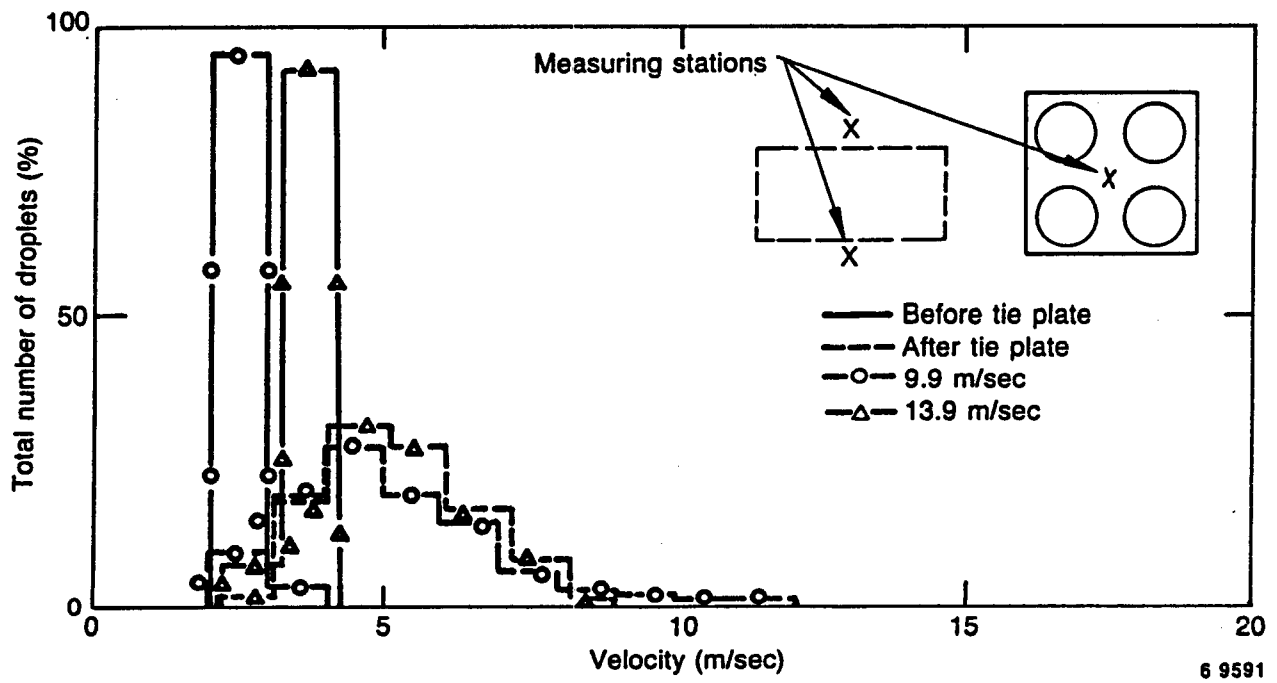


Figure C-20. Droplet velocity distribution.

#### C.6.4.4 Heated or Cooled Thermocouples (See Pages IV.2-1 through 42 of Reference C-3)

- A. Description. Measurement of low flow rates is difficult because the commonly used flow measuring devices (such as turbines) lose accuracy at low flow velocities in the range of 1 in./sec. The heated or cooled thermocouple (TC) measures the change of enthalpy downstream of a heat source or sink and has the capability to measure low velocities in this range. From the enthalpy change and the heat input, the flow rate can be determined based upon a previously calibrated relationship. INEL developed a heated thermocouple for subcooled water which has bidirectional sensing capability as indicated in Figure C-21. However, the heated TC does not work properly when the liquid temperature is close to saturation because nucleate boiling results and its sensing capability is affected. Thus, there is a limitation to its applicability and under this condition, a cooled TC is more useful. A cooled TC flowmeter was developed by INEL and tested at Semiscale.
- B. Results. Typical Semiscale data traces for the cooled TC and for a turbine flowmeter at the same location shown in Figure C-22 indicate the same velocity trends and also show that the cooled TC has greater sensitivity to velocity variations. Cooled TCs were also used in the lower plenum of the Japanese CCTF-II facility to sense velocities under core flood conditions.

#### C.6.4.5 Optical Liquid Level Detectors (OLLD)

- A. Description. As an alternative to the conductance liquid level detectors described in Section C.5.4, optical liquid level detectors (OLLD) were developed by INEL for measurement of liquid levels, local voids and water pockets along the length of the OLLD. By using an array of OLLDs, the structure of a steam-water mixture within a three-dimensional volume can be determined. The OLLD consists of the following components:
- o A low voltage light source.
  - o Optical fibers to guide the light to the sapphire probe tip.
  - o Optical fibers to return reflected light from the probe tip to a detector.

Since a greater fraction of the incident light is reflected from the probe tip when it is exposed to steam as compared with water, the OLLD has the capability to detect the presence of steam or water when properly calibrated.

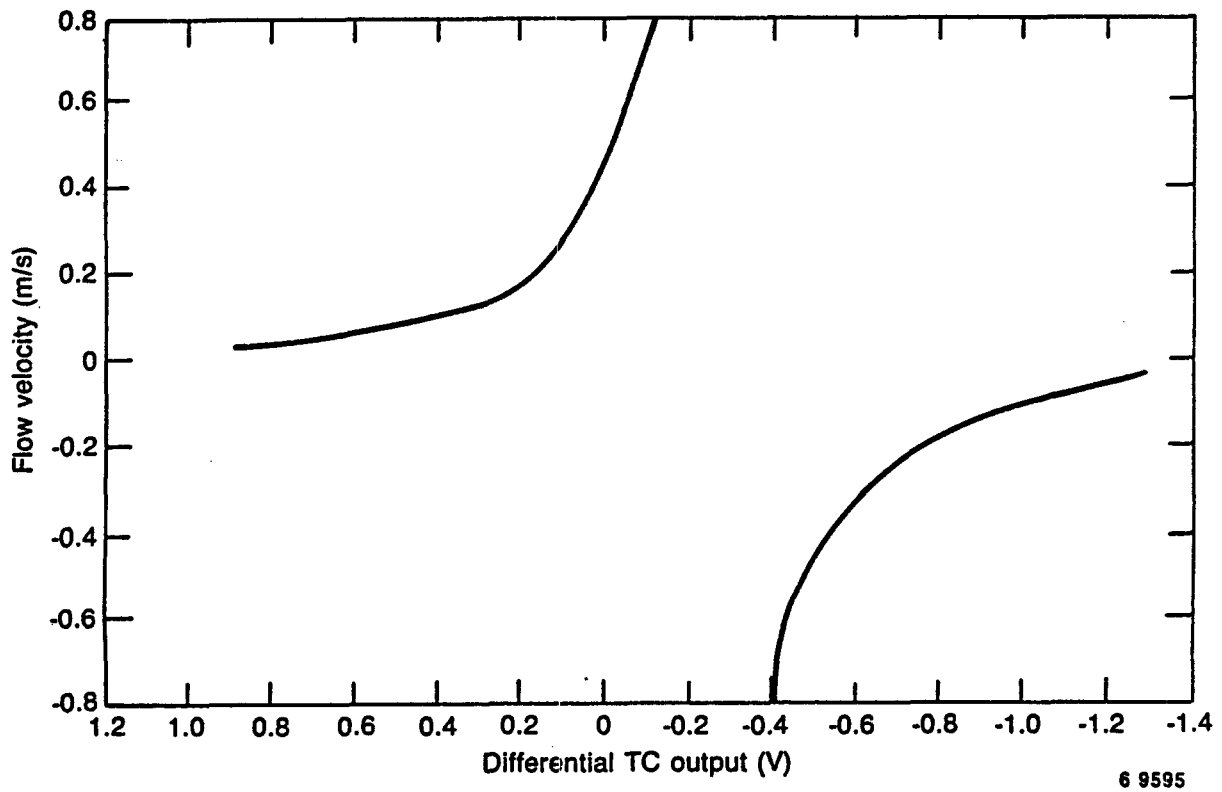


Figure C-21. Bi-directional heated thermal flowmeter velocity data.

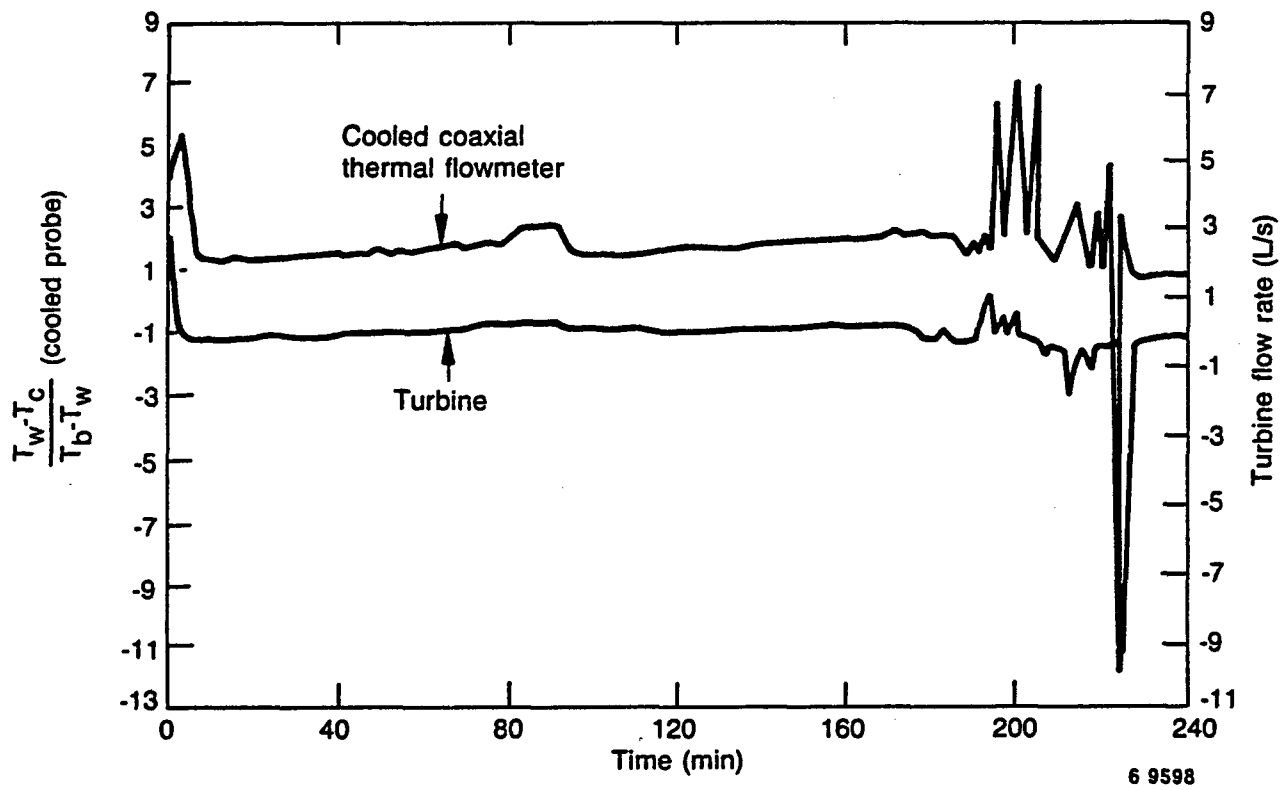


Figure C-22. Semiscale test data for cooled thermocouple.

- B. Results. The OLLDs, configured as three-dimensional fluid distribution grids, were used to measure the steam-water distribution in the downcomer, lower plenum and upper plenum regions of both the German UPTF and Japanese CCTF-II facilities.

## REFERENCES

- C-1 Review Group Meeting on Two-Phase Flow Instrumentation, NUREG/CP-0006, March 1978.
- C-2 Review Group Conference on Advanced Instrumentation for Reactor Safety Research, edited by A. L. Hon, T. Weber, NUREG/CP-0007, July 1980.
- C-3 Review Group Conference on Advanced Instrumentation Research for Reactor Safety, edited by A. L. Hon et al., NUREG/CP-0015, July 1980.
- C-4 "Drag Devices for Two-Phase Mass Flow Measurements," NUREG/CR-1361, 1980.
- C-5 "Development of the LOFT Prototype Drag Screen - Transient Steam-Water Testing," NUREG/CR-0270, 1978.
- C-6 "Factors that Affect the Calibration of Turbines in Single-Phase Flow," TREE-NUREG-1082, 1977.
- C-7 "LOFT Three-Beam Densitometer Interpretation," TREE-NUREG-1111, 1977.
- C-8 "Two-Phase Flow Measurements with Advanced Instrumented Spool Pieces," NUREG/CR-1529, 1980.
- C-9 "A Model to Calculate Mass Flow Rate and Other Quantities of Two-Phase Flow in a Pipe with a Densitometer, a Drag Disk and a Turbine Meter," ORNL-TM-4759, 1975.
- C-10 "Some Aspects of Interpreting Two-Phase Flow Measurements in Instrumented Piping Spool Pieces," NUREG-0280, 1977.
- C-11 "Fabrication of Sensors for High-Temperature Steam Instrumentation Systems," NUREG/CR-1359, 1980.
- C-12 "Transient Testing of an In-Core Impedance Flow Sensor in a 9-Rod Heated Bundle," NUREG/CR-1909, 1981.
- C-13 "Mass Flow Measurements Under PWR Reflood Conditions in a Downcomer and at a Core Barrel Vent Valve Location," NUREG/CR-2710, 1982.
- C-14 "ORNL Instrumentation Performance for Slab Core Test Facility (SCTF)-Core I Reflood Test Facility," NUREG/CR-3286, 1983.
- C-15 "Assessment of the Adequacy of ORNL Instrumentation in Reflood Test Facilities," NUREG/CR-3651, 1985.
- C-16 "Assessment of Current High-Temperature Strain Gages," ORNL/TM-7025, 1979.

- C-17 "Determination of Mass Flow Rates Across the Core/Upper Plenum Interface," 2D/3D Coordination Meeting, USNRC, November 10-14, 1978.
- C-18 "Measurement of Two-Phase Flow at the Core/Upper Plenum Interface for a PWR Geometry Under Simulated Reflood Conditions," NUREG/CR-3138, 1984.
- C-19 "Two-Phase Flow Measurement by Pulsed Neutron Activation Techniques," ANC-NUREG-C7-78-17, 1978.
- C-20 "Measurement of Slow Flow Velocities at the PKL Facility," NUREG/CR-1622, 1980.
- C-21 "Neutron Generator for Two-Phase Flow Calibration," NUREG/CR-0480, 1978.
- C-22 "Development of a Laser Doppler Anemometer for the Measurement of Two-Phase Dispersed Flow," NUREG/CR-0457, 1978.
- C-23 "Characterization of Two-Phase Flow using Neutron Fluctuations," NUREG/CR-3141, 1983.



NRC FORM 335 (2-84) NRCM 1102, 3201, 3202	U.S. NUCLEAR REGULATORY COMMISSION	1. REPORT NUMBER (Assigned by TIDC, add Vol. No., if any)
<b>BIBLIOGRAPHIC DATA SHEET</b>		<b>NUREG-1230</b>
SEE INSTRUCTIONS ON THE REVERSE		3. LEAVE BLANK
2. TITLE AND SUBTITLE		4. DATE REPORT COMPLETED
Compendium of ECCS Research for Realistic LOCA Analysis Final Report		MONTH   YEAR
5. AUTHOR(S)		October   1988
7. PERFORMING ORGANIZATION NAME AND MAILING ADDRESS (Include Zip Code)		6. DATE REPORT ISSUED
Division of Systems Research Office of Nuclear Regulatory Research U.S. Nuclear Regulatory Commission Washington, DC 20555		MONTH   YEAR
10. SPONSORING ORGANIZATION NAME AND MAILING ADDRESS (Include Zip Code)		8. PROJECT/TASK/WORK UNIT NUMBER
Same as 7, above.		9. FIN OR GRANT NUMBER
12. SUPPLEMENTARY NOTES		11a. TYPE OF REPORT
13. ABSTRACT (200 words or less)		Staff Technical Report
<p>Emergency Core Cooling Systems (ECCS) are required on all light water reactors (LWRs) in the United States to provide cooling of the reactor core in the event of a break in the reactor piping. These accidents are called loss-of-coolant accidents (LOCA), and they range from small leaks to a postulated full break of the largest pipe in the reactor cooling system. Federal government regulations require that calculations of the LOCA be performed to show that the ECCS will maintain fuel rod cladding temperatures, cladding oxidation, and hydrogen production within certain limits. The Nuclear Regulatory Commission (NRC) and others have completed an extensive investigation of fuel rod behavior and ECCS performance. The technology has been advanced to the point that it is now possible to make a realistic estimate of ECCS performance during a LOCA and to quantify the uncertainty of this calculation. This report serves as a general reference for ECCS research. The report (1) summarizes the understanding of LOCA phenomena in 1974, (2) reviews experimental and analytical programs developed to address the phenomena, (3) describes best-estimate computer codes developed by the NRC, (4) discusses the salient technical aspects of LOCA phenomena and our current understanding of them, (5) discusses probabilistic risk studies and (6) examines the impact of research on the ECCS regulations.</p>		b. PERIOD COVERED (Inclusive dates)
14. DOCUMENT ANALYSIS -- a. KEYWORDS/DESCRIPTORS		15. AVAILABILITY STATEMENT
Emergency Core Cooling System (ECCS) Loss-of-coolant accident (LOCA) Best-Estimate Computer Codes		<b>UNLIMITED</b>
b. IDENTIFIERS/OPEN-ENDED TERMS		16. SECURITY CLASSIFICATION
Light Water Reactor (LWR)		(This page) <b>UNCLASSIFIED</b>
		(This report) <b>UNCLASSIFIED</b>
		17. NUMBER OF PAGES
		18. PRICE